NASA TECHNICAL MEMORANDUM

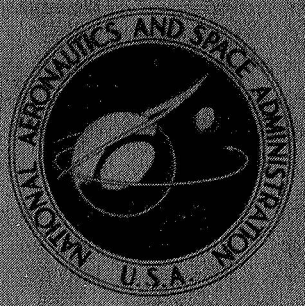

NASA TM X-1844

NASA TM X-1844

FLIGHT PERFORMANCE OF ATLAS-CENTAUR AC-13, AC-14, AC-15 IN SUPPORT OF THE SURVEYOR LUNAR LANDING PROGRAM

Lewis Staff

Lewis Research Center

Cleveland, Ohio

NATIONAL AERONAUTICS AND SPACE ADMINISTRATION • WASHINGTON, D. C. • FEBRUARY 1970

1. Report No. NASA TM X-1844	2. Government Accession No.	3. Recipient's Catalog No.
4. Title and Subtitle FLIGHT PERFORMANCE OF ATLAS-CENTAUR AC-13, AC-14, AC-15 IN SUPPORT OF THE SURVEYOR LUNAR LANDING PROGRAM		5. Report Date January 1970 6. Performing Organization Code
7. Author(s) Lewis Staff		8. Performing Organization Report No. E-5057
9. Performing Organization Name and Address Lewis Research Center National Aeronautics and Space Administration Cleveland, Ohio 44135		10. Work Unit No. 491-05-00-03-22 11. Contract or Grant No.
12. Sponsoring Agency Name and Address National Aeronautics and Space Administration Washington, D.C. 20546		13. Type of Report and Period Covered Technical Memorandum 14. Sponsoring Agency Code
15. Supplementary Notes		

16. Abstract

Atlas-Centaur launch vehicles AC-13, AC-14, and AC-15 successfully boosted Surveyors V, VI, and VII, respectively, into lunar intercept trajectories. These launch vehicles used the indirect (two-burn) mode of ascent. Surveyor VII, launched on January 7, 1968, concluded the Surveyor lunar landing program. This report discusses the flight performance of the AC-13, AC-14, and AC-15 launch vehicles from lift-off through Centaur retromaneuver.

17. Key Words *(Suggested by Author(s))*	18. Distribution Statement Unclassified - unlimited		
19. Security Classif. (of this report) Unclassified	20. Security Classif. (of this page) Unclassified	21. No. of Pages 244	22. Price * $3.00

*For sale by the Clearinghouse for Federal Scientific and Technical Information
Springfield, Virginia 22151

CONTENTS

I. SUMMARY

The Atlas-Centaur launch vehicles AC-13, AC-14, and AC-15, with Surveyor spacecraft V, VI, and VII, respectively, were successfully launched from the Eastern Test Range to complete the Surveyor lunar landing program. AC-13 was launched September 8, 1967; followed by AC-14 on November 7, 1967, and AC-15 on January 7, 1968. All three flights were flown using an indirect (parking orbit) mode of ascent wherein the Centaur and Surveyor were first injected into a near circular 167-kilometer (90-n. mi.) Earth orbit. After orbital coast periods of 7 minutes in duration for AC-13, 13 minutes in duration for AC-14, and 22 minutes in duration for AC-15, the Centaur main engines were restarted, and the spacecraft were inserted into the desired lunar transfer orbit. Orbital insertions were very accurate and only slight midcourse velocity corrections were required to place the Surveyors on the desired touchdown sites. All three Surveyors successfully touched down on the lunar surface. Elapsed time for a Surveyor lunar transit was about 66 hours.

This report contains a summary evaluation of the Atlas-Centaur systems in support of the last three Surveyor missions. Their flights were so similar that the results are combined in a single report.

II. INTRODUCTION

Atlas-Centaur launch vehicles AC-13, AC-14, and AC-15 launched Surveyors V, VI, and VII, respectively, from Cape Kennedy Complex 36. The launches occurred between early September 1967 and early January 1968.

Centaur was first developed as a high-energy second stage for a modified Atlas missile. It underwent an extensive development program which was divided into two phases. The first phase occurred from May 1962 to August 1965. In this phase, the Centaur demonstrated the capability to perform a lunar mission using a single, continuous thrusting period. This type of mission is called a direct-ascent mission. The second phase occurred from April 1966 to October 1966. During this phase, the ability was developed to perform a lunar mission using two distinct periods of thrusting separated by a coast phase. The development of this indirect mode of ascent was undertaken to provide greater launch flexibility than is provided with a direct mode of ascent. For example, the direct-ascent mode restricts lunar launches to the summer months, while the indirect-ascent mode permits launches every month of the year. In addition to providing more potential launch days, the indirect mode of ascent allows longer launch windows on each launch day.

The first operational Atlas-Centaur vehicle used the direct mode of ascent and was successfully launched in May 1966. Its payload was Surveyor I. Subsequently, vehicles AC-7 and AC-11 used the direct mode of ascent to successfully inject Surveyors II and IV into the proper lunar transfer ellipses. These launches occurred in September 1966 and July 1967, respectively. The flight of AC-12 with Surveyor III in April 1967 was the first operational flight to use the indirect mode of ascent. In this indirect mode, the Centaur fires for two distinct periods separated by a coast phase. During the coast phase, the orbit of the Centaur vehicle is nearly circular at an altitude of 169 kilometers (90 n. mi.). The Centaur engine second firing then transfers the Surveyor from the nearly circular, low-energy parking orbit to the highly elliptical, higher-energy lunar transfer orbit. The last three Centaur-Surveyor missions, AC-13, AC-14, and AC-15, used the indirect mode of ascent.

The overall objectives of the Surveyor project were (1) to accomplish soft landings on the Moon, as demonstrated by successful spacecraft operation subsequent to landing, (2) to provide basic data in support of the Apollo manned lunar landing program, and (3) to perform lunar surface operations designed to contribute new scientific knowledge about the Moon and provide further data in support of Apollo. The role of Atlas-Centaur

in the Surveyor program was to support the Surveyor project in carrying out these design goals.

This report presents a final performance evaluation of the AC-13, AC-14, and AC-15 launch vehicles from lift-off through completion of the Centaur post-spacecraft-separation retromaneuver.

III. LAUNCH VEHICLE DESCRIPTION

by Eugene E. Coffey

The Atlas-Centaur is a two-stage launch vehicle consisting of an Atlas first stage and a Centaur second stage connected by an interstage adapter. Both stages are 3.05 meters (10 ft) in diameter, and the composite vehicle is 35.66 meters (117 ft) in length. The vehicle weight at lift-off approximates 147 000 kilograms (324 000 lbm). The basic structure of the Atlas and Centaur stages utilizes thin-wall, pressure-stabilized, main propellant tank sections of monocoque construction.

The first-stage SLV-3C Atlas (fig. III-1) is 21.03 meters (69 ft) long. It is powered by a Rocketdyne MA-5 propulsion system consisting of a booster engine with two thrust chambers and with a total thrust at sea level of 149.453×10^4 newtons (336 000 lbf), a sustainer engine with a thrust at sea level of 257.98×10^3 newtons (58 000 lbf), and two small vernier engines each with a thrust at sea level of 2980 newtons (670 lbf). All engines use liquid oxygen and RP-1 (kerosene) as propellants and are ignited prior to lift-off. The booster engine thrust chambers are gimbaled for pitch, yaw, and roll control during the booster phase of the flight. This phase is completed at booster engine cutoff, which occurs when the vehicle acceleration reaches about 5.7 g's; the booster engine section is jettisoned 3.1 seconds later. The sustainer engine and the vernier engines continue to burn after booster engine cutoff for the Atlas sustainer phase of the flight. During this phase the sustainer engine is gimbaled for pitch and yaw control, while the vernier engines are gimbaled for roll control only. The sustainer and vernier engines fire until propellant depletion. The Atlas is severed from the Centaur by the firing of a shaped-charge system located on the interstage adapter. The firing of a retrorocket system then separates the Atlas - interstage adapter from the Centaur.

The configuration of the Centaur second stage is shown in figure III-2. This stage, including the nose fairing, is 14.63 meters (48 ft) long. Centaur is a high-performance stage (specific impulse, approx. 442 sec) powered by two Pratt & Whitney RL10A-3-3 engines which generate a total thrust at sea level of approximately 133.45×10^3 newtons (30 000 lbf). These engines use liquid hydrogen and liquid oxygen as the propellants. The Centaur main engines are gimbaled to provide pitch, yaw, and roll control during Centaur powered flight. Fourteen hydrogen peroxide engines mounted on the aft periphery of the tank provide various thrust levels for attitude control, propellant settling and retention during the coast phase, and vehicle reorientation after spacecraft separation. The

Centaur hydrogen tank is shielded with four insulation panel sections, each 2.54 centimeters (1 in.) thick. Each section consists of a polyurethane-foam-filled honeycomb core, covered with fiber glass lamination. A fiber glass nose fairing is used to provide an aerodynamic shield for the Surveyor spacecraft, guidance equipment, and electronic packages during ascent. The insulation panels and nose fairing are jettisoned during the Atlas sustainer phase.

The AC-13, AC-14, and AC-15 launch vehicles were designed for an indirect (parking orbit) mode of ascent. For this mode of ascent, it was necessary to install a "slosh" baffle in the hydrogen tank to damp disturbances in the liquid residuals at Centaur main engine cutoff and during the low-gravity coast period. In addition, energy-dissipating devices were installed in the propellant (fuel) return lines to reduce disturbances induced by main engine cutoff.

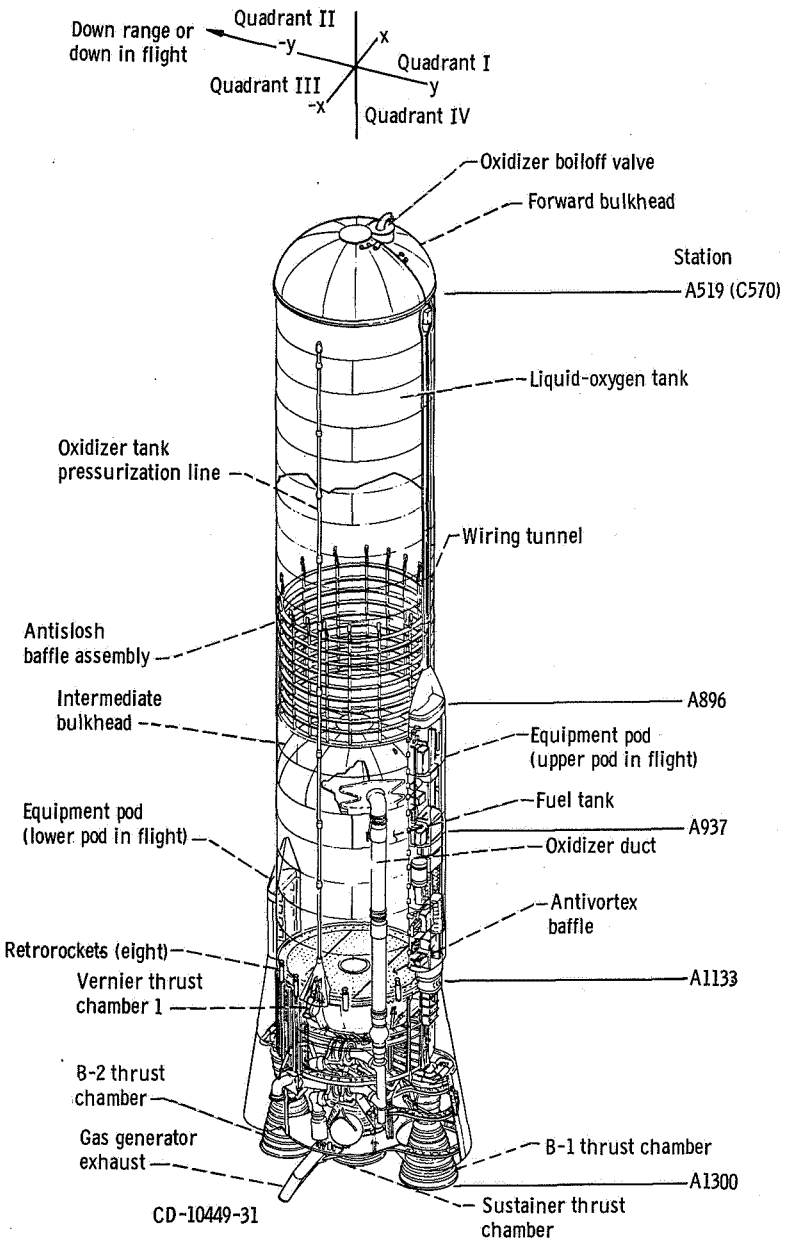

Figure III-1. - General arrangement of Atlas launch vehicle, AC-13, AC-14, and AC-15.

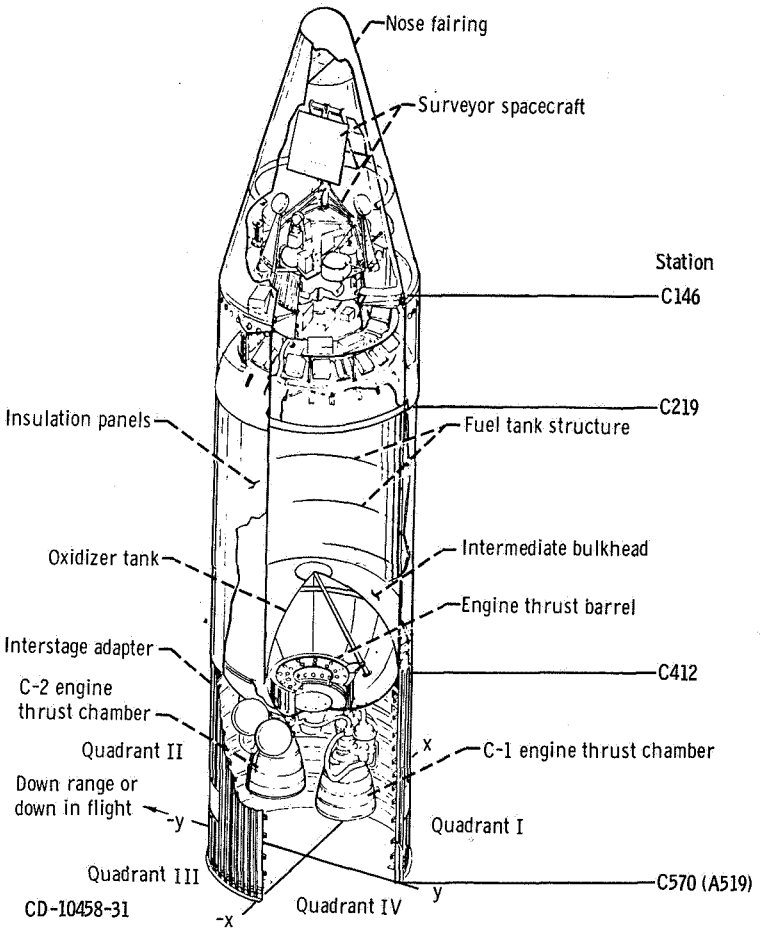

Figure III-2. - General arrangement of Centaur vehicle; AC-13, AC-14, and AC-15.

IV. MISSION PERFORMANCE

by William A. Groesbeck

The Surveyor lunar landing program was completed with the launching of Atlas-Centaur vehicles AC-13, AC-14, and AC-15. The AC-13 was launched at 0257 hours (EST) on September 8, 1967; AC-14 at 0239 hours (EST) on November 7, 1967; and AC-15 at 0130 hours (EST) on January 7, 1968. Launch vehicle system performance was successful on all flights. Surveyors V, VI, and VII, respectively, were accurately injected into the required lunar transfer orbit using an indirect (parking orbit) mode of ascent. Touchdown of the three Surveyors on the lunar surface was also successfully accomplished.

A compendium of the typical Atlas-Centaur mission profile and the Surveyor lunar transfer trajectory are shown in figures IV-2 and IV-2. Listings of postflight vehicle weights summary, atmospheric sounding data, Surveyor launch windows, and flight events records are given in the TRAJECTORY AND PERFORMANCE section for AC-15 and in appendix A for AC-13 and AC-14.

The AC-13, AC-14, and AC-15 Atlas-Centaur flights were so similar that the following discussion is centered around the AC-15 flight performance as being typical of all three. However, any mission events peculiar to the other two flights are included when appropriate.

ATLAS FLIGHT PHASE

Ignition and thrust buildup of the Atlas engines were normal, and the vehicle lifted off (T + 0 sec) with a combined vehicle weight of 147 000 kilograms (324 000 lbm) and a thrust to weight ratio of 1.22. Two seconds after lift-off, the vehicle started a programmed roll from the launcher azimuth (fixed) of 105^{o} to the required flight azimuth of 102.914^{o}. At T + 15 seconds, the vehicle had rolled to the flight azimuth, and it began a preprogrammed pitchover maneuver which lasted through booster engine cutoff. Pitch rate commands for the pitchover maneuver were supplied to the flight control system by the Atlas displacement gyros. The Centaur inertial guidance system was operating during this time, but guidance-generated steering commands were not admitted to the flight control system until after booster staging.

The preset Atlas pitch program used to command the vehicle during the booster flight was augmented by incremental pitch and yaw inputs which acted to reduce vehicle bending loads resulting from wind shear forces. This supplemental program, one of a series selected on the basis of measured prelaunch upper air soundings, was stored in the airborne computer. The incremental commands were then algebraically summed with the fixed program commands issued by the Atlas flight programmer. Booster engine gimbal angles for thrust vector control were accordingly reduced and did not exceed 2.0° (well within previous experience) during the atmospheric ascent.

Vehicle acceleration during the boost phase proceeded according to the mission plan. Centaur guidance issued the booster engine cutoff signal when the vehicle acceleration reached 5.78 g's. Approximately 3 seconds later at T + 155.5 seconds, the Atlas programmer issued the staging command, causing separation of the booster engine section from the vehicle. Staging transients were small, and the maximum vehicle angular rate in pitch, yaw, or roll did not exceed 2.03 degrees per second. Normal low-amplitude "slosh" was excited in the Atlas liquid-oxygen tank but was damped out within a few seconds.

Vehicle steering by the inertial guidance system was initiated about 4 seconds after Atlas booster staging. At the start of guidance steering, the vehicle was slightly off the required steering vector by about 7.2° nose low in pitch and 6.4° nose right in yaw. This error was within the expected dispersion limits, and the guidance system issued commands to correct the error and to continue the pitchover maneuver during the Atlas sustainer flight phase.

Insulation panels were jettisoned during the sustainer flight phase at T + 197.1 seconds. The insulation panel assembly was completely severed in four sections along the joint seams by a shaped charge, and the cut sections fell away from the vehicle. The nose fairing unlatch command was given at T + 226.4 seconds; the thruster bottles, firing 0.5 second later, rotated the fairing halves away from the vehicle. Vehicle angular rates, caused by the jettisoning of the insulation panels and nose fairing, were insignificant.

Sustainer and vernier engine system performance was satisfactory throughout the flight. Sustainer engine cutoff was initiated at T + 248.7 seconds because of liquid-oxygen depletion.

Coincident with sustainer engine cutoff, the guidance steering commands to the flight control system were discontinued, allowing the vehicle to coast in a nondisturbed flight mode until Atlas-Centaur separation. The Atlas staging command was issued by the flight programmer at T + 250.6 seconds. A shaped charge was fired to cut the interstage adapter and sever the two stages. Eight retrorockets on the Atlas then fired to push the Atlas stage away from the Centaur. Only minor disturbances were noted during the staging sequences.

CENTAUR FLIGHT PHASE

Centaur Main Engine First Burn

The main engine start sequence for the Centaur stage was initiated prior to sustainer engine cutoff. Propellant boost pumps were started at T + 214.5 seconds. The required net positive suction pressure to prevent boost pump cavitation, during the near-zero-gravity period from sustainer engine cutoff until main engine start, was provided by increasing the ullage pressure in the propellant tanks with helium. Eight seconds prior to main engine start, the Centaur programmer issued prestart commands for engine firing. Engine inlet valves were opened to flow liquid propellants through the lines and chill down the supply lines and engine turbopumps. Chilldown of the system was provided to ensure liquid at the pump inlets and prevent cavitation of the turbopump while the engines are accelerating. This engine conditioning made possible a uniform and rapid thrust buildup after main engine start. At T + 260.2 seconds, the main engine start command was issued by the flight programmer, and engine thrust increased to full flight levels.

Guidance steering for the Centaur stage was initiated at 4 seconds after main engine start by the vehicle timer. Guidance steering commands were delayed until after the engine start sequence to prevent excessive vehicle angular rates, which could be induced by gimbaling the engines to correct for vehicle position errors. The total residual angular rates and disturbing torques induced during this staging interval resulted in only a 2.4^{o} vehicle drift off the steering vector in the pitch plane. This attitude drift error was within the expected dispersions and was corrected within 4 seconds after start of guidance steering.

Through the remainder of the Centaur main engine firing period, the guidance system provided the necessary steering commands to acquire the injection velocity vector for the desired parking orbit. At T + 593.2 seconds, the guidance computed velocity for injection was attained, and the engines were commanded off. Orbital insertion at an altitude of 162.9 kilometers (87.9 n. mi.) occurred approximately 2040 kilometers (1100 n. mi.) southeast of Cape Kennedy at a velocity of 7380 meters (24 199 ft) per second.

Throughout the flight, the propellant utilization system performed satisfactorily and accurately controlled the mixture ratio of propellants consumed by the engines.

Centaur Coast Phase

At main engine cutoff, the vehicle began a 22-minute orbital coast. Guidance flight control commands continued to maintain vehicle attitude and rate control by means of the hydrogen peroxide engine system.

Control of the propellants during the coast phase was successfully accomplished by using energy-dissipating devices and a programmed low-level-thrust schedule. Propellant tank configuration and propellant control technique for this phase of the mission were the same as those successfully demonstrated on the AC-8 and AC-9 research and development flights (refs. 1 and 2). Coincident with main engine cutoff, two 222-newton-(50-lbf-) thrust engines were fired to provide an acceleration level of 6.9×10^{-3} g's for 75.8 seconds. This thrust level suppressed any disturbance of the liquid residuals excited by engine shutdown transients and retained the propellants in the bottom of the tanks. Energy-dissipating devices, such as slosh baffles around the hydrogen tank and diffusers on propellant return flow lines into the tank, served to attenuate and dissipate the disturbance inputs to the residual propellants. After the first 75.8 seconds of the coast, the liquid disturbances were damped out, and the thrust level was reduced to 26.7 newtons (6 lbf) or an acceleration of 4.1×10^{-4} g's. This thrust was sufficient to retain the propellants in a settled condition through the remainder of the coast.

Attitude control of the vehicle throughout the coast phase was achieved without incident. Disturbance torques were experienced, as on previous flights, during the firing of the hydrogen peroxide engines for propellant settling. Control of the disturbances required a 50-percent duty cycle of the attitude control engines (ref. 1). Hydrogen venting through the nonpropulsive vent system did not produce any disturbing torques on the vehicle. Venting of the hydrogen tank during the coast phase occurred at about 600 seconds after main engine cutoff when the ullage pressure increased to the regulating range of the primary vent valve. Hydrogen gas was then vented intermittently as required to maintain tank pressure throughout the remainder of the coast. The oxygen tank was not vented at any time during the coast.

Forty seconds prior to main engine restart, the thrust level on the vehicle was increased to 444 newtons (100 lbf) to give added assurance of proper propellant settling. At the same time, the hydrogen tank vent valve was closed, and the tank pressures were increased by injecting helium gas into the ullage. The engine inlet valves were opened 17 seconds prior to engine start to allow liquid propellants to chill the propellant feed lines and the engine turbopumps. Tank pressurization, thermal conditioning of the engines, and control of the propellants throughout the coast phase, were all completely successful and supported a restart of the main engines.

Centaur Main Engine Second Burn

The Centaur main engines were successfully restarted on command at T + 1939.3 seconds. At engine restart, all hydrogen peroxide engines were commanded off. At 4 seconds after engine start, Centaur guidance steering was resumed to steer the vehicle toward the velocity vector required for injection of the spacecraft into a lunar intercept

trajectory. All systems performed properly. At T + 2054.9 seconds, the required injection velocity for the lunar intercept was attained, and the guidance system issued commands to shut down the engines.

The propellant utilization system controlled propellant mixture ratio to an average value of 5.03 to 1. Burnable residual propellants could have provided an additional 10.4 seconds of engine firing. This margin indicated an adequate propellant reserve and satisfactory vehicle performance.

SPACECRAFT SEPARATION

Coincident with the main engine second cutoff, the guidance steering commands were temporarily discontinued, and the coast-phase hydrogen peroxide engines system was again activated to maintain attitude control. Angular rates imparted to the vehicle by engine shutdown transients were small and were quickly reduced to rates below the design threshold of 0.2 degree per second. The residual vehicle motion below the rate threshold allowed only a negligible drift in vehicle attitude.

The Centaur with the Surveyor coasted in a near-zero-gravity field for about 61 seconds. This time period was allowed to damp out any residual vehicle rates and to prepare the spacecraft for separation. Commands were given by the Centaur timer to the spacecraft to turn on transmitter high power, arm the spacecraft separation pyrotechnics, and extend landing gear and omnidirectional antennas. All commands were properly received by the spacecraft.

At T + 2115.3 seconds, the command for spacecraft separation was given. The hydrogen peroxide attitude control system was commanded off, the pyrotechnically operated latches were fired, and the springs separated the Surveyor from the Centaur. Full extension of all three springs occurred within 1 millisecond of each other, and the separation velocity imparted to the spacecraft was about 0.213 meter (0.75 ft) per second. Angular rates of the spacecraft after separation did not exceed 0.50 degree per second. This rate was well below the allowable rate of 3.0 degrees per second.

CENTAUR RETROMANEUVER

Following spacecraft separation, the Centaur stage was commanded to perform a reorientation and retrothrust maneuver. This maneuver was necessary to increase the Centaur-Surveyor separation distance and thus eliminate the possibility of the Surveyor star sensor acquiring the reflected light of Centaur rather than the star Canopus. A second objective of the retromaneuver was to alter the Centaur orbit in order to prevent the Centaur from impacting on the Moon.

A guidance steering vector for the Centaur reorientation (turnaround) was selected that was the reciprocal of the velocity vector at main engine second cutoff. Execution of the turnaround was commanded 5 seconds after spacecraft separation at T + 2120.3 seconds. The guidance system accounted for any vehicle drift after main engine cutoff and issued steering commands which rotated the vehicle in the shortest arc from its actual position to the new vector. Angular rates during the turnaround were limited to a maximum of 1.6 degrees per second.

About halfway through the turnaround, two 222-newton- (50 lbf-) thrust hydrogen peroxide engines were fired for 20 seconds to provide additional longitudinal separation from the spacecraft. This increased separation distance was necessary to minimize the possible impingement of frozen particles on the spacecraft during the subsequent discharge of residual Centaur propellants through the main engines. While these 222-newton- (50-lbf-) thrust engines were firing, the exhaust plumes produced high impingement forces on the vehicle, causing a clockwise roll disturbing torque. To correct this torque, the 15.55- and 26.6-newton- (3.5- and 6.0-lbf-) thrust attitude control engines were required to operate 50 percent of the time.

The turnaround maneuver was completed at about T + 2220 seconds, after rotating the vehicle through 172^{o}. After the retrovector was acquired, the attitude control system maintained the vehicle on the vector within 1.5^{o}.

At T + 2355 seconds, the retrothrust portion of the retromaneuver was commanded by the Centaur timer. The main engines were gimbaled to aline the thrust vector with the newly acquired steering vector, the engine prestart valves were opened, the residual propellants were allowed to discharge through the engines. The propellant dischare provided sufficient thrust to increase the separation distance from the spacecraft and to alter the Centaur orbit in order to avoid impact on the Moon. The relative separation distance between the spacecraft and the Centaur at the end of 5 hours was 1423 kilometers. This distance was about 4.3 times the required minimum.

At completion of the retromaneuver at T + 2705 seconds, the hydrogen and oxygen tank vent valves were enabled to the relief or normal regulating mode. A postmission exercise was then conducted to determine the amount of residual hydrogen peroxide. This test was accomplished by firing the 222-newton- (50-lbf-) thrust engines until the hydrogen peroxide propellant was depleted. The engines fired for 50 seconds. For normal consumption, this firing time indicated a usable residual of about 16.4 kilograms (36.2 lbm) of hydrogen peroxide at the end of the basic mission. Following this test, all systems were deenergized, and the vehicle continued in orbit in a nonstabilized flight mode.

SURVEYOR LUNAR TRANSIT

The Surveyor VII was accurately injected into its lunar intercept trajectory. A lunar touchdown at the design target site would have required only a slight midcourse velocity correction of 0.33 meter per second (miss only) at 20 hours after injection. However, after the vehicle was launched, a different target site was selected. An actual correction of 11.05 meters per second (for miss only) was made about 17 hours after lift-off in order to impact the newly selected target. The Surveyor VII successfully touched down on the lunar surface at 2005 hours eastern standard time on January 9, 1968. Elapsed flight time for the mission was about 66 hours. The actual touchdown point on the Moon was at a position of 40.92° South latitude and 11.45° West longitude. This position was within 3 kilometers of the final targeted aiming point.

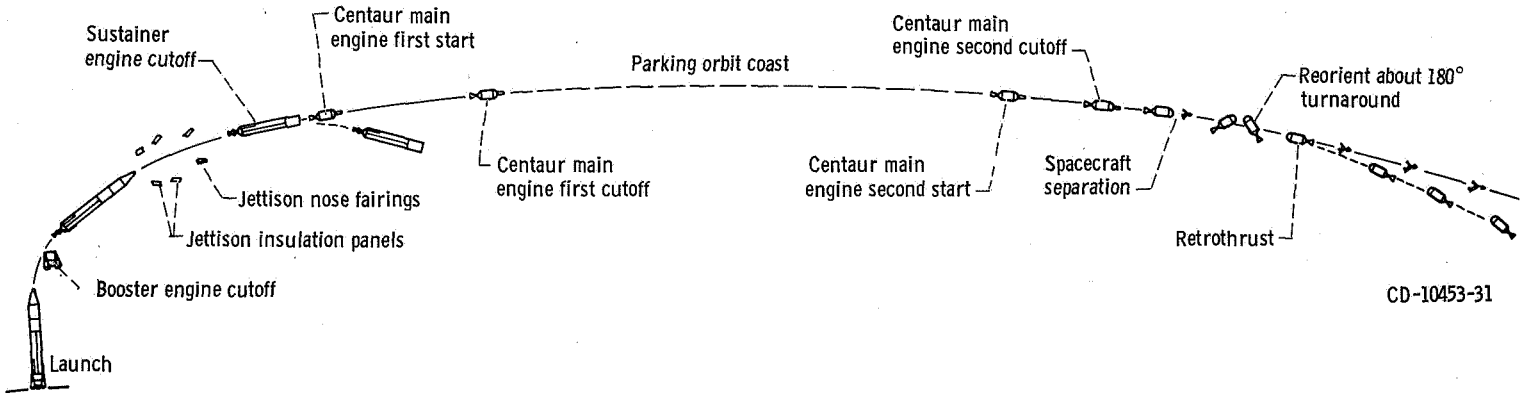

Figure IV-1. - Atlas-Centaur flight compendium for indirect-ascent mode; AC-13, AC-14, and AC-15.

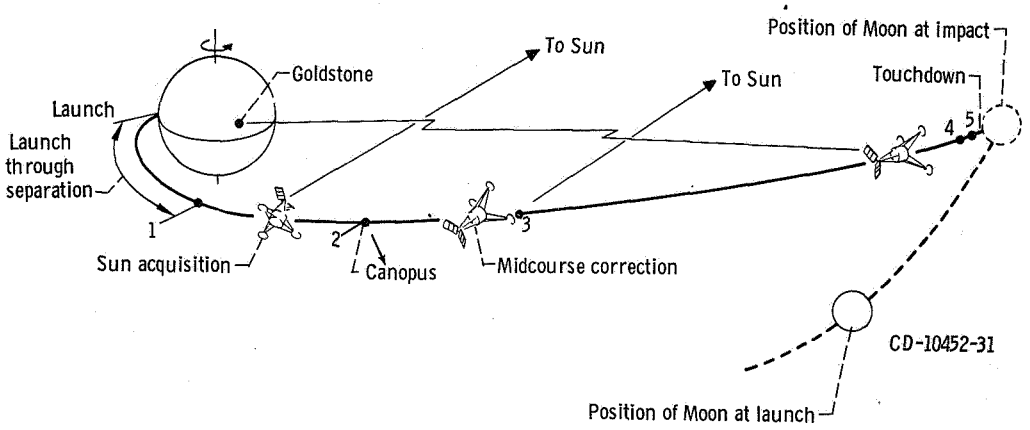

Figure IV-2. - Surveyor Earth-Moon trajectory. 1, injection and separation; 2, star acquisition and verification; 3, reacquisition of Sun and star after midcourse correction; 4, retrophase initiated about 60 miles (96 km) from Moon; 5, vernier descent initiated 35 000 feet (10 700 m) above surface of Moon; AC-13, AC-14, and AC-15.

V. TRAJECTORY AND PERFORMANCE

by John J. Nieberding

MISSION PLAN

The AC-13, AC-14, and AC-15 Atlas-Centaur flights were so similar that only a typical Surveyor mission plan (AC-15) is presented.

The mission plan was to launch the Centaur-Surveyor into a nearly circular parking orbit at an altitude of approximately 167 kilometers (90 n. mi.). The launch vehicle - spacecraft combination then coasts for a period in the parking orbit under very low thrust until restart of the Centaur main engines. A second main engine firing is necessary to transfer the Centaur-Surveyor from the nearly circular, near-Earth parking orbit to the highly elliptical lunar intercept trajectory. Following the Centaur second burn, the spacecraft is separated. The Centaur then performs a retromaneuver to prevent impact of the Centaur on the Moon and to minimize the possibility of the star sensor on the Surveyor mistaking the light reflected from Centaur for the star Canopus.

The spacecraft flight sequence after separation consists of first executing an antenna - solar panel positioning and Sun acquisition maneuver to establish the desired attitude of the spacecraft roll axis and ensure an adequate supply of solar energy during the translunar coast period. After this attitude-stabilized coast phase, a midcourse trajectory correction is performed at about 15 to 20 hours after launch. This midcourse correction is followed by a second attitude-stabilized coast phase, and finally a terminal descent phase for a controlled, soft landing on the Moon. Touchdown on the Moon occurs after approximately 66 hours of flight.

TRAJECTORY RESULTS

The discussion in this section is generally centered around the trajectory and performance data of AC-15 because this flight is typical of the AC-13, AC-14, and AC-15 flights. Trajectory data (figs. V-1 to V-10 and data tables V-1 to V-6) are presented in this section. Corresponding data for AC-13 and AC-14 are included in appendix A. The data for AC-13 and AC-14 are not discussed except in cases when the AC-15 trajectory and performance data are not typical for these flights. Also included in appendix A

are AC-13 and AC-14 flight events records, postflight vehicle weight summaries, and a brief countdown history for AC-13, AC-14, and AC-15.

Lift-Off Through Atlas Booster Phase

Launch related data are summarized in the following table:

	Units	AC-13 Surveyor V	AC-14 Surveyor VI	AC-15 Surveyor VII
Launch day	---	9/8/67	11/7/67	1/7/68
Launch time (EST)	---	0257:01.257	0239:01.1	0130:00.545
Launch complex	---	36B	36B	36A
Flight azimuth	deg	79.517	82.995	102.914
Separated space-craft weight	kg	1006	1007	1039
	lbm	2217	2219	2291

Atmospheric conditions at the launch site were determined by a series of weather balloons sent aloft beginning about 18 hours prior to launch. Measured temperatures and pressures are compared with values predicted on the basis of characteristic weather for the Cape Kennedy area in figures V-1 and V-2. Wind speed and wind azimuth data as a function of altitude are compared with expected data for the Cape Kennedy area in figures V-3 and V-4. The wind data plotted are actual data and should not be smoothed. Note that, for the purpose of this report, wind azimuth is defined as the direction towards which the wind is blowing. A wind azimuth of 90^{o}, for example, is a wind blowing out of the west, towards the east. Wind azimuth differs from wind direction by 180^{o}.

Radar tracking data indicated that the AC-15 flight path during the Atlas booster phase was very close to the predicted path. Maximum dynamic pressure occurred at about T + 78 seconds; Mach 1 occurred at about T + 64 seconds. Time histories of dynamic pressure and Mach number are shown in figures V-5 and V-6. Atlas booster engine cutoff occurred at T + 152.4 seconds, when the vehicle axial acceleration reached 5.78 g's (fig. V-7). This cutoff was 1 second earlier than predicted. The deviation of actual trajectory parameters from predicted parameters at booster engine cutoff was as follows:

	Units	Predicted	Actual
Altitude	km	59.0	60.5
	n. mi.	31.9	32.7
Surface range	km	90.3	90.1
	n. mi.	48.8	48.7
Earth relative velocity	m/sec	2595	2588
	ft/sec	8515	8490

These data show that there were no significant deviations from predictions. The slight "lofting" of the trajectory at booster engine cutoff resulted from the vehicle pitching over 0.9° less than predicted. Consequently, the surface range was lower than expected. Plots of altitude against time and altitude against surface range are presented in figures V-8 and V-9.

Atlas Sustainer Phase

An abrupt decrease in acceleration occurred at T + 152.4 seconds because the booster engine cut off (fig. V-7). A small but sudden increase in acceleration occurred 3.1 seconds after booster engine cutoff when the booster engine section, weighing 3341 kilograms (7366 lbm), was jettisoned. Following booster jettison, the constantly decreasing vehicle propellant weight caused the thrust acceleration (axial load factor) to increase smoothly, except for small perturbations caused by sudden weight losses when the insulation panels (555 kg, 1224 lbm) and nose fairing (922 kg, 2032 lbm) were jettisoned at T + 197.1 and 226.9 seconds, respectively. Sustainer and vernier engine cutoff occurred at T + 248.7 seconds, 0.7 second earlier than expected. At this time, the deviation of actual from predicted trajectory parameters was as follows:

	Units	Predicted	Actual
Altitude	km	134.4	138.8
	n. mi.	72.6	75.0
Surface range	km	371.1	368.2
	n. mi.	200.5	198.9
Earth relative velocity	m/sec	3669	3644
	ft/sec	12 038	11 957

These data show that at sustainer engine cutoff the trajectory remained (as at booster engine cutoff) slightly more "lofted" than predicted. Consequently, the surface range was less than expected. This "lofting" also increased the velocity losses caused by gravity and, thus, resulted in an actual velocity lower than predicted. The axial acceleration at sustainer engine cutoff abruptly dropped to zero, thereby reflecting the end of thrust from the sustainer and vernier engines.

Centaur First Firing Phase

Atlas-Centaur separation is timed to occur 1.9 seconds after sustainer engine cutoff. Consequently, because the cutoff was 0.7 second early, separation at T + 250.6 seconds and Centaur main engine start at T + 260.2 seconds were also 0.7 second early. Figure V-7 verifies the early initiation of Centaur thrust. Subsequently, the uniformly decreasing Centaur propellant weight caused the axial acceleration to increase smoothly (no sudden weight losses occur in this phase) until termination of the Centaur main engine first firing at T + 593.2 seconds, 12.7 seconds later than expected. This firing was 13.4 seconds longer than predicted. A major contributing factor to the longer firing period was lower than nominal Centaur thrust (PROPULSION SYSTEMS). This low-thrust effect can be seen in figure V-10, where the actual inertial velocities are lower than predicted. However, the longer Centaur firing increased the velocity to the required value at cutoff. After main engine shutdown, two 222-newton- (50-lbf-) thrust hydrogen peroxide engines were fired for a period of 75.8 seconds to settle the propellants remaining aboard the Centaur. The energy at which the Centaur main engines cut off was biased so that with the additional energy from the propellant settling engines, the proper total energy for an approximately 167-kilometer (90-n. mi.) circular parking orbit was achieved. The orbit actually achieved, referenced to a time 6.9 seconds after the settling engines were shut down, is shown in table V-1.

Centaur Coast Phase

The duration of the coast phase between Centaur main engine first cutoff and Centaur main engine second start varies as a function of the time of launch to account for the Earth's rotation. The actual AC-15 coast time was 1346.1 seconds, compared to the planned coast period of 1354.2 seconds. (Coast periods for AC-13 and AC-14 can be obtained from tables A-4, A-5, and A-6.) After the coast phase, the Centaur main engines fired for the second time at T + 1939.3 seconds.

Centaur Second Firing Phase and Spacecraft Separation

The second firing of the Centaur engines accelerated the Centaur-Surveyor combination from the nearly circular parking orbit into the highly elliptical lunar transfer ellipse. Centaur main engine second cutoff occurred at T + 2054.9 seconds and was 2.2 seconds longer than expected. Following second cutoff the Centaur-spacecraft coasted for approximately 1 minute, and at T + 2115.3 seconds the spacecraft was separated from the Centaur. The Surveyor VII orbital parameters are presented in table V-2.

For an evaluation of launch vehicle injection accuracy refer to the section GUIDANCE AND FLIGHT CONTROL SYSTEMS. A dicsussion of the spacecraft midcourse velocity correction is presented in appendix A. The midcourse summary correction in appendix A (provided for general interest only) summarizes the flight times, midcourse maneuvers, and landing conditions for Surveyors V, VI, and VII. The data presented in this summary reflect the re-aiming of the Surveyor after launch and, consequently, differ from the values shown in the GUIDANCE AND FLIGHT CONTROL SYSTEMS section.

Centaur Retromaneuver

At T + 2120.3 seconds, the Centaur fired its hydrogen peroxide attitude control engines to begin the retromaneuver. This retromaneuver was required to prevent impact of the Centaur on the Moon and also to minimize the possibility of the Surveyor star sensor mistaking the light reflected from Centaur for the star Canopus. After the retromaneuver, the Centaur orbit was an ellipse of lower energy than that of the spacecraft. The Centaur orbit is described in table V-3.

TABLE V-1. - CENTAUR PARKING ORBIT PARAMETERS, AC-15

Parameter[a]	Units	Value
Time from 2-inch motion	sec	675.9
Epoch (Greenwich mean time)	hr	0.641:16.9 (Jan. 7)
Apogee altitude	km	172.2
	n. mi.	93.0
Perigee altitude	km	164.8
	n. mi.	89.0
Injection energy, C_3	km^2/sec^2	-60.92
	ft^2/sec^2	-65.57×10^7
Semimajor axis	km	6541
	n. mi.	3532
Eccentricity		0.00061
Orbital inclination	deg	30.692
Period	min	87.74
Inertial velocity at Centaur main engine first cutoff	m/sec	7881.04
	ft/sec	25 856.43
Earth relative velocity at Centaur main engine first cutoff	m/sec	7478.37
	ft/sec	24 535.34
Geocentric latitude at Centaur main engine first cutoff	deg, North	22.362
Longitude at Centaur main engine first cutoff	deg, West	60.825

[a]These parameters are based on tracking data.

TABLE V-2. - SURVEYOR ORBIT PARAMETERS, AC-15

Parameter	Units	Value
Time from 2-inch motion	sec	3419.0
Epoch (Greenwich mean time)	hr	0727:00.0 (Jan. 7)
Apogee Altitude	km	710 184
	n. mi.	383 469
Perigee altitude	km	170.4
	n. mi.	92
Injection energy, C_3	km^2/sec^2	-1.102
	ft^2/sec^2	-1.186×10^7
Semimajor axis	km	361 555
	n. mi.	195 224
Eccentricity		0.98189
Orbital inclination	deg	30.699
Period	days	25.04
Longitude of ascending node	deg	8.858
Argument of perigee	deg	228.02

TABLE V-3. - CENTAUR POSTRETROMANEUVER

ORBITAL PARAMETERS, AC-15

Parameter	Units	Value
Time from 2-inch motion	sec	(2819.0
Epoch (Greenwich mean time)	hr	0717:00.0 (Jan. 7)
Apogee altitude	km	447 575
	n. mi.	241 671
Perigee altitude	km	168.5
	n. mi.	91.0
Injection energy, C_3	km^2/sec^2	-1.73
	ft^2/sec^2	-1.86215×10^7
Semimajor axis	km	230 246
	n. mi.	124 323
Eccentricity		0.97157
Orbital inclination	deg	30.685
Period	days	12.73

TABLE V-4. - CENTAUR VEHICLE POSTFLIGHT WEIGHT SUMMARY, AC-15

Item	Weight	
	kg	lbm
Basic hardware:		
Body	420	927
Propulsion group	556	1 226
Guidance group	151	333
Control group	69	152
Pressurization group	84	185
Electrical group	130	286
Separation group	37	81
Flight instrumentation	114	252
Miscellaneous equipment	65	143
Total	1 626	3 585
Jettisonable hardware:		
Nose fairing	922	2 032
Insulation panels	555	1 224
Ablated ice	23	50
Total	1 500	3 306
Centaur residuals:		
Liquid hydrogen	94	207
Liquid oxygen	300	662
Gaseous hydrogen	31	68
Gaseous oxygen	78	171
Hydrogen peroxide	19	41
Helium	2	4
Ice	5	12
Total	529	1 165

Item	Weight	
	kg	lbm
Centaur expendables:		
Main impulse hydrogen	2 182	4 811
Main impulse oxygen	11 076	24 419
Gas boiloff on ground, hydrogen	4	8
Gas boiloff on ground, oxygen	0	0
Inflight chill hydrogen	32	71
Inflight chill oxygen	46	102
Booster phase vent, hydrogen	24	53
Booster phase vent, oxygen	30	66
Sustainer phase vent, hydrogen	14	30
Sustainer phase vent, oxygen	27	60
Engine shutdown loss, hydrogen:		
First	3	6
Second	3	6
Engine shutdown loss, oxygen:		
First	8	18
Second	8	18
Parking orbit vent, hydrogen	8	17
Parking orbit vent, oxygen	0	0
Parking orbit leakage, hydrogen	1	1
Parking orbit leakage, oxygen	1	2
Hydrogen peroxide	89	196
Helium	2	5
Total	13 558	29 889
Total tanked weight	17 213	37 945
Ground vent	4	8
Total Centaur weight at lift-off	17 209	37 937

TABLE V-5. - ATLAS VEHICLE POSTFLIGHT

WEIGHT SUMMARY, AC-15

Item	Weight	
	kg	lbm
Booster jettison weight:	2 852	6 287
Booster dry weight	251	554
Oxygen residual	221	487
Fuel (RP-1) residual	17	38
Unburned lubrication oil		
Total		
Sustainer jettison weight:		
Sustainer dry weight	2 718	5 993
Oxygen residual	271	598
Fuel (RP-1) residual	93	206
Interstage adapter	459	1 012
Unburned lubrication oil	7	15
Total	3 548	7 824
Flight expendables:		
Main impulse fuel (RP-1)	37 849	83 443
Main impulse oxygen	83 798	184 743
Helium-panel purge	2	5
Oxygen vent loss	7	15
Lubrication oil	84	185
Total	121 740	268 391
Ground expendables:		
Fuel (RP-1)	256	564
Oxygen	789	1 740
Lubrication oil	1	3
Exterior ice	24	54
Liquid nitrogen in helium shrouds	113	250
Pre-ignition gaseous oxygen loss	204	450
Total	1 387	3 061
Total Atlas tanked weight	130 019	286 642
Ground run	1 387	3 061
Total Atlas weight at lift-off	128 632	283 581
Spacecraft weight	1 039	2 291
Total Atlas-Centaur-Spacecraft lift-off weight	146 880	323 809

TABLE V-6. - FLIGHT EVENTS RECORD, AC-15

Event	Programmer time, sec	Preflight time, sec	Actual time, sec
Lift-off (2-in. motion)	T + 0.0	T + 0.0	T + 0.0
Start roll	T + 2.0	T + 2.0	T + 2.0
End roll	T + 15.0	T + 15.0	T + 15.0
Start pitchover	T + 15.0	T + 15.0	T + 15.0
Booster engine cutoff (BECO)	BECO	T + 153.4	T + 152.4
Jettison booster engines	BECO + 3.1	T + 156.5	T + 155.5
Jettison insulation panels	BECO + 45	T + 198.4	T + 197.1
Start Centaur boost pumps	BECO + 62	T + 215.4	T + 214.5
Jettison nose fairing	BECO + 75	T + 228.4	T + 226.9
Sustainer engine cutoff (SECO); vernier engine cutoff (VECO); start Centaur programmer	SECO	T + 249.4	T + 248.7
Atlas-Centaur separation	SECO + 1.9	T + 251.3	T + 250.6
Centaur main engine first start (MES-1)	SECO + 11.5	T + 260.9	T + 260.2
Centaur main engine first cutoff (MECO-1)	MECO-1	T + 580.5	T + 593.2
Start propellant settling engines	MECO-1	T + 580.5	T + 593.2
Stop propellant settling engines; start propellant retention engines	MECO-1 + 76	T + 656.5	T + 669.0
Stop propellant retention engines; start propellant settling engines	MES-2 - 40	T + 1894.7	T + 1899.3
Start Centaur boost pumps	MES-2 - 28	T + 1906.7	T + 1191.3
Centaur main engine second start (MES-2)	MES-2	T + 1934.7	T + 1939.3
Stop propellant settling engine	MES-2	T + 1934.7	T + 1939.3
Centaur main engine second cutoff (MECO-2)	MECO-2	T + 2048.1	T + 2054.9
Preseparation arming signal; extend landing gear signal	MES-2 + 134	T + 2068.7	T + 2073.3
Unlock omnidirectional antennas on signal	MES-2 + 144.5	T + 2079.2	T + 2083.8
High power transmitter on signal	MES-2 + 165	T + 2099.7	(a)
Spacecraft separate	MES-2 + 176.0	T + 2110.7	T + 2115.3
Start turnaround	MES-2 + 181.0	T + 2115.7	T + 2120.3
Start propellant settling engines	MES-2 + 221.0	T + 2155.7	T + 2160.3
Stop propellant settling engines	MES-2 + 241.0	T + 2175.7	T + 2180.3
Start discharge of Centaur residual propellants	MES-2 + 416	T + 2350.7	T + 2355.3
End discharge of Centaur residual propellants; start propellant settling engines[b]	MES-2 + 666	T + 2600.7	T + 2605.3
Energize power changeover	MES-2 + 766	T + 2700.7	T + 2705.3

[a]Undetermined because of noisy data.

[b]Postmission hydrogen peroxide depletion experiment.

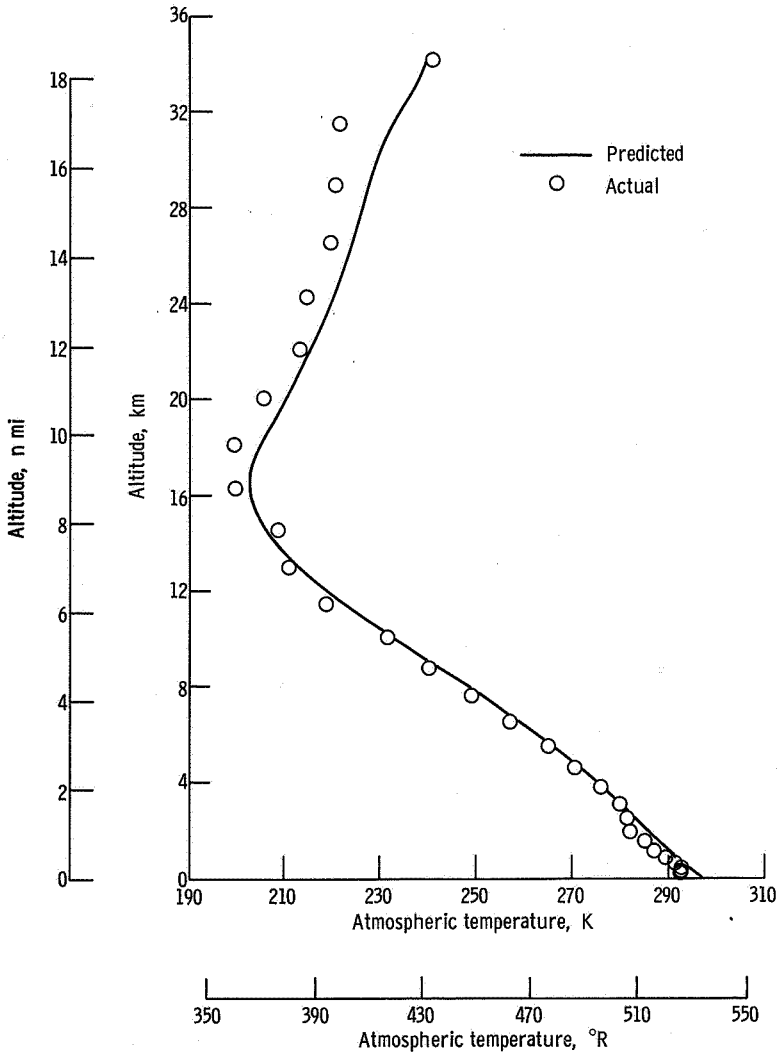

Figure V-1. - Altitude as function of temperature, AC-15.

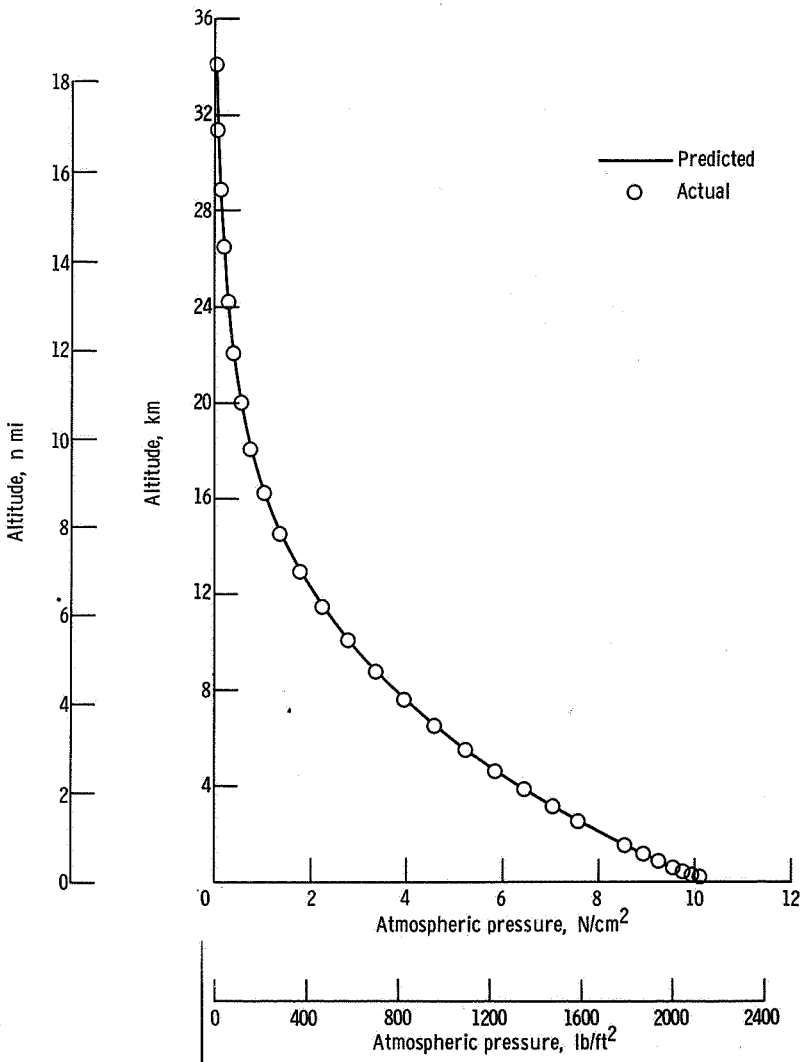

Figure V-2. - Altitude as function of pressure, AC-15.

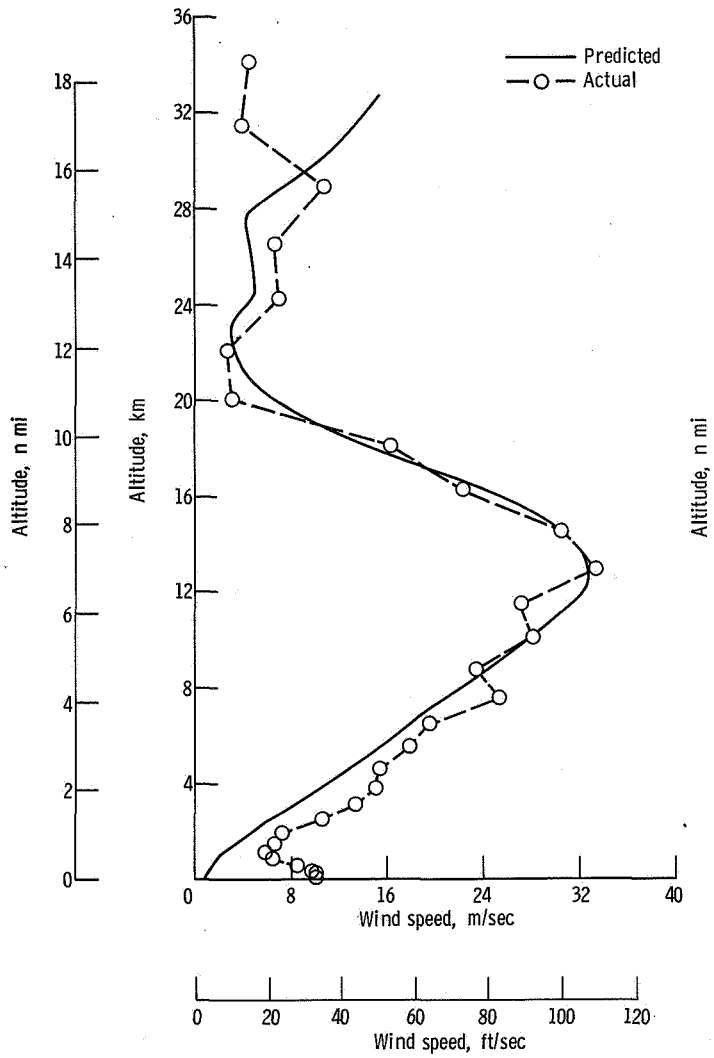

Figure V-3. - Altitude as function of wind speed, AC-15.

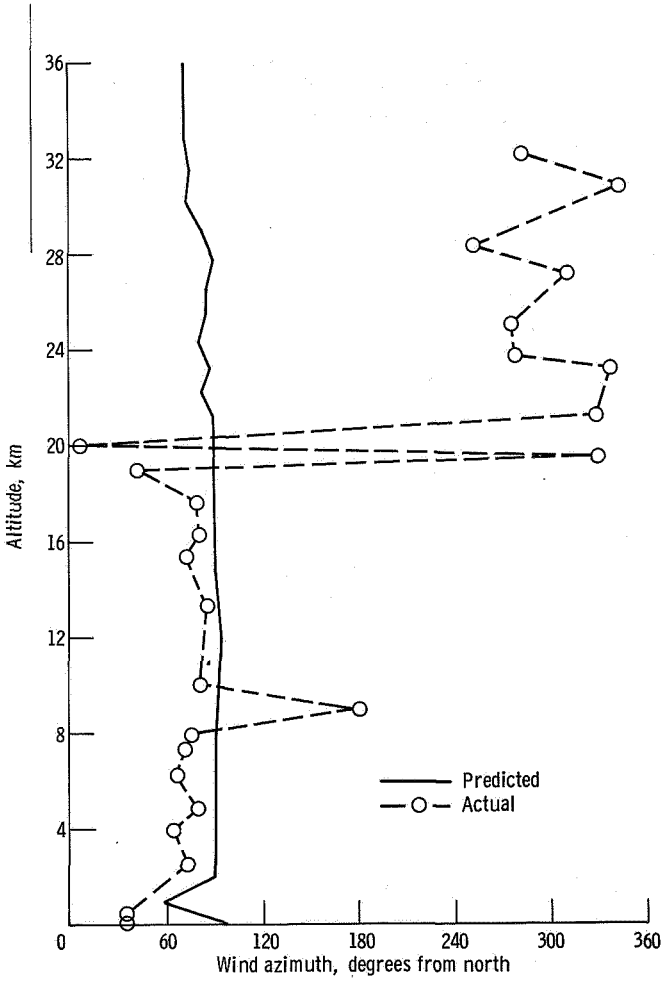

Figure V-4. - Altitude as function of wind azimuth, AC-15.

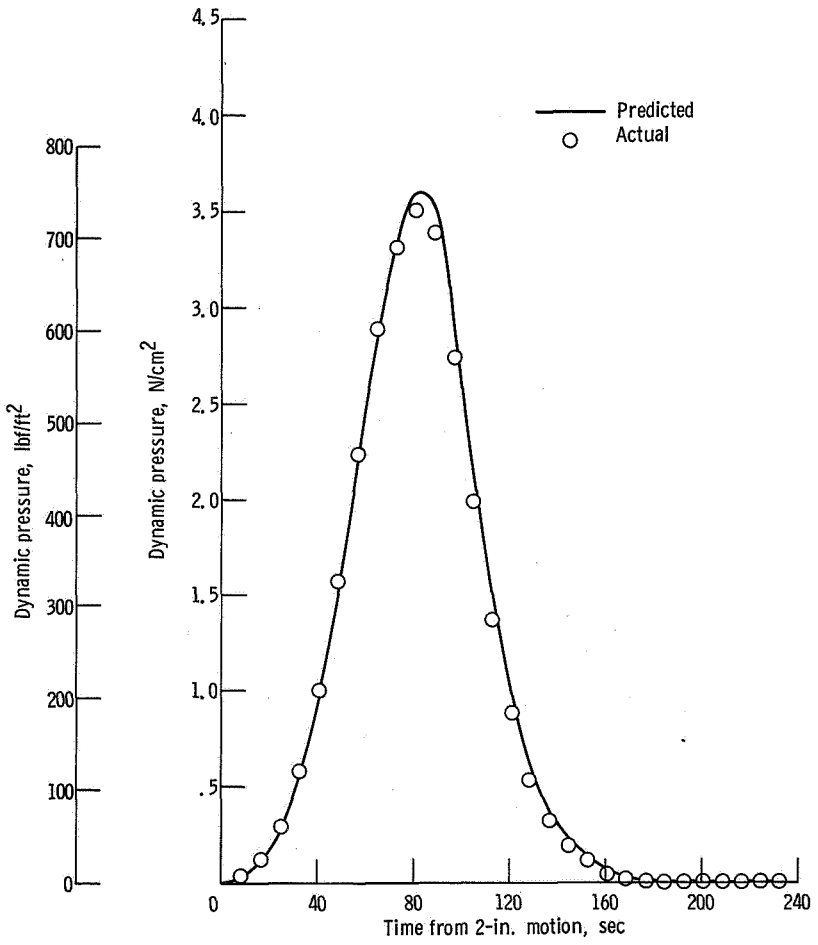

Figure V-5. - Dynamic pressure as function of time, AC-15.

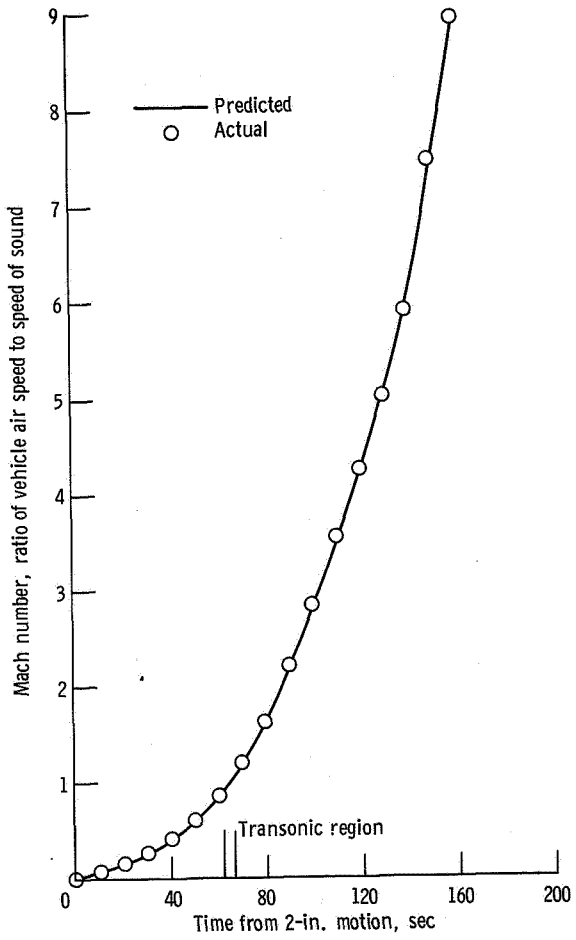

Figure V-6. - Mach number as function of time, AC-15.

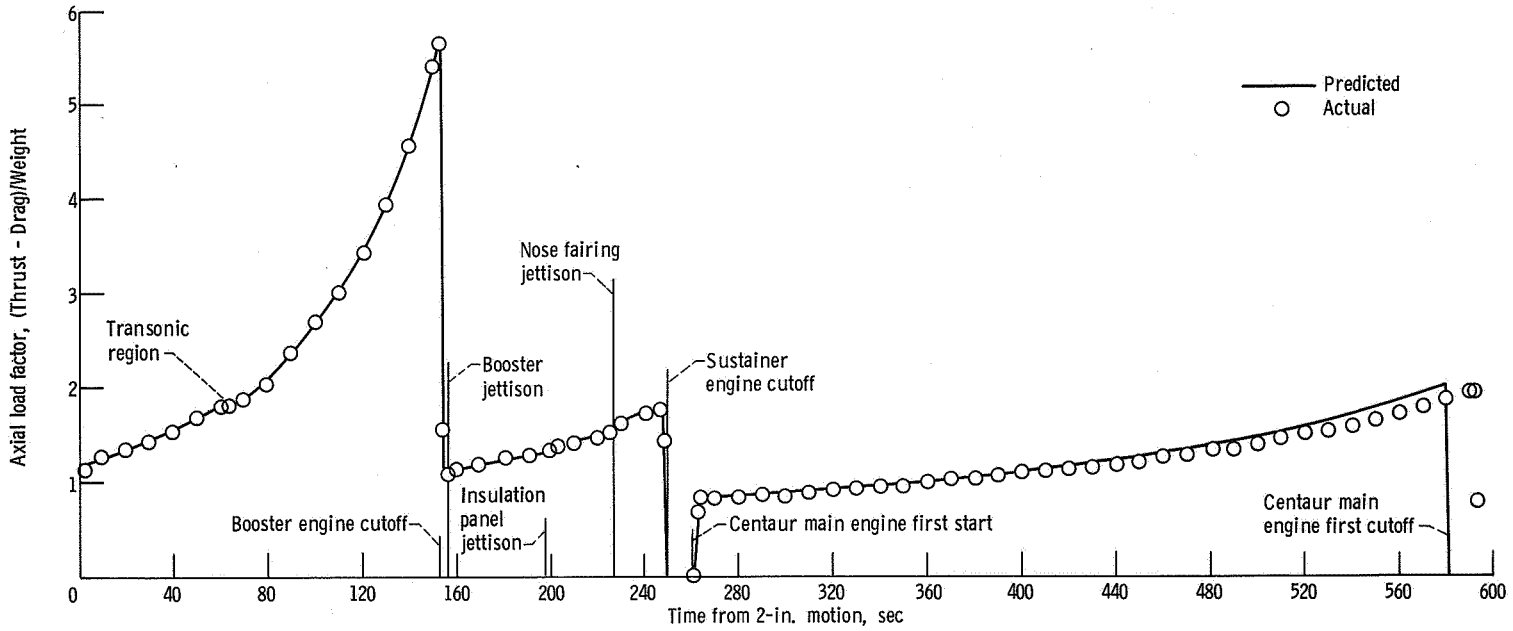

Figure V-7. - Axial load factor as function of time, AC-15.

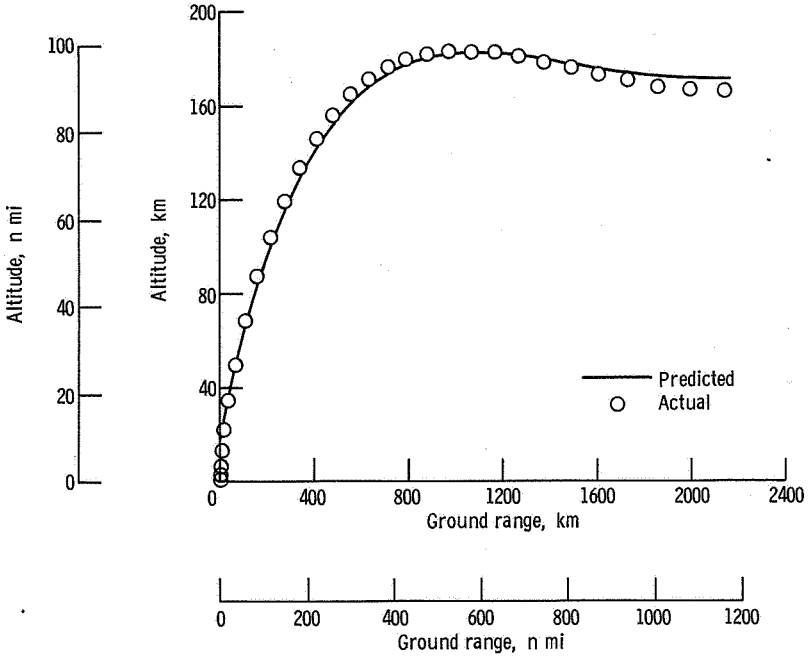

Figure V-8. - Altitude as function of surface range, AC-15.

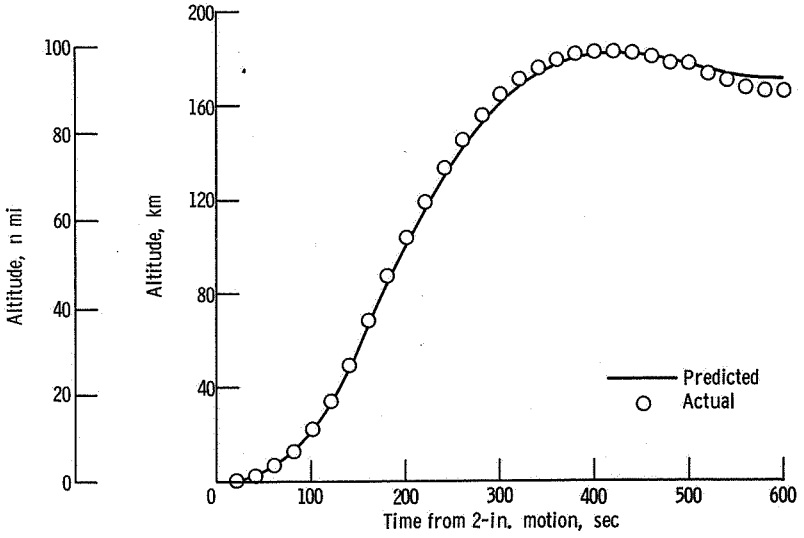

Figure V-9. - Altitude as function of time, AC-15.

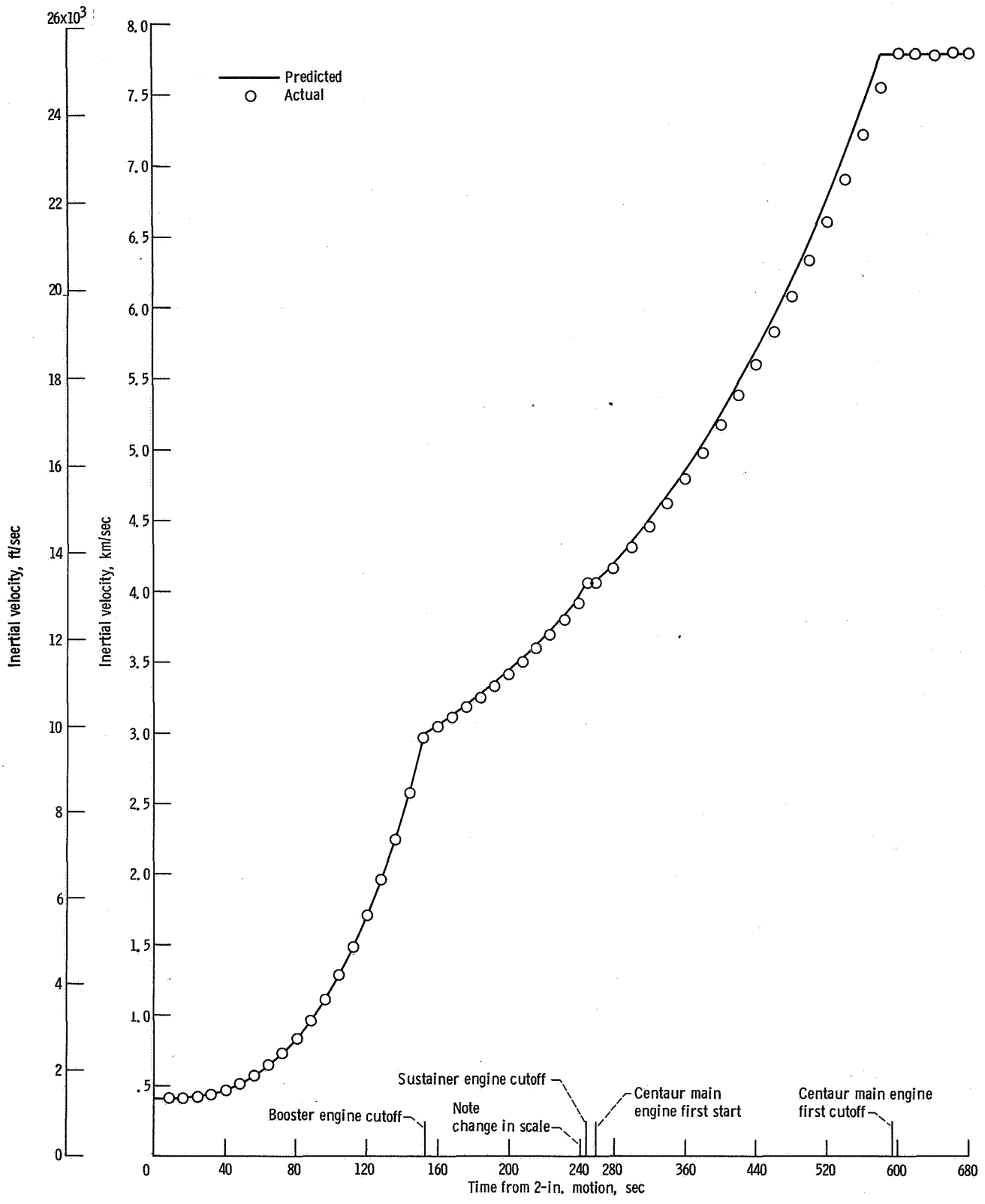

Figure V-10. - Inertia velocity as function of time, AC-15. Note change in scale at 240 seconds.

VI. LAUNCH VEHICLE SYSTEM ANALYSIS

PROPULSION SYSTEMS

by James A. Berns, Ronald W. Ruedele, Kenneth W. Baud, and Donald B. Zelten

Atlas Engines

System description. - The Rocketdyne MA-5 engine system used by the Atlas consisted of a booster engine system, a sustainer engine system, a vernier engine system, an engine start system, a logic control subsystem, and an electric subsystem. The systems are shown schematically in figure VI-1.

All engines were single-start, fixed-thrust rocket engines using liquid oxygen (oxidizer) and RP-1 (fuel) as propellants. The engines were hypergolically ignited using pyrophoric fuel cartridges. The pyrophoric fuel preceded the RP-1 into the combustion chambers and initiated ignition with the liquid oxygen. Combustion was then sustained by RP-1 and liquid oxygen. All thrust chambers were regeneratively cooled with RP-1.

The rated thrust values in newtons (lbf) for these type engines approximate

Booster engine (two thrust chambers total) . . . . . 1494×10^3 (336×10^3)
Sustainer engine (one thrust chamber) . . . . . 258×10^3 (58×10^3)
Vernier engines (two thrust chambers total) . . . . . 5.96×10^3 (1.34×10^3)

The booster engine system consisted of two gimbaled thrust chambers, one gas generator and two turbopumps, and a supporting control system. The sustainer engine was a gimbaled engine assembly consisting of a thrust chamber, a gas generator, a turbopump, and a supporting control system. The two vernier engines consisted of thrust chambers, propellant valves, and gimbal assemblies. The engine start system consisted of an oxidizer start tank, a fuel start tank, and the associated controls. In general, during the ignition stage, the propellant tanks are pressurized; the gas generator igniters are fired; propellants and the hypergolic fluids are introduced into the vernier, booster, and sustainer thrust chambers; and combustion starts.

System performance. - Engine start and thrust buildup appeared normal, and engine system requirements for start were adequately met, as given in table VI-1.

Booster engine system operation during these flights was satisfactory. Booster engine thrust calculated from chamber pressure data is compared with predicted thrust

levels in the following table. Booster engine cutoff times and axial acceleration are also shown.

	Units	T + 10 sec			Booster engine cutoff		
					T +153.2 sec	T +153.2 sec	T +152.4 sec
		AC-13	AC-14	AC-15	AC-13	AC-14	AC-15
Predicted thrust	N	1 480 000	1 470 000	1 330 000	1 690 000	1 690 000	1 690 000
	lbf	334 000	331 000	330 000	381 000	382 000	381 000
Actual thrust	N	1 460 000	1 480 000	1 490 000	1 670 000	1 710 000	1 700 000
	lbf	329 000	334 000	335 000	377 000	386 000	383 000
Acceleration	g's	--------	--------	--------	5.73	5.76	5.78

Telemetered booster engine data are summarized in table VI-2.

The in-flight operation of the sustainer and vernier engines was also satisfactory. Sustainer and vernier engine cutoff occurred due to liquid oxygen depletion as planned, by activation of the pressure switches in the sustainer fuel injection manifold. Predicted and actual combined sustainer and vernier engine axial thrust data are presented in the following table. Actual thrust was calculated from flight chamber pressure data.

Thrust	Units	T + 10 sec			Booster engine cutoff			Sustainer engine cutoff		
					T+153.2 sec	T+153.2 sec	T+152.4 sec	T+246.3 sec	T+245.8 sec	T+248.7 sec
		AC-13	AC-14	AC-15	AC-13	AC-14	AC-15	AC-13	AC-14	AC-15
Predicted	N	266 000	260 000	259 000	363 000	365 000	366 000	364 000	375 000	360 000
	lbf	59 100	59 000	58 900	82 600	82 200	82 400	82 000	82 100	81 000
Actual	N	254 000	266 000	261 000	365 000	374 000	362 000	361 000	368 000	356 000
	lbf	57 300	59 100	58 600	83 100	84 100	81 500	81 200	82 700	80 100

Telemetered sustainer and vernier engine flight data are also summarized in table VI-2.

TABLE VI-1. - ATLAS ENGINE SYSTEM REQUIREMENTS AT ENGINE START, AC-13, AC-14, AND AC-15

Parameter	Units[a]	Value at engine start		
		AC-13	AC-14	AC-15
Booster gas generator liquid-oxygen regulator reference pressure	N/cm^2	459	451	446
	psi	668	656	665
Sustainer gas generator liquid-oxygen regulator reference pressure	N/cm^2	584	583	596
	psi	850	849	867
Booster engine turbine inlet temperature, number 2 turbopump	K	293	292	(b)
	^oF	69	72	---
Sustainer engine turbine inlet temperature	K	292	287	(b)
	^oF	73	57	---
Liquid-oxygen temperature at fill and drain valve	K	(c)	30	29
	^oF	---	-306	-304

[a]All pressures are gage.

[b]Data not taken.

[c]Malfunction in telemetry.

TABLE VI-2. - ATLAS ENGINE SYSTEM PERFORMANCE, AC-13, AC-14, AND AC-15

Parameter	Units[a]	T + 10 sec			Booster engine cutoff[b]			Sustainer engine[b] cutoff		
		AC-13	AC-14	AC-15	AC-13	AC-14	AC-15	AC-13	AC-14	AC-15
Booster engine:										
Number 1 thrust chamber:										
Pressure	N/cm^2	384	404	405	384	404	408	----	------	------
	psi	559	586	588	559	586	592	----	------	------
Pump speed	rpm	6490	6384	6421	6510	6364	6412	----	------	------
Oxidizer pump inlet pressure	N/cm^2	43.4	43.4	45.5	60	60	59.3	----	------	------
	psi	63	63	66	87	87	86	----	------	------
Fuel pump inlet pressure	N/cm^2	51.6	51.6	51.6	41.3	41.3	41.3	----	------	------
	psi	75	75	75	60	60	60	----	------	------
Number 2 thrust chamber:										
Pressure	N/cm^2	396	400	408	396	400	408	----	------	------
	psi	560	581	592	560	581	592	----	------	------
Pump speed	rpm	6443	6191	6399	6413	6191	6399	----	------	------
Oxidizer pump inlet pressure	N/cm^2	44.7	48.3	(c)	64	64.8	(c)	----	------	------
	psi	64	70	------	93	94	(c)	----	------	------
Gas generator combustion chamber pressure	N/cm^2	371	372	376	381	372	376	----	------	------
	psi	539	540	545	554	540	545	----	------	------
Liquid-oxygen-regulator reference pressure	N/cm^2	473	464	465	465	458	455	----	------	------
	psi	686	672	675	676	665	665	----	------	------
Sustainer engine:										
Chamber pressure	N/cm^2	483	483	482	477	479	488	463	479	475
	psi	702	715	699	692	695	709	672	695	688
Pump speed	rpm	9975	10 414	10 228	10 034	10 384	10 258	9958	10 429	10 243
Fuel pump discharge pressure	N/cm^2	618	651	621	618	651	614	618	646	614
	psi	898	945	900	898	945	890	898	937	890
Oxidizer regulator reference pressure	N/cm^2	590	589	593	579	582	593	579	582	593
	psi	856	855	860	841	845	860	841	845	860
Gas generator discharge pressure	N/cm^2	460	441	441	460	441	441	460	441	441
	psi	669	640	640	669	640	640	660	640	640
Fuel pump inlet pressure	N/cm^2	55	52.4	54.5	48.3	46.9	48.3	33	34.5	33
	psi	80	76	79	70	68	70	48	50	48
Oxidizer pump inlet pressure	N/cm^2	46.1	46.1	46.1	84.6	66.8	66.8	26.8	22.8	22.8
	psi	67	67	67	94	97	97	39	33	33
Vernier engine:										
Engine 1 chamber pressure	N/cm^2	165	176	181	165	176	181	165	126	181
	psi	240	256	262	240	256	262	240	256	262
Engine 2 chamber pressure	N/cm^2	186	172	178	186	174	178	186	172	178
	psi	260	250	258	260	252	258	260	250	258

[a]All pressures are absolute.

[b]Data points actually taken 2 sec prior to booster and sustainer engine cutoff.

[c]Data not taken.

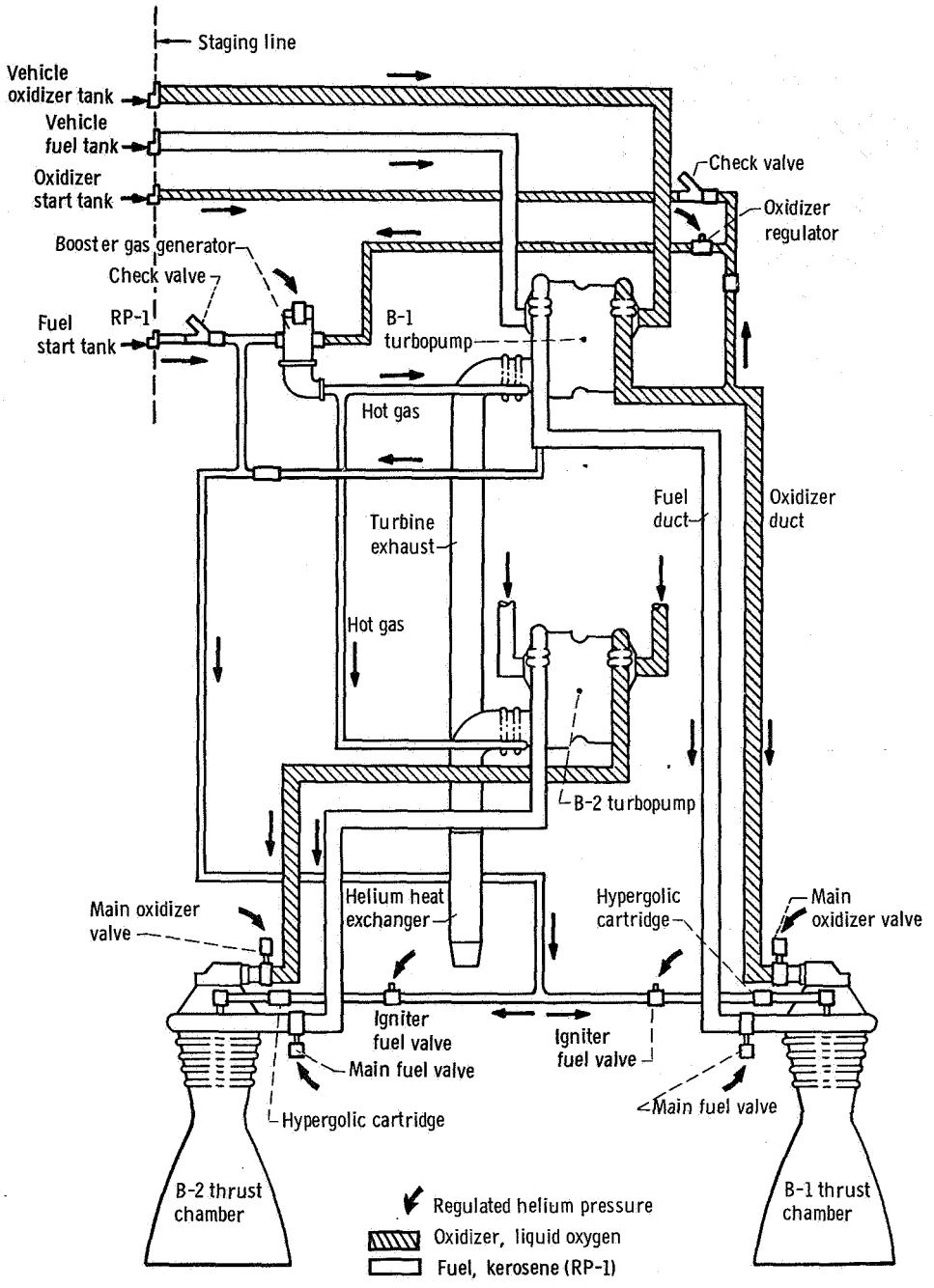

(a) Atlas vehicle booster engine.

Figure VI-1. - Atlas propulsion system; AC-13, AC-14, and AC-15.

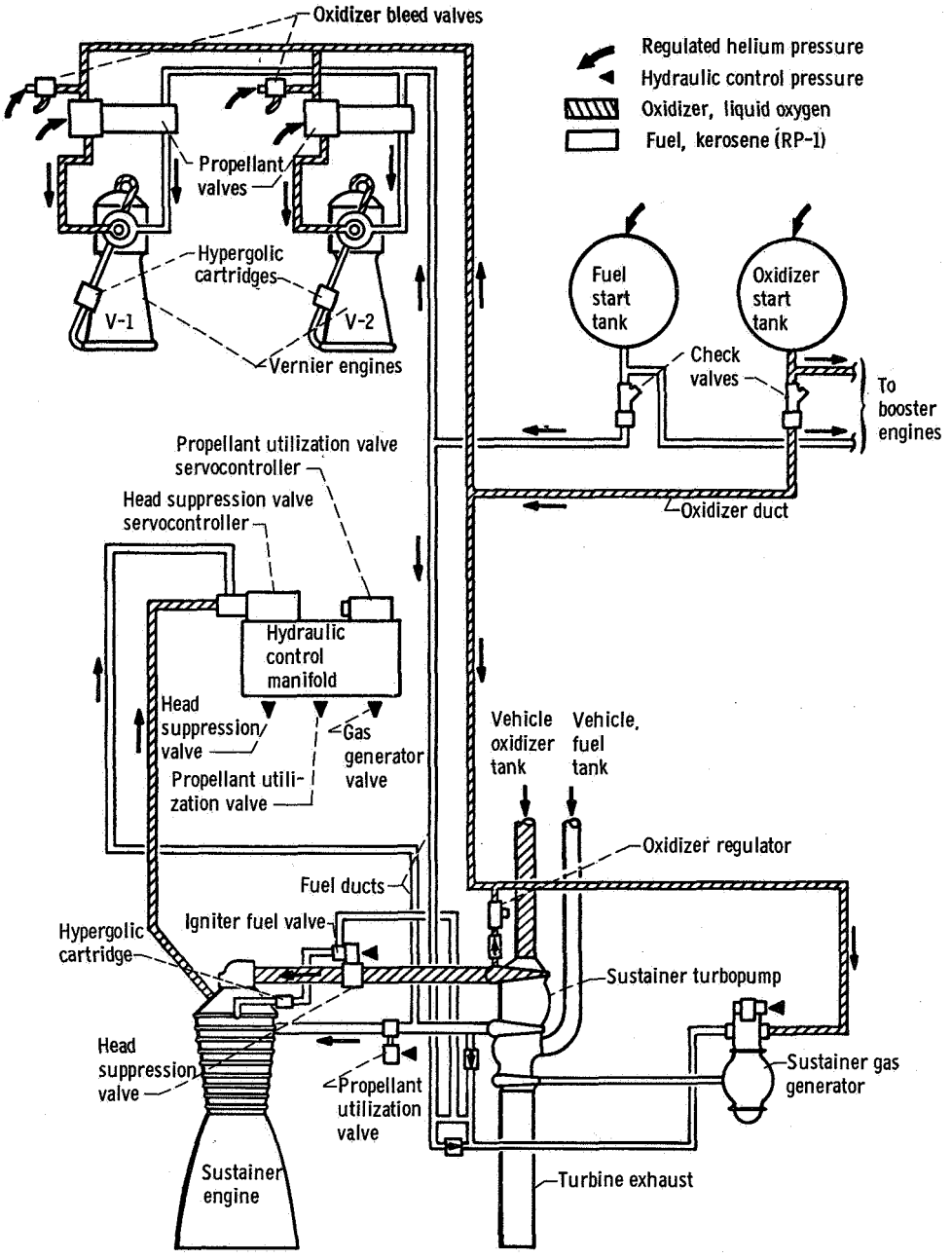

(b) Atlas vehicle sustainer and vernier engines.

Figure VI-1. - Concluded.

Centaur Main Engines

System description. - Two Pratt & Whitney RL10A-3-3 engines (identified as C-1 and C-2) are used to provide thrust for the Centaur stage. Each engine has a single thrust chamber and is regeneratively cooled and turbopump fed. Propellants are liquid oxygen and liquid hydrogen injected at an oxidizer-to-fuel mixture ratio of approximately 5 to 1. Engine rated thrust is 66 700 newtons (15 000 lbf) at an altitude of 61 000 meters (200 000 ft) and a design combustion chamber pressure of 274 newtons per square centimeter (400 psi). The thrust chamber nozzle expansion area ratio is 57 to 1, and the design specific impulse is 444 seconds.

These engines use a "bootstrap" process: pumped fuel is circulated through the thrust chamber tubes and is then expanded through a turbine which drives the propellant pumps (fig. VI-2). This routing of fuel through the thrust chamber tubes serves the dual purpose of cooling the thrust chamber walls and adding energy to the fuel prior to expansion through the turbine. After passing through the turbine, the fuel is injected into the combustion chamber. The pumped oxidizer is supplied directly to the combustion chamber after passing through the propellant utilization (mixture ratio control) valve.

Thrust control is achieved by regulating the amount of fuel by-passed around the turbine as a function of combustion chamber pressure. Ignition is accomplished by means of a spark igniter recessed in the propellant injector face. Starting and stopping are controlled by pneumatically operated valves. Helium pressure to these valves is supplied through engine-mounted solenoid valves which are controlled by discrete commands from the vehicle control system.

System performance, engine first firing. - In-flight turbopump chilldown was commanded 8.0 seconds prior to main engine first start for all flights. This chilldown was accomplished by opening both the oxidizer and the fuel pump inlet valves. The oxidizer passed through the pump and into the combustion chamber; the fuel flowed through the pump and discharged through separate cooldown valves, one located downstream of each pump stage (fig. VI-2). The chilldown successfully prevented cavitation of the turbopumps during the engine start transients.

Main engine first start was commanded at T + 257.8, T + 257.3, and T + 260.2 seconds for AC-13, AC-14, and AC-15, respectively. The engine start transients appeared normal. The start transient chamber pressure rises are presented in figures VI-3(a) to (f). Engine acceleration times and values of start total impulse are presented in table VI-3(a). All values of differential impulse between engines were within the allowable 3σ limit of approximately 25 000 newton-seconds (5700 lbf-sec).

Fuel and oxidizer pump inlet conditions throughout the main engine first firing durations are presented in figures VI-4(a) to (f). The pump inlet pressures and temperatures indicated that the propellant pressures remained well above saturation at all

times during engine operation. The margin between the steady-state operating limit and the actual inlet conditions ensured satisfactory values of net positive suction pressure.

Steady-state operating conditions for the engine first firing are summarized and compared with their predicted values in table VI-4. The values of main engine chamber pressure at 90 seconds after main engine first start were below acceptance test levels by 2.7 and 2.7 newtons per square centimeter (3.9 and 3.9 psi) on AC-13, by 1.8 and 3.0 newtons per square centimeter (2.6 and 4.4 psi) on AC-14, and by 6.1 and 6.3 newtons per square centimeter (8.8 and 9.1 psi) and AC-15, for the C-1 and C-2 engines, respectively. A corresponding change in engine internal operating parameters substantiated an engine thrust shift on AC-15. On AC-13 and AC-14, however, the internal parameters did not substantiate a thrust shift. The variation in internal operating parameters on AC-15 consisted of higher values of turbine inlet temperature and lower values of venturi upstream pressures and pump speeds than were experienced during the acceptance tests. Engine thrust shifts were also noted during the flights of AC-9 and AC-12. The exact cause for these shifts has not been found to date.

Main engine performance, in terms of thrust, specific impulse, and mixture ratio, is shown in figures VI-5(a) to (f). Performance was calculated using both the Pratt & Whitney regression and the characteristic velocity C^* techniques. An explanation of these techniques is given in appendix B of this report. During the first 90 seconds of main engine operation, while the propellant utilization valves were "nulled", engine performance should have been stable. However, the scatter in performance values for the C^* technique reflects the sensitivity of the chamber pressure data used in this technique. The lower values of thrust for the C^* technique are a reflection of the lower than expected chamber pressure levels previously discussed (which are not used in the regression technique). The performance changes during the latter portion of the first firing (following main engine start +90 seconds) were normal and resulted from the operation of the propellant utilization system.

Main engine first cutoff was commanded at T + 587.0, T + 581.2, and T + 593.2 seconds for AC-13, AC-14, and AC-15, respectively. The engine systems responded as expected to the cutoff commands. Engine cutoff total impulse values of 13 000, 12 900, and 13 700 newton-seconds (2920, 2900, and 3095 lbf-sec) were noted on AC-13, AC-14, and AC-15, respectively. These values were all within the 3σ tolerance limits. The main engine first firing durations for AC-13, AC-14, and AC-15 were 329.2, 323.9, and 333.0 seconds, respectively; these values were 9.0, 6.9, and 13.4 seconds longer than the predicted values. The indicated thrust shift on AC-15 would cause the engine firing duration to increase by 7.9 seconds. However, no explanation is available for the longer firing durations on AC-13 and AC-14, nor the remaining time on AC-15.

Coast phase. - Stainless-steel heat shields were used on the engine pumps and the adjacent downstream plumbing to protect these areas from impingement heating by the ex-

haust products of the hydrogen peroxide engines. An experiment was conducted on AC-14 and AC-15 in an attempt to further reduce the coast-phase heat input to the engine turbopumps. A set of specially plated heat shields (gold internal surface and black external surface) was used on the AC-14 C-2 engine and on the AC-15 C-1 engine. Two additional temperature patches were provided on the C-1 engine for AC-14 and AC-15: one located on the internal surface of the shield, and the other mounted on the nearest location of the fuel turbopump surface immediately below. Table VI-5 compares the significant component temperatures during the coast phases of AC-13, AC-14, and AC-15 with those of AC-9 (a two-burn flight not employing engine heat shields). The times shown for the coast phase in table VI-5 were selected primarily when the 222-newton (50-lbf) hydrogen peroxide engines were cycled. The 222-newton (50-lbf) engines were commanded on for the first 76 seconds following main engine first cutoff and for the 40-second period prior to main engine second start. Although significant temperature reductions resulted from the use of the heat shields, little additional reduction was observed with the plated shields.

Main engine second firing. - Because of the heat input to both the main engine turbopumps and the propellant feedlines during the coast period, a longer prestart duration (17 sec) was employed prior to main engine second start. For all three flights, engine prechill was satisfactorily accomplished prior to the main engine start command.

Main engine start was commanded to T + 989.5, T + 1352.9, and T + 1939.3 seconds for AC-13, AC-14, and AC-15, respectively. The start transients for AC-13 and AC-15 were normal. However, that of AC-14 was not: a momentary cavitation of both oxidizer turbopumps occurred while the engines were accelerating. Main engine chamber pressure rise for all flights is presented in figures V-6(a) to (f). Nothing abnormal can be seen in any of these figures, including those of AC-14. Engine acceleration times and values of start total impulse are presented in table VI-3(b). All values were within their expected tolerance limits. The only noticeable difference in the start transient on AC-14 was a delay in chamber pressure rise with respect to turbopump speed. Normally, chamber pressure rises more rapidly in relation to pump speed during the second start transient than during the first start transient; on AC 14 this situation was reversed. Plots of chamber pressure rise as a function of turbopump speed are presented in figures VI-7(a) to (f).

Fuel and oxidizer pump inlet pressure and inlet temperature data throughout the main engine second firing durations are presented in figures VI-8(a) to (f). The more severe dip in the oxidizer pump inlet conditions during the AC-14 start transient can be readily observed. At all other times, the inlet pressures remained well above saturation.

The cause for the temporary oxidizer pump cavitation on AC-14 was considered to be the result of insufficient "burp" pressurization of the oxygen tank. This combined with warm propellants would cause the oxidizer boost pump to cavitate, which in turn would cause the engine oxidizer pumps to cavitate momentarily during the high-flow

acceleration period of the engine start transient. For AC-15, the "burp" pressure level was increased to prevent a recurrence of cavitation. This problem is further discussed in the sections Centaur Boost Pump and Propellant Supply System and Centaur Pneumatics.

Engine second firing steady-state operating conditions are summarized and compared with their predicted values in table VI-6. The values of chamber pressure at 100 seconds after main engine second start were greater than expected by 2.0 and 0.6 newton per square centimeter (2.9 and 0.8 psi) on AC-13, less than expected by 3.4 and 1.4 newtons per square centimeter (4.9 and 2.0 psi) on AC-14, and less than expected by 3.0 and 4.9 newtons per square centimeter (4.3 and 7.1 psi) on AC-15, for the C-1 and C-2 engines respectively. Only on AC-15 was any thrust shift substantiated by engine internal operating parameters.

Main engine second firing performance in terms of thrust, specific impulse, and mixture ratio was calculated by the same techniques as for the engine first firing and is presented in figures VI-5(a) to (f). The high mixture ratios and high thrusts at the start of the second firing are a result of the oxidizer-rich propellant utilization valve settings during this time. During approximately the last 25 seconds of the engine second firing, the propellant utilization valves were again nulled. The difference in thrust values between flights, as calculated by the C* technique, are a direct reflection of the chamber pressure levels as previously discussed.

Main engine cutoff was commanded at T + 1103.6, T + 1468.6, and T + 2054.9 seconds for AC-13, AC-14, and AC-15, respectively. All engine systems responded as expected to the cutoff commands. Cutoff total impulse was calculated to be 13 000 newton-seconds (2920 lbf-sec) on AC-13, 13 300 newton-seconds (2990 lbf-sec) on AC-14, and 12 600 newton-seconds (2840 lbf-sec) on AC-15. These values were within their 3σ tolerance limits. The respective main engine second firing durations were 114.1, 115.7, and 115.6 seconds for AC-13, AC-14, and AC-15. These values were 1.2, 2.6, and 2.2 seconds longer than their respective predictions. The suspected thrust shift for AC-15 would account for approximately 1.4 seconds of its long burn time. No explanation is available for the longer firing durations on AC-13 and AC-14, nor the remaining time on AC-15.

Retromaneuver. - Significant engine component temperatures during the period between main engine second cutoff and the initiation of the retrothrust operation are presented in table VI-5. The retrothrust was provided by opening the engine inlet valves and allowing the propellants in the tanks to discharge through the main engines. Flow through the engines was verified by pump inlet pressure and temperature measurements following the retrothrust command (main engine second cutoff +300 sec). Liquid or two-phase flow was indicated by the engine inlet temperature measurements throughout the retrothrust operations. Engine pump inlet pressures closely correlated with propellant tank ullage pressures.

TABLE VI-3. - CENTAUR MAIN ENGINE STARTING CHARACTERISTICS

(a) Engine first firing

Characteristic	Units	Engine					
		C-1	C-2	C-1	C-2	C-1	C-2
		AC-13		AC-14		AC-15	
Engine acceleration time	sec	1.58	1.62	1.50	1.50	1.49	1.44
Start total impulse	N-sec	41 500	35 300	43 100	43 100	45 100	43 700
	lbf-sec	9 320	7 940	9 710	9 690	10 150	9 820

(b) Engine second firing

Characteristic	Units	Engine					
		C-1	C-2	C-1	C-2	C-1	C-2
		AC-13		AC-14		AC-15	
Engine acceleration time	sec	1.50	1.55	1.50	1.45	1.60	1.50
Start total impulse	N-sec	43 400	42 600	44 300	43 000	41 300	45 200
	lbf-sec	9 760	9 590	9 950	9 680	9 290	10 180

TABLE VI-4. - CENTAUR MAIN ENGINE OPERATING DATA, ENGINE FIRST FIRING

Parameter	Units	Expected value	Main engine start +					
			90 sec		200 sec		320 sec	
			C-1	C-2	C-1	C-2	C-1	C-2
AC-13								
Fuel pump inlet total pressure, absolute	N/cm^2	17.2 to 24	21.6	21.2	20.4	20.4	19.0	19.9
	psi	24.9 to 35.3	31.4	30.8	29.6	29.6	27.6	28.9
Fuel pump inlet temperature	K	20.3 to 21.9	21.3	21.1	21.0	20.9	20.6	20.4
	^oR	36.5 to 39.5	38.3	38.0	37.8	37.6	37.0	36.7
Oxidizer pump inlet total pressure, absolute	N/cm^2	35.5 to 53.8	45.2	45.6	45.3	46.3	45.3	44.6
	psi	51.5 to 78.0	65.8	66.2	65.7	67.1	65.7	64.7
Oxidizer pump inlet temperature	K	95.6 to 101.6	98.6	98.5	98.5	98.2	98.0	97.8
	^oR	172.0 to 183.0	177.6	177.3	177.4	176.8	176.3	176.0
Oxidizer pump speed	rpm	[a]12 163±347	12 380	12 280	12 220	12 290	12 460	12 350
Fuel venturi upstream pressure, absolute	N/cm^2	[a]508±17	503.4	508.7	502.5	508.1	506.2	509.5
	psi	[a]737±25	730.1	737.8	728.8	736.9	734.2	738.9
Fuel turbine inlet temperature	K	[a]207±12	203.4	211.1	200.0	204.9	200.4	205.3
	^oR	[a]372±22	366.1	380.0	360.1	368.9	360.7	369.5
Oxidizer injector differential pressure	N/cm^2	[a]31.7±6.9	32.2	25.6	30.2	26.8	32.9	25.6
	psi	[a]46±10	46.6	37.2	43.7	38.8	47.8	37.1
Engine chamber pressure, absolute	N/cm^2	[a]270.8±3.7	266.8	268.9	385.7	390.1	386.2	389.1
	psi	[a]392.4±5.4	386.9	390.0	385.7	390.1	386.2	389.1
AC-14								
Fuel pump inlet total pressure, absolute	N/cm^2	17.2 to 24.4	22.1	22.0	20.6	21.0	19.2	19.6
	psi	24.9 to 35.3	32.0	31.9	29.3	30.5	27.9	28.4
Fuel pump inlet temperature	K	20.3 to 21.9	21.6	21.6	21.2	21.3	20.8	20.9
	^oR	36.5 to 39.5	38.9	38.8	38.2	38.3	37.5	37.6
Oxidizer pump inlet total pressure, absolute	N/cm^2	35.5 to 53.8	43.6	44.3	44.7	45.1	41.8	43.3
	psi	51.5 to 78.0	63.3	64.3	64.8	65.4	60.6	62.8
Oxidizer pump inlet temperature	K	95.6 to 101.6	98.5	98.5	98.0	98.0	97.7	97.7
	^oR	172.0 to 183.0	177.3	177.3	176.6	176.7	175.9	175.9
Oxidizer pump speed	rpm	[a]12 163±347	11 920	12 250	11 900	12 300	11 900	12 160
Fuel venturi upstream pressure, absolute	N/cm^2	[a]508±17	514.7	521.1	514.5	521.4	510.9	516.2
	psi	[a]737±25	746.5	755.7	746.2	756.2	740.9	748.6
Fuel turbine inlet temperature	K	[a]207±12	216.9	213.4	213.0	207.5	215.6	212.9
	^oR	[a]372±22	390.5	384.2	383.5	373.6	388.2	383.2
Oxidizer injector differential pressure	N/cm^2	[a]31.7±6.9	26.5	31.2	26.9	29.0	27.6	29.1
	psi	[a]46±10	38.4	45.2	39.0	42.0	40.0	42.2
Engine chamber pressure, absolute	N/cm^2	[a]270.8±3.7	268.3	268.9	266.8	267.5	267.5	268.4
	psi	[a]392.4±5.4	389.1	390.0	386.9	387.9	387.9	389.3
AC-15								
Fuel pump inlet total pressure, absolute	N/cm^2	17.2 to 24.4	20.4	19.7	19.6	20.3	19.1	19.1
	psi	24.9 to 35.3	29.6	38.6	38.5	29.4	27.7	27.7
Fuel pump inlet temperature	K	20.3 to 21.9	21.6	21.6	21.3	21.3	20.9	20.9
	^oR	36.5 to 39.5	38.8	38.8	38.3	38.3	37.6	37.6
Oxidizer pump inlet total pressure, absolute	N/cm^2	35.5 to 53.8	44.3	44.0	44.1	44.7	46.8	45.1
	psi	51.5 to 78.0	64.3	63.9	64.0	64.7	67.9	65.4
Oxidizer pump inlet temperature	K	95.6 to 101.6	98.3	98.4	98.0	98.0	97.5	97.5
	^oR	172.0 to 183.0	177.0	177.1	176.7	176.7	175.7	175.8
Oxidizer pump speed	rpm	[a]12 163±347	12 040	12 010	12 070	11 860	12 000	11 810
Fuel venturi upstream pressure, absolute	N/cm^2	[a]508±17	501.4	494.0	504.3	494.7	496.6	490.0
	psi	[a]737±25	727.2	716.4	731.4	717.5	720.3	710.6
Fuel turbine inlet temperature	K	[a]207±12	214.9	206.3	206.0	196.1	210.7	197.5
	^oR	[a]372±22	386.9	371.4	370.8	353.1	379.3	355.5
Oxidizer injector differential pressure	N/cm^2	[a]31.7±6.9	29.3	24.9	28.6	22.2	30.5	23.2
	psi	a [a]46±10	42.5	36.1	41.4	32.1	44.2	33.7
Engine chamber pressure, absolute	N/cm^2	[a]270.8±3.7	264.5	264.6	263.6	265.3	265.5	264.2
	psi	[a]392.4±5.4	383.6	383.6	383.7	382.3	385.0	383.2

[a]Expected value with nominal inlet conditions and nulled propellant utilization valve angle.

TABLE VI-5. - CENTAUR MAIN ENGINE COMPONENT TEMPERATURE TRENDS[a]

Temperature	Flight	Engine	Units	First prestart, MES-1 -8 sec	Main engine first cutoff			Main engine second start		Main engine second cutoff		
					MECO-1	MECO-1 +75 sec	MECO-1 +200 sec	MES-2 -40 sec	Second prestart, MES-2 17 sec	MECO-2	MECO-2 +10 sec	MECO-2 +300 sec
Fuel turbine inlet	AC-13	C-1	K	220	214	194	(b)	194	194	208	192	194
			°R	395	368	348	↓	350	350	374	345	350
	AC-13	C-2	K	199	209	212	↓	198	198	212	196	198
			°R	359	377	382	↓	356	356	382	358	356
	AC-14	C-1	K	198	214	211	↓	176	(b)	218	202	200
			°R	357	386	379	↓	316	↓	392	362	360
	AC-14	C-2	K	195	214	209	↓	176	↓	215	200	200
			°R	350	385	377	↓	316	↓	387	360	360
	AC-15	C-1	K	225	208	200	200	163	166	215	198	196
			°R	405	373	360	360	294	300	387	356	353
	AC-15	C-2	K	215	198	190	190	152	152	218	190	188
			°R	386	356	343	343	273	273	374	341	338
	AC-9	C-1	K	217	200	200	202	174	174	213	204	203
			°R	390	360	360	364	314	314	383	367	365
	AC-9	C-2	K	207	203	201	198	170	170	210	202	200
			°R	372	365	362	357	306	306	378	363	360
Fuel pump housing	AC-13	C-1	K	94	31	63	(b)	99	101	41	44	89
			°R	170	55	114	↓	178	182	73	79	160
	AC-13	C-2	K	94	36	63	↓	97	100	44	44	89
			°R	169	65	114	↓	174	180	80	80	160
	AC-14	C-1	K	89	60	115	↓	111	(b)	34	37	84
			°R	160	108	207	↓	200	↓	62	67	151
	AC-14	C-2	K	88	55	120	↓	106	↓	34	36	85
			°R	159	99	216	↓	190	↓	61	66	153
	AC-15	C-1	K	100	60	66	79	130	131	66	67	84
			°R	181	108	119	142	234	236	120	121	150
	AC-15	C-2	K	98	28	56	70	104	115	32	37	80
			°R	177	52	101	126	206	208	158	66	143
	AC-9	C-1	K	99	37	83	92	141	144	40	42	89
			°R	178	67	150	166	254	260	70	75	160
	AC-9	C-2	K	96	40	89	88	133	136	50	50	83
			°R	172	73	143	158	240	245	90	90	150

Fuel pump housing skin	AC-14	C-1	K	88	(c)	(c)	(b)	108	(b)	(c)	(c)	(c)
			°R	158	(c)	(c)	(b)	195	(b)	(c)	(c)	(c)
	AC-15	C-1	K	99	40	65	83	130	132	43	46	88
			°R	179	73	117	149	235	237	78	83	158
Fuel pump shield	AC-14	C-1	K	312				285		169	173	251
			°R	416				513		304	312	452
	AC-15	C-1	K	243	103	246	234	300	326	202	192	264
			°R	437	185	443	421	541	589	363	345	474
Oxidizer pump housing	AC-13	C-1	K	223	105	147	(b)	169	188	114	174	223
			°R	402	189	266		304	339	206	313	402
	AC-13	C-2	K	228	107	151		(d)	(d)	114	136	228
			°R	410	192	271		(d)	(d)	205	246	410
	AC-14	C-1	K	213	(c)	(c)		160	(b)	136	214	213
			°R	384				288		245	385	384
	AC-14	C-2	K	216				[d]62		104	121	216
			°R	370				111		187	218	370
	AC-15	C-1	K	105	144	147	181	181	190	106	123	196
			°R	353	190	260	264	326	343	191	221	353
	AC-15	C-2	K	226	104	144	135	165	179	106	118	226
			°R	407	187	260	242	296	322	191	212	407
	AC-9	C-1	K	256	106	200	178	208	228	106	125	256
			°R	460	190	360	320	375	410	190	225	460
	AC-9	C-2	K	228	117	186	175	205	220	117	144	228
			°R	410	210	345	315	370	395	210	260	410

[a]Temperature levels at MES-2 - 40 sec can vary depending on both the duration of the coast period and time of launch for each flight were

AC-9 - 1457 sec; 06:12 EST Oct. 26, 1966

AC-13 - 346 sec; 02:57 EST Sept. 8, 1967

AC-14 - 888 sec; 02:39 EST Nov. 7, 1967

AC-15 - 1344 sec; 01:30 EST Jan. 7, 1968

[b]No telemetry coverage.

[c]Measurement not recording.

[d]Measurement value questionable.

TABLE VI-6. - CENTAUR MAIN ENGINE OPERATING DATA, ENGINE SECOND FIRING

Parameter	Units	Expected	Main engine start +			
			50 sec		100 sec	
			C-1	C-2	C-1	C-2
AC-13						
Fuel pump inlet total pressure, absolute	N/cm^2	16.6 to 27.1	26.0	25.4	21.1	21.9
	psi	24.1 to 39.3	37.7	36.9	30.6	31.7
Fuel pump inlet temperature	K	20.1 to 24.1	18.5	18.9	20.9	20.8
	^oR	36.2 to 43.4	33.3	34.1	37.6	37.4
Oxidizer pump inlet total pressure, absolute	N/cm^2	34.4 to 43.2	45.2	44.6	42.6	42.9
	psi	49.9 to 71.2	65.5	64.7	61.8	62.1
Oxidizer pump inlet temperature	K	95.0 to 99.6	98.0	97.6	97.0	96.9
	^oR	171.0 to 179.2	176.2	175.7	174.6	174.4
Oxidizer pump speed	rpm	[a]12 163±347	12 300	12 240	12 360	12 310
Fuel venturi upstream pressure, absolute	N/cm^2	[a]508±17	507.1	507.7	506.1	512.2
	psi	[a]737±25	735.4	736.4	734.0	742.8
Fuel turbine inlet temperature	K	[a]207±12	200.1	202.5	207.5	211.6
	^oR	[a]372±22	360.3	364.6	373.5	380.9
Oxidizer injector differential pressure	N/cm^2	[a]31.7±6.9	31.6	25.5	32.9	26.2
	psi	[a]46±10	45.9	37.0	47.7	38.0
Engine chamber pressure, absolute	N/cm^2	[a]270.8±3.7	269.3	269.5	271.5	272.1
AC-14						
Fuel pump inlet total pressure, absolute	N/cm^2	16.6 to 27.1	22.8	23.2	21.0	22.5
	psi	24.1 to 39.3	33.0	33.7	30.4	32.6
Fuel pump inlet temperature	K	20.1 to 24.1	21.2	21.2	21.4	21.4
	^oR	36.2 to 43.4	38.1	38.2	38.4	38.5
Oxidizer pump inlet total pressure, absolute	N/cm^2	34.4 to 49.2	43.1	43.8	42.0	43.6
	psi	49.9 to 71.2	62.5	63.5	61.0	63.2
Oxidizer pump inlet temperature	K	96.0 to 99.2	97.5	97.5	96.9	97.0
	^oR	171.0 to 179.2	175.5	175.5	174.4	174.5
Oxidizer pump speed	rpm	[a]12 163±347	11 890	12 120	11 870	12 140
Fuel venturi upstream pressure, absolute	N/cm^2	[a]508±17	513.4	526.2	511.3	518.2
	psi	[a]737±25	744.6	763.2	763.2	751.5
Fuel turbine inlet temperature	K	[a]207±12	208.3	204.9	213.7	212.4
	^oR	[a]372±22	375.0	368.8	384.7	382.4
Oxidizer injector differential pressure	N/cm^2	[a]31.7±6.9	27.1	30.2	27.8	28.5
	psi	[a]46±10	39.3	43.8	40.3	41.3
Engine chamber pressure, absolute	N/cm^2	[a]270.8±3.7	267.7	271.7	266.7	270.6
	psi	[a]392.4±5.4	388.3	394.1	386.8	392.4
AC-15						
Fuel pump inlet total pressure, absolute	N/cm^2	16.6 to 27.1	23.1	23.9	21.6	23.9
	psi	24.1 to 39.3	33.5	34.7	31.4	34.6
Fuel pump inlet temperature	K	20.1 to 24.1	21.3	21.3	21.5	21.6
	^oR	36.2 to 43.4	38.4	38.4	38.7	38.8
Oxidizer pump inlet total pressure, absolute	N/cm^2	34.4 to 49.2	43.9	44.6	43.2	43.2
	psi	49.9 to 71.2	63.6	64.6	62.6	62.6
Oxidizer pump inlet temperature	K	95.0 to 99.6	97.8	97.6	97.0	97.1
	^oR	171.0 to 179.2	176.0	175.7	174.5	174.7
Oxidizer pump speed	rpm	[a]12 163±347	12 380	12 060	11 960	11 720
Fuel venturi upstream pressure, absolute	N/cm^2	[a]508±17	504.2	498.5	503.4	491.5
	psi	[a]737±25	731.2	723.0	730.1	712.9
Fuel turbine inlet temperature	K	[a]207±12	200.3	193.0	213.3	207.0
	^oR	[a]372±22	360.6	347.5	383.9	372.7
Oxidizer injector differential pressure	N/cm^2	[a]31.7±6.9	32.5	26.9	33.0	27.2
	psi	[a]46±10	47.1	39.0	47.8	39.4
Engine chamber pressure, absolute	N/cm^2	[a]270.8±3.7	269.2	267.2	267.6	265.9
	psi	[a]392.4±5.4	390.5	387.5	388.1	385.7

[a]Expected value with nominal inlet conditions and nulled propellant utilization valve angle.

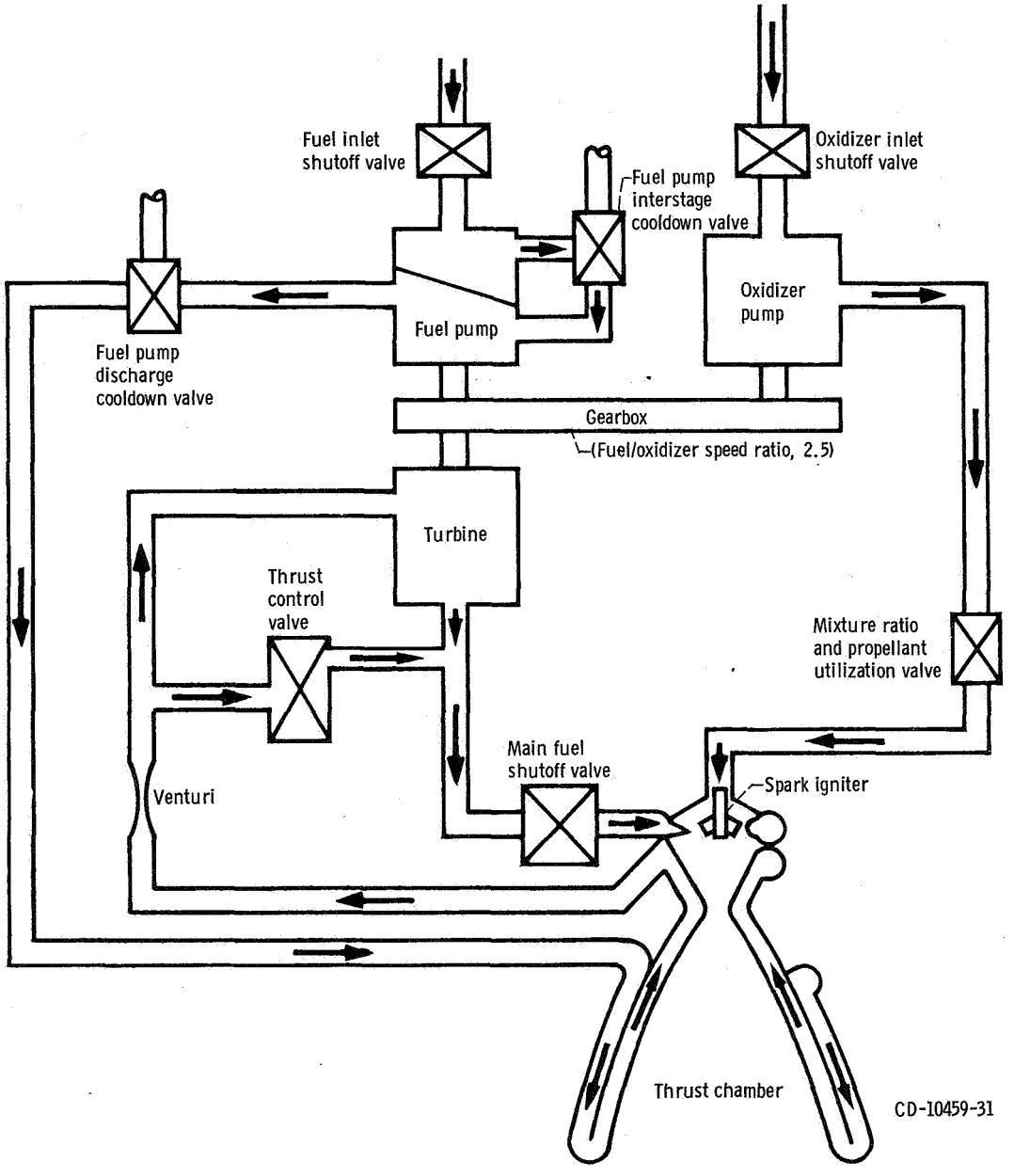

Figure VI-2. - Centaur propulsion system; AC-13, AC-14, and AC-15.

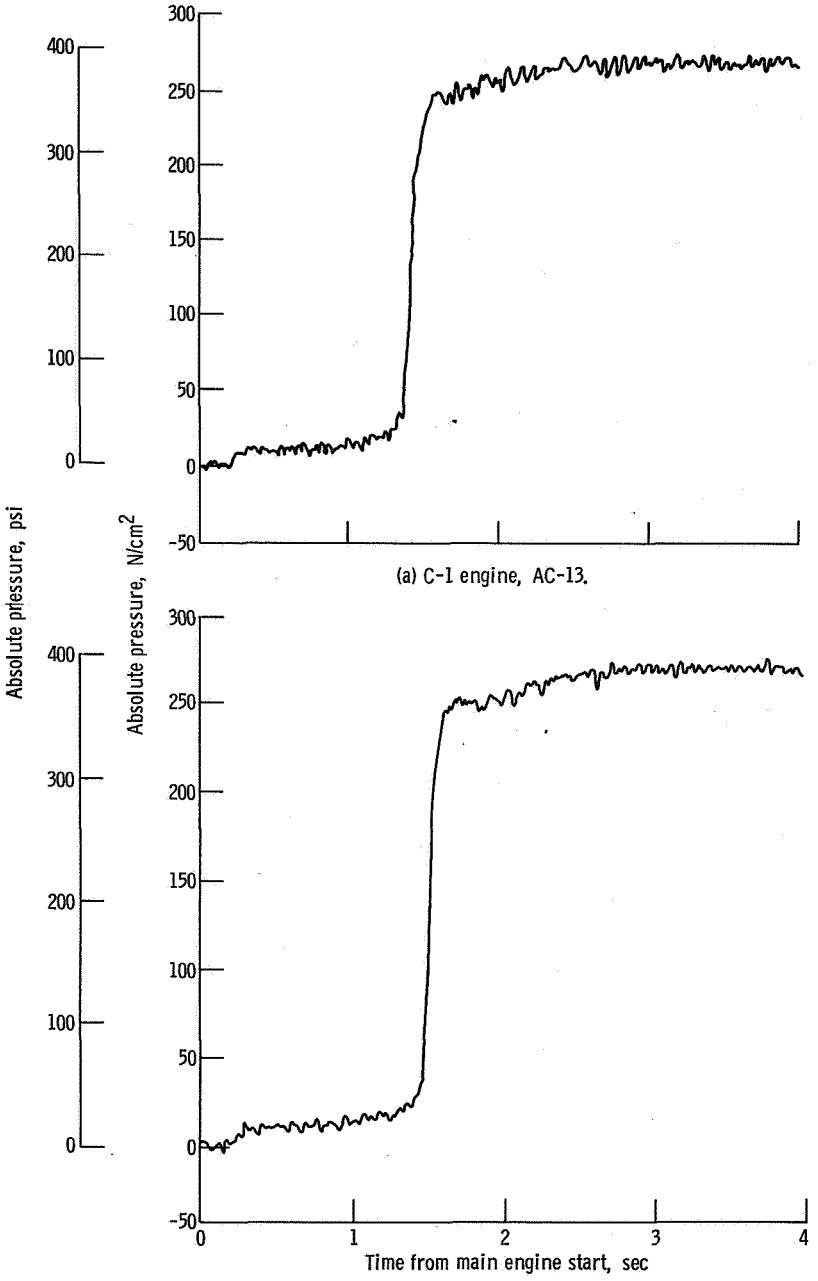

(a) C-1 engine, AC-13.

(b) C-2 engine, AC-13.

Figure VI-3. - Centaur main engine chamber pressure first start transients; AC-13, AC-14, and AC-15.

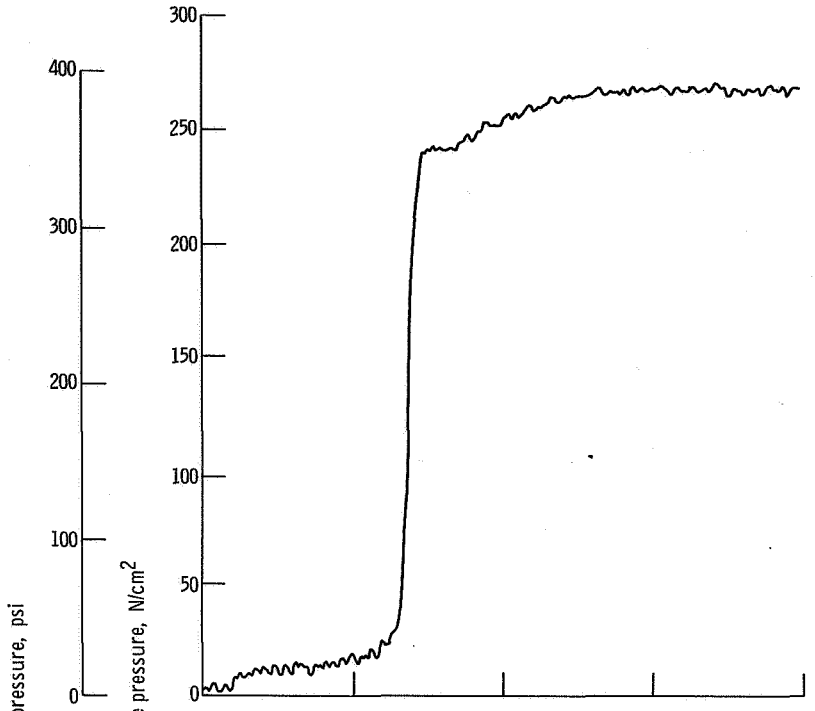

(c) C-1 engine, AC-14.

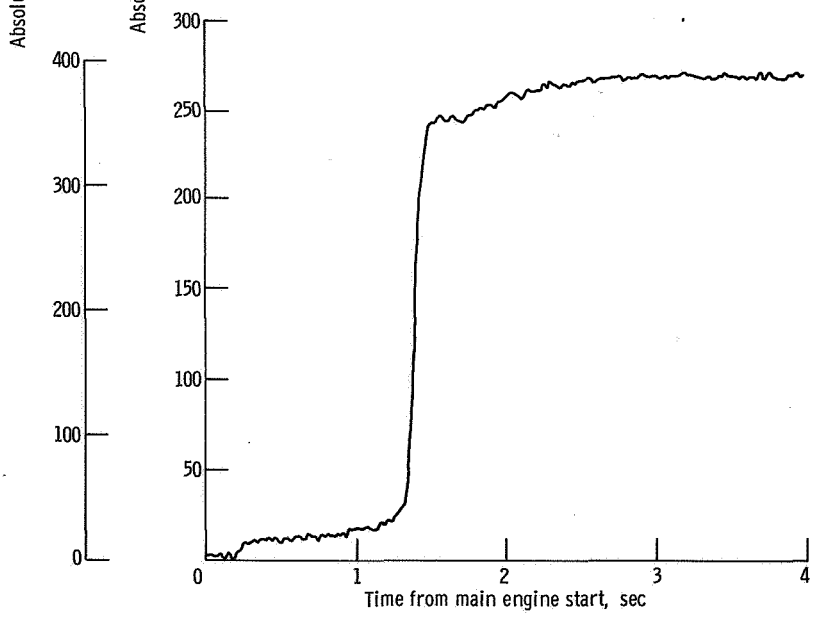

(d) C-2 engine, AC-14.

Figure VI-3. - Continued.

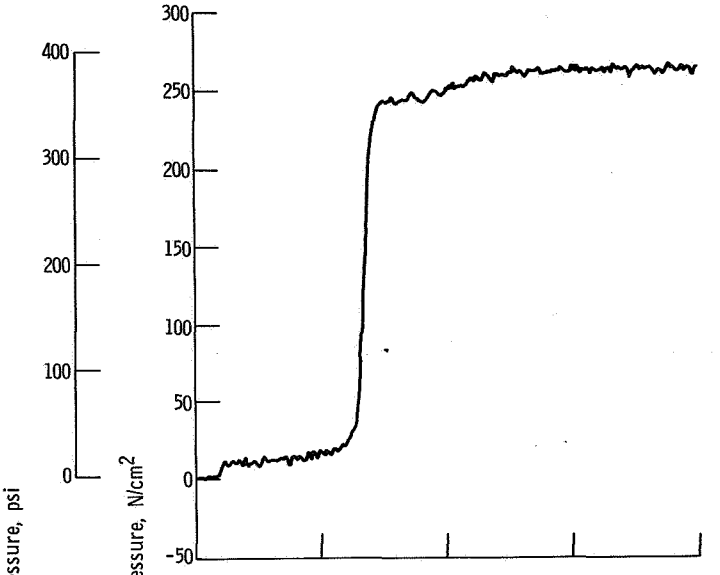

(e) C-1 engine, AC-15.

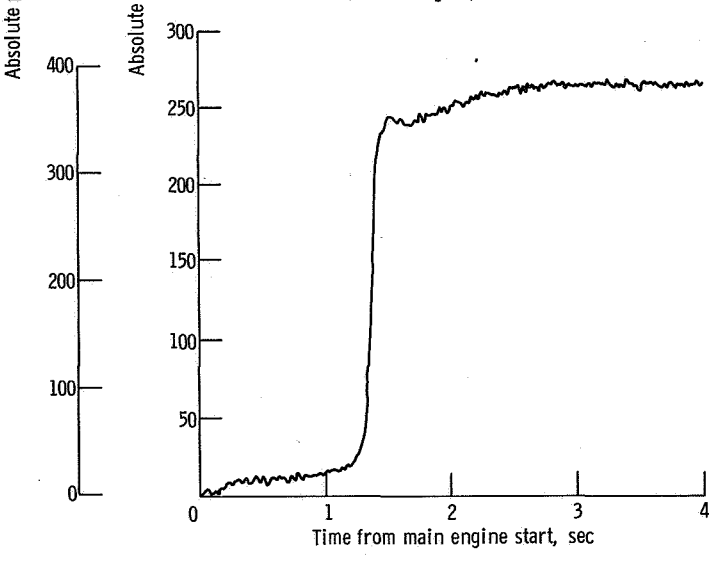

(f) C-2 engine, AC-15.

Figure VI-3. - Concluded.

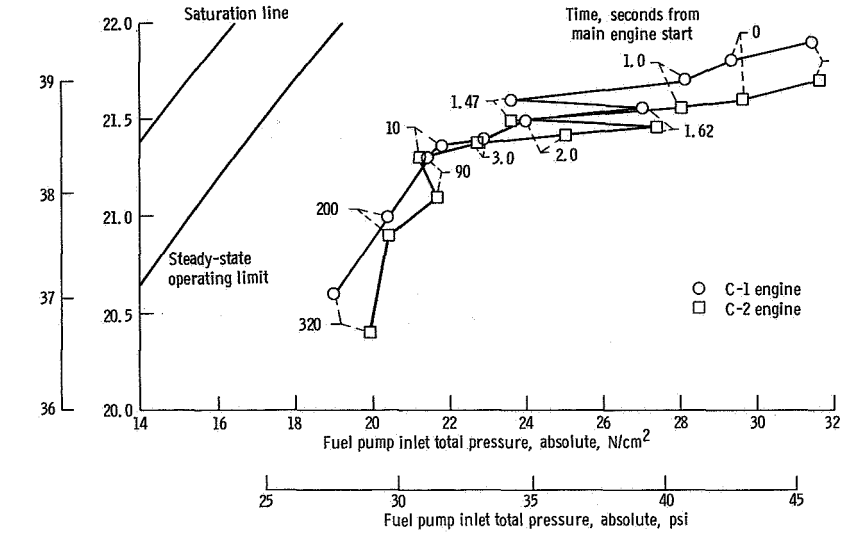

(a) Fuel pump, AC-13.

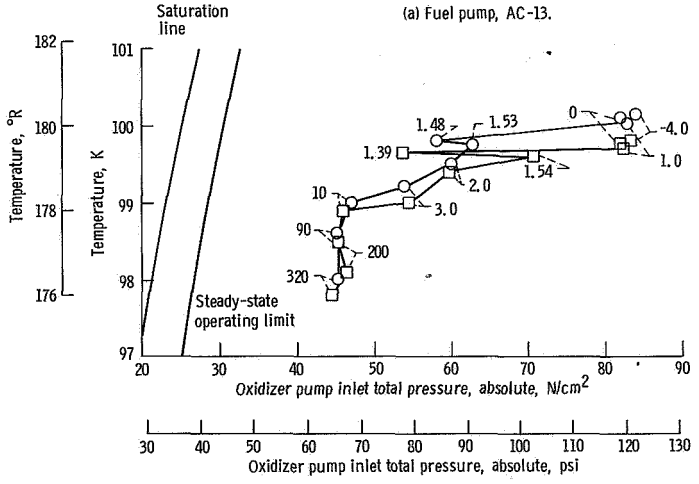

(b) Oxidizer pump, AC-13.

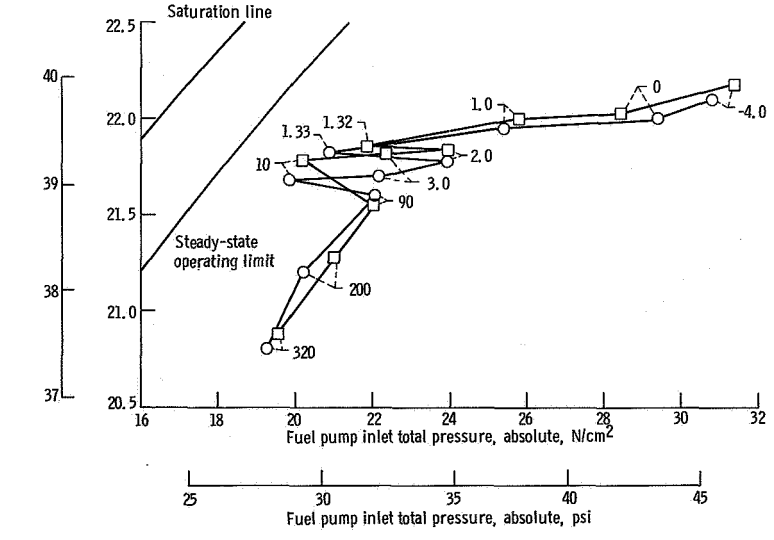

(c) Fuel pump, AC-14.

Figure VI-4. - Centaur fuel pump and oxidizer pump inlet conditions, engine first firing; AC-13, AC-14, and AC-15.

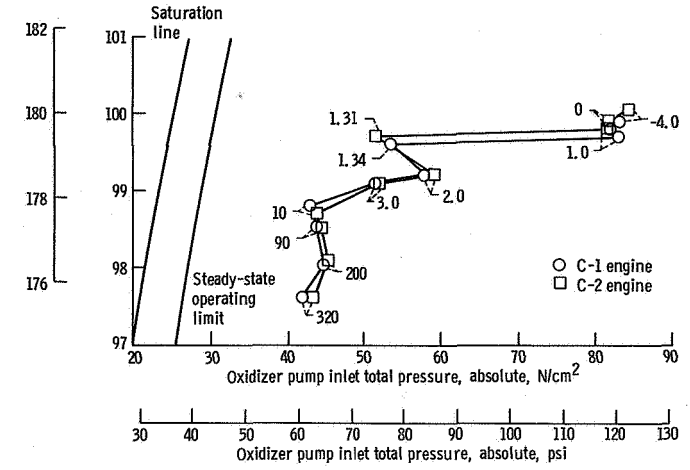

(d) Oxidizer pump, AC-14.

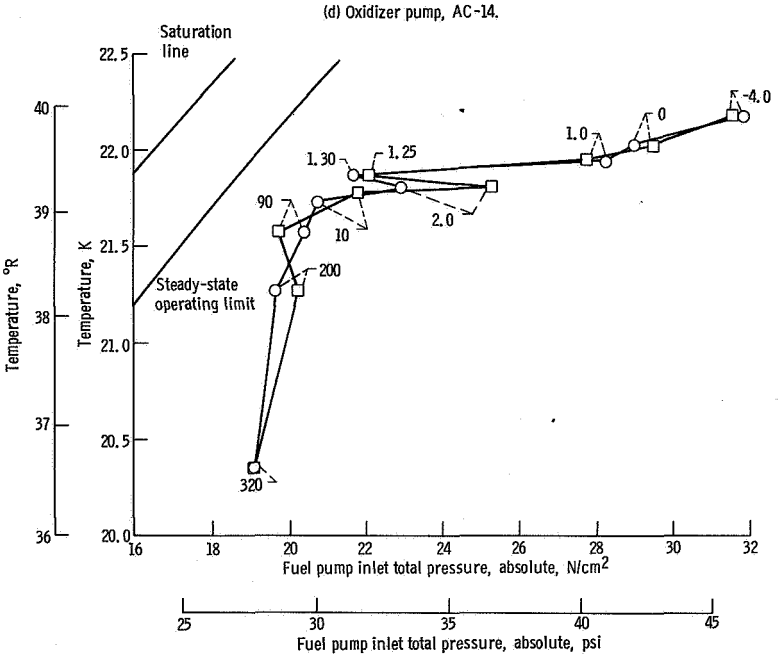

(e) Fuel pump, AC-15.

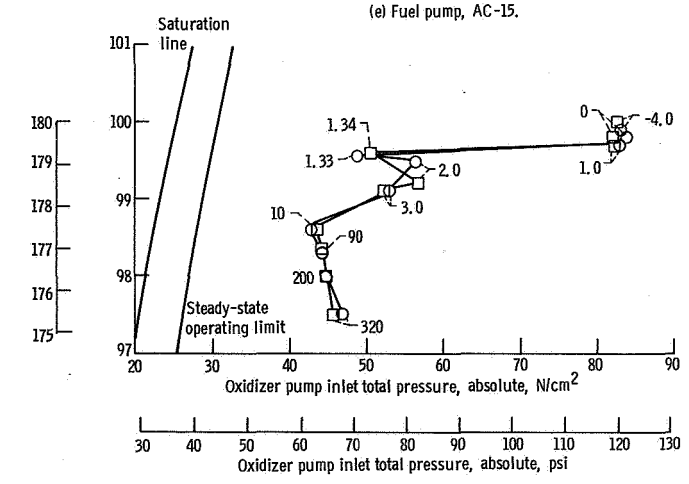

(f) Oxidizer pump, AC-15.

Figure VI-4. - Concluded.

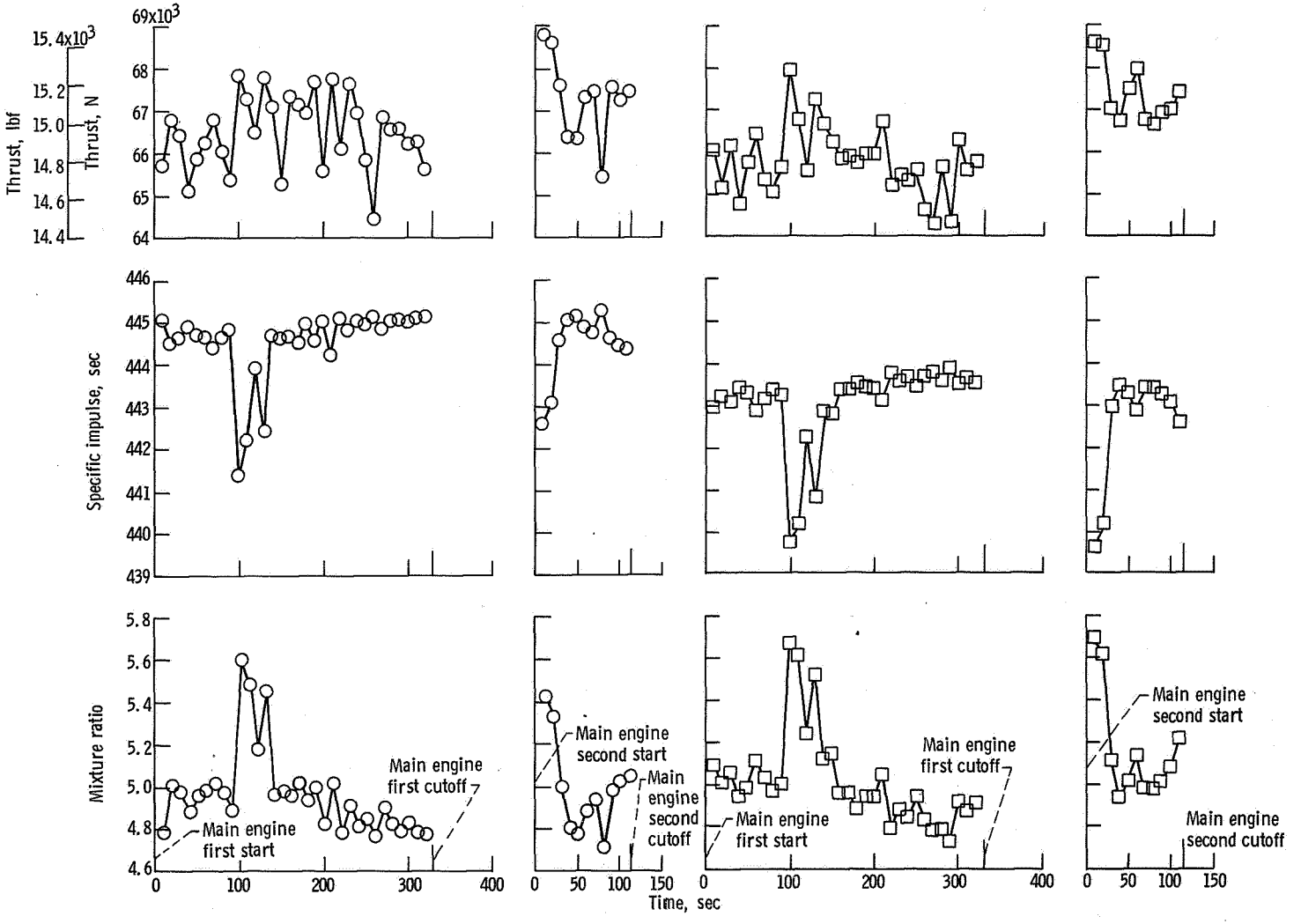

(a-1) C-1 engine.

(a-2) C-2 engine.

(a) C* technique, AC-13.

Figure VI-5. - Centaur main engine performance.

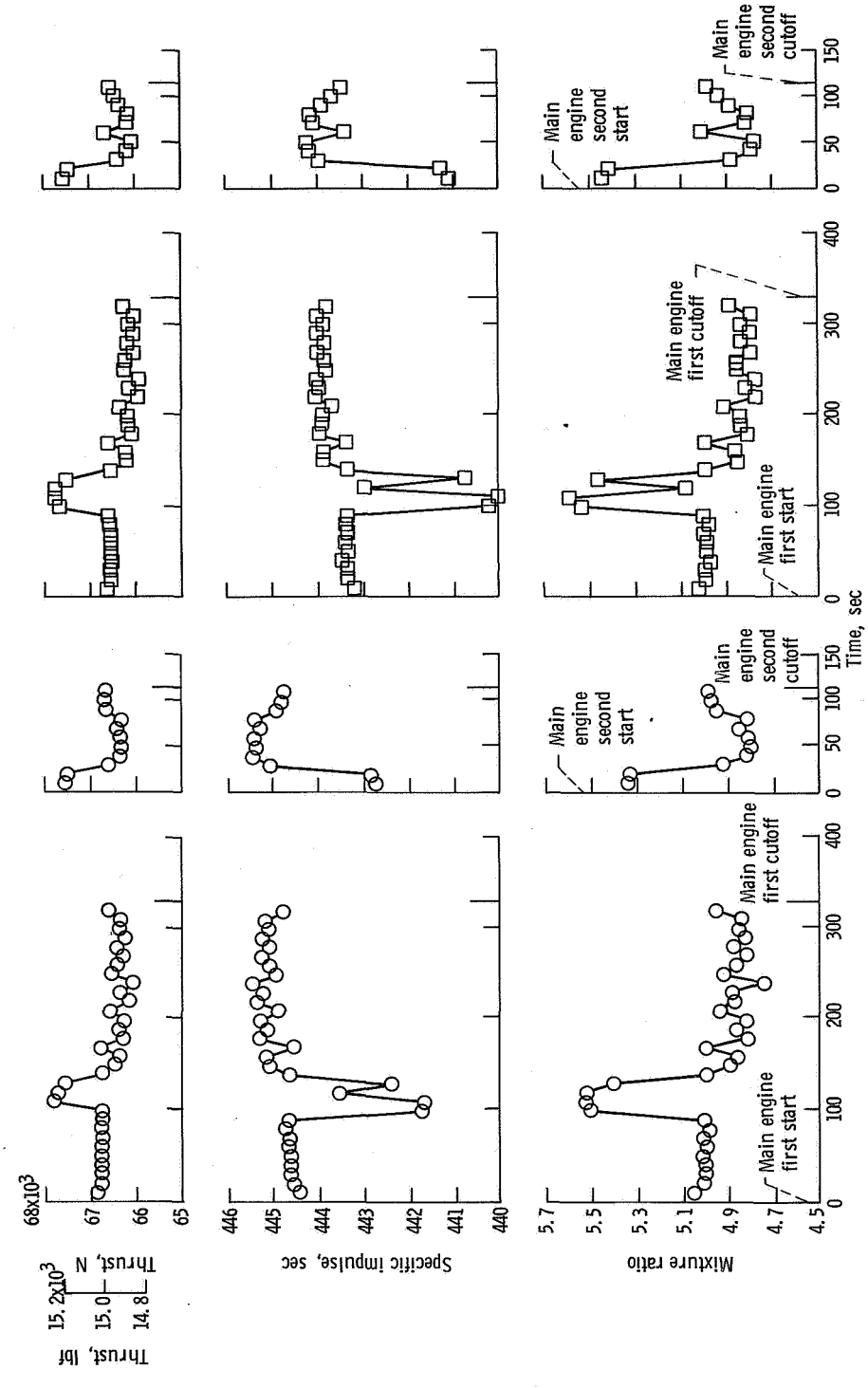

(b-1) C-1 engine.

(b-2) C-2 engine.

(b) Regression technique, AC-13.

Figure VI-5. - Continued.

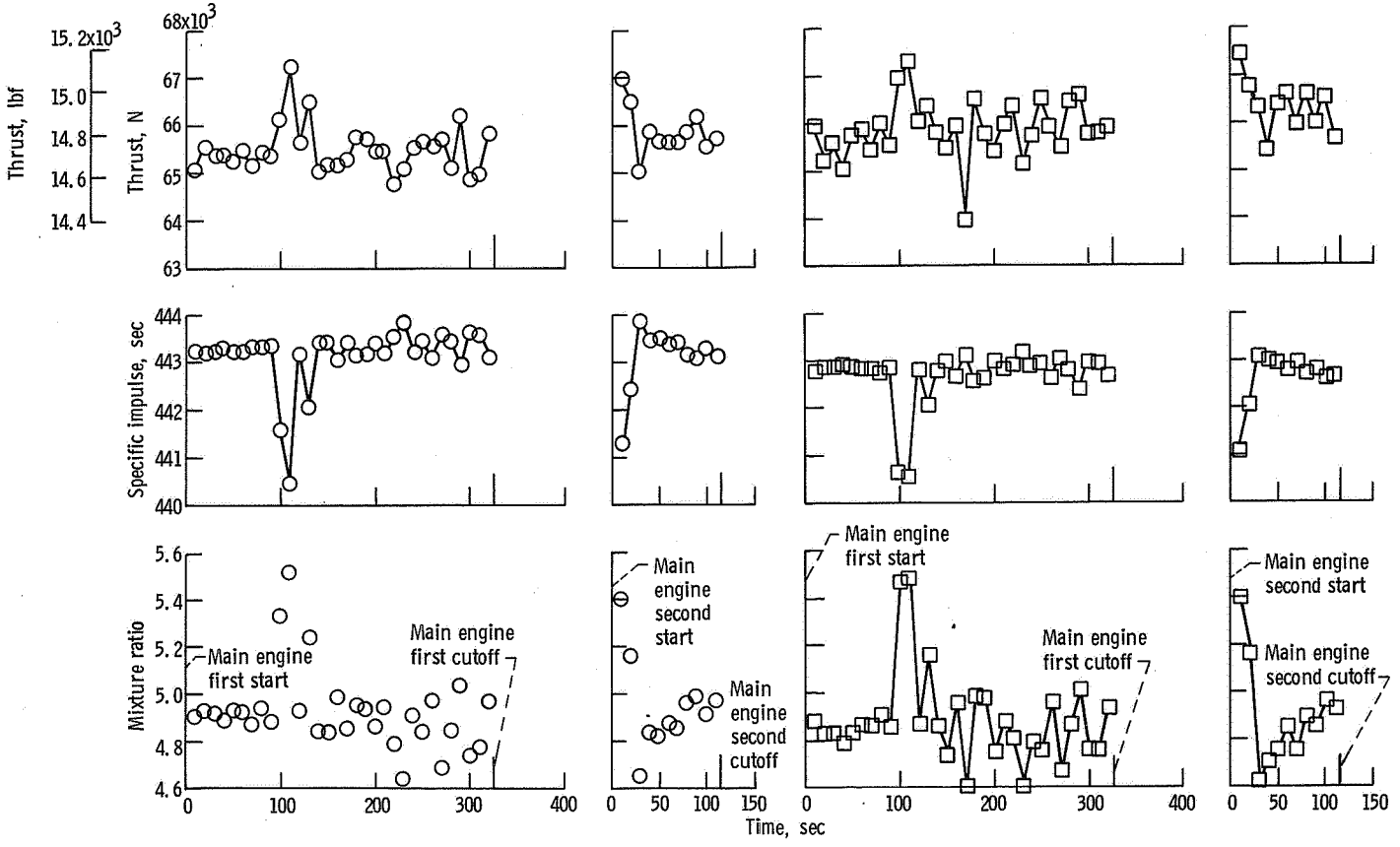

(c-1) C-1 engine.

(c-2) C-2 engine.

(c) C* technique, AC-14.

Figure VI-5. - Continued.

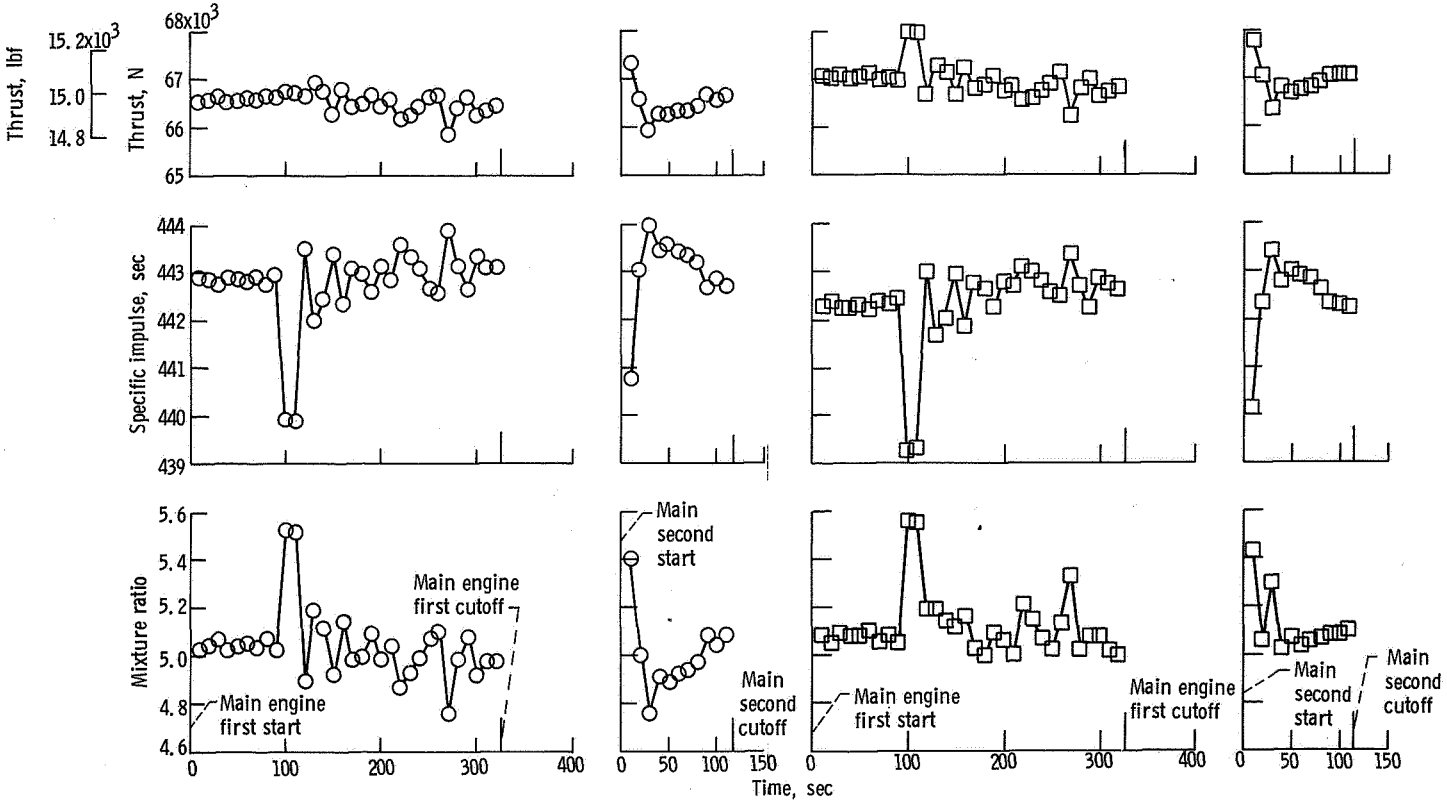

(d-1) C-1 engine.

(d-2) C-2 engine.

(d) Regression technique, AC-14.

Figure VI-5. - Continued.

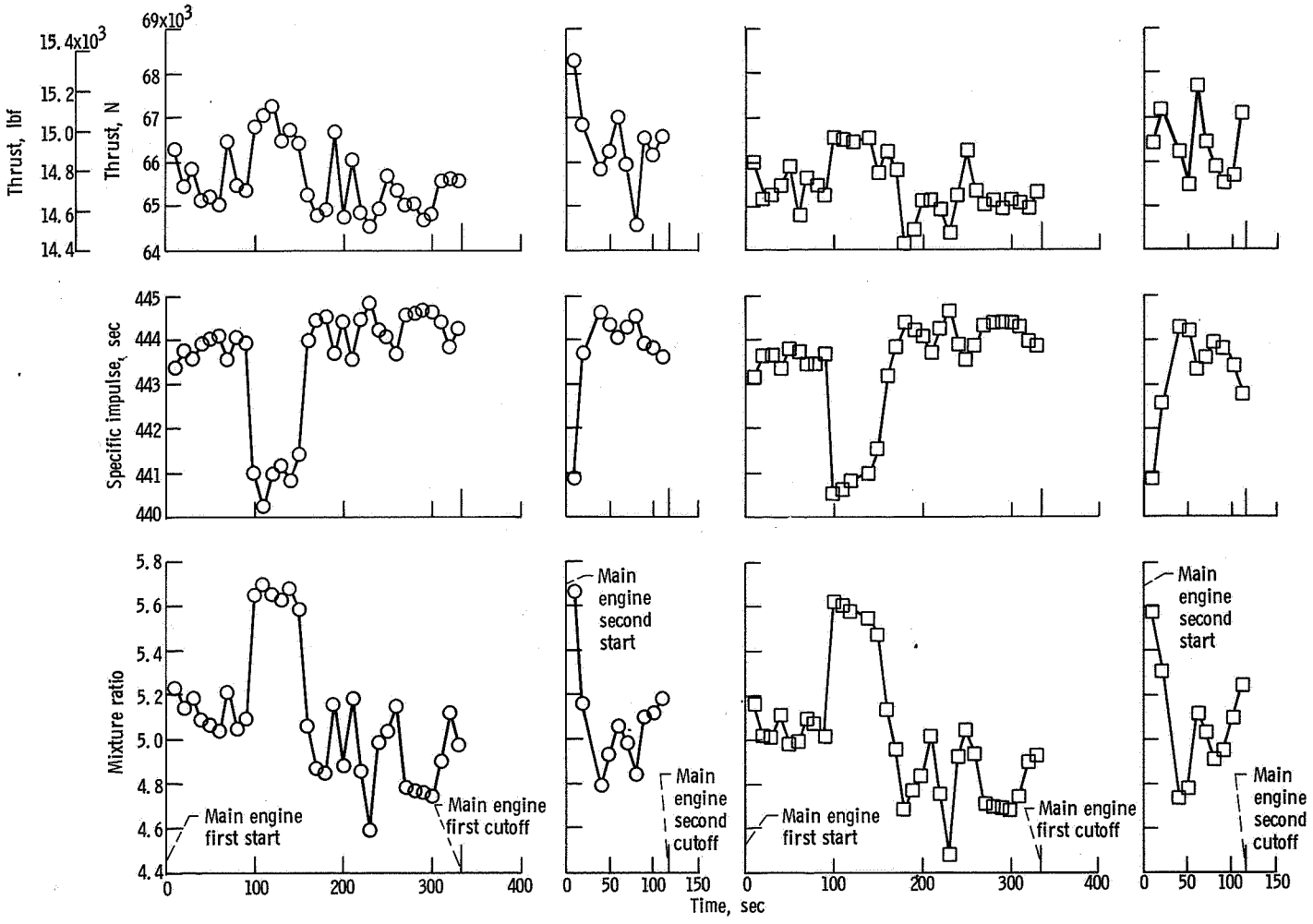

(e-1) C-1 engine.

(e-2) C-2 engine.

(e) C* technique, AC-15.

Figure VI-5. - Continued.

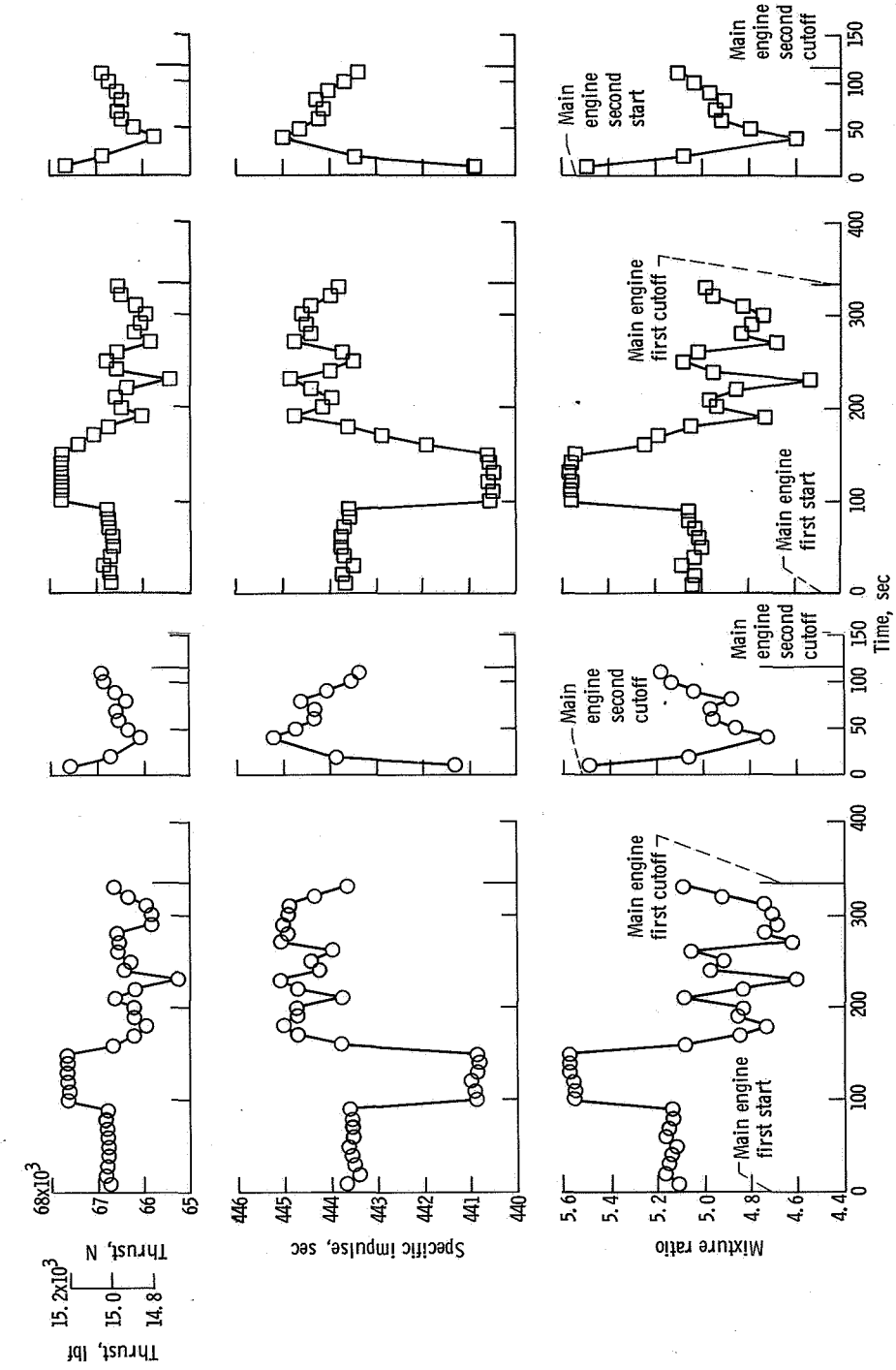

(f-1) C-1 engine.

(f-2) C-2 engine.

(f) Regression technique, AC-15.

Figure VI-5. - Concluded.

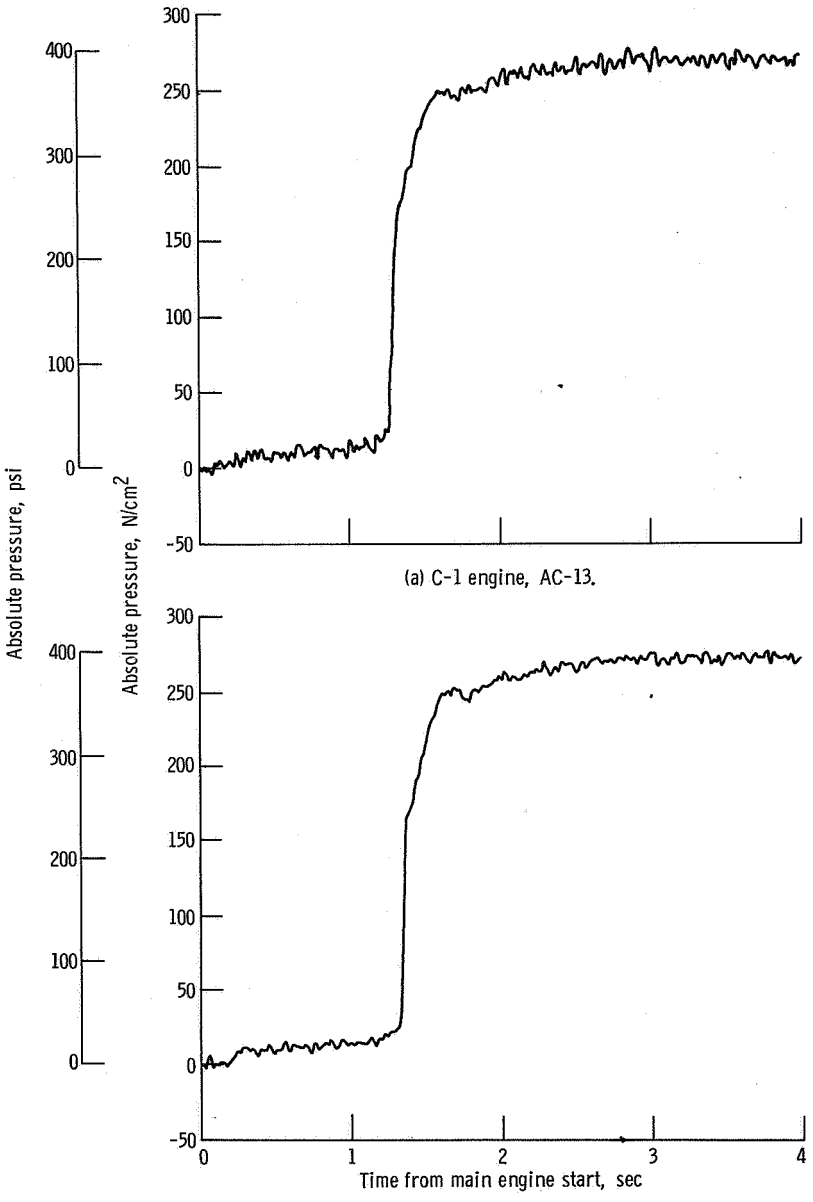

(a) C-1 engine, AC-13.

(b) C-2 engine, AC-13.

Figure VI-6. - Centaur main engine chamber pressure, second start transients; AC-13, AC-14, and AC-15.

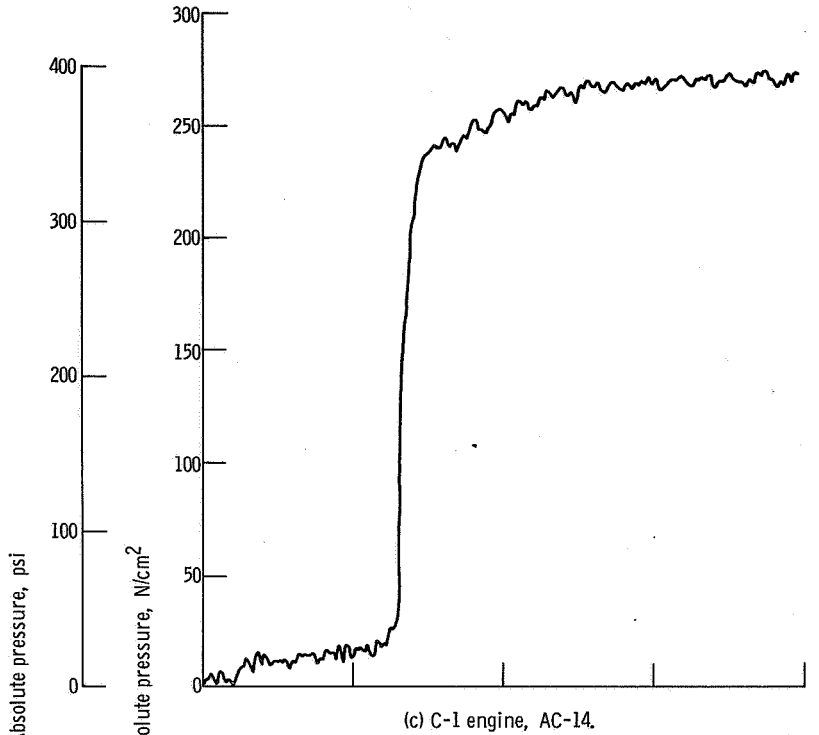

(c) C-1 engine, AC-14.

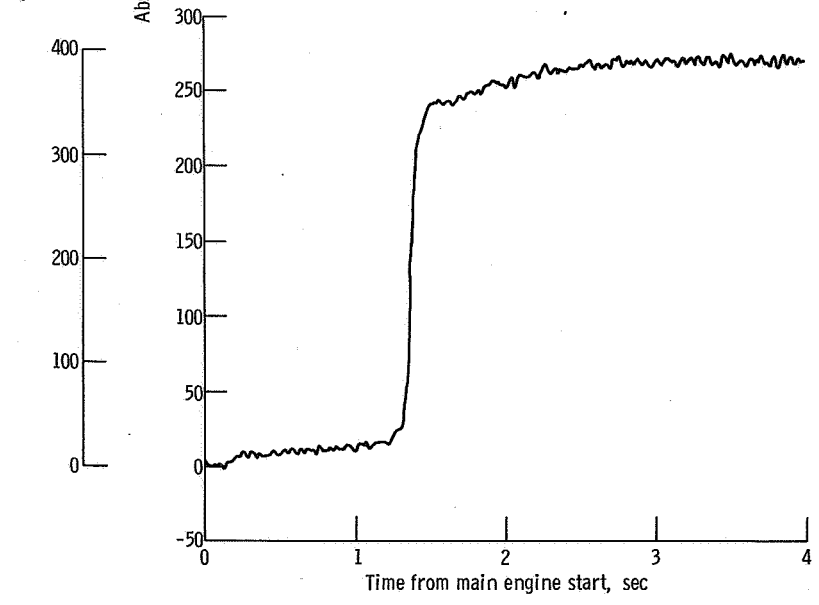

(d) C-2 engine, AC-14.

Figure VI-6. - Continued.

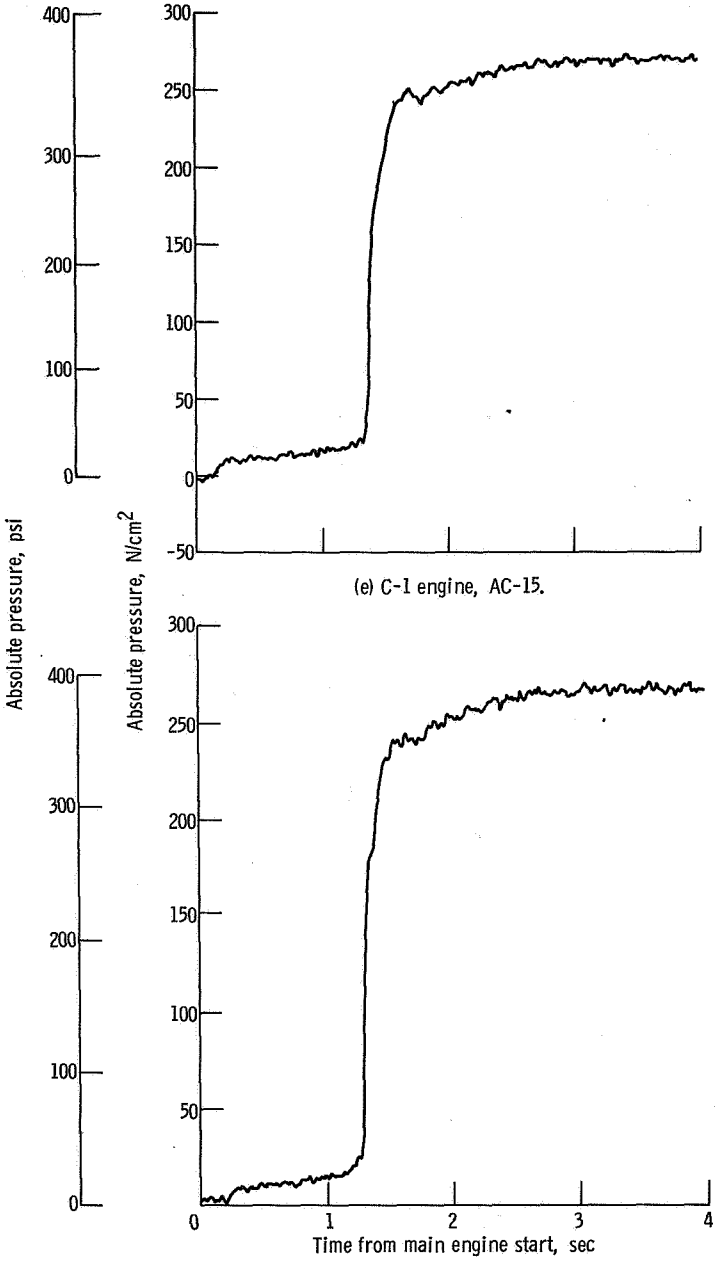

(e) C-1 engine, AC-15.

(f) C-2 engine, AC-15.

Figure VI-6. - Concluded.

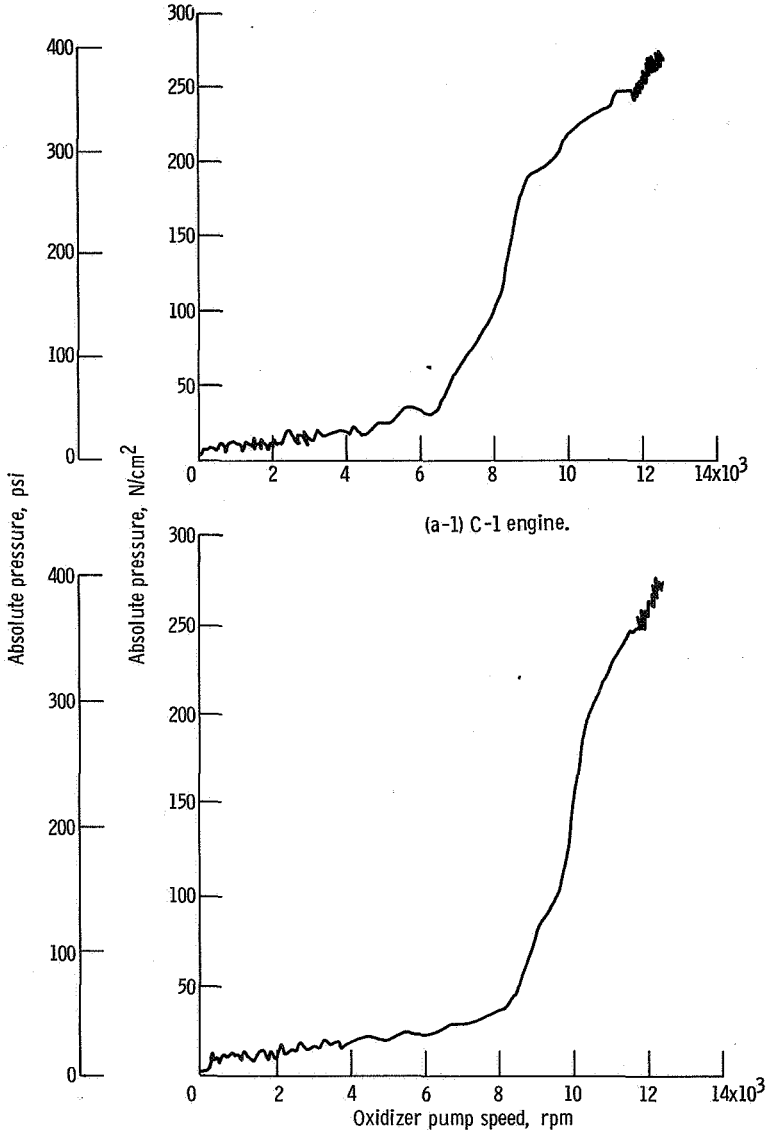

(a-1) C-1 engine.

(a-2) C-2 engine.

(a) First firing, AC-13.

Figure VI-7. - Centaur main engine accelerating characteristics; AC-3, AC-14, and AC-15.

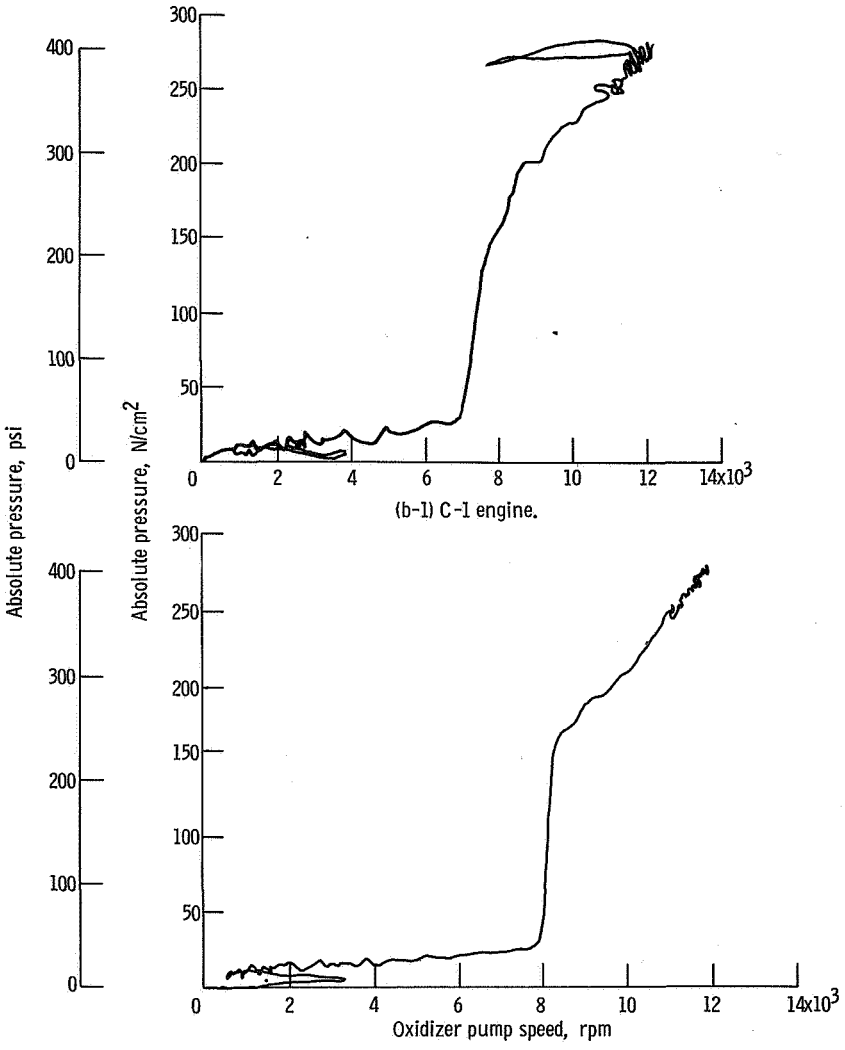

(b-1) C-1 engine.

(b-2) C-2 engine.

(b) Second firing, AC-13.

Figure VI-7. - Continued.

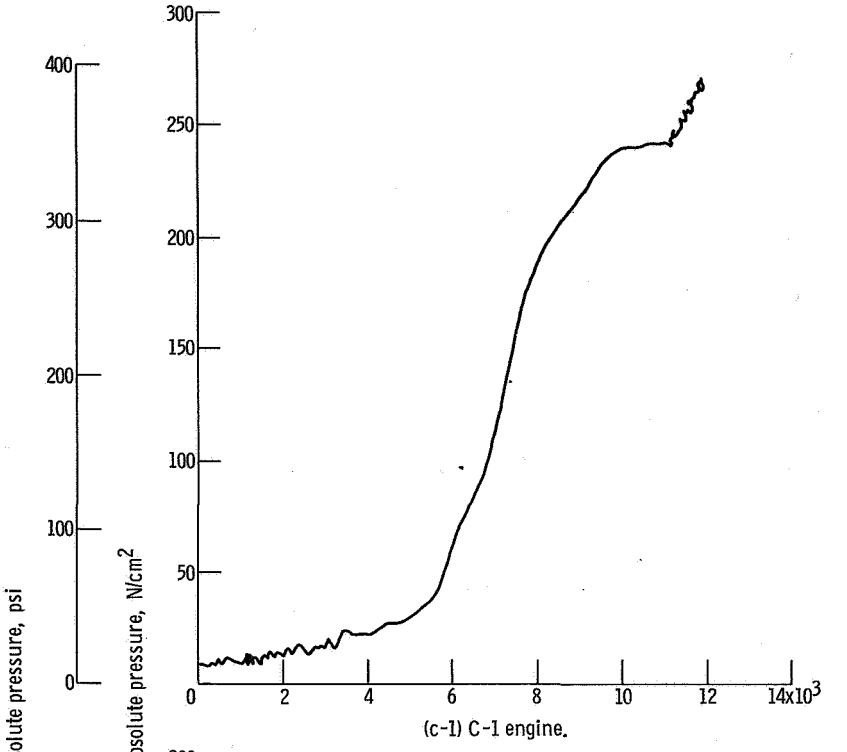

(c-1) C-1 engine.

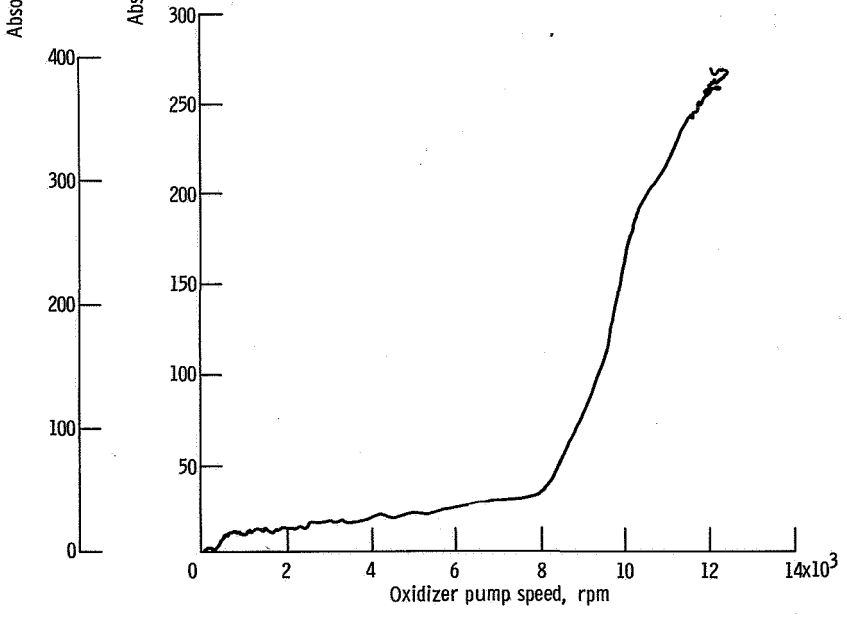

(c-2) C-2 engine.

(c) First firing, AC-14.

Figure VI-7. - Continued.

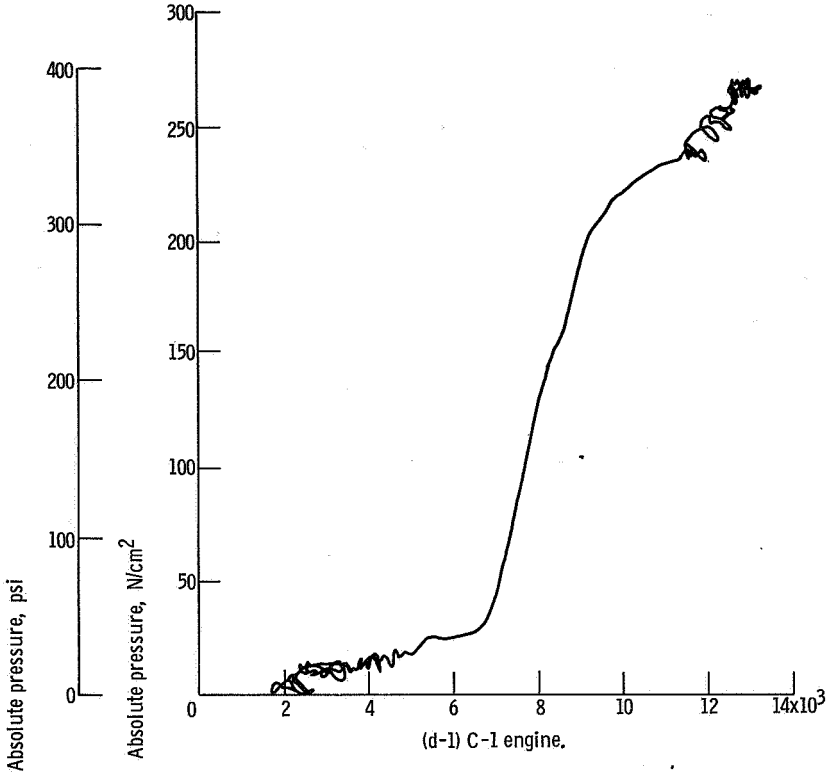

(d-1) C-1 engine.

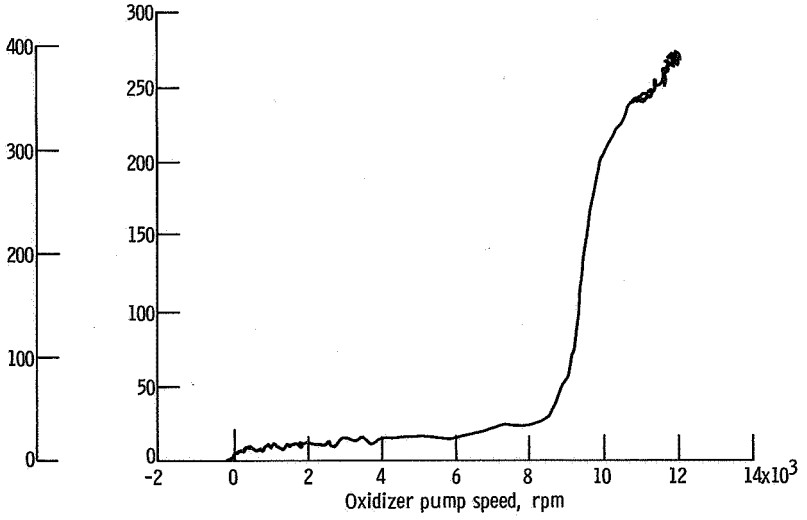

(d-2) C-2 engine.

(d) Second firing, AC-14.

Figure VI-7. - Continued.

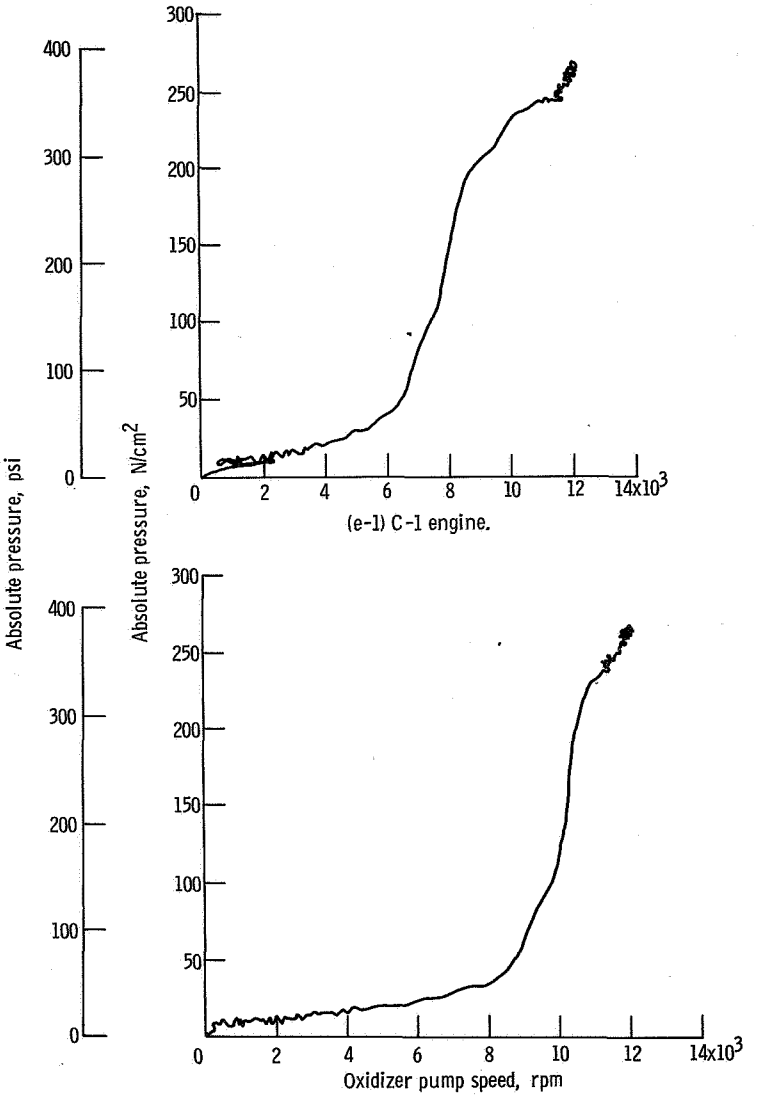

(e-1) C-1 engine.

(e-2) C-2 engine.

(e) First firing, AC-15.

Figure VI-7. - Continued.

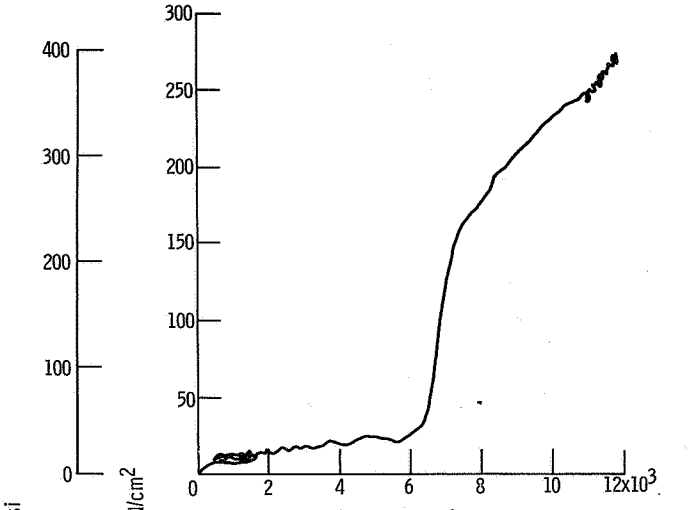

(f-1) C-1 engine.

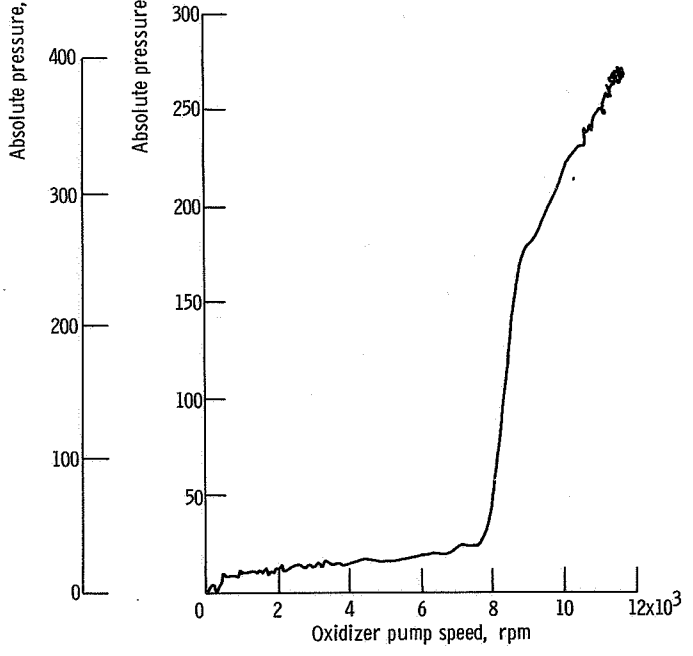

(f-2) C-2 engine.

(f) Second firing, AC-15.

Figure VI-7. - Concluded.

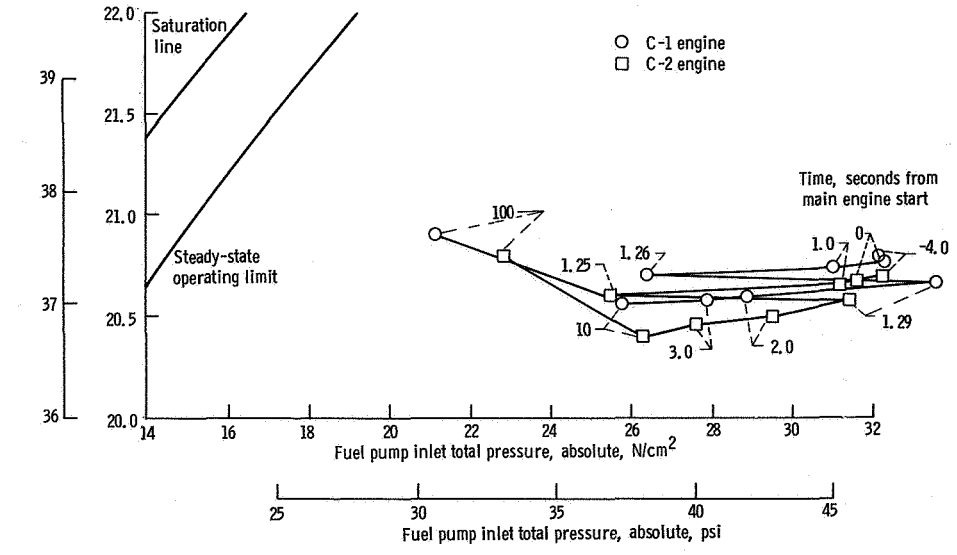

(a) Fuel pump, AC-13.

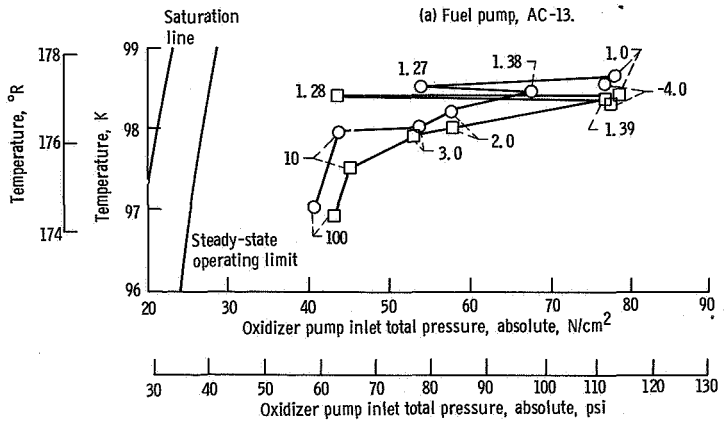

(b) Oxidizer pump, AC-13.

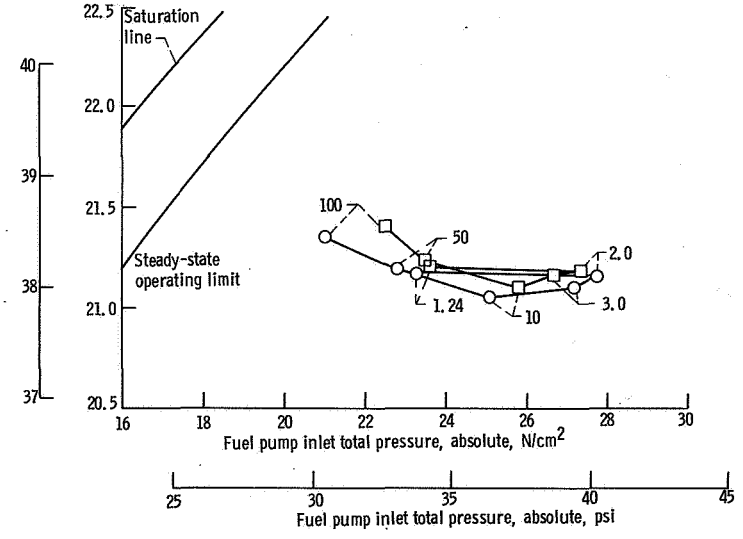

(c) Fuel pump, AC-14.

Figure VI-8. - Centaur fuel pump and oxidizer pump inlet conditions, engine second firing; AC-13, AC-14, and AC-15.

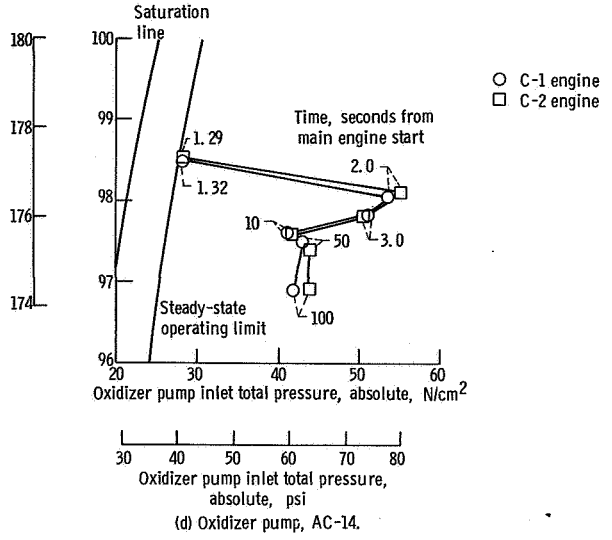

(d) Oxidizer pump, AC-14.

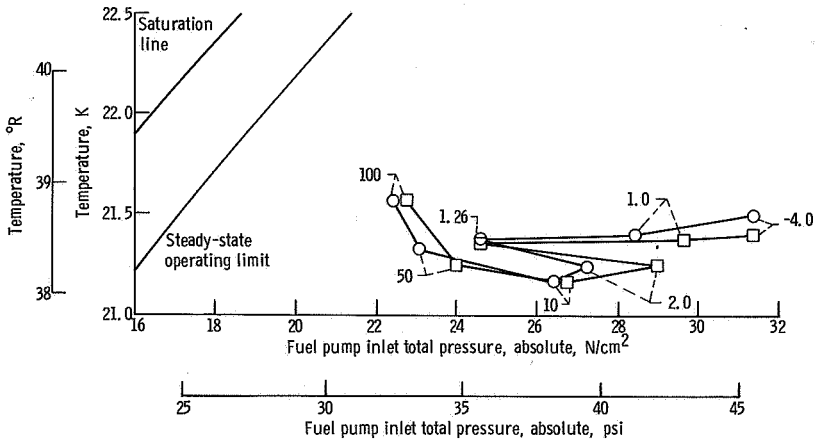

(e) Fuel pump, AC-15.

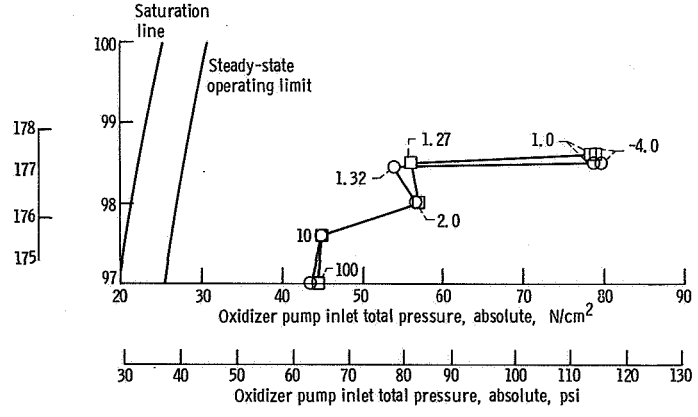

(f) Oxidizer pump, AC-15.

Figure VI-8. - Concluded.

Centaur Boost Pump and Propellant Supply System

System description. - A single boost pump is used in each propellant tank to supply propellants to the main engine turbopumps at the required inlet pressures. Each boost pump is a mixed-flow centrifugal type and is powered by a hot-gas-driven turbine. The hot gas consists of superheated steam and oxygen from the catalytic decomposition of 90 percent concentration hydrogen peroxide. Constant turbine power is maintained on each pump by metering the hydrogen peroxide through fixed orifices upstream of the catalyst bed. A speed-limiting control system is provided on each turbine to prevent overspeed under abnormal operating conditions. The complete boost pump and hydrogen peroxide supply systems are shown in figures VI-9 to VI-12. Flow from each boost pump discharge is routed to the main engine pump inlet through insulated propellant supply lines. Recirculation lines with flow-limiting venturis are connected to the supply lines immediately upstream of the main engine inlet valves. The purpose of these recirculation lines is to remove trapped gases from the supply lines prior to main engine first start and to aid in supply line chilldown prior to main engine second start. A schematic of the supply and recirculation lines is shown in figure VI-2.

Boost pump performance. - Performance of the boost pumps was satisfactory during both the first and second operating periods of all three flights (AC-13, AC-14, and AC-15). Minor abnormal conditions were observed but had little effect on the overall main engine and boost pump system performance. Boost pump start and cutoff times, referenced to main engine start time, are listed in table VI-7 for all three flights.

The turbine inlet pressure delay times (time from boost pump start signal to time of first indication of turbine inlet pressure rise) ranged from a minimum of 0.5 second to a maximum of 1.2 seconds for all three flights. The liquid-oxygen boost pump turbine inlet pressure transducer exhibited a very slow response to pressure changes during the first operating period on AC-13 and during the second operating periods of AC-14 and AC-15. This transducer completely failed to respond during the AC-15 first operating period. It is believed that the improper functioning of this transducer was caused by moisture (from the hydrogen peroxide decomposition products) freezing and blocking the transducer sensing line. Corrective action has been taken for future flights to thermally isolate the sensing line from the liquid-oxygen tank with nonconductive clamps and insulation blocks.

Steady-state turbine inlet pressure values for all flights are compared with the expected values in table VI-8. Expected values were obtained from prelaunch acceptance test data for each turbine. The flight turbine inlet pressures were within 1.5 percent of the expected values for all flights.

A momentary decrease in turbine inlet pressures occurred shortly after main engine second start on all three flights (figs. VI-13 and VI-14). This same phenomenon has

been observed on previous two-burn flights. The greatest reduction in pressure on AC-13, AC-14, and AC-15 was approximately 50 percent of the steady-state pressure. The longest duration of reduced pressure was approximately 3 seconds. The momentary decrease in turbine inlet pressure has been attributed to entrainment of a small amount of gas into the liquid flow from the hydrogen peroxide supply bottle. The configuration of the hydrogen peroxide supply bottle is such that a small quantity of gas could be trapped at the top of the bottle. This small quantity of gas was probably dislodged by disturbances during the engine start transient and was subsequently entrained in the liquid flow to the boost pumps. The assumption that the gas bubbles were dislodged by disturbances at main engine start is substantiated by calculated times of 3 and 10 seconds for a bubble to flow from the hydrogen peroxide supply bottle to the liquid-oxygen and liquid-hydrogen boost pump turbine catalyst beds, respectively. To simplify the calculations it was assumed that a gas bubble would move at the same velocity as the fluid flow velocity. From figures VI-13 and VI-14, it is apparent that the first bubbles arrived at the turbine catalyst beds at 7 seconds (oxidizer boost pump) and at 11 to 13 seconds (fuel boost pump) after main engine start signal. The longer gas flow times for the flight case can be partially attributed to the fact that gas bubbles do not move at the same velocity as the fluid, but actually move more slowly since their movement is dependent on the drag forces produced on the bubble by the fluid stream.

The momentary decreases in turbine inlet pressure had little effect on the boost pump performance. The largest effect was on the AC-14 liquid-hydrogen boost pump, where a speed decrease of approximately 1200 rpm was noted. This speed decrease did not affect main engine performance.

Boost pump turbine data are presented in figures VI-15 and VI-16 for the first operating period, and in figures VI-17 and VI-18 for the second operating period, for all flights. As shown in these figures, the initial acceleration of each boost pump to full operating speed prior to main engine start was almost identical on all flights. The small deviation in steady-state turbine speeds (after main engine start) for the three flights was due to the differences in turbine power calibration. Steady-state turbine speeds are compared to the expected values (expected values were obtained from prelaunch acceptance test data for each turbine) in table VI-8. As shown in the table, the actual flight values were consistently higher than the expected values (maximum difference was approximately 5 percent higher than expected speeds for AC-13). These differences may be partially attributed to the accuracy of the telemetry and instrumentation system. However, the fact that the flight speeds were consistently higher than the ground test values indicated that the higher flight turbine speeds were probably valid. This latter position has been substantiated by previous flights where higher than expected turbine speeds were also noted, and were accompanied by a higher than expected pressure rise across the pumps. We believe that this shift in turbine performance is primarily

caused by the inability to exactly duplicate the flight conditions during ground test calibration of each boost pump (simulation of backpressure at the turbine exhaust, hydrogen peroxide supply flow rate, liquid propellant flow rate through the pump, etc.).

Liquid-hydrogen and liquid-oxygen boost pump turbine bearing temperature data are presented by figures VI-19 and VI-20, respectively, for all three flights. The first and most significant rise in temperatures occurred during the first boost pump operating periods. During the coast periods, the temperatures continued to rise, but at a slower rate, as a result of heat transfer from the hot turbine rotor and exhaust casing. During the second operating period, the temperature rise rates again increased until termination of the second operating period. For a short period of time following the boost pump second cutoff, the temperatures continued to rise as a result of the heat transfer previously mentioned. Subsequently, a very slow decrease in temperatures occurred as the hot turbines gradually cooled because of thermal radiation to the space environment.

As previously discussed in the section Centaur Main Engines, a momentary cavitation of both main engine oxidizer turbopumps occurred during the high-flow acceleration period of the second engine start on AC-14. A similar, but more severe, cavitation of the main engine oxidizer turbopumps occurred on the AC-6 flight during main engine first start (ref. 3). The AC-6 problem was attributed to insufficient pressurization of the liquid-oxygen tank. The lack of sufficient pressure in the tank resulted in oxidizer boost pump cavitation, and subsequent cavitation of the main engine oxidizer turbopumps.

We believe that the AC-14 engine pump cavitation problem was also caused by insufficient oxidizer tank pressurization and subsequent boost pump cavitation. On AC-6, a significant increase in oxidizer boost pump turbine speed occurred during the time of main engine turbopump cavitation (main engine start + 1.2 sec); no increase was noted on AC-14. A boost pump turbine speed increase at this time in the start sequence is strong evidence of boost pump cavitation.

An analysis of the AC-14 data at 1.2 seconds after main engine start revealed that the ullage pressure was 0.1 newton per square centimeter (0.2 psi) less than the saturation pressure of the fluid at the boost pump inlet. The boost pump inlet pressure must be at least 0.27 newton per square centimeter (0.4 psi) greater than the saturation pressure to prevent pump cavitation. Based on this analysis, it was concluded that insufficient tank pressurization was the most likely cause of the AC-14 problem. The pressurization flow to the liquid-oxygen tank was increased on AC-15 to ensure sufficient pressure at the boost pump inlet. This corrective action appeared to be satisfactory since there was no recurrence of the cavitation problem on AC-15. The oxygen tank ullage pressures, the fluid saturation pressures at the liquid-oxygen boost pump inlet, and the differences between ullage and saturation pressures are given in the following table for the AC-13, AC-14, and AC-15 flights:

	Units	AC-13	AC-14	AC-15
Tank ullage absolute pressure, P_u	N/cm^2	21.3	21.1	22.0
	psi	30.9	30.5	31.9
Boost pump inlet saturation absolute pressure, P_s	N/cm^2	19.6	21.2	21.0
	psi	28.4	30.7	30.4
Pressure difference, $P_u - P_s$	N/cm^2	+1.7	-0.1	+1.0
	psi	+2.5	-.2	+1.5

Propellant supply lines. - A problem unique to the use of cyrogenic propellants for a two-burn vehicle is the required thermal preconditioning of the propellant supply lines and engine turbopumps prior to the main engine second start. Solar and Earth thermal radiation results in heating of these components during the coast phase. Unless these components are adequately cooled, main engine turbopump cavitation may occur during the second start sequence.

Cooling of the propellant supply lines and main engine turbopumps is accomplished on Centaur by opening the main engine inlet valves. This permits liquid oxygen and liquid hydrogen to flow through the supply lines and engine turbopumps.

Ground testing of the combined engine and propellant supply systems prior to the AC-13 flight (utilizing maximum predicted component temperatures for the tests) was conducted to determine an acceptable second-start prechill sequence. From these tests it was determined that a period of 17 seconds provided satisfactory chilldown. This 17-second prechill period was used on the AC-13, AC-14, and AC-15 flights for the second start sequence.

Temperature transducers were located in the propellant supply lines immediately upstream of the engine turbopump inlet valves on AC-13, AC-14, and AC-15. These transducers generally indicate the presence of liquid when they are on-scale, and gas conditions when they are off-scale high. A sudden rise in temperature towards off-scale high can be interpreted as local evaporation of the cryogenic liquids in the line. A sudden decrease in temperature from off-scale high can be interpreted as the replacement of the gas by liquid. The response of these transducers during the coast and restart sequence gave a relative indication of the amount of heat input to the propellants in the supply lines, and of the amount of heat absorbed by the propellant supply lines during the coast period.

Unfortunately, no data were obtained from these transducers on the AC-13 and AC-14 flights during the time periods of most interest (due to either no telemetry coverage or poor quality data). However, the desired data were obtained during the AC-15 flight. The usable data from each flight are compared in figure VI-21. On the AC-13 flight, the coast period was very short, which resulted in only the liquid-hydrogen lines drying at the engine inlets during the coast. On the AC-14 flight, the coast period was

approximately twice as long as on the AC-13 flight and resulted in local drying of the liquid-hydrogen lines and the C-1 engine liquid-oxygen line. The duration of the AC-15 coast period was more than three times that of the AC-13 flight and resulted in local drying of all lines. Liquid conditions were reestablished at the engine inlets on all three flights well in advance of main engine second start. Liquid conditions were reestablished on the C-1 liquid-oxygen line on AC-14 and AC-15 by the slight increase in longitudinal acceleration produced when the two 222-newton- (50-lbf-) thrust propellant settling engines were activated prior to boost pump second start. In all other cases, liquid conditions were reestablished either before, or a few seconds after, the initiation of the in-flight chilldown period. It was concluded from these data (and similar data from previous Centaur two-burn flights) that, for coast periods of as long as 25 minutes, only 3 or 4 seconds of the in-flight chilldown period is required to assure liquid conditions at the engine inlets.

TABLE VI-7. - CENTAUR BOOST PUMP START AND CUTOFF TIMES

	AC-13	AC-14	AC-15
Time of boost pump first start referenced to main engine first start, sec	MES-1 - 42.8	MES-1 - 41.9	MES-1 - 45.7
Time of boost pump first cutoff referenced to main engine first start, sec	MES-1 + 329.3	MES-1 + 323.9	MES-1 + 332.9
Time of boost pump second start referenced to main engine second start, sec	MES-2 - 28	MES-2 - 28	MES-2 - 28
Time of boost pump second cutoff referenced to main engine second start, sec	MES-2 + 114.1	MES-2 + 115.7	MES-2 + 115.6

TABLE VI-8. - COMPARISON OF EXPECTED AND FLIGHT CENTAUR BOOST PUMP STEADY-STATE TURBINE PERFORMANCE

Data Source		Liquid-oxygen boost pump turbine			Liquid-hydrogen boost pump turbine		
		Turbine inlet absolute pressure		Turbine speed, rpm	Turbine inlet absolute pressure		Turbine speed, rpm
		N/cm^2	psi		N/cm^2	psi	
AC-13	Flight values from first operating period	64.6	93.7	34 200	65.6	95.4	42 050
	Flight values from second operating period	64.6	93.7	34 200	65.6	95.4	42 750
	Expected values from ground calibration tests	65.5	95.0	32 600	66.4	96.3	40 500
AC-14	Flight values from first operating period	65.6	95.5	33 500	67.7	98.3	40 300
	Flight values from second operating period	64.9	94.2	34 100	67.7	98.3	40 600
	Expected values from ground calibration tests	65.2	94.7	33 500	67.8	98.4	39 400
AC-15	Flight values from first operating period	(a)	(a)	34 000	67.5	98.0	41 700
	Flight values from second operating period	(a)	(a)	34 000	67.2	97.5	41 700
	Expected values from ground calibration tests	65.1	94.4	33 500	68.1	98.7	40 250

[a]No data due to transducer failure.

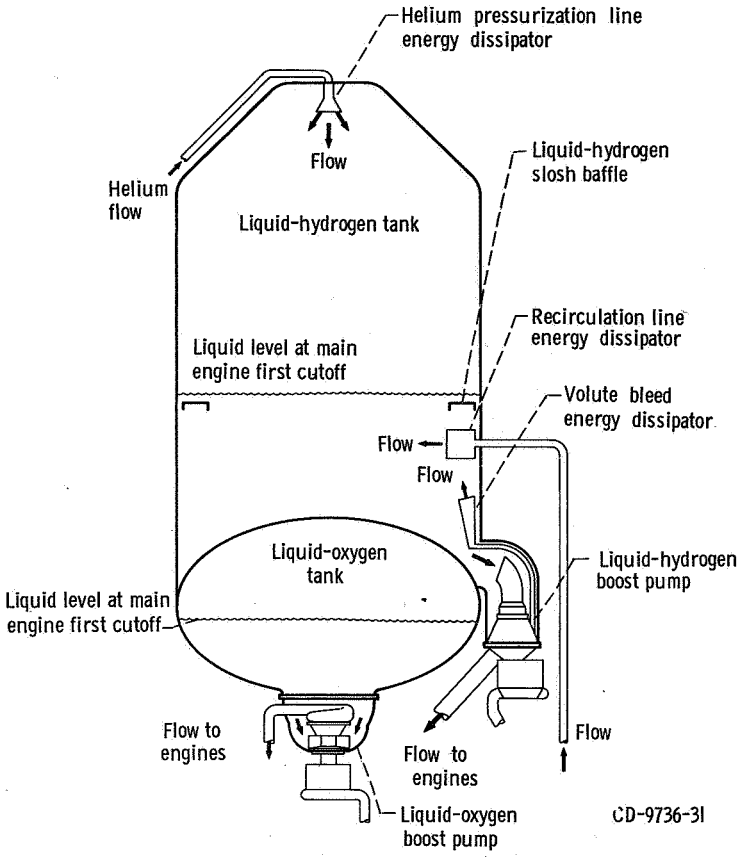

Figure VI-9. - Location of Centaur liquid-hydrogen and liquid-oxygen boost pumps; AC-13, AC-14, and AC-15.

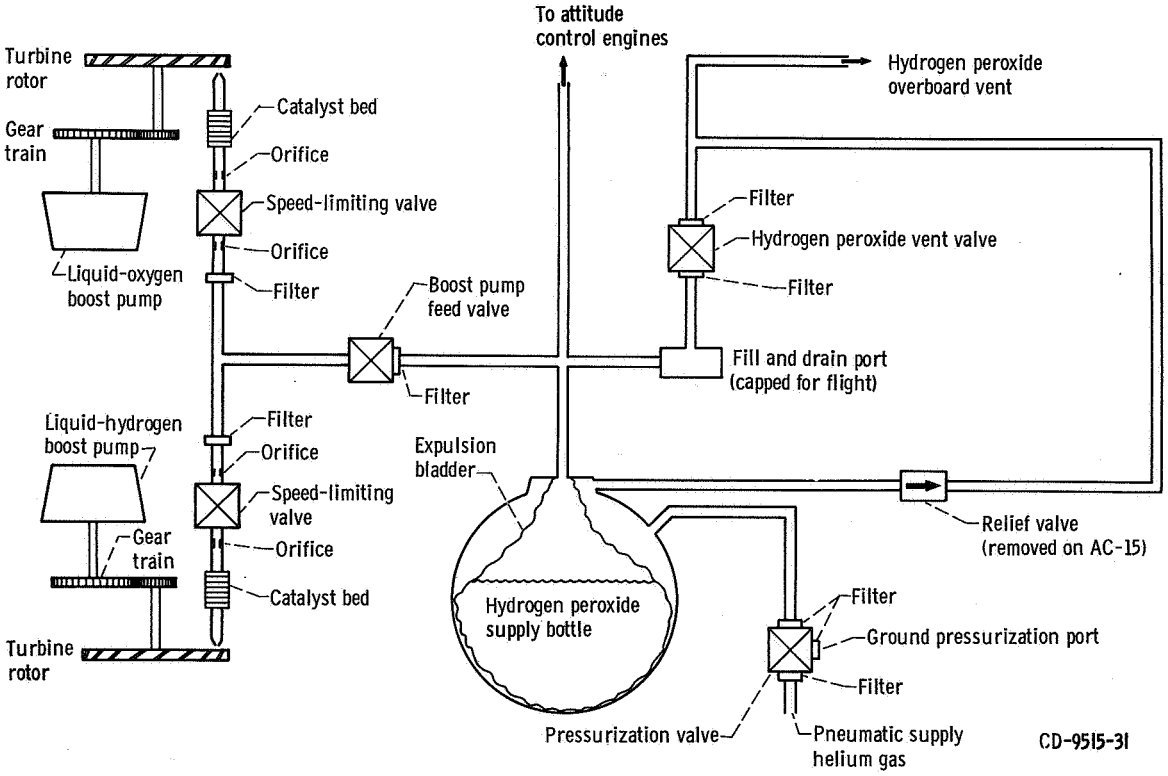

Figure VI-10. - Schematic drawing of Centaur boost pump hydrogen peroxide supply; AC-13, AC-14, and AC-15.

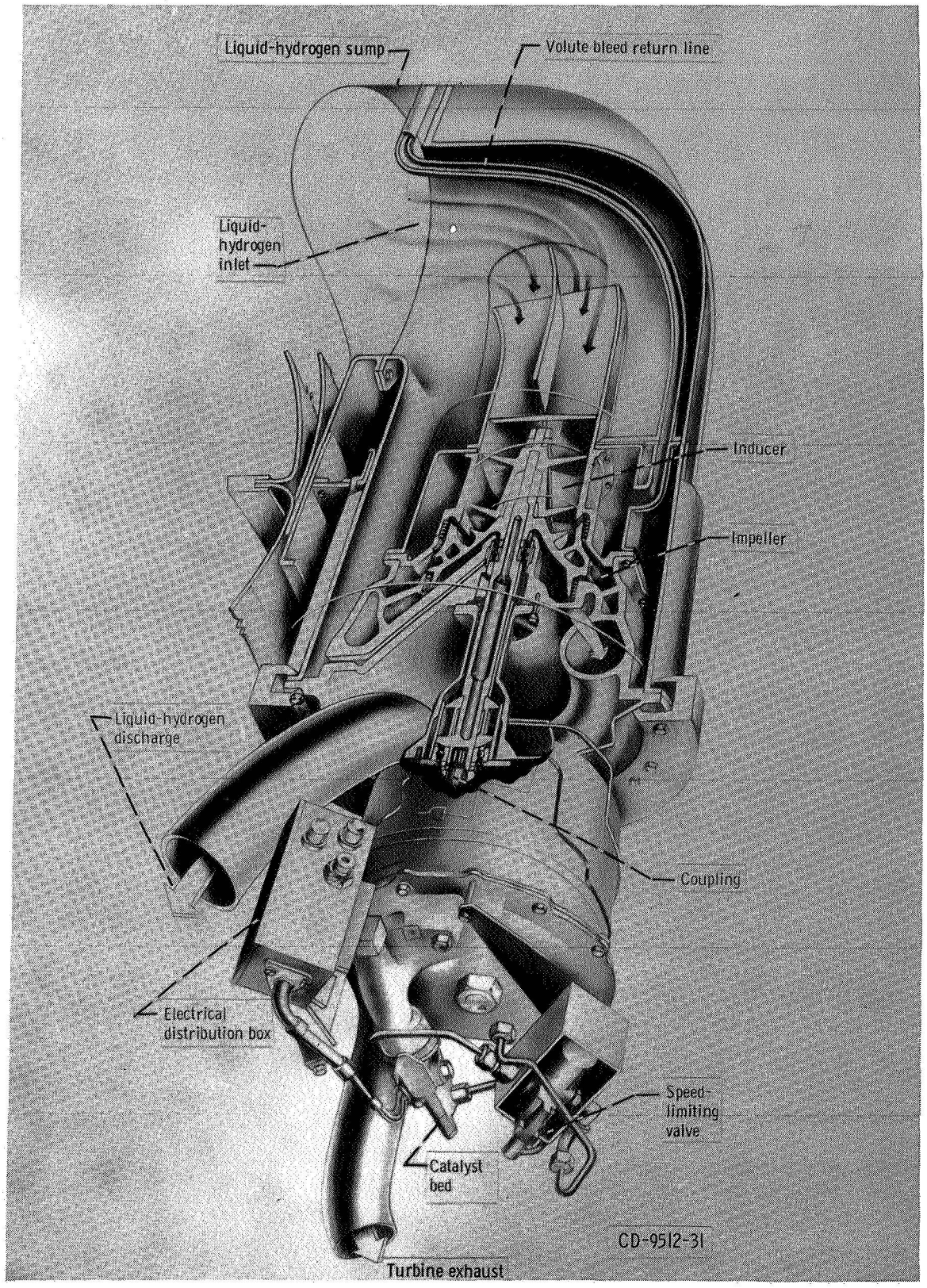

Figure VI-11. - Centaur liquid-hydrogen boost pump and turbine cutaway; AC-13, AC-14, and AC-15.

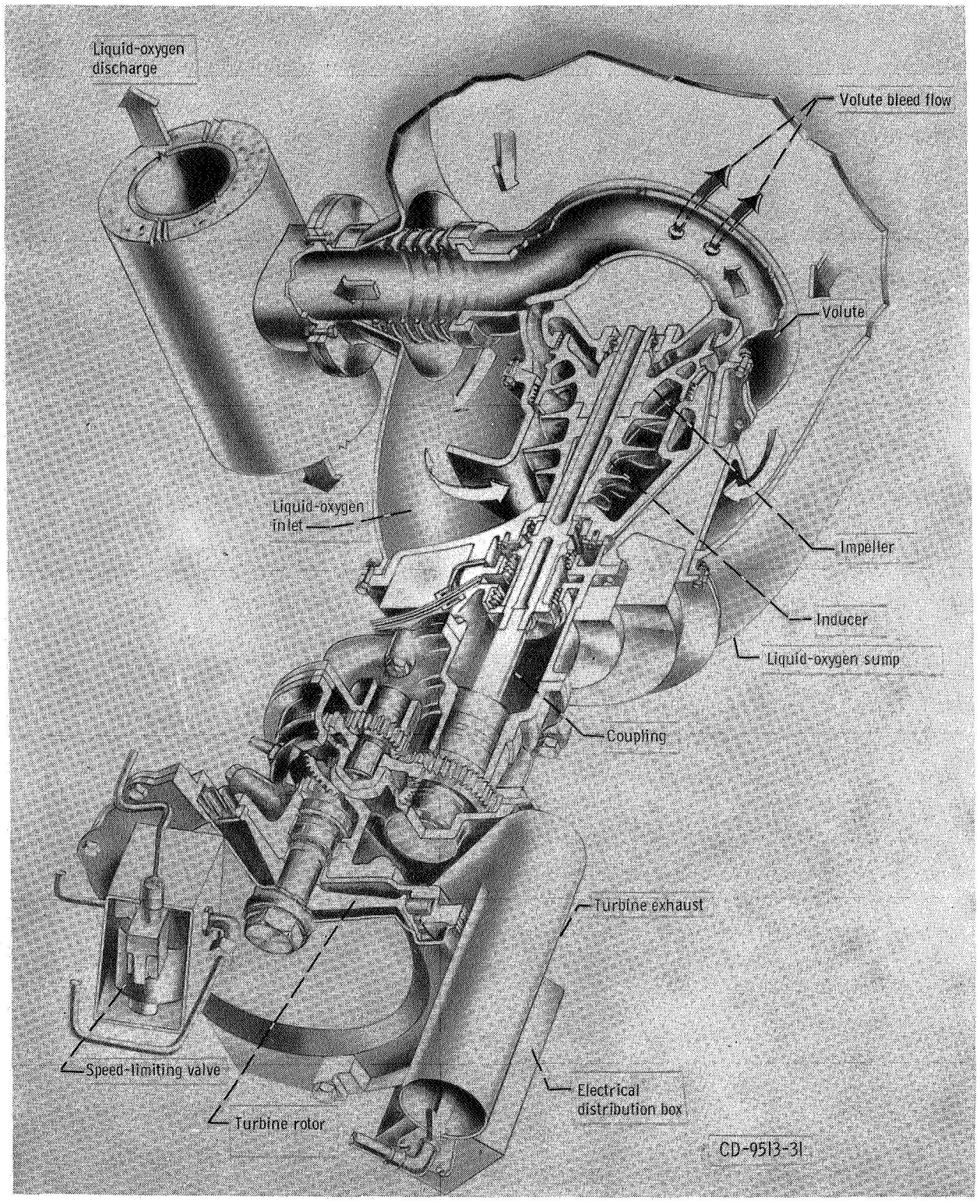

Figure VI-12. - Centaur liquid-oxygen boost pump and turbine cutaway; AC-13, AC-14, and AC-15.

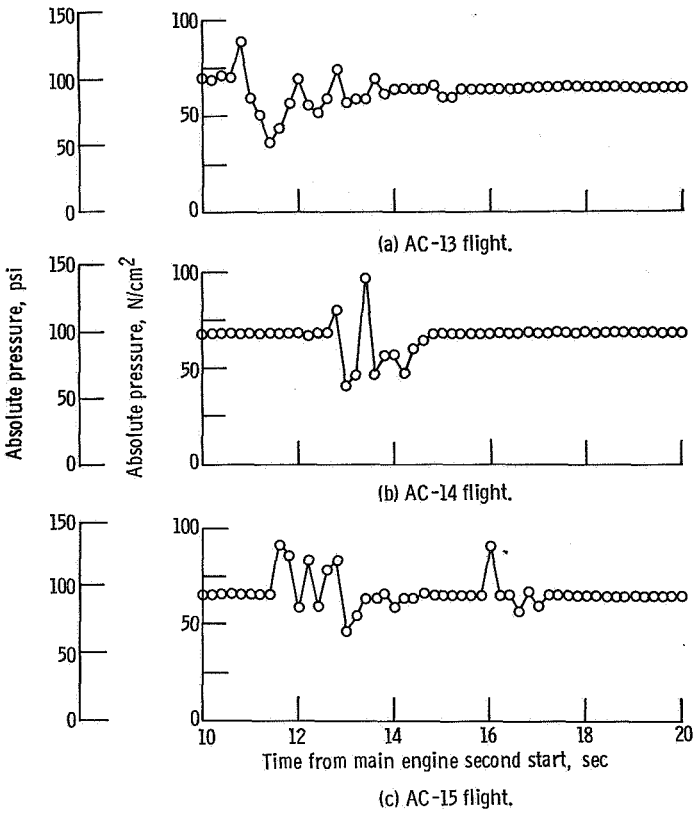

(a) AC-13 flight.

(b) AC-14 flight.

(c) AC-15 flight.

Figure VI-13. - Centaur liquid-hydrogen boost pump turbine inlet pressure comparison during main engine second firing; AC-13, AC-14, and AC-15.

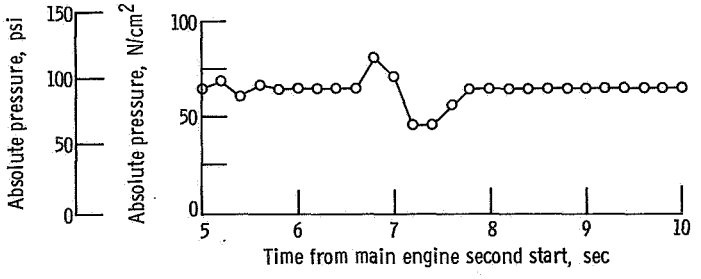

Figure VI-14. - Centaur liquid-oxygen boost pump turbine inlet pressure during main engine second firing, AC-13. Data for AC-14 and AC-15 are not available because of a transducer failure.

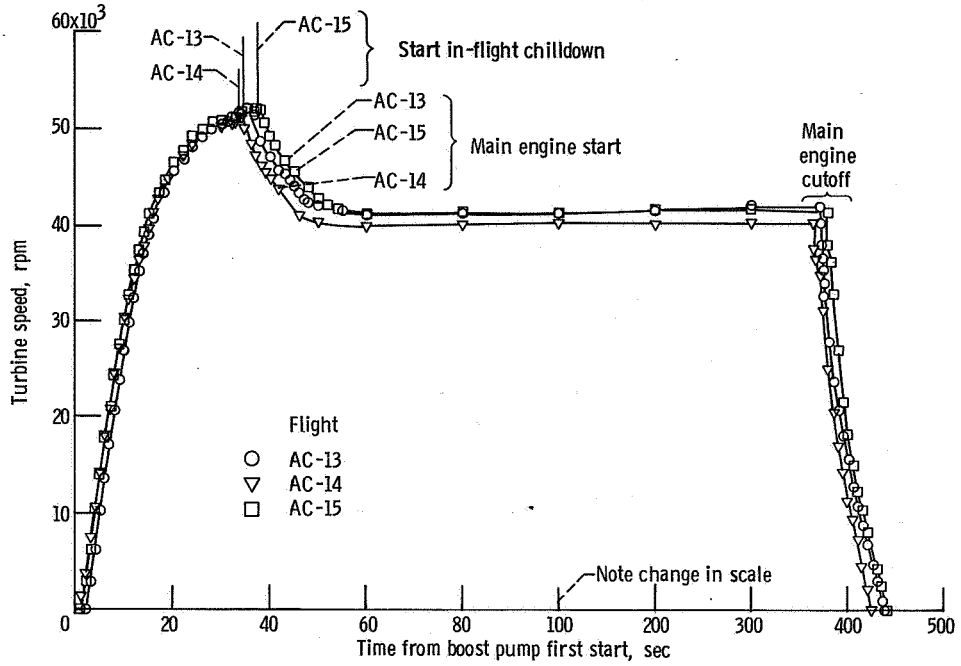

Figure VI-15. - Centaur liquid-hydrogen boost pump turbine speed comparison, first operating period; AC-13, AC-14, and AC-15.

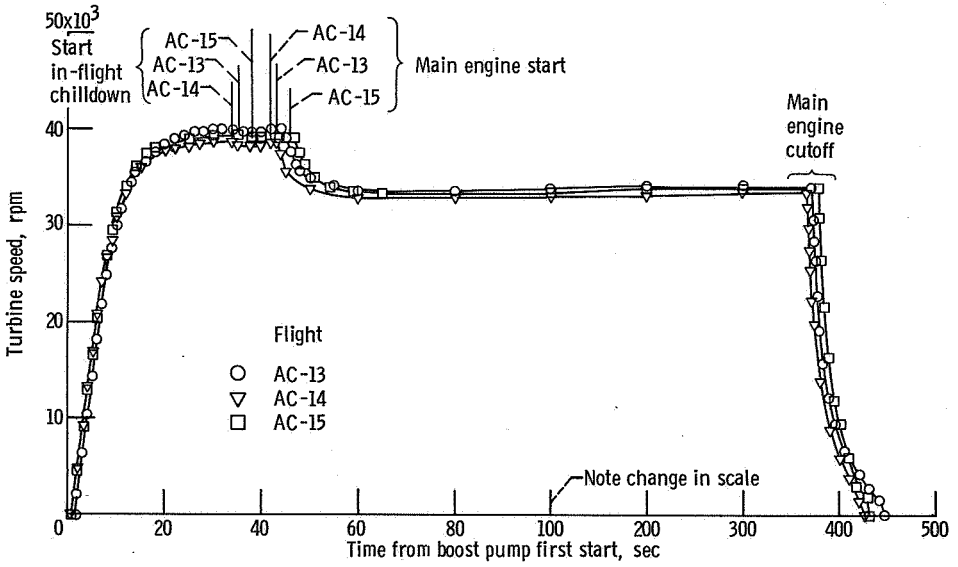

Figure VI-16. - Centaur liquid-oxygen boost pump turbine speed comparison, first operating period; AC-13, AC-14, and AC-15.

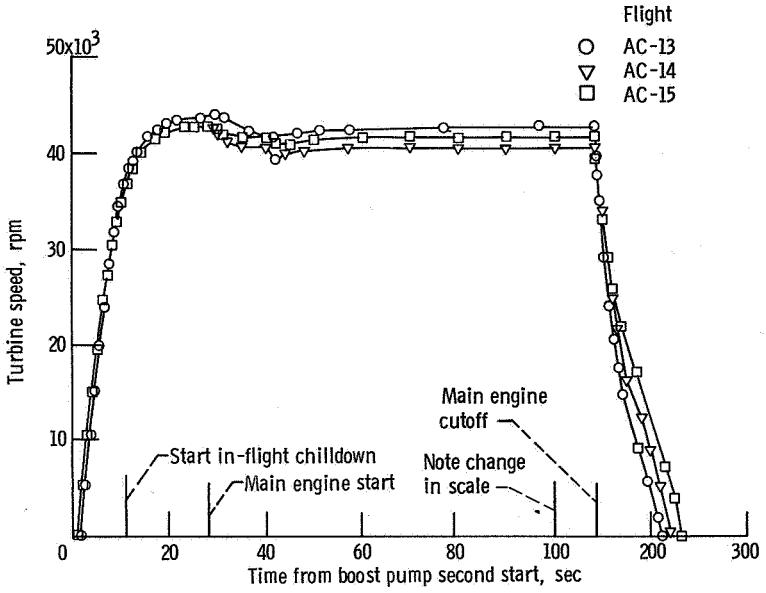

Figure VI-17. - Centaur liquid-hydrogen boost pump turbine speed comparison, second operating period; AC-13, AC-14, and AC-15. No data coverage on AC-14 until main engine start.

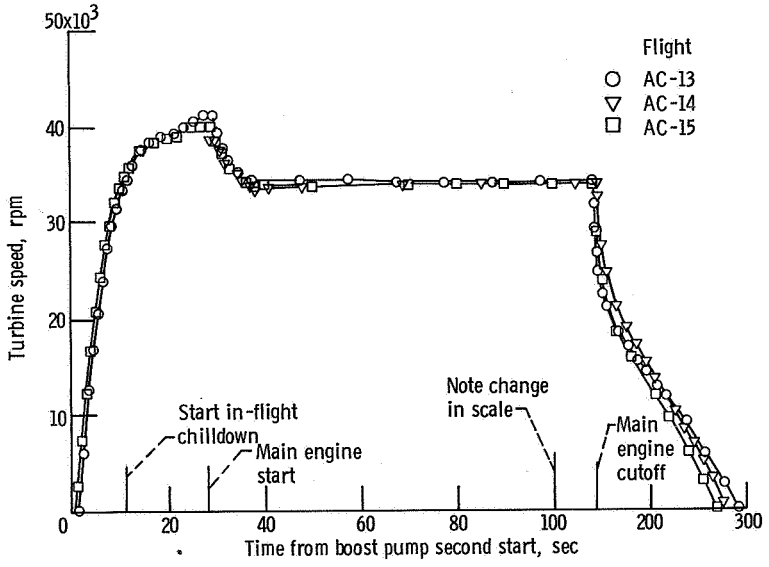

Figure VI-18. - Centaur liquid-oxygen boost pump turbine speed comparison, second operating period; AC-13, AC-14, and AC-15. No data coverage on AC-14 until main engine start.

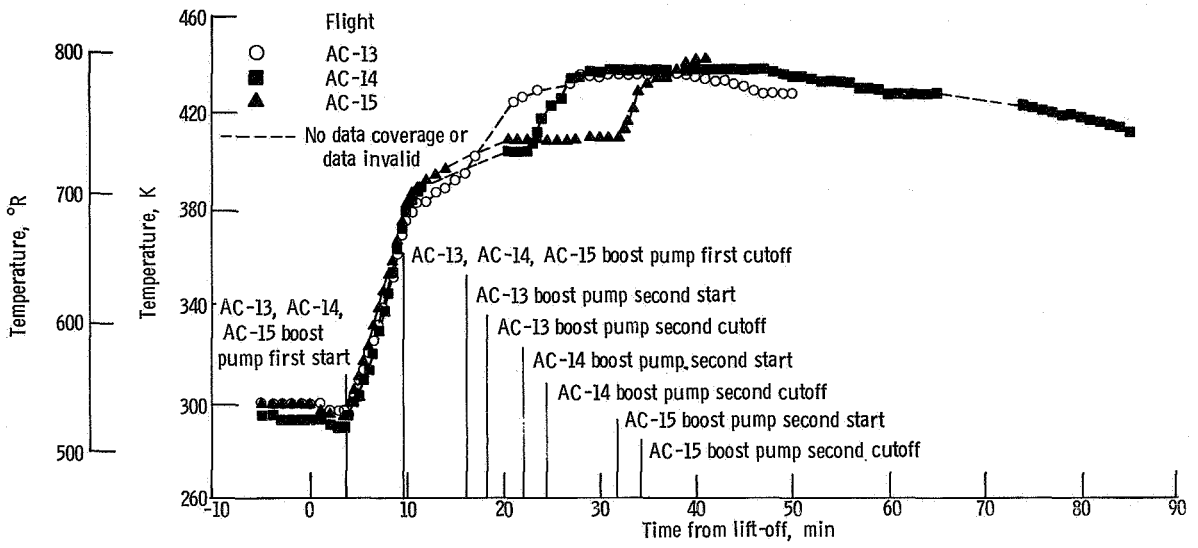

Figure VI-19. - Centaur liquid-hydrogen boost pump turbine bearing temperature; AC-13. AC-14, and AC-15.

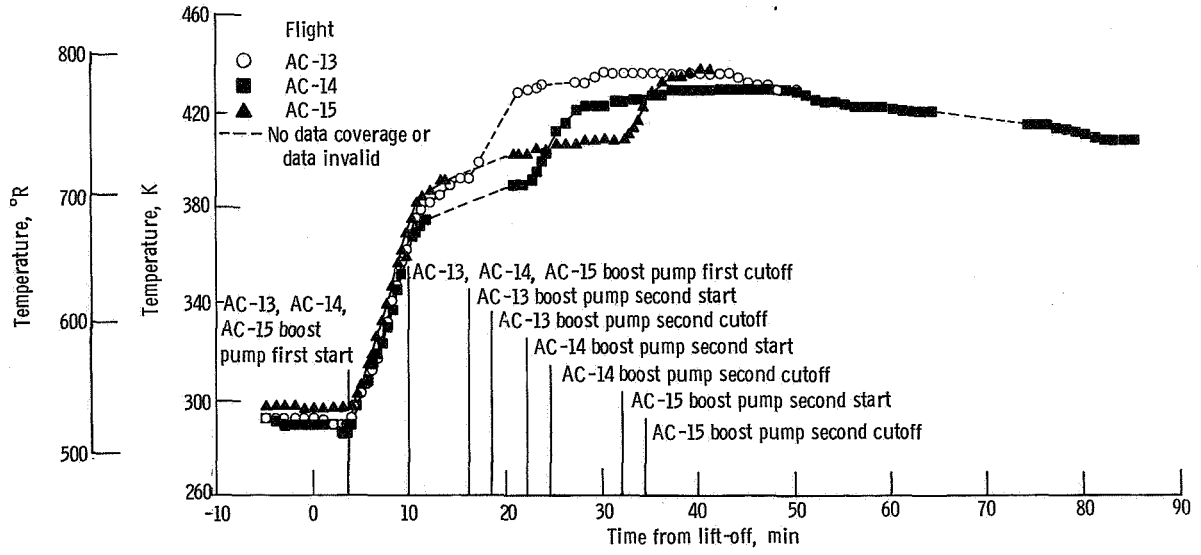

Figure VI-20. - Centaur liquid-oxygen boost pump turbine bearing temperature; AC-13, AC-14, and AC-15.

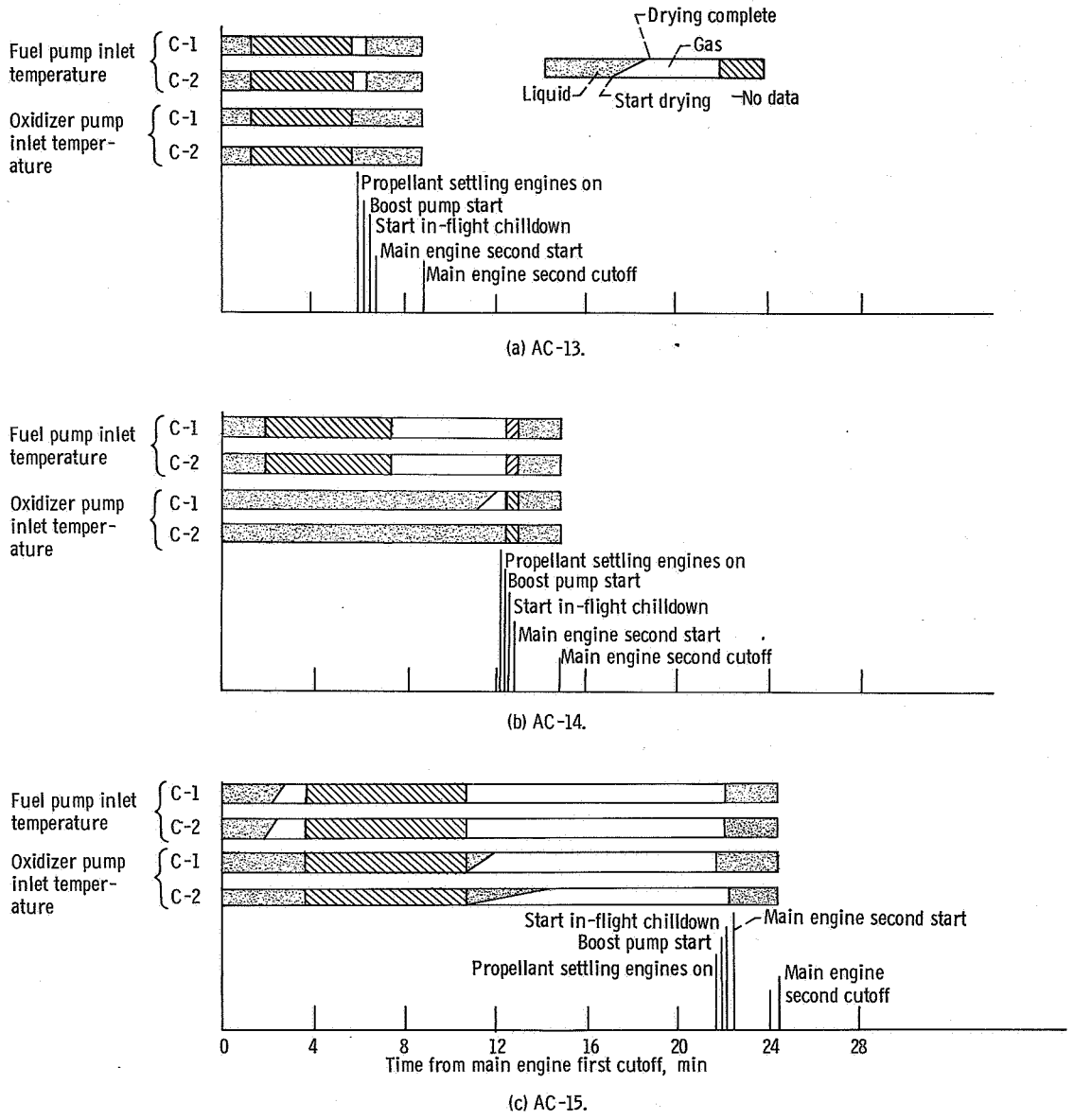

Figure VI-21. - Comparison of Centaur main engine turbopump inlet temperature transducer liquid/gas indication during coast and main engine second firing; AC-13, AC-14, and AC-15.

Hydrogen Peroxide Supply and Engine System

System description. - The hydrogen peroxide engines are used during the nonpowered portion of flight for attitude control, for propellant settling and retention, and to provide the initial thrust for the retromaneuver. There are four 13-newton- (3-lbf-) thrust engines, four 222-newton- (50-lbf-) thrust engines, and two clusters each of which consists of two 16-newton- (3.5-lbf-) thrust engines and one 27-newton- (6-lbf-) thrust engine. The 13-newton- (3-lbf-) and the 222-newton- (50-lbf-) thrust engines are used primarily for propellant settling and retention, and the clusters are used for attitude control (see table VI-24 GUIDANCE AND FLIGHT CONTROL SYSTEMS section). Propellant is supplied to the engines from a positive-expulsion, bladder-type storage tank which is pressurized to an absolute pressure of about 210 newtons per square centimeter (305 psi) by the pneumatic system. The hydrogen peroxide is decomposed in the engine catalyst beds, and the hot decomposition products are expanded through converging-diverging nozzles to provide thrust. Hydrogen peroxide is also provided to drive the boost pump turbines. The system is shown in figures VI-10 and VI-22.

System performance. - Engine chamber surface temperatures were recorded for two of the 222-newton- (50-lbf-) thrust engines (designated V-2 and V-4) and two of the 13-newton- (3-lbf-) thrust engines (designated S-2 and S-4). The firing commands to all of the engines were also recorded. All temperature data, with the exception of one measurement on AC-13, indicated the hydrogen peroxide engines performed satisfactorily on command. The temperature of the S-4 engine did not indicate normal performance. It should have been almost identical to that of the S-2 engine but, as shown in figure VI-23, it varied considerably. During the Centaur coast period when the engines were firing in the S-half-on mode (see table VI-24), the temperature of the S-4 engine indicated a maximum of 550 K (530^{o} F); it should have reached approximately 900 K (1160^{o} F). Then during the hydrogen peroxide experiment at the end of the mission, the temperature of S-4 engine indicated an increase from 371 K (209^{o} F) to 468 K (384^{o} F). There should not have been an increase in temperature at this time since the engine was not firing. The unusual thermal history of the S-4 engine cannot be definitely explained. However, it did not appear to be an engine performance problem because the vehicle rate gyro data did not indicate any abnormal forces on the vehicle. The problem is attributed to instrumentation.

On all three flights, the boost pump data indicated momentary gas flow (instead of liquid hydrogen peroxide) to the catalyst beds shortly after main engine second start (see the Centaur Boost Pump and Propellant Supply System section). On AC-13 and AC-14, attitude engine firing interruptions after the start of vehicle turnaround were also indicative of gas bubbles in the hydrogen peroxide supply system. This condition has been noted in past flights and is not considered to be serious because of the small amount of gas involved. The gas is assumed to originate from the hydrogen peroxide

bottle. Most of it is air trapped in the bottle prior to launch, and a small amount is gaseous oxygen evolved from decomposition of the hydrogen peroxide during the coast period. The small amount of gas flow has never seriously affected boost pump or attitude engine performance.

The postmission hydrogen peroxide experiment consisted of commanding the 222-newton- (50-lbf-) thrust engines to fire in the V-half-on mode for 100 seconds. The purpose of the experiment was to establish the time of hydrogen peroxide depletion and thereby determine propellant residuals. These data were useful in verifying estimated propellant consumption rates. On AC-13, the engines fired the entire duration of 100 seconds. At estimated consumption rates, this time period corresponded to approximately 32.7 kilograms (72.2 lbm) of propellant consumption. Since propellant depletion never occurred, the residual at the end of the normal mission was greater than this quantity. The reason for the large residual on this flight was the small amount of hydrogen peroxide used during the short coast period. The "S" engines fire continuously in the S-half-on mode during the coast period. On AC-14 and AC-15, propellant depletion occurred after 83 and 50.1 seconds, respectively. These times corresponded to 27.2 and 16.4 kilograms (60.0 and 36.2 lbm) of propellant, respectively. The difference in residuals was due to the different length of the coast periods. These experiments further verified that there was sufficient hydrogen peroxide available for the standard Surveyor indirect-ascent mission.

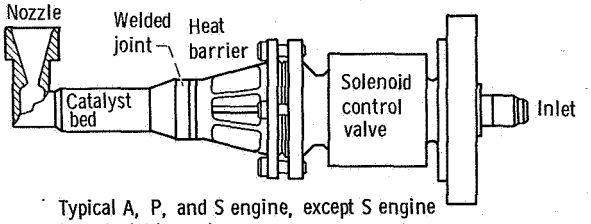

Typical A, P, and S engine, except S engine has straight nozzle

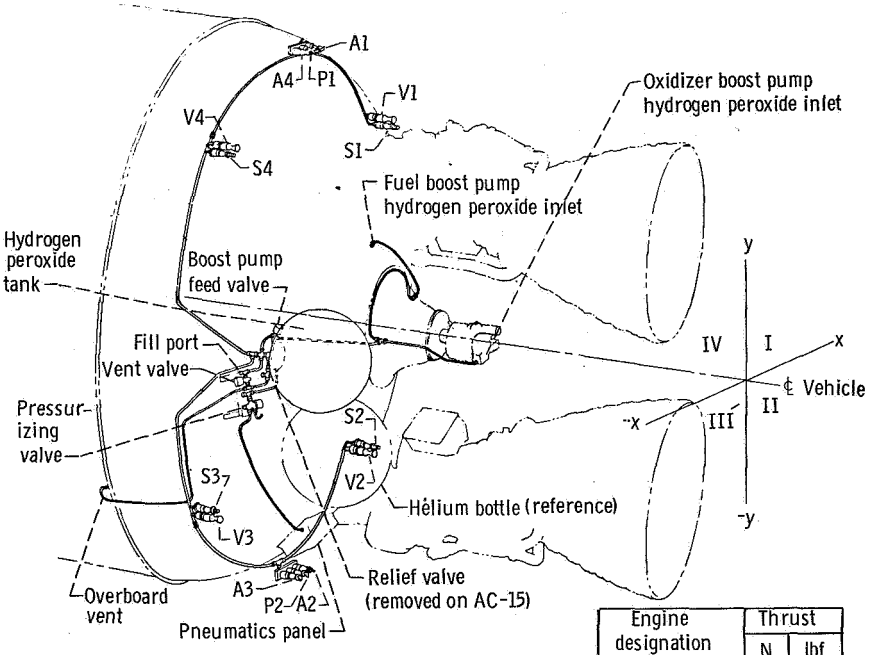

Hydrogen peroxide control system

Engine designation	Thrust	
	N	lbf
V1, V2, V3, V4	222	50
S1, S2, S3, S4	13	3
A1, A2, A3, A4	16	3.5
P1, P2	27	6

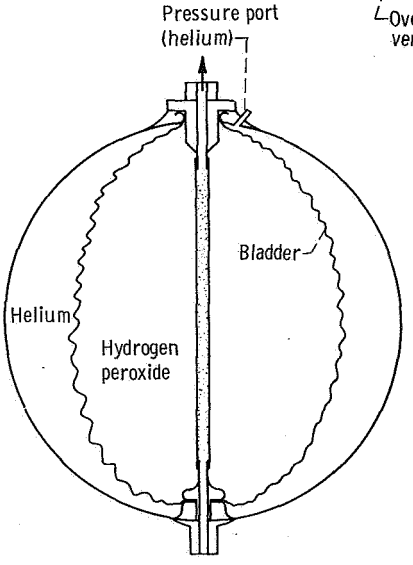

Hydrogen peroxide tank

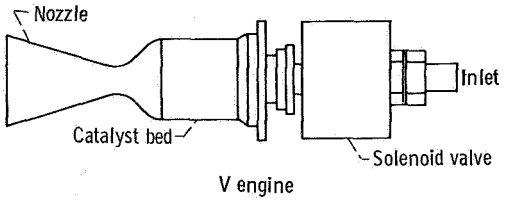

V engine

CD-9781-31

Figure VI-22. - Hydrogen peroxide system isometric; AC-13, AC-14, and AC-15.

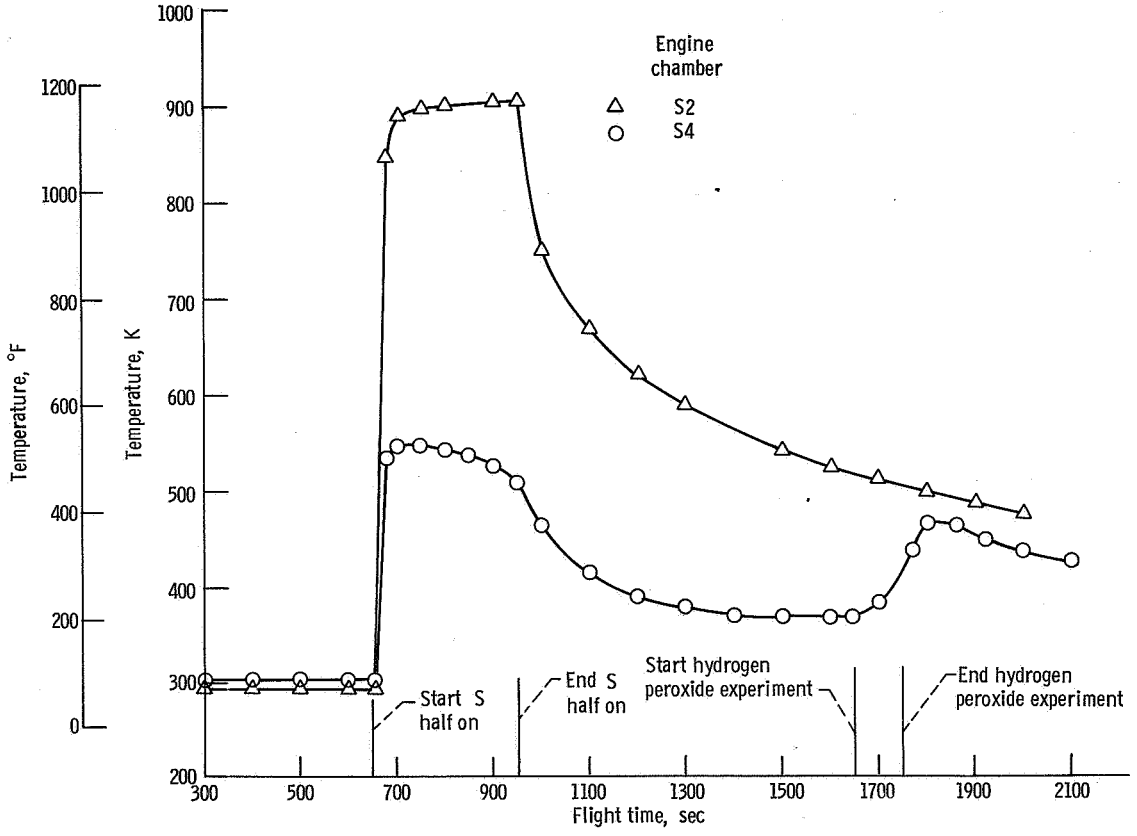

Figure VI-23. - Engine chamber surface temperatures, AC-13.

PROPELLANT LOADING AND PROPELLANT UTILIZATION SYSTEMS

by James A. Berns

Propellant Level Indicating Systems for Propellant Loading

System description. - Atlas liquid-oxygen loading levels are determined by liquid-level sensors (fig. VI-24) located at discrete points in the liquid-oxygen tank. The RP-1 (fuel) loading levels are determined by a fuel sight gage. The sight gage replaced the liquid-level sensor used in previous flights.

The sensors in the liquid-oxygen tank are platinum hot-wire sensors. The control unit for the platinum hot-wire liquid-oxygen sensors is an amplifier that detects a change in voltage level. The amplified signal is applied to an electronic trigger circuit. The liquid-oxygen sensors are supplied with a nearly-constant current of approximately 200 milliamperes. The voltage drop across a sensor reflects the resistance value of the sensor. The sensing element is a platinum wire (0.001 in. diam) which has a linear resistance temperature coefficient. When dry, the wire has a high resistance and, therefore, a high voltage drop. When immersed in a cryogenic fluid, it has a low resistance and voltage drop. When the sensor is wetted, a control relay is deenergized, and a signal is sent for the propellant loading operator.

The fuel sight gage is a portable unit which mounts directly on the vehicle and connects to the existing fuel probe by two sensing lines. Visual fuel level readings are taken during tanking. After tanking, the fuel sight gage assembly is removed, and the connection points on the vehicle are secured.

The Centaur propellant level indicating system (fig. VI-25) uses hot-wire liquid-level sensors in both the liquid-oxygen and liquid-hydrogen tanks. These sensors are similar in operation to the ones used in the Atlas liquid-oxygen tank.

Propellant weights. - Atlas fuel (RP-1) and liquid-oxygen weights tanked for AC-13, AC-14, and AC-15 are shown in table VI-9. These weights were calculated based on densities of 0.8 and 1.1 grams per cubic centimeter (49 and 69 lbm/ft^3), respectively.

Centaur propellant loading was satisfactorily accomplished. Calculated propellant weights at lift-off are also shown in table VI-9. Data used to calculate these propellant weights are given in table VI-10.

Atlas Propellant Utilization System

System description. - The Atlas propellant utilization system (fig. VI-26) is used to ensure nearly simultaneous depletion of the propellants and minimum propellant residuals at sustainer engine cutoff. This is accomplished by controlling the propellant

mixture ratio (oxidizer flow rate to fuel flow rate) to the sustainer engine. The system consists of two mercury manometer assemblies, a computer-comparator, a hydraulically actuated propellant utilization fuel valve, sensing lines, and associated electrical harnessing. During flight, the manometers sense propellant head pressures which are indicative of propellant mass. The mass ratio is then compared to a reference ratio (2.27 at lift-off) in the computer-comparator. If needed, a correction signal is sent to the propellant utilization valve controlling the fuel flow to the sustainer engine. The oxidizer flow is regulated by the head suppression valve. This valve senses propellant utilization valve movement and moves in a direction opposite to that of the propellant utilization valve. This opposite movement thus alters propellant mixture ratio to maintain constant combined propellant mass flow to the engine.

System performance. - The Atlas propellant utilization system operation was satisfactory. The propellant utilization system valve angles during flights are shown in figure VI-27.

The valve operated at the center position for approximately the first 13 seconds of flight because the error signal to the valve was grounded. The error signal was grounded to eliminate abnormal system behavior during this period.

The valves on AC-13, AC-14, and AC-15 were in the fuel-rich position from T + 13 seconds to approximately T + 120 seconds; and then operated about their center positions until approximately T + 230 seconds. After T + 230 seconds, the valves were on the oxygen-rich stop and remained there to ensure sustainer engine cutoff by usable oxygen depletion.

Atlas propellant residuals. - The residuals above the sustainer engine pump inlets at sustainer engine cutoff for AC-13, AC-14, and AC-15 are shown in the following table:

Propellant	Units	Atlas propellant residuals		
		AC-13	AC-14	AC-15
RP-1	kg	161	107	93
	lb	355	236	206
Liquid oxygen	kg	143	276	271
	lb			

These residuals were calculated by using the head sensing port uncovery times as reference points. Propellants consumed from port uncovery to sustainer engine cutoff include the effect of flow rate decay for liquid-oxygen depletion.

Centaur Propellant Utilization System

System description. - The Centaur propellant utilization system is used during flight to control propellant consumption by the main engines and provides minimum propellant residuals. The system is shown schematically in figure VI-28. It is also used during tanking to indicate propellant levels. The mass of propellant remaining in each tank is sensed by a capacitance probe, and the mass ratio is compared in a bridge balancing circuit. If the mass ratio of propellants remaining varies from a predetermined value (oxidizer-to-fuel ratio, 5 to 1), an error signal is sent to the proportional servopositioners which control the liquid-oxygen flow control valves. When the mass ratio is greater than 5 to 1, the liquid-oxygen flow is increased to return the ratio to 5 to 1. If the ratio is less than 5 to 1, the liquid-oxygen flow is decreased. Since the sensing probes do not extend to the top of the tanks, system control is not commanded on until approximately 90 seconds after main engine first start. For this 90 seconds of engine firing, the bridge is nulled, locking the liquid-oxygen flow control valves at a 5 to 1 propellant mixture ratio.

System performance. - All prelaunch checks and calibrations of the system were within specification. The in-flight operation of the system was satisfactory during both main engine firing periods. The system liquid-oxygen flow control valve positions during the engine firings are shown in figure VI-29. The system was commanded on by the vehicle programmer at approximately 90 seconds after main engine first start. The valves then moved to the oxygen-rich stop and remained there until the system compensated for an excess amount of oxygen. The results for AC-13, AC-14, and AC-15 are shown in the following table:

Event	Units	Propellant corrections after main engine first start		
		AC-13	AC-14	AC-15
Valves on oxygen-rich stop	sec	18	20	2.3
Excess of oxygen burned	kg	45	67	12
	lb	100	147	26

These corrections resulted from

(1) Engine consumption error during the first 90 seconds of engine firing

(2) Propellant loading errors

(3) System bias to ensure that liquid oxygen depleted first

(4) System bias to compensate for liquid-hydrogen boiloff during coast (No liquid oxygen was vented, and, if this compensation was not made, the mass ratio in the tanks at main engine second start would not be 5 to 1.)

The system commanded the valve to control mainly in a hydrogen-rich position during the remainder of the engine first firing period.

At main engine first cutoff, the valves moved to the oxygen-rich stop. Approximately 10 seconds after engine shutdown, the system bias for the coast-phase liquid-hydrogen boiloff was removed from the system. At this time, the valves began to move to the hydrogen-rich stop, in response to the hydrogen-rich propellant ratio in the tanks. After main engine first cutoff, the propellants began to rise in the sensing probes as a result of capillary action. By approximately 100 seconds after main engine cutoff, capillary action had caused the propellants to rise into the probes sufficiently to result in an indication of an oxygen-rich propellant mass ratio, which caused the valves to move to the oxygen-rich stop. Discussion of capillary rise is found in reference 4. The valves remained at the oxygen-rich stop until after main engine second start (fig. VI-29) After engine second start, the valves moved from the stop and then controlled at a hydrogen-rich valve angle. The length of time the valves were on their stops varied with each flight because of the errors in tank mixture ratio. Approximately 25 seconds prior to main engine second cutoff, the valves were commanded to the 5 to 1 mixture ratio position. This was done because the sensing probes do not extend to the bottoms of the tanks, and system control is ended after the liquid level drops below the bottoms of the probes.

Propellant residuals. - The propellant residuals were calculated by using data obtained from the propellant utilization system. The gaseous hydrogen residual at main engine first cutoff was calculated by using density data obtained from flights AC-8 and AC-9. The gaseous oxygen residuals were calculated by assuming saturated oxygen gas at main engine first cutoff.

The propellant residuals and the corresponding liquid levels (station numbers) at main engine first cutoff, are shown in the following table:

Event	Units	Propellant					
		Hydrogen			Oxygen		
		AC-13	AC-14	AC-15	AC-13	AC-14	AC-15
Liquid residual at main engine first cutoff	kg	684	717	698	3225	3404	3232
	lbm	1507	1580	1538	7111	7504	7127
Gaseous residual at main engine first cutoff	kg	24	23.8	24.1	43	42	43.5
	lbm	53.5	52.9	53.4	95.5	92.8	96.0
Liquid level, station number[a]	---	327.5	324.7	326.13	423.9	427.9	423.9

[a]See fig. III-2 for vehicle station numbers.

The propellant residuals remaining at main engine second cutoff were calculated by using the times that the propellant levels passed the bottoms of the probes as reference points. The propellant residuals and the corresponding station numbers at main engine second cutoff are shown in the following table:

Event	Units	Propellant					
		Hydrogen			Oxygen		
		AC-13	AC-14	AC-15	AC-13	AC-14	AC-15
Total propellant residual	kg	91	107	94	327	382	300
	lbm	201	235	207	722	843	662
Usable propellant residual	kg	61	77	64	293	348	265
	lbm	135	169	141	647	768	585
Firing time remaining to depletion	sec	10.1	15.0	12.4	8.3	13.6	10.4
Liquid level, station number[a]	---	378.2	375.5	377.7	444.3	443.7	444.7

[a]See fig. III-2 for vehicle station numbers.

TABLE VI-9. - PROPELLANT WEIGHTS

Propellant	Units	Weight for flight -		
		AC-13	AC-14	AC-15
Atlas				
RP-1	kg	38 283	38 374	38 419
	lbm	84 400	84 600	84 700
Liquid oxygen	kg	85 411	85 502	85 320
	lbm	188 300	188 500	188 100
Centaur				
Liquid hydrogen	kg	2 383	2 384	2 390
	lbm	5 253	5 257	5 270
Liquid oxygen	kg	11 553	11 557	11 574
	lbm	25 471	25 480	25 518

TABLE VI-10. - CENTAUR PROPELLANT LOADING

Quantity or event	Units	Propellant tank					
		Hyrodgen			Oxygen		
		AC-13	AC-14	AC-15	AC-13	AC-14	AC-15
Amount of sensor required to be wet:							
At T - 90 seconds	percent	99.8	99.8	99.8	------	------	------
At T - 75 seconds	percent	------	------	------			
Sensor location (vehicle station number)	-------	175	175	175	373	373	373
Tank volume at sensor[a]	m^3	35.6	35.6	35.6	10.5	10.5	10.5
	ft^3	1257	1257	1257	371	371	371
Ullage volume at sensor	m^3	0.32	0.32	0.32	0.19	0.19	0.19
	ft^3	11.2	11.2	11.2	6.6	6.6	6.6
Liquid-hydrogen sensor 99.8 percent dry at -	sec	T - 51	T - 56	T - 32	------	------	------
Liquid-oxygen sensor 100.2 percent dry at -	sec	------	------	------	T - 61	T - 0	T - 0
Ullage pressure at time sensor goes dry, absolute	N/cm^2	15.3	15.1	14.8	21.4	21.4	20.8
	psi	22.2	21.9	21.5	31.1	31.0	30.1
Density at time sensor goes dry[b]	g/cm^3	66.9	66.9	67.0	1099	1099	1131
	lb/ft^3	4.19	4.19	4.2	68.7	68.7	68.8
Propellant weight in tank when sensor is dry	kg	2389	2392	2394	11 561	11 557	11 574
	lbm	5267	5273	5278	25 488	25 480	25 518
Liquid-hydrogen boiloff to vent valve close[c]	kg	6.3	7.45	3.64	------	------	------
	lbm	14	16.4	8.10	------	------	------
Liquid-oxygen boiloff to lift-off[c]	kg	------	------	------	7.65	0	0
	lbm	------	------	------	17	0	0
Ullage volume at lift-off	m^3	0.50	0.53	0.45	0.24	0.23	0.23
	ft^3	14.5	15.3	13.2	7	6.6	6.6
Weight at lift-off[d]	kg	2383	2384	2390	11 553	11 557	11 574
	lbm	5253	5257	5270	25 471	25 480	25 518

[a]Volumes include 0.05 m^3 (1.85 ft^3) of liquid oxygen and 0.72 m^3 (2.53 ft^3) of liquid hydrogen for lines from boost pumps to engine turbopump inlet valves.

[b]Liquid-hydrogen density taken from ref. 5; liquid-oxygen density taken from ref. 6.

[c]Boiloff rates determined from tanking test are, for AC-13, 0.14 kg/sec (0.3 lbm/sec) liquid hydrogen and 0.15 kg/sec (0.28 lbm/sec liquid oxygen; for AC-14, 0.11 kg/sec (0.294 lbm/sec) liquid hydrogen and 0.149 kg/sec (1.33 lbm/sec) liquid oxygen; for AC-15, 0.095 kg/sec (0.253 lbm/sec) liquid hydrogen and 0.109 kg/sec (0.29 lbm/sec) liquid oxygen.

[d]Propellant loading accuracy: hydrogen, ±3.2 percent; oxygen, ±1.5 percent.

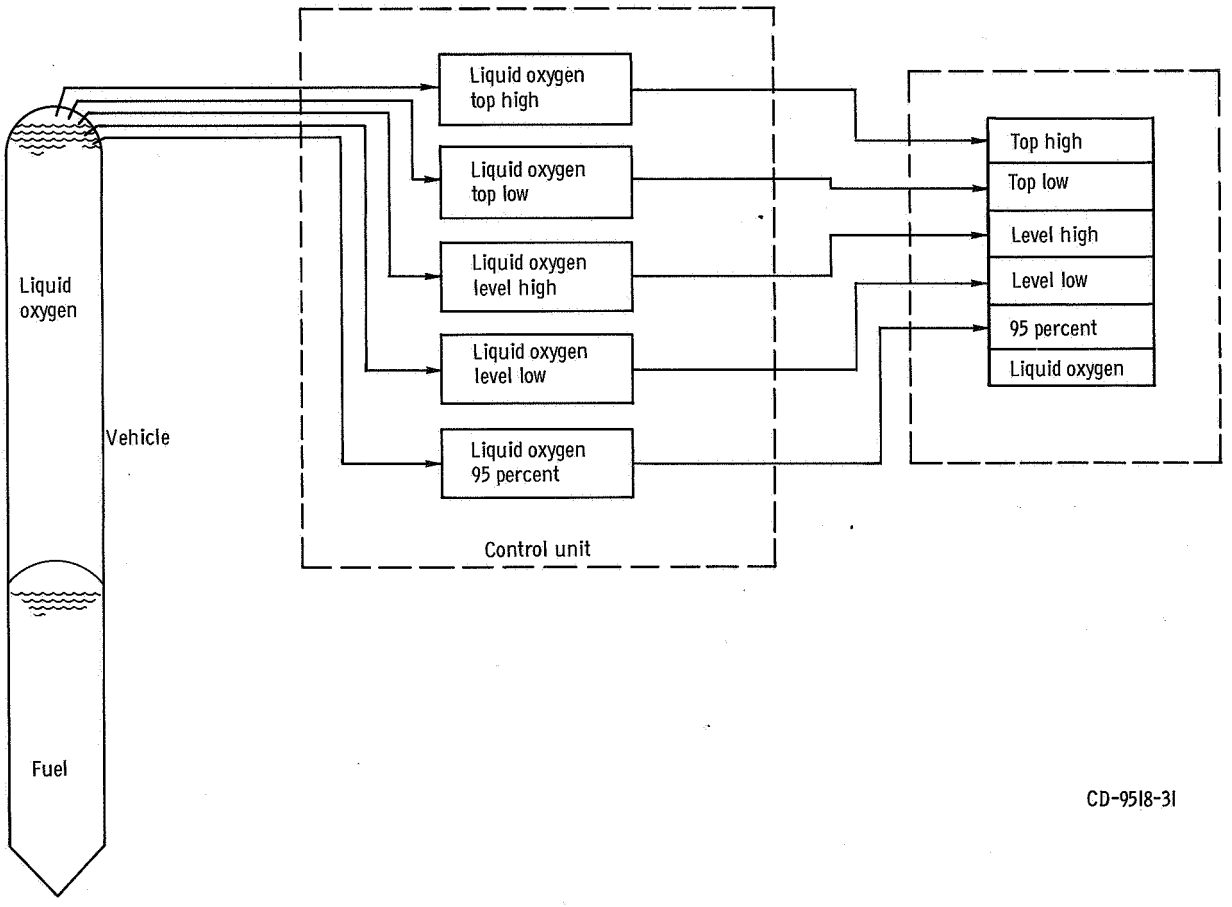

Figure VI-24. - Propellant level indicating system for Atlas propellant loading; AC-13, AC-14, and AC-15. (Lights on launch control panel indicate if sensor is wet or dry. Percent levels are indications of required flights levels and not percent of total tank volume.)

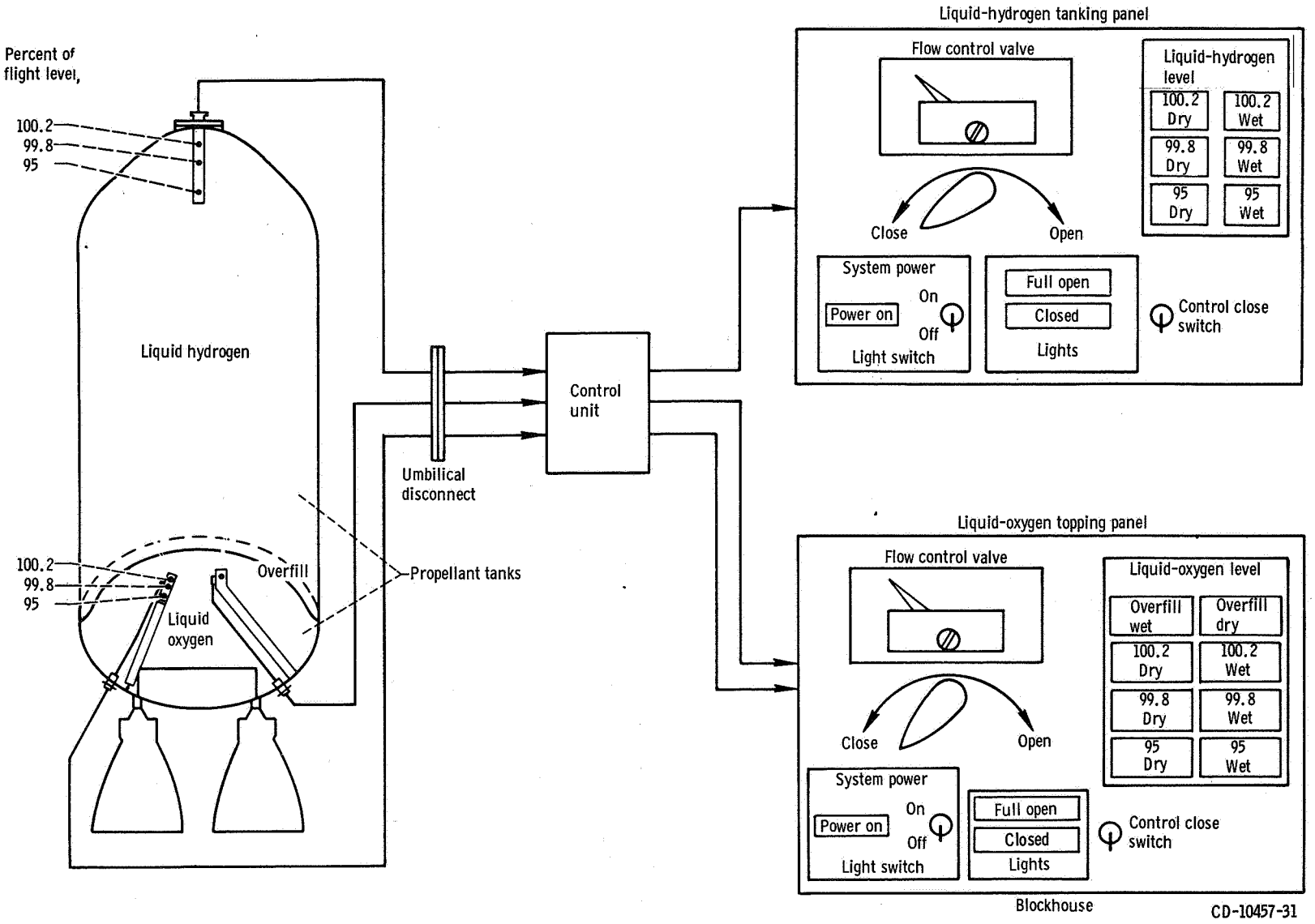

Figure VI-25. - Propellant level indicating system for Centaur propellant loading; AC-13, AC-14, and AC-15.

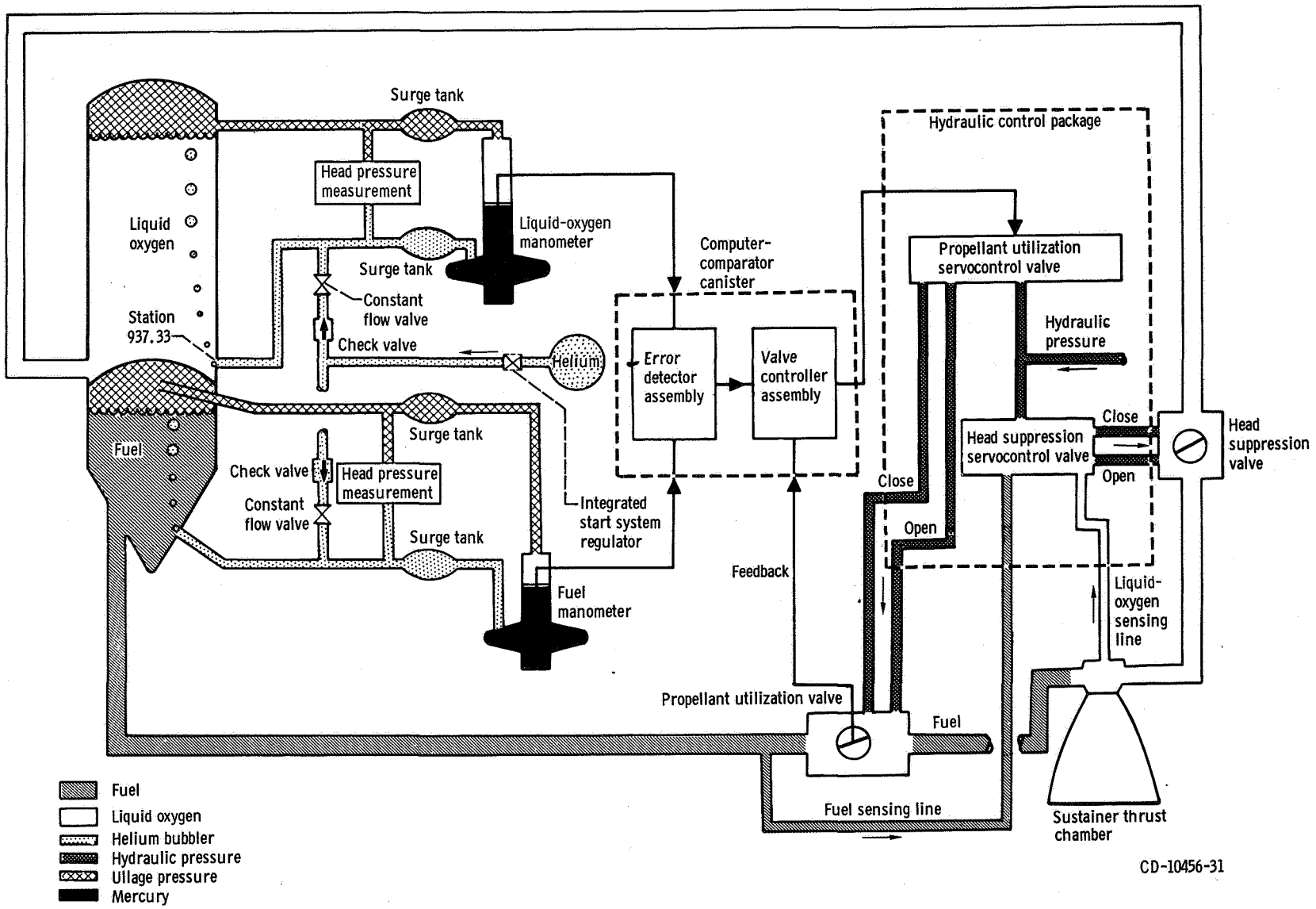

Figure VI-26. - Atlas propellant utilization system; AC-13, AC-14, and AC-15.

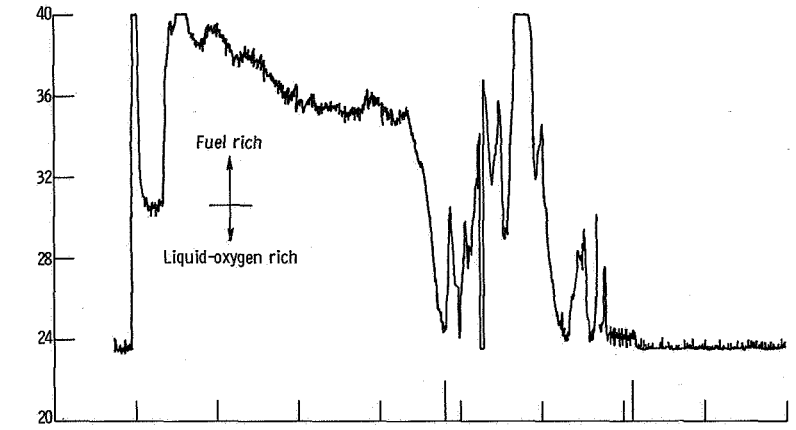

(a) AC-13.

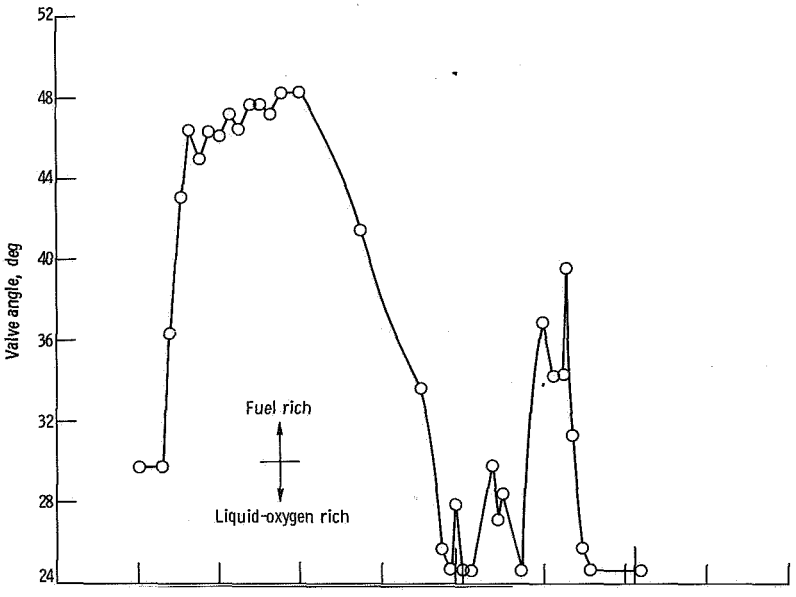

(b) AC-14.

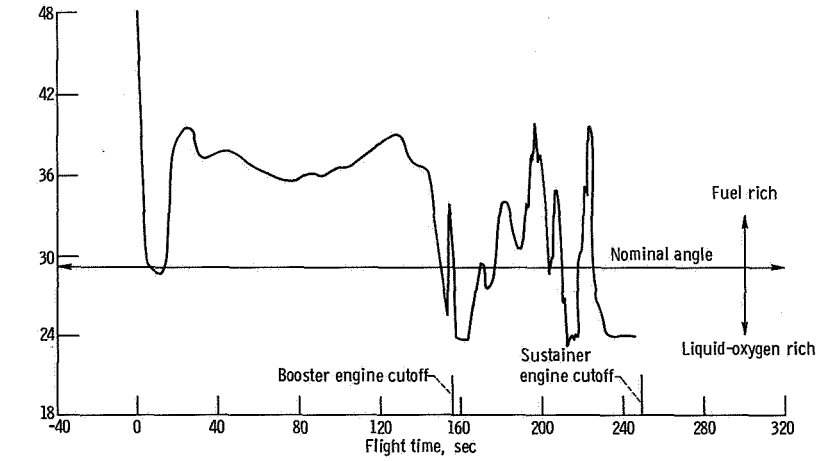

(c) AC-15.

Figure VI-27. - Atlas propellant utilization valve angles.

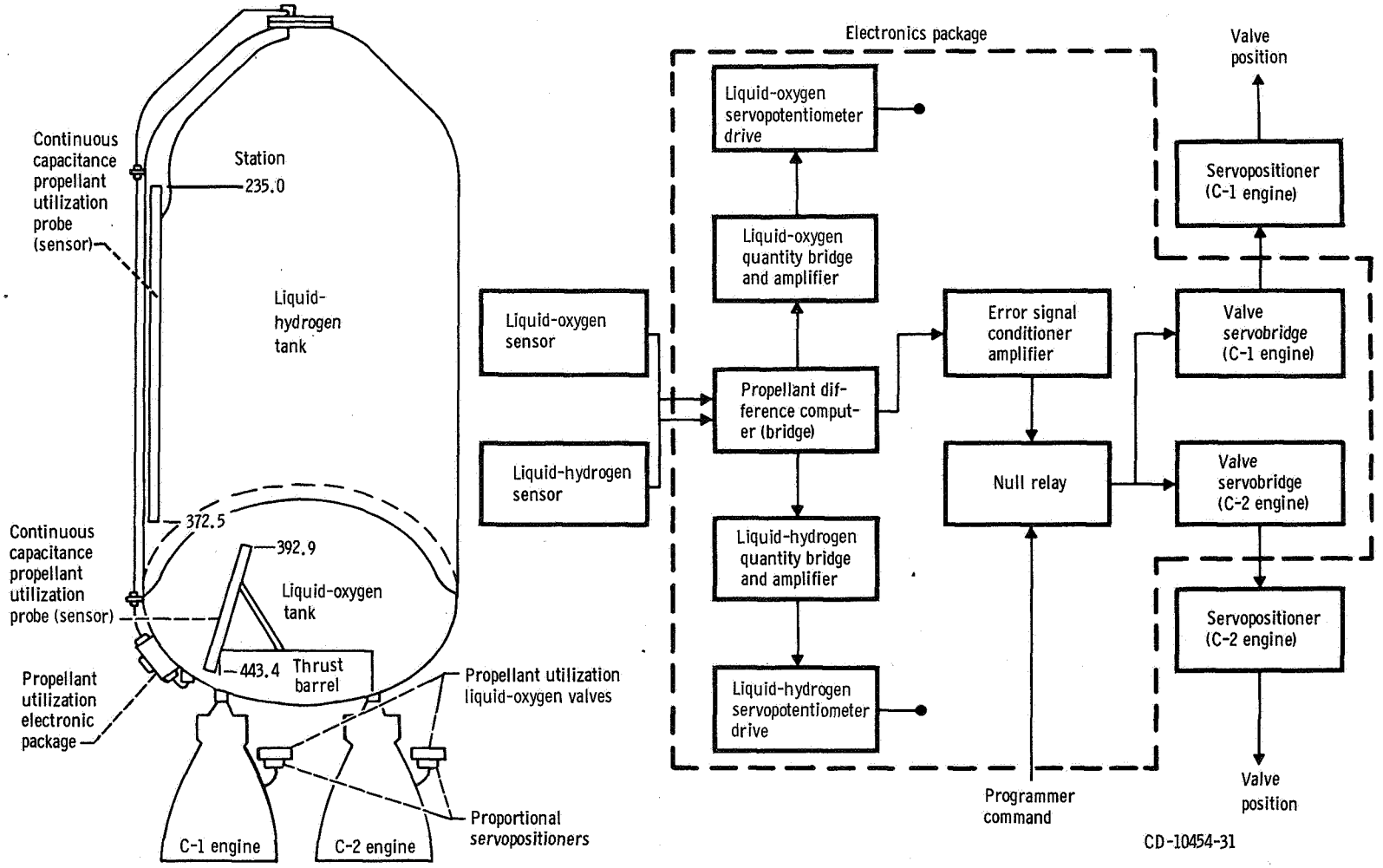

Figure VI-28. - Centaur propellant utilization system; AC-13, AC-14, and AC-15.

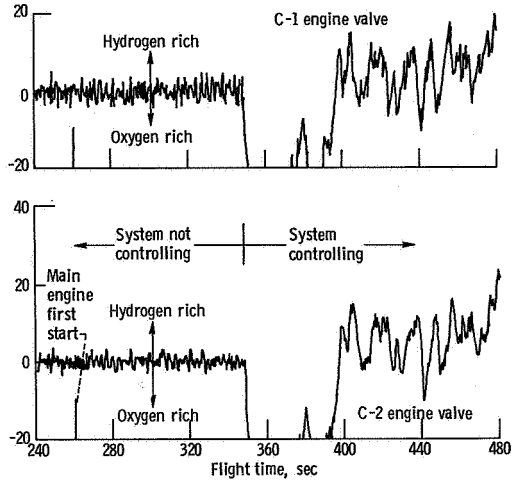

(a-1) Flight time, 240 to 480 seconds.

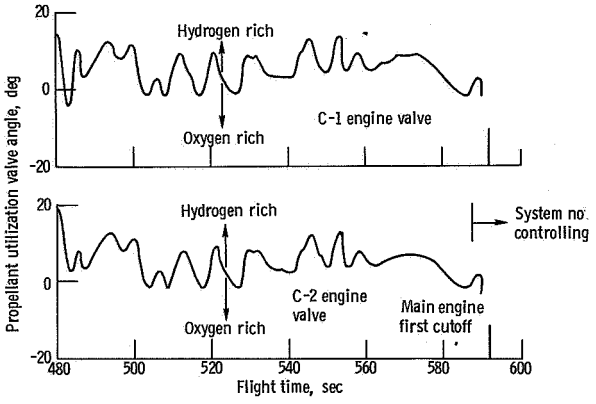

(a-2) Flight time, 480 to 600 seconds.

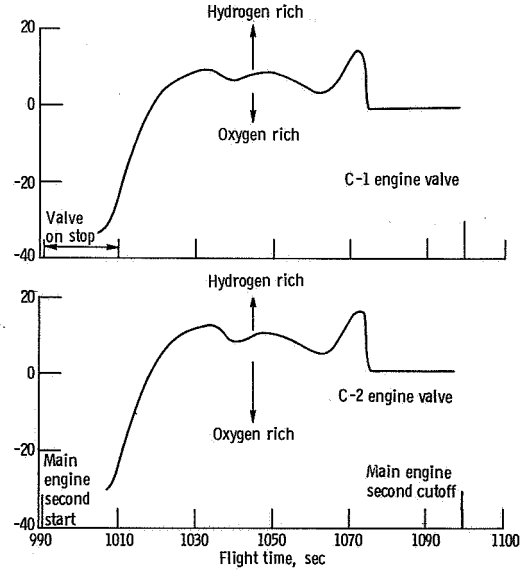

(a-3) Flight time, 990 to 1100 seconds.

(a) AC-13.

Figure VI-29. - Centaur propellant utilization valve angles; AC-13, AC-14, and AC-15.

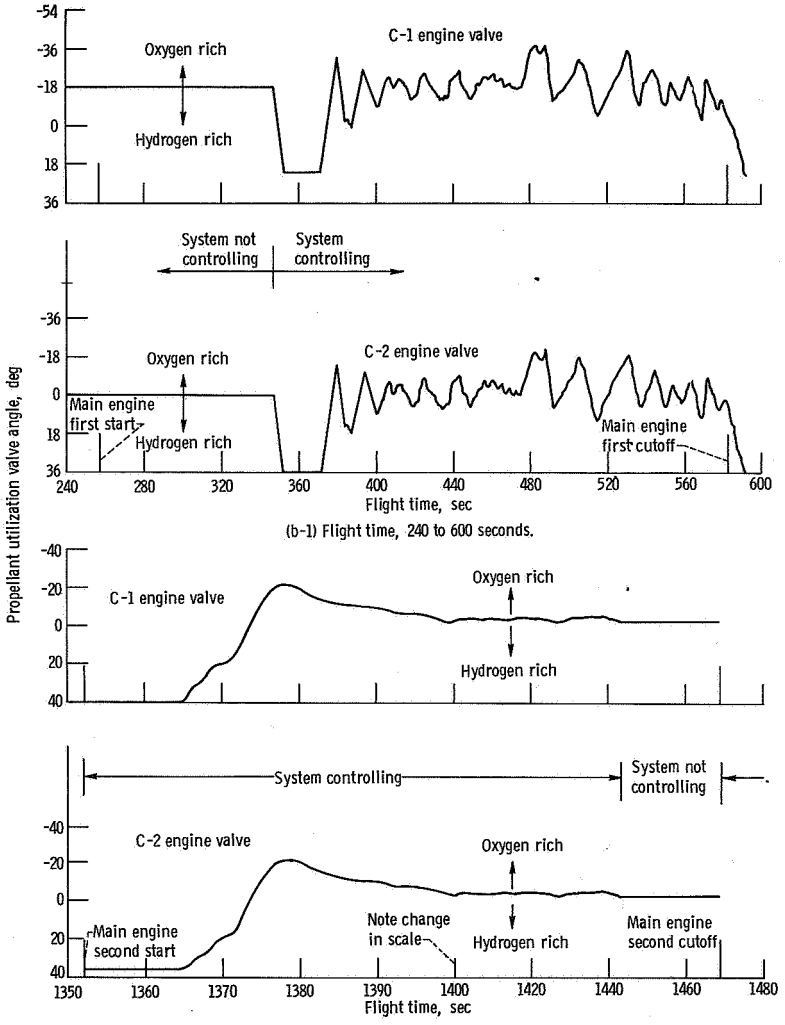

(b-1) Flight time, 240 to 600 seconds.

(b-2) Flight time, 1350 to 1480 seconds.

(b) AC-14.

Figure VI-29. - Continued.

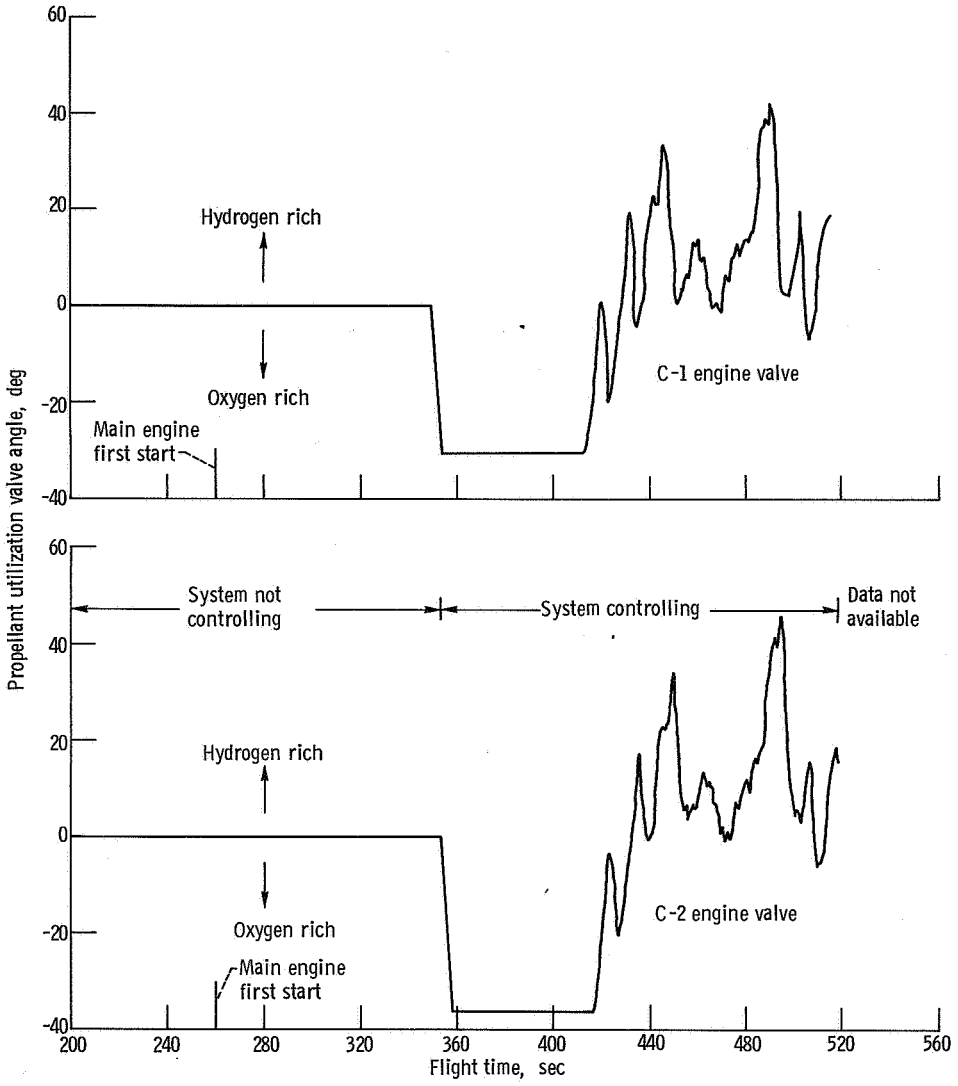

(c-1) Flight time, 200 to 560 seconds.

(c) AC-15.

Figure VI-29. - Continued.

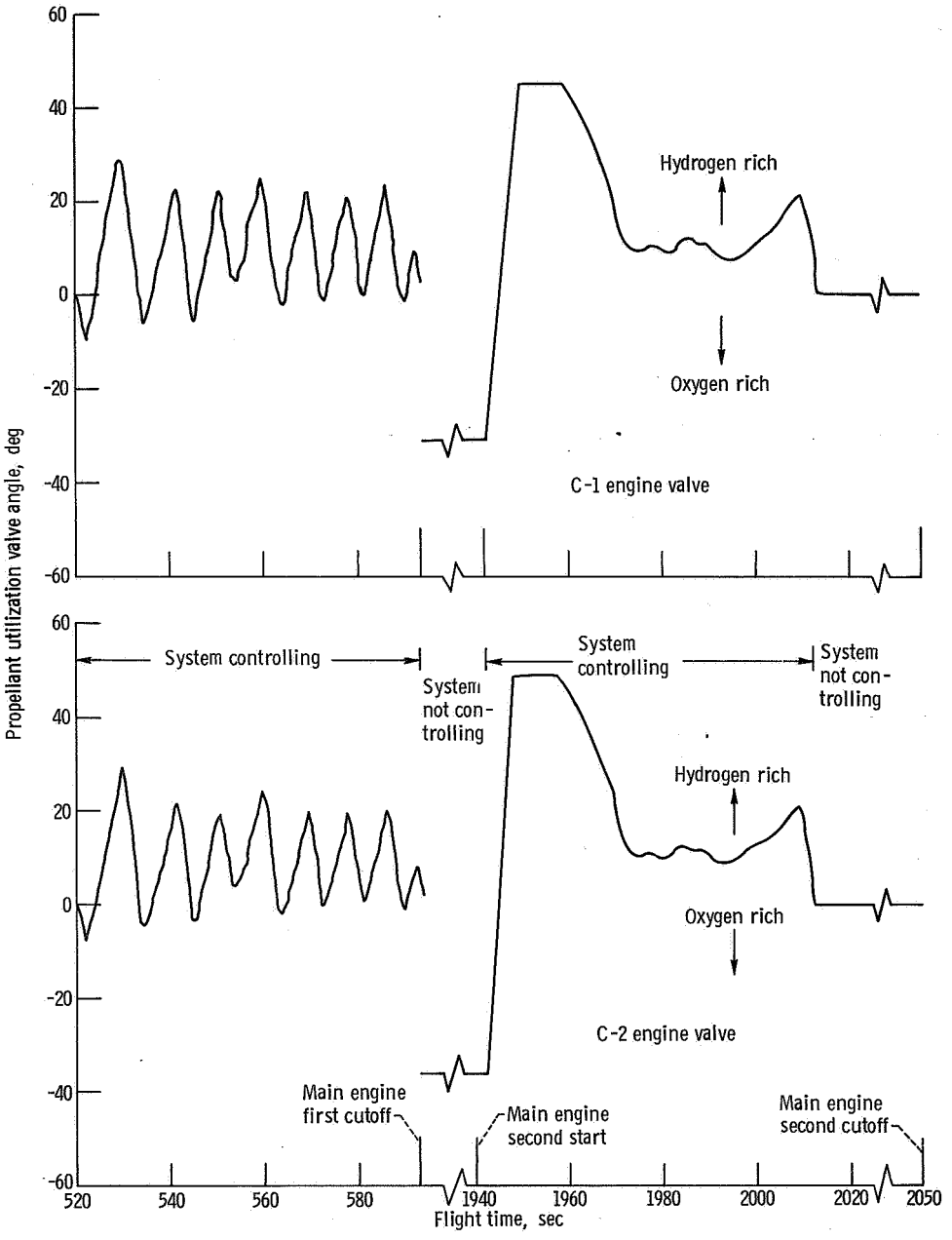

(c-2) Flight time, 520 seconds to main engine second cutoff.

(c) Concluded.

Figure VI-29. - Concluded.

PNEUMATIC SYSTEMS

by William A. Groesbeck and Merle L. Jones

Atlas Pneumatics

System description. - The Atlas pneumatic system supplied helium gas for tank pressurization and for various vehicle control functions. The system comprises three independent subsystems: propellant tank pressurization, engine control, and booster section jettison. This system schematic is shown in figure VI-30.

Propellant tank pressurization subsystem: This subsystem is used to maintain propellant tank pressures at required levels (1) to support the pressure stabilized tank structure, and (2) to satisfy the inlet pressure requirements of the engine turbopumps. In addition, helium is supplied from the fuel tank pressurization line to pressurize the hydraulic reservoirs and turbopump lubricant storage tanks. The subsystem consists of eight shrouded helium storage bottles, a heat exchanger, and fuel and oxidizer tank pressure regulators and relief valves. The eight shrouded helium storage bottles with a total capacity of 967 000 cubic centimeters (59 000 in.^{3}) are mounted in the jettisonable booster engine section. The bottle shrouds are filled with liquid nitrogen during prelaunch operations to chill the helium in order to provide a maximum storage capacity at about 2070 newtons per square centimeter (3000 psia). The liquid nitrogen drains from the shrouds at lift-off. During flight the cold helium passes through a heat exchanger located in the booster engine turbine exhaust duct before being supplied to the tank pressure regulators.

Propellant tank pressurization: - Tank pressurization control switched from the ground to the airborne systems at about T - 60 seconds. Airborne regulators are set to maintain tank gage pressure between 44.9 and 46.2 newtons per square centimeter (64 and 67 psi) and oxidizer tank pressure between 22.1 and 24.1 newtons per square centimeter (32.0 and 35.0 psi). However, from about T - 2 minutes to T + 20 seconds the liquid-oxygen regulator is biased by a helium "bleed" flow into the line which senses ullage pressure. The bias causes the regulator to control tank pressure at a lower level than the normal regulator setting. Depressing the liquid-oxygen tank pressure increases the differential pressure across the bulkhead between the propellant tanks. The increased differential pressure counteracts the launch transient loads that act in a direction to cause bulkhead reversal. At T + 20 seconds, the bias is removed by closing an explosively actuated valve, and the ullage pressure in the liquid-oxygen tank increases to the normal regulator control range. The increased pressure then provides sufficient vehicle structural stiffness to withstand bending loads during the remainder of the ascent. Pneumatic regulation of tank pressure is terminated at booster

staging. Thereafter, the fuel tank pressure decays slowly, but the oxidizer tank pressure is sustained by liquid-oxygen boiloff.

Engine controls subsystem: This subsystem supplies helium pressure for actuation of engine control valves, for pressurization of the engine start tanks, for purging booster engine turbopump seals, and for the reference pressure to the regulators which control oxidizer flow to the gas generator. Control pressure in the system is maintained through Atlas-Centaur separation. These pneumatic requirements are supplied from a 76 000-cubic-centimeter (4650-in.^{3}) storage bottle pressurized to a gage pressure of about 2070 newtons per square centimeter (3000 psi) at lift-off.

Booster engine jettison subsystem: This subsystem supplies pressure for release of the pneumatic staging latches to separate the booster engine package. A command from the Atlas flight control system opens two explosively actuated valves to supply helium pressure to the 10 piston-operated staging latches. Helium for the system is supplied by a single 14 260-cubic-centimeter (870-in.^{3}) bottle charged to a gage pressure of 2070 newtons per square centimeter (3000 psi).

System performance. - The Atlas pneumatic system performance was satisfactory throughout the AC-13, AC-14, and AC-15 flights. The individual subsystem performance on these three flights is discussed in the following paragraphs.

Propellant tank pressurization: Control of propellant tank pressures was switched from ground to the airborne subsystem at approximately T - 49 seconds. Ullage pressures were properly controlled throughout the flight. Tank pressurization data for the flights are shown in figure VI-31 and table VI-11. The fuel tank pressure regulator controlled at a gage pressure of about 45.5 newtons per square centimeter (66 psi) until termination of pneumatic control at booster staging. During sustainer engine firing, the fuel tank pressure decreased normally and was 37.9 newtons per square centimeter (55 psi) on AC-13 and AC-15 and 36.8 newtons per square centimeter (53.7 psi) on AC-14 at engine shutdown. Oxidizer tank gage pressure in newtons per square centimeter (psi), on switching to airborne regulation prior to lift-off, was steady at 20.1 (29.2) on AC-13, at 20.8 (30.2) on AC-14, and at 20.6 (29.9) on AC-15. The pressure decreased momentarily at engine start and then indicated only a very slow pressure rise. At T + 20 seconds, the regulator bias was terminated, and pneumatic regulation immediately increased the ullage pressure to a level within the normal regulator control range of 22 to 24 newtons per square centimeter (32 to 35 psi). The regulator continued to control tank pressure within required limits until termination of pneumatic regulation at booster engine shutdown. At this time, the ullage pressure increased slightly as the result of the sudden decrease in propellant outflow and an increase in liquid-oxygen boiloff rate. The boiloff rate increased because of the abrupt reduction in hydrostatic pressure caused by the decrease in vehicle acceleration from about 5 g's to about 1.1 g's. After booster staging, the ullage pressure in newtons per square centimeter (psi) gradually decreased from 23.1 to 22.4 (33.5 to 32.5) on AC-13, from 23.1 to 21.6 (33.5 to 31.4) on AC-14,

and from 23.3 to 22.3 (33.8 to 32.4) on AC-15, at sustainer engine shutdown.

Engine control subsystem: The booster and sustainer pneumatic regulators provided the required helium pressures for engine control throughout the flight. Significant performance values are shown in tavle VI-11.

Booster section jettison subsystem: System performance was satisfactory. The explosive actuated valves were opened on command at about T + 156 seconds, allowing high-pressure helium to actuate the 10 booster staging latches.

Centaur Pneumatics

System description. - The Centaur pneumatic system, which is shown schematically in figure VI-32, consists of five subsystems: propellant tank venting, propellant tank pressurization, propulsion pneumatics, helium purge, and nose fairing pneumatics.

The structural stability of the propellant tanks is maintained throughout each flight by the propellant boiloff gas pressures. These pressures are controlled by a vent system on each propellant tank. Two pilot-controlled, pressure-actuated vent valves and ducting comprise the hydrogen tank vent system. The primary vent valve is fitted with a continuous-duty solenoid valve which, when energized, locks the vent valve and prevents operation. The secondary hydrogen vent valve does not have this solenoid valve. The relief range of the secondary valve is above that of the primary valve and prevents overpressurization of the hydrogen tank when the primary vent valve is locked. Until nose fairing jettison, the vent gases are ducted overboard through a single vent. After jettison, the venting occurs through diametrically opposed nozzles which balance the vent thrust forces. The oxygen tank vent system uses a single vent valve which is fitted with the control solenoid valve. The vented gases are ducted overboard through the interstage adapter. The duct, which remains with the Centaur after separation from the interstage adapter, is oriented to aline the venting thrust vector with the vehicle center of gravity.

The vent valves are commanded to the locked mode at specific times (1) to permit the hydrogen tank pressure to increase during the atmospheric ascent to satisfy the structural requirements of the pressure-stabilized tank, (2) to permit controlled pressure increases in the tanks to satisfy the boost pump pressure requirements, (3) to restrict oxygen venting during nonpowered flight to avoid vehicle disturbing torques, and (4) to restrict hydrogen venting to nonhazardous times. (A fire could conceivably occur during the early part of the atmospheric ascent if a plume of vented hydrogen washes back over the vehicle and is exposed to an ignition source. A similar hazard could occur at Atlas booster engine staging when residual oxygen envelopes a large portion of the vehicle.)

The propellant tank pressurization subsystem supplies helium gas in controlled

quantities for in-flight pressurization, in addition to that provided by the propellant boiloff gases. It consists of two normally closed solenoid valves and orifices and a pressure switch assembly which senses oxygen tank pressure. The solenoid valves and orifices provide metered flow of helium to the propellant tanks for step pressurization during main engine start sequences. The pressure sensing switch controls the pressure in the oxygen tank from boost pump first start to main engine first start.

The propulsion pneumatics subsystem supplies helium gas at regulated pressures for actuation of main engine control valves and pressurization of the hydrogen peroxide storage bottle. It consists of two pressure regulators, which are referenced to ambient pressure, and two relief valves. Pneumatic pressure supplied through the engine controls regulator is used for actuation of the engine inlet valves, the engine chilldown valves, and the main fuel shutoff valve. The second regulator, located downstream of the engine controls regulator, further reduces the pressure to provide expulsion pressurization for the hydrogen peroxide storage bottle. A relief valve downstream of each regulator prevents overpressurization.

A ground-airborne helium purge subsystem is used to prevent cryopumping and icing under the insulation panels and in propulsion system components. A common airborne distribution system is used for prelaunch purging from a ground helium source and postlaunch purging from an airborne helium storage bottle. This subsystem distributes helium gas for purging the cavity between the hydrogen tank and the insulation panels, the seal between the nose fairing and the forward bulkhead, the propellant feedline insulation, the boost pump seal vents, the engine gearbox seal vents, the engine chilldown ventducts, the engine thrust chambers, and the hydraulic power packages. The umbilical charging connection for the airborne bottle can also be used to supply the purge from the ground source should an abort occur after ejection of the ground purge supply line.

The nose fairing pneumatic subsystem provides the required thrust for nose fairing jettison. It consists of a nitrogen storage bottle and an explosive actuated valve with an integral thruster nozzle in each fairing half. Release of the gas through the nozzles provides the necessary thrust to propel the fairing halves away from each other and from the vehicle.

Propellant tank pressurization and venting. - The ullage pressures in the hydrogen and oxygen tanks for AC-13, AC-14, and AC-15 flights are shown in figures VI-33 to VI-35, respectively. The sequence of events for all three vehicles was the same, but the timing of some of the events varied. At approximately T - 8 seconds, the primary hydrogen vent valve on each vehicle was locked, causing an increase in the tank pressure. In each case, the pressure increased to the relief setting of the secondary hydrogen vent valve which then began to regulate the tank pressure. The relief absolute pressure on AC-13 was 17.9 newtons per square centimeter (25.9 psi), and on AC-14 and AC-15 it was 18.1 newtons per square centimeter (26.2 psi). The tank pressure rise rate during this period was, in newtons per square centimeter per minute (psi/min), 310 (4.50) on

AC-13, 3.12 (4.52) on AC-14, and 3.37 (4.89) on AC-15. At approximately T + 90 seconds, the primary hydrogen tank vent valves were enabled. The tank pressures were then reduced and were regulated by these vent valves.

The primary hydrogen vent valve on each vehicle was again locked at the beginning of Atlas booster engine staging and remained locked for approximately 7.5 seconds. Following booster engine staging, the vent valves were again enabled and allowed to regulate tank pressure. At Atlas sustainer engine cutoff, the primary hydrogen vent valves were locked, and the tanks were pressurized with helium for 1 second as a part of the Centaur main engine start sequence. In each case, the pressure increased approximately 1 newton per square centimeter (1.4 psi) and then decreased as the warm helium in the tank was cooled by the hydrogen gas (see figs. VI-33(a) and (b), VI-34(a) and (b), and VI-35(a) and (b)).

The ullage pressure in the oxygen tank remained relatively constant for the first 40 seconds of each flight until the increasing vehicle acceleration suppressed propellant boiling sufficiently to cause the pressure to decrease. Thereafter, the pressure decreased until the oxygen vent valve reseated and venting ceased. The pressure then varied between the operating limits of the vent valve until Atlas booster engine cutoff. At that time, the sudden reduction in the acceleration caused an increase in the liquid-oxygen boiloff and a resulting pressure rise in the tanks. As thermal equilibrium was reestablished, the pressures decreased to their original level.

At approximately 62 seconds after Atlas booster engine cutoff, the oxygen tank vent valve on each vehicle was locked, and the helium pressurization of the oxygen tank was initiated. The tank pressure increased to the upper limit of the pressurization switch, which opened and terminated pressurization. As the helium cooled in the AC-13 tank, the pressure decreased until the heat input from the boost pump recirculation flow increased boiloff and caused the pressure to increase again. On AC-14 and AC-15, the pressure decreased to the lower limit of the pressurization switch which closed, causing additional helium to be injected into the tank. Following this second cycle, heat input from the boost pump recirculation flow increased the boiloff, causing the pressure to increase before it reached the lower limit of the pressurization switch again. The pressure in the AC-13, AC-14, and AC-15 vehicle oxygen tanks continued to increase from heat input until Centaur main engine first prestart. The pressure in each case then decreased gradually until Centaur main engine first start, when it decreased abruptly to the saturation pressure of the ullage gas (see figs. VI-33(b), VI-34(b), and VI-35(b)).

The ullage pressures in both propellant tanks of the three vehicles decreased normally during the main engine first firing. After main engine cutoff, the primary hydrogen vent valves were enabled, while the oxygen vent valves remained locked (see figs. VI-33(c), VI-34(c), and VI-35(c).

Forty seconds prior to main engine second start, the primary hydrogen vent valves were locked. At the same time, the pressures in the oxygen tank and hydrogen tank, on

each vehicle, were increased by the injection of helium. The pressurization of the oxygen tanks was timed to last 18 seconds. The pressure sensing switches, used prior to Centaur main engine first start, were electrically bypassed. The pressurization of the hydrogen tanks was also a timed function lasting 40 seconds. These time periods for pressurization were the same for all three flights; however, the pressure increase in the oxidizer tank was greater on AC-15 than on previous vehicles (see figs. VI-33(d) and VI-35(e)) because of a larger orifice in the AC-15 oxygen tank pressurization line. The change from a 1.09-millimeter- (0.043-in.-) diameter orifice on previous vehicles to a 1.50-millimeter- (0.059-in.-) diameter orifice on AC-15 was made because of a possible oxidizer boost pump cavitation on the AC-14 flight (see Centaur Boost Pump and Propellant Supply System section). It has been concluded that the net positive suction pressure at the boost pump for AC-14 was marginal at the time of Centaur main engine second start. In order to provide increased net positive suction pressure through a greater tank pressure increase on AC-15, the larger orifice was installed in the pressurization line.

Following main engine second cutoff, the hydrogen tank ullage pressures increased until the start of lateral thrust in the Centaur turnaround maneuver, when a sudden pressure decrease occurred. This decrease in pressure indicated the splashing of liquid hydrogen into the ullage gas. The pressures increased again until the start of retrothrust. The oxygen tank ullage pressure on each of the three vehicles increased slightly after main engine second cutoff and then remained essentially constant (see figs. VI-33(e), VI-34(e), and VI-35(e)).

After the start of retrothrust, the hydrogen tank ullage pressure on each of the three vehicles decreased (indicating either gaeeous or two-phase outflow) except for a short period of time when the pressures remained constant (indicating liquid outflow). During the period of retrothrust, the oxygen tank ullage pressures remained essentially constant (indicating liquid outflow). At the termination of the retrothrust, the primary hydrogen vent valves and the oxygen vent valves were enabled to prevent rupture of the tanks in space (see figs. VI-33(e), VI-34(e), and VI-35(f)).

Propulsion pneumatics. - The engine controls regulators and the hydrogen peroxide bottle pressure regulators maintained proper system pressure levels throughout the three flights. The AC-13 engine controls regulator output absolute pressure was 328 newtons per square centimeter (476 psi) at lift-off while that of the hydrogen peroxide bottle pressure regulator was 227 newtons per square centimeter (329 psi). The corresponding values for AC-14 were 324 and 223 newtons per square centimeter (470 and 324 psi), respectively, and those for AC-15 were 316 and 222 newtons per square centimeter (459 and 322 psi), respectively. After lift-off, all regulator output pressures decreased, corresponding to the decrease in ambient pressure and remained relatively constant after the ambient pressure had decreased to zero.

Helium purge subsystem. - The total helium purge flow rate to AC-13 at T - 10 seconds was 89 kilograms per hour (196 lbm/hr). The flow rates to AC-14 and AC-15 were 87 and 84 kilograms per hour (184 and 191 lbm/hr), respectively. The differential pressure, in newtons per square centimeter (psi), across the insulation panels after hydrogen tanking was 0.13 (0.18) on AC-13, 0.17 (0.25) on AC-14, and 0.19 (0.28) on AC-15. The minimum allowable differential pressure required to prevent cryopumping and icing is 0.02 newton per square centimeter (0.03 psi). At a nominal time of T - 9 seconds, the airborne purge system on each vehicle was activated; and at T - 4 seconds, the ground purge was terminated. The supply of helium in each vehicle purge bottle lasted through most of the atmospheric ascent.

Nose fairing pneumatics. - There was no airborne instrumentation in this system on any of the vehicles. Normal jettisoning of the nose fairing on each flight indicated that the system functioned properly each time.

TABLE VI-11. - ATLAS PNEUMATICS SYSTEM DATA SUMMARY; AC-13, AC-14, AND AC-15

Pneumatic subsystem	Measurement	Event time	Units	Requirement at lift-off	Flight values for Atlas-Centaur launch vehicle		
					AC-13	AC-14	AC-15
Propellant tank pressurization	Liquid-oxygen tank ullage gage pressure	Lift-off	N/cm^2	19.6 to 22.3	20.2	20.9	20.6
			psi	28.4 to 32.3	29.3	30.3	29.9
		Booster engine cutoff	N/cm^2	----------	22.9	22.3	22.7
			psi	----------	33.2	32.5	33.0
		Sustainer engine cutoff	N/cm^2	----------	22.4	21.6	22.3
			psi	----------	32.6	31.3	32.4
	Fuel tank ullage gage pressure	Lift-off	N/cm^2	44.7 to 47.3	45.5	45.2	45.3
			psi	64.8 to 68.7	66.0	65.7	66.0
		Booster engine cutoff	N/cm^2	----------	45.5	45.0	45.2
			psi	----------	66.0	65.5	65.5
		Sustainer engine cutoff	N/cm^2	----------	37.9	36.8	37.9
			psi	----------	55.0	53.5	55.0
	Helium usage	Through booster engine cutoff	kg	----------	52.0	51.0	51.0
			lbm	----------	115.0	112.0	112.0
Engine controls	Booster engine pneumatic regulator outlet gage pressure	Lift-off	N/cm^2	493 to 541	510	523	517
			psi	715 to 785	740	760	750
		Booster engine cutoff	N/cm^2	----------	510	516	517
			psi	----------	740	750	750
	Sustainer engine pneumatic regulator outlet gage	Lift-off	N/cm^2	388 to 438	412	426	410
			psi	565 to 635	598	618	594
		Booster engine cutoff	N/cm^2	----------	412	425	403
			psi	----------	598	616	585
		Sustainer engine cutoff	N/cm^2	----------	412	425	403
			psi	----------	598	616	585
	Helium storage bottle gage pressure	Lift-off	N/cm^2	2000 to 2340	2270	2250	2255
			psi	2900 to 3400	3290	3265	3270
		Booster engine cutoff	N/cm^2	----------	1905	1940	1930
			psi	----------	2763	2820	2800
		Sustainer engine cutoff	N/cm^2	----------	1820	1800	1855
			psi	----------	2640	2610	2690
Booster jettison	Helium storage bottle gage pressure	Lift-off	N/cm^2	2000 to 2340	2280	2250	2280
			psi	2900 to 3400	3310	3270	3312

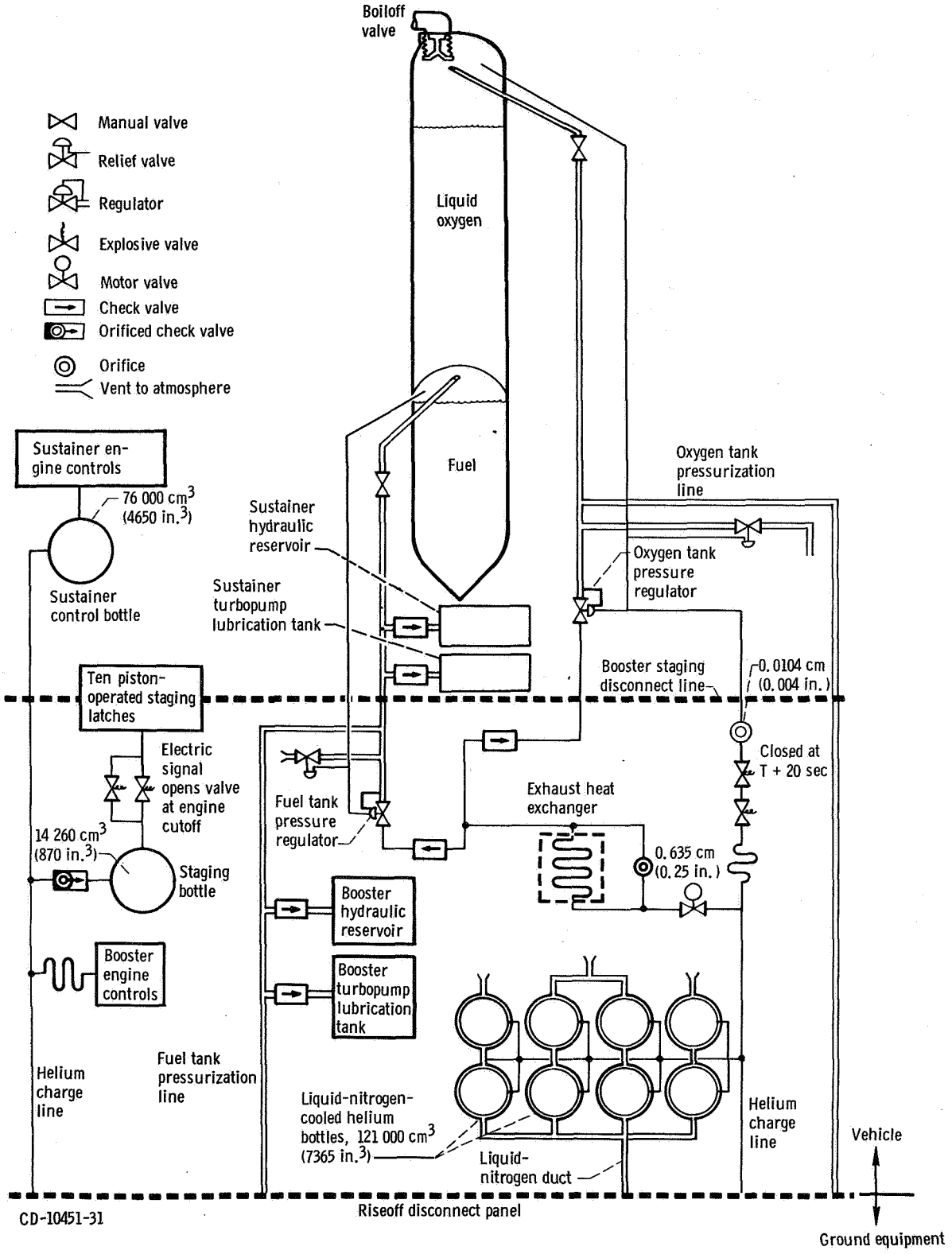

Figure VI-30. - Atlas vehicle pneumatic system; AC-13, AC-14, and AC-15.

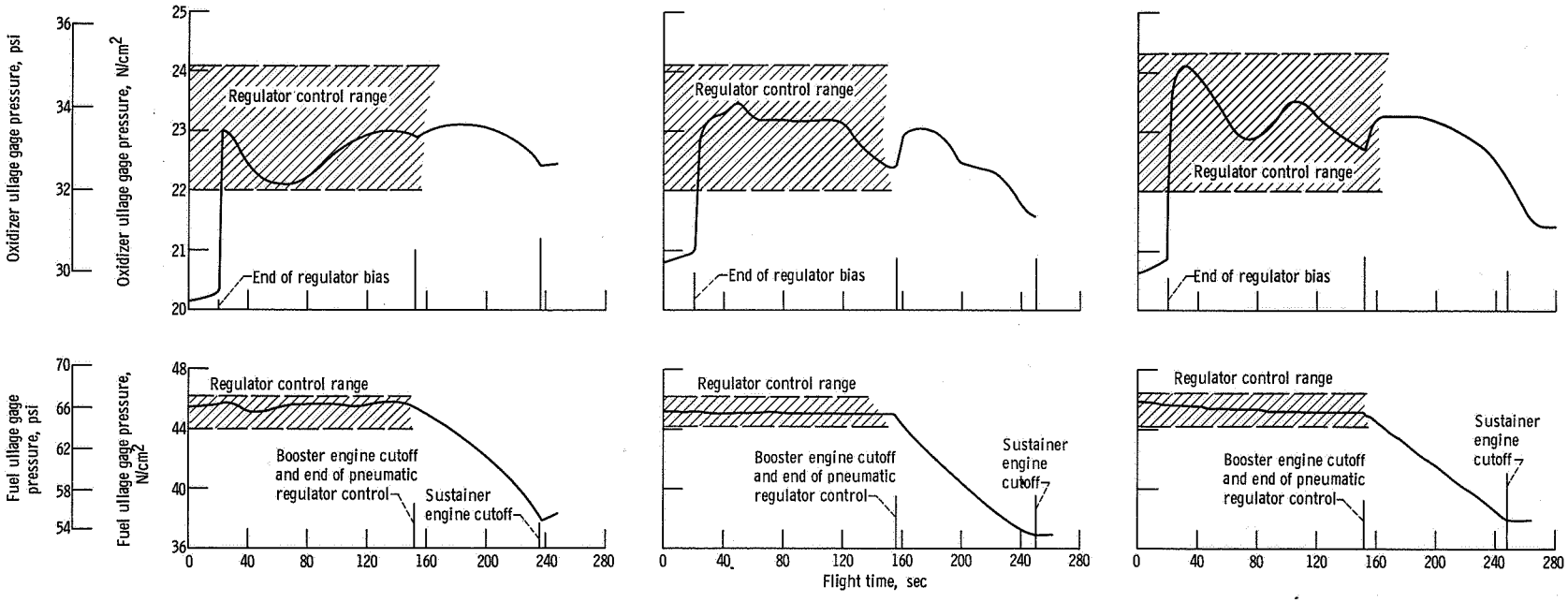

(a) AC-13.

(b) AC-14.

(c) AC-15.

Figure VI-31. - Atlas propellant tank pressures.

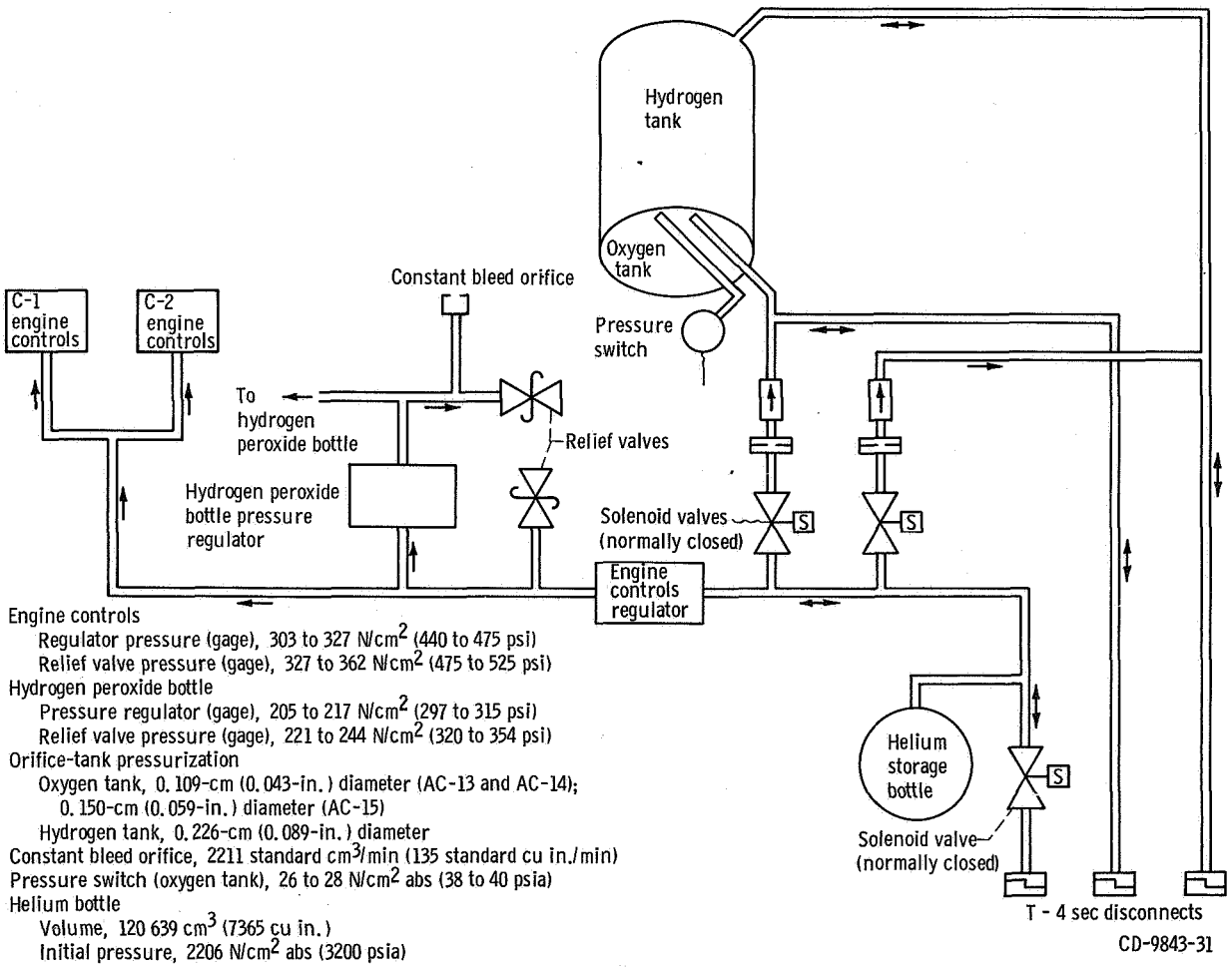

Engine controls
- Regulator pressure (gage), 303 to 327 N/cm^2 (440 to 475 psi)
- Relief valve pressure (gage), 327 to 362 N/cm^2 (475 to 525 psi)

Hydrogen peroxide bottle
- Pressure regulator (gage), 205 to 217 N/cm^2 (297 to 315 psi)
- Relief valve pressure (gage), 221 to 244 N/cm^2 (320 to 354 psi)

Orifice-tank pressurization
- Oxygen tank, 0.109-cm (0.043-in.) diameter (AC-13 and AC-14); 0.150-cm (0.059-in.) diameter (AC-15)
- Hydrogen tank, 0.226-cm (0.089-in.) diameter

Constant bleed orifice, 2211 standard cm^3/min (135 standard cu in./min)

Pressure switch (oxygen tank), 26 to 28 N/cm^2 abs (38 to 40 psia)

Helium bottle
- Volume, 120 639 cm^3 (7365 cu in.)
- Initial pressure, 2206 N/cm^2 abs (3200 psia)

(a) Tank pressurization and propulsion pneumatic subsystems.

Figure VI-32. - Centaur pneumatic system; AC-13, AC-14, and AC-15.

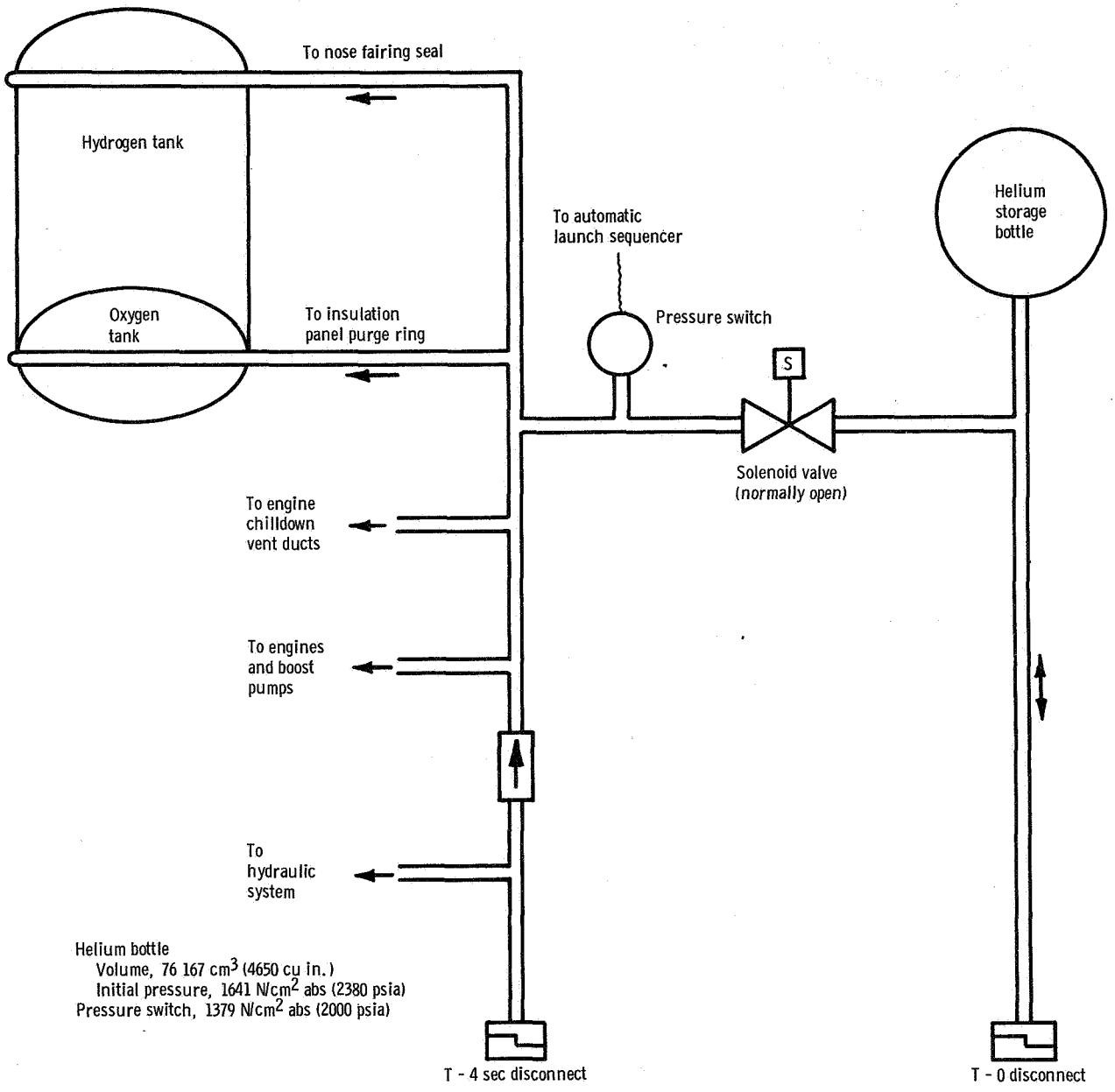

(b) Helium purge subsystem.

Figure VI-32. - Continued.

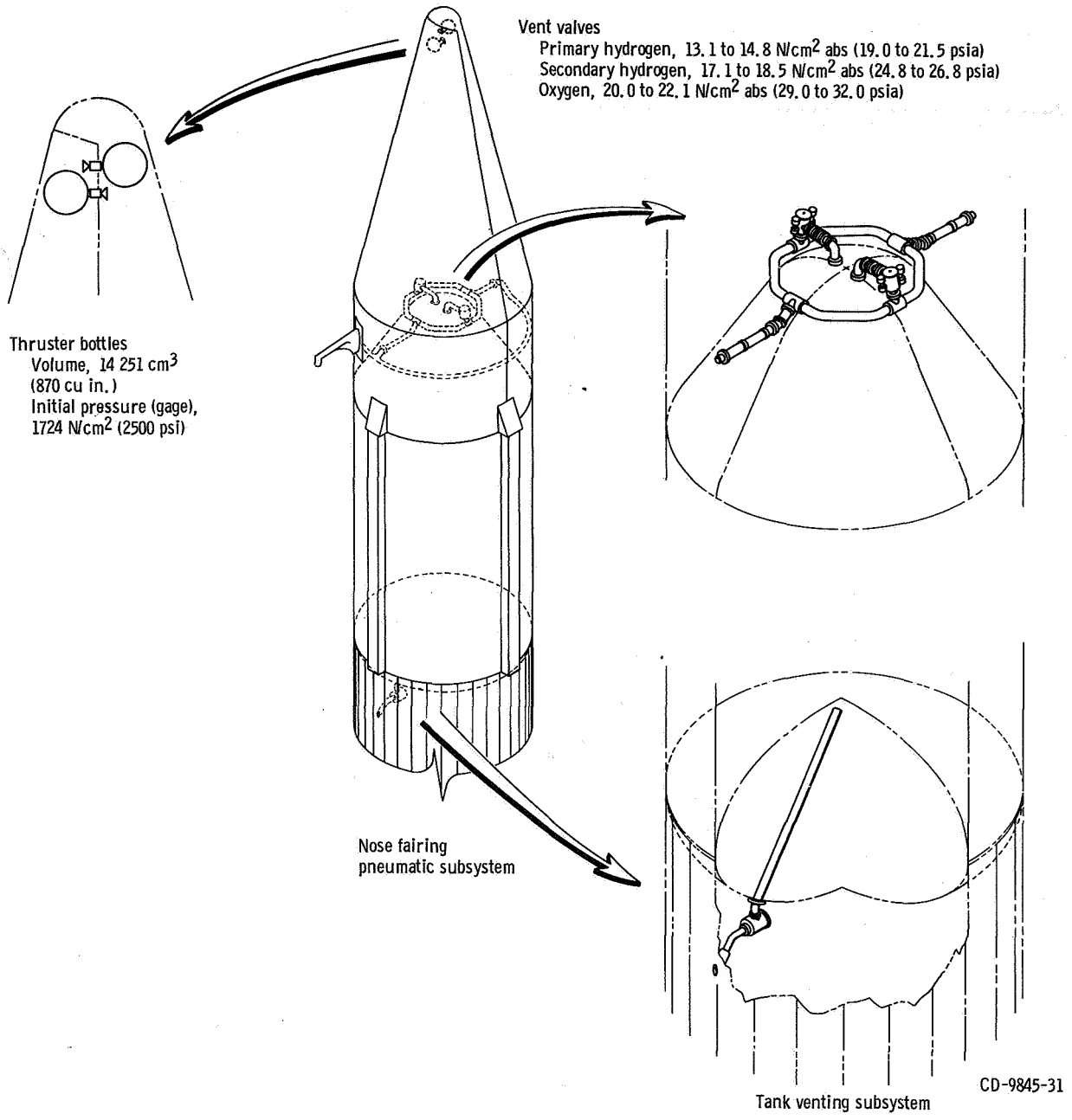

(c) Tank venting and nose fairing pneumatic subsystems.

Figure VI-32. - Concluded.

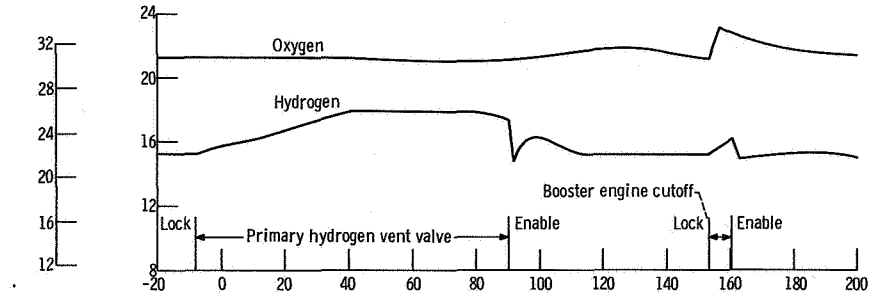

(a) Flight time, -20 to 200 seconds.

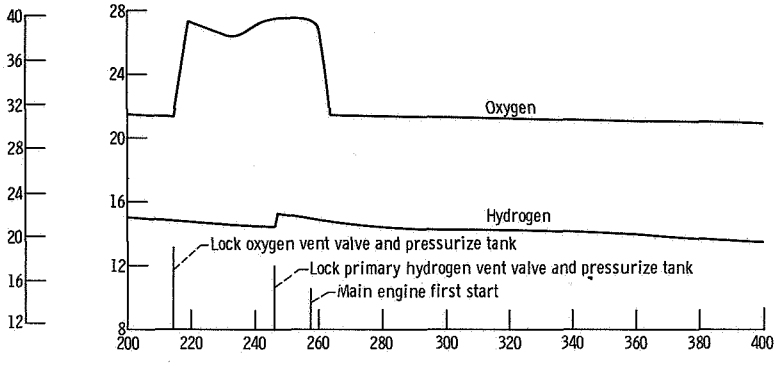

(b) Flight time, 200 to 400 seconds.

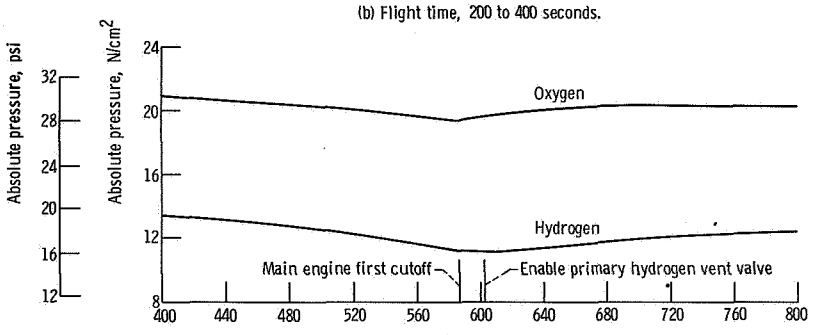

(c) Flight time, 400 to 800 seconds.

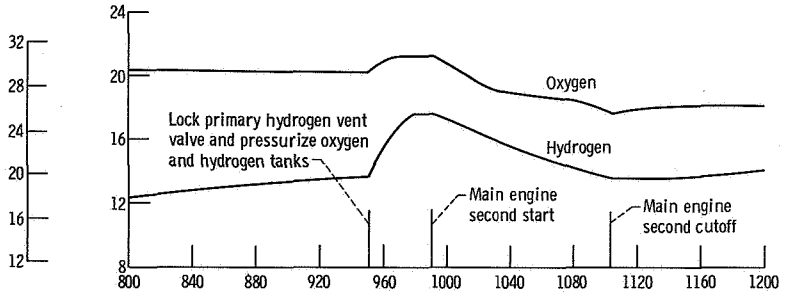

(d) Flight time, 800 to 1200 seconds.

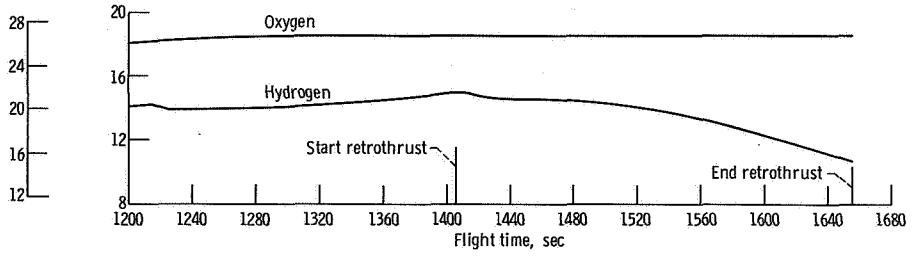

(e) Flight time, 1200 seconds to end of retrothrust.

Figure VI-33. - Centaur tank pressure history, AC-13.

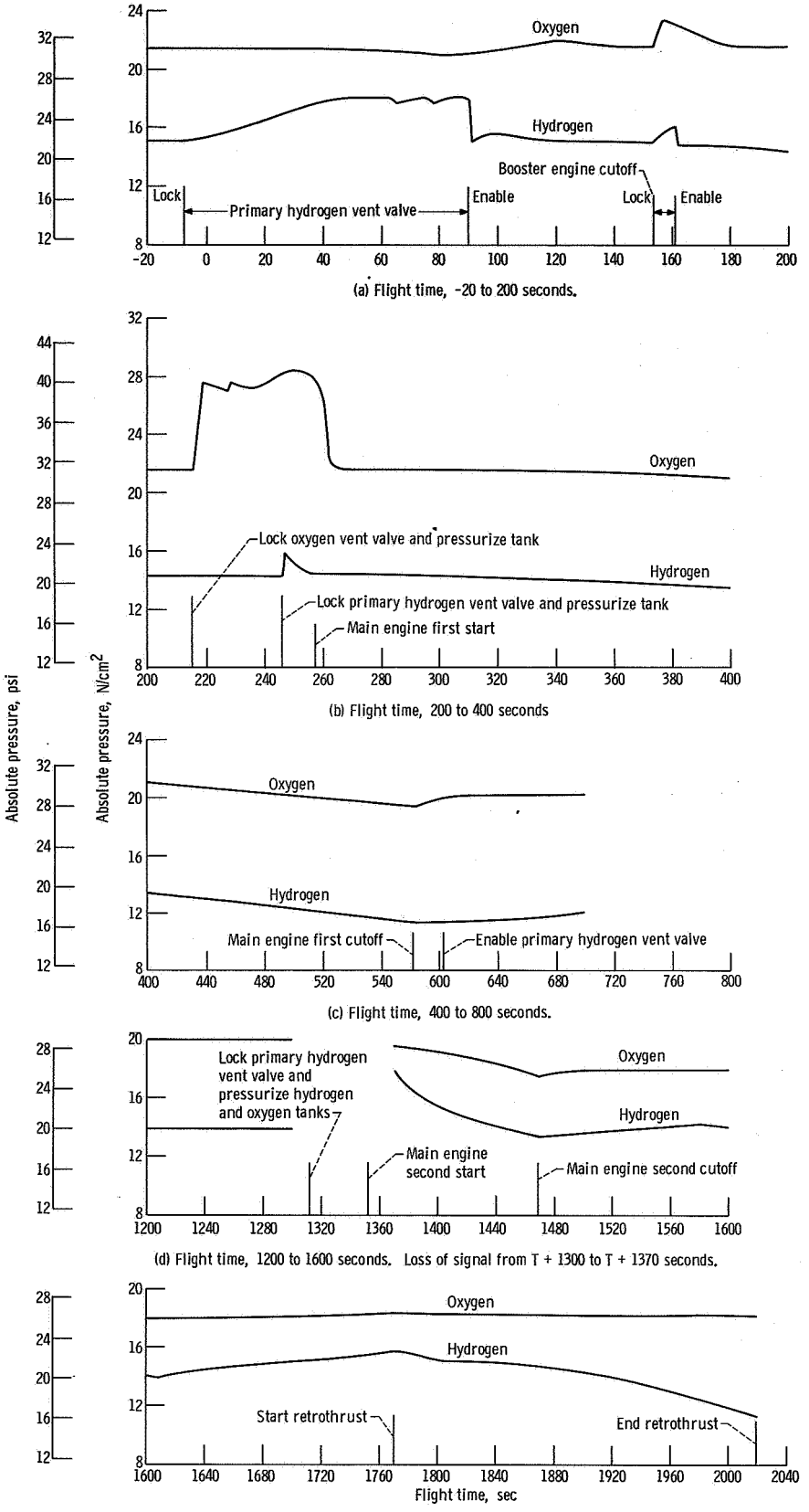

(a) Flight time, -20 to 200 seconds.

(b) Flight time, 200 to 400 seconds

(c) Flight time, 400 to 800 seconds.

(d) Flight time, 1200 to 1600 seconds. Loss of signal from T + 1300 to T + 1370 seconds.

(e) Flight time, 1600 seconds to end of retrothrust.

Figure VI-34. - Centaur tank pressure history, AC-14.

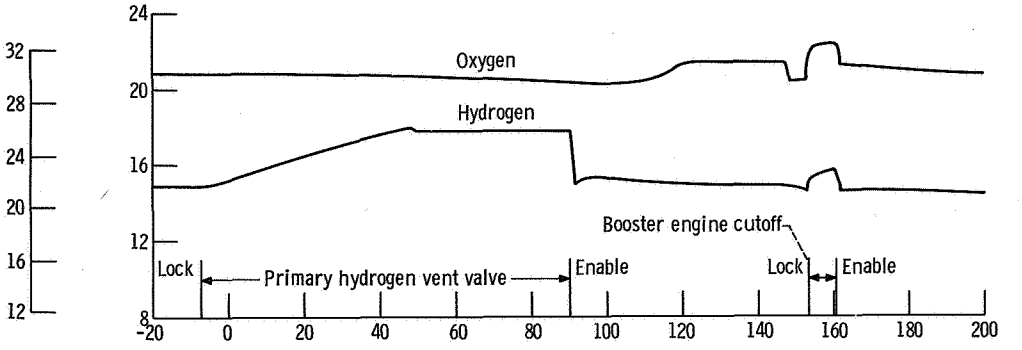

(a) Flight time, -20 to 200 seconds.

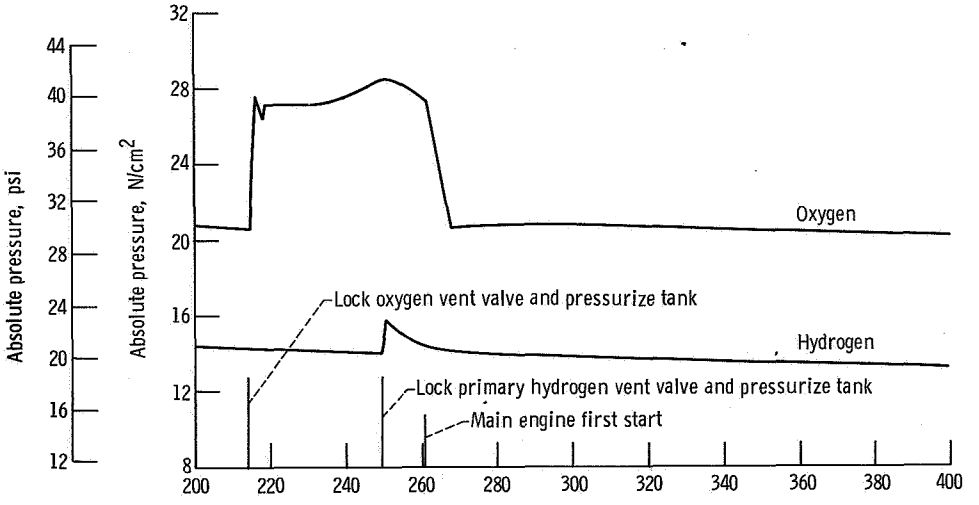

(b) Flight time, 200 to 400 seconds.

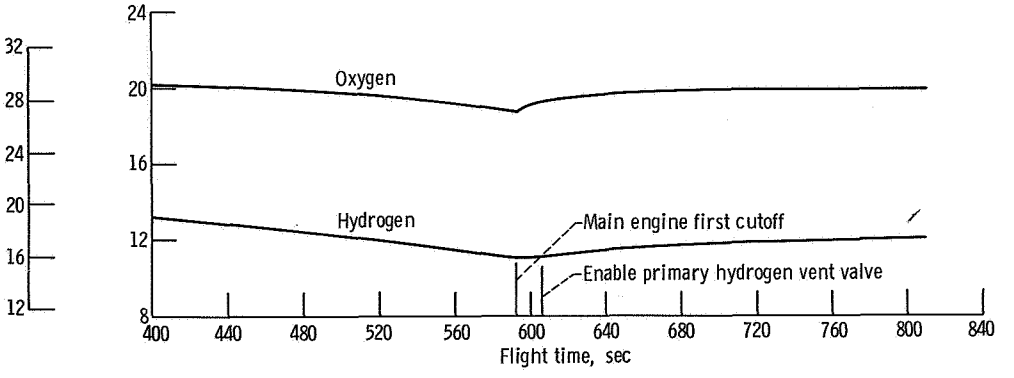

(c) Flight time, 400 to 800 seconds. Loss of signal from T + 810 to T + 1240 seconds.

Figure VI-35. - Centaur tank pressure history, AC-15.

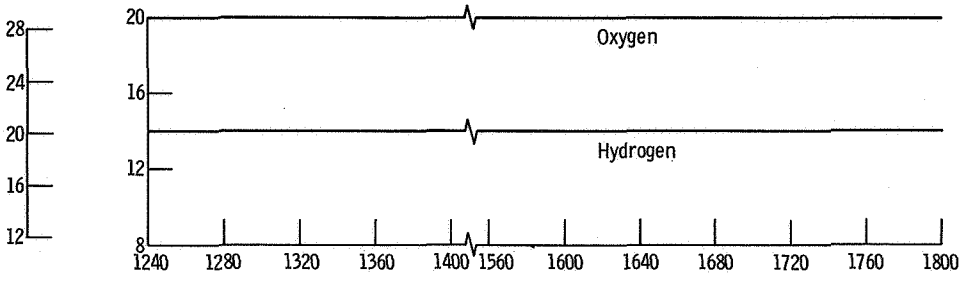

(d) Flight time, 1240 to 1800 seconds.

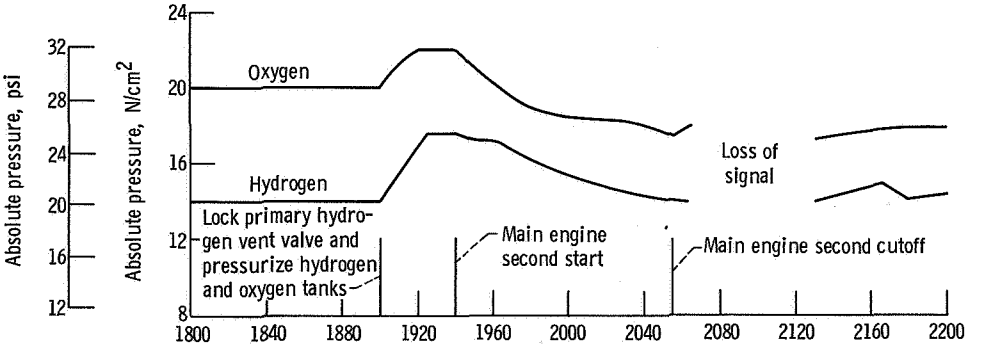

(e) Flight time, 1800 to 2200 seconds. Loss of signal from T + 2064 to T + 2130 seconds.

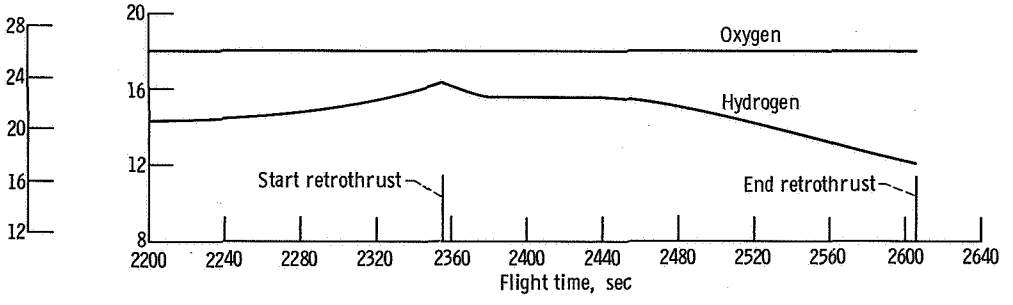

(f) Flight time, 2200 seconds to end of retrothrust.

Figure VI-35. - Concluded.

HYDRAULIC SYSTEMS

by Eugene J. Fourney

Atlas Hydraulics

System description. - Two hydraulic systems (fig. VI-36) are used on the Atlas stage to supply fluid power for operation of sustainer control valves and for thrust vector control of all engines. One system is used for the booster engine and the other for the sustainer engine and vernier engines. Both the booster and sustainer accumulator subsystems used on AC-13, AC-14, and AC-15 were identical but differed from those used on AC-12 and earlier flight vehicles.

The booster hydraulic system provides power solely for gimbaling the two thrust chambers of the booster engine system. System pressure is supplied by a single, pressure compensated, variable displacement pump driven by the engine turbopump accessory drive. Other components of the system include four servocylinders, a high-pressure relief valve, an accumulator, and a reservoir. Two isolated accumulators were used on previous vehicles. Vehicles AC-13, AC-14, and AC-15 used a single accumulator with a lower precharge pressure. Engine gimbaling in response to flight control commands is accomplished by the servocylinders which provide separate pitch, yaw, and roll control during the booster phase of flight. The maximum booster engine gimbal angle capability is $\pm 5^{\circ}$ in both the pitch and yaw planes.

The sustainer stage uses a system similar to that of the booster but, in addition, provides hydraulic power for sustainer engine control valves and gimbaling of the two vernier engines. The high-precharge-pressure-type accumulator system was replaced with the lower-precharge-pressure type, identical to that used on the booster.

The sustainer engine is held in the centered position until booster engine cutoff. Any disturbances created by the booster engine differential cutoff impulses would be damped by gimbaling the sustainer and vernier engines. The sustainer engine is again centered during booster engine package jettison. Vehicle engine roll control is maintained throughout the sustainer phase by differential gimbaling of the vernier engines. Actuator limit travel of the vernier engines is $\pm 70^{\circ}$, and that of the sustainer engine is $\pm 3^{\circ}$.

System performance. - Hydraulic system pressure data for both the booster and sustainer circuits are shown in figures VI-37 to VI-39. All pressures were stable throughout the boost phase of flight except the sustainer return system pressure on AC-15. The return pressures oscillated ±21 newtons per square centimeter (±30 psi) about an absolute pressure of 80 newtons per square centimeter (115 psia) at a frequency of 0.3 hertz from T + 62 seconds to T + 150 seconds. This particular pressure normally

remains steady except for a few seconds during the transients of sustainer engine start, booster engine package jettison, and sustainer engine cutoff. This problem is attributed to instrumentation rather than a malfunction of the hydraulic system.

The transfer of fluid power on AC-13, AC-14, and AC-15 from ground to airborne hydraulic systems was normal. Hydraulic pump discharge pressures increased at T - 2 seconds to flight levels in less than 2 seconds. Engine start transients produced a normal overshoot of about 10 percent in the hydraulic pump discharge pressures. Absolute pressures in the booster and sustainer systems stabilized at the values shown in the following table:

Flight	Units	Absolute pressures at lift-off	
		Booster	Sustainer
AC-13	N/cm^2	2053	2144
	psi	2977	3110
AC-14	N/cm^2	2157	2137
	psi	3130	3100
AC-15	N/cm^2	2118	2117
	psi	3070	3070

Maximum engine gimbaling during the flights occurred during the period of maximum dynamic pressure. Only $\pm 1^{\circ}$ of the $\pm 5^{\circ}$ engine gimbal capacility was required during this period.

Centaur Hydraulics

System description. - Two separate but identical hydraulic systems (fig. VI-40) are used on the Centaur stage. Each system gimbals one engine. Together they provide pitch, yaw, and roll control. Each system consists of two servocylinders and an engine-coupled power package containing high- and low-pressure pumps, a reservoir, an accumulator, a pressure intensifying bootstrap piston, and relief valves for pressure regulation. Hydraulic pressure and flow are provided by a constant-displacement vane-type pump driven by the liquid-oxygen turbopump accessory drive shaft. An electrically powered recirculation pump is used to provide low pressure for engine gimbaling requirements during prelaunch checkout, to aline the engines prior to main engine start, and to provide limited thrust vector control during the Centaur retrothrust operation.

Maximum engine gimbal capacility is $\pm 3^{o}$.

System performance. - The hydraulic systems on AC-13, AC-14, and AC-15 properly performed all guidance and flight control commands throughout the flight. System pressures and temperatures as a function of the flight times are shown in figures VI-41 to VI-43. Values at selected times are shown in tables VI-12 and VI-13.

TABLE VI-12. - C-1 SYSTEM ABSOLUTE PRESSURE AND MANIFOLD TEMPERATURE; AC-13, AC-14, AND AC-15

Event	Measurement	Units	Flight values for-		
			AC-13	AC-14	AC-15
Main engine first start	System pressure	N/cm^2	789	808	786
		psi	1142	1170	1138
	Recirculation pressure	N/cm^2	94	87	77
		psi	136	126	112
	Manifold temperature	K	291	285	287
		^{o}F	64	53	57
Main engine first cutoff	System pressure	N/cm^2	789	808	786
		psi	1142	1170	1138
	Manifold temperature	K	344	339	340
		^{o}F	160	150	153
Main engine second start	System pressure	N/cm^2	789	800	786
		psi	1142	1160	1138
	Recirculation pressure	N/cm^2	94	87	77
		psi	136	126	112
	Manifold temperature	K	332	314	314
		^{o}F	138	106	106
Main engine second cutoff	System pressure	N/cm^2	789	800	786
		psi	1142	1160	1138
	Manifold temperature	K	350	342	343
		^{o}F	171	156	158

TABLE VI-13. - C-2 SYSTEM ABSOLUTE PRESSURE AND MANIFOLD TEMPERATURE; AC-13, AC-14, AND AC-15

Event	Measurement	Units	Flight values for -		
			AC-13	AC-14	AC-15
Main engine first start	System pressure	N/cm^2	776	798	794
		psi	1126	1157	1151
	Recirculation pressure	N/cm^2	82	88	96
		psi	119	127	139
	Manifold temperature	K	291	282	288
		^oF	64	48	59
Main engine first cutoff	System pressure	N/cm^2	776	798	794
		psi	1126	1157	1151
	Manifold temperature	K	347	340	339
		^oF	165	153	151
Main engine second start	System pressure	N/cm^2	776	780	794
		psi	1126	1131	1151
	Recirculation pressure	N/cm^2	82	88	96
		psi	119	127	139
	Manifold temperature	K	330	324	315
		^oF	135	123	108
Main engine second cutoff	System pressure	N/cm^2	776	780	794
		psi	1126	1131	1151
	Manifold temperature	K	352	344	341
		^oF	174	160	155

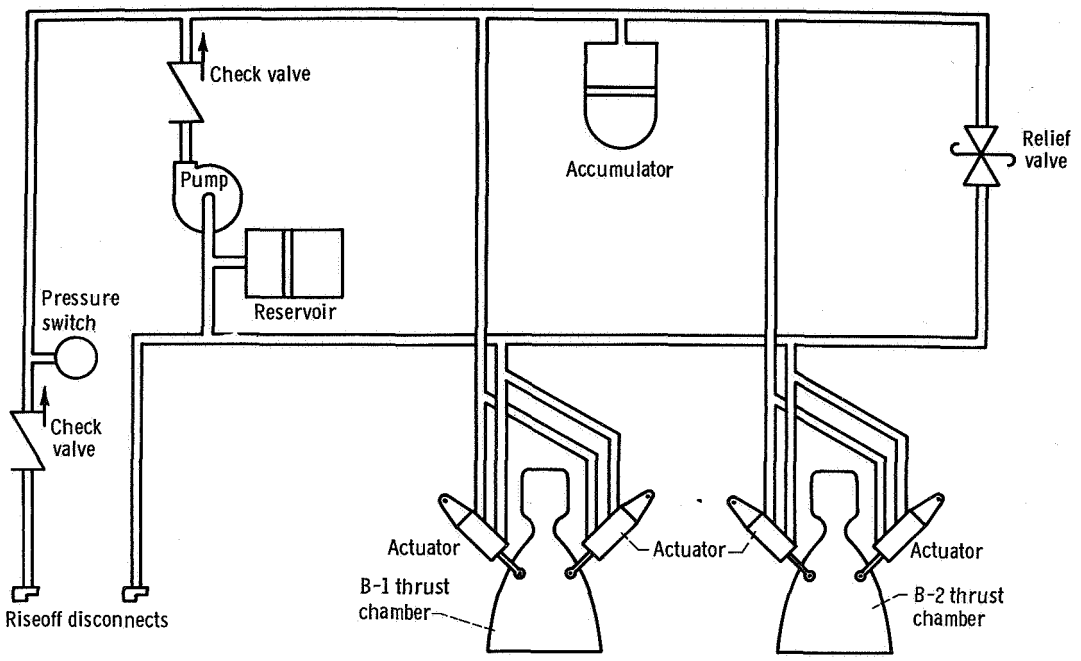

(a) Booster.

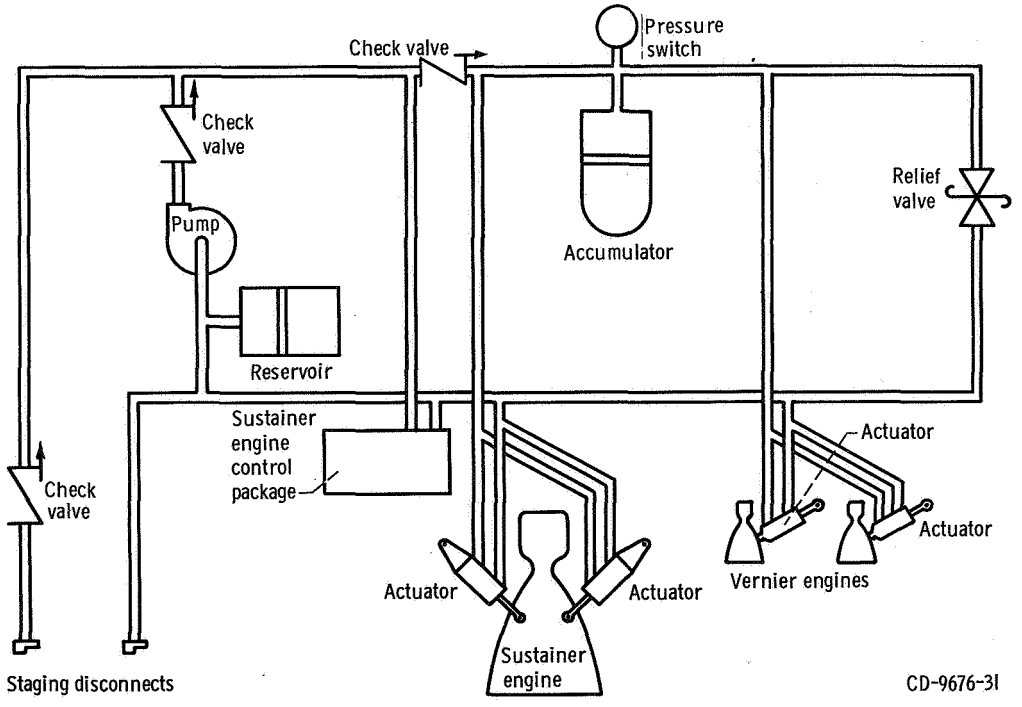

(b) Sustainer.

Figure VI-36. - Atlas hydraulic systems; AC-13, AC-14, and AC-15.

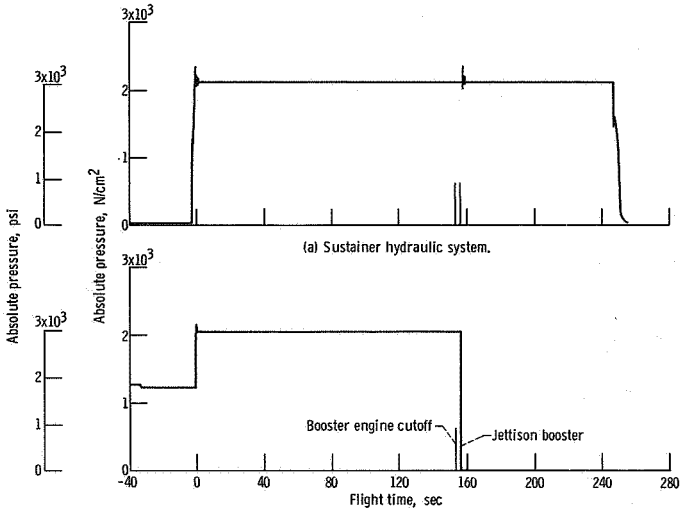

(b) Booster hydraulic system.

Figure VI-37. - Atlas hydraulic system pressures, AC-13.

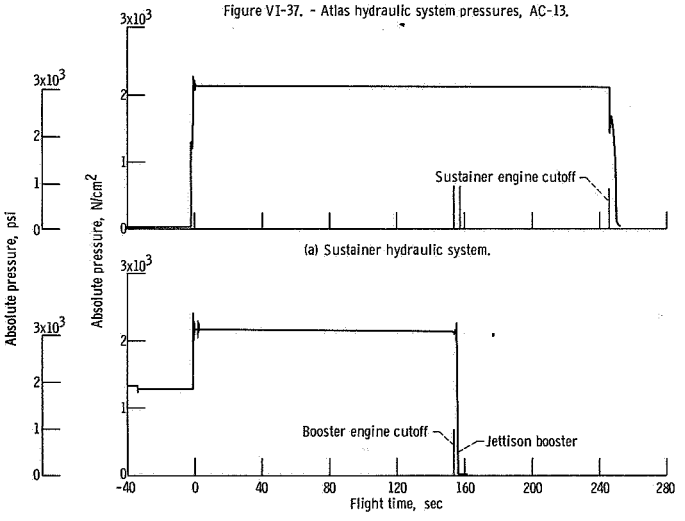

(b) Booster hydraulic system.

Figure VI-38. - Atlas hydraulic system pressures, AC-14.

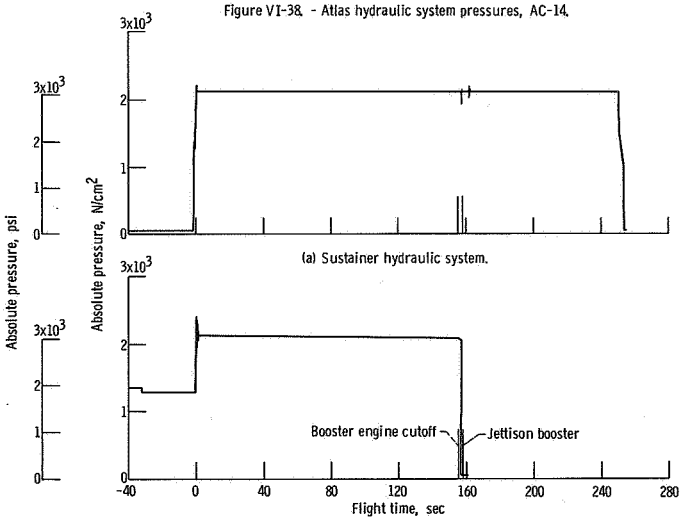

(b) Booster hydraulic system.

Figure VI-39. - Atlas hydraulic system pressures, AC-15.

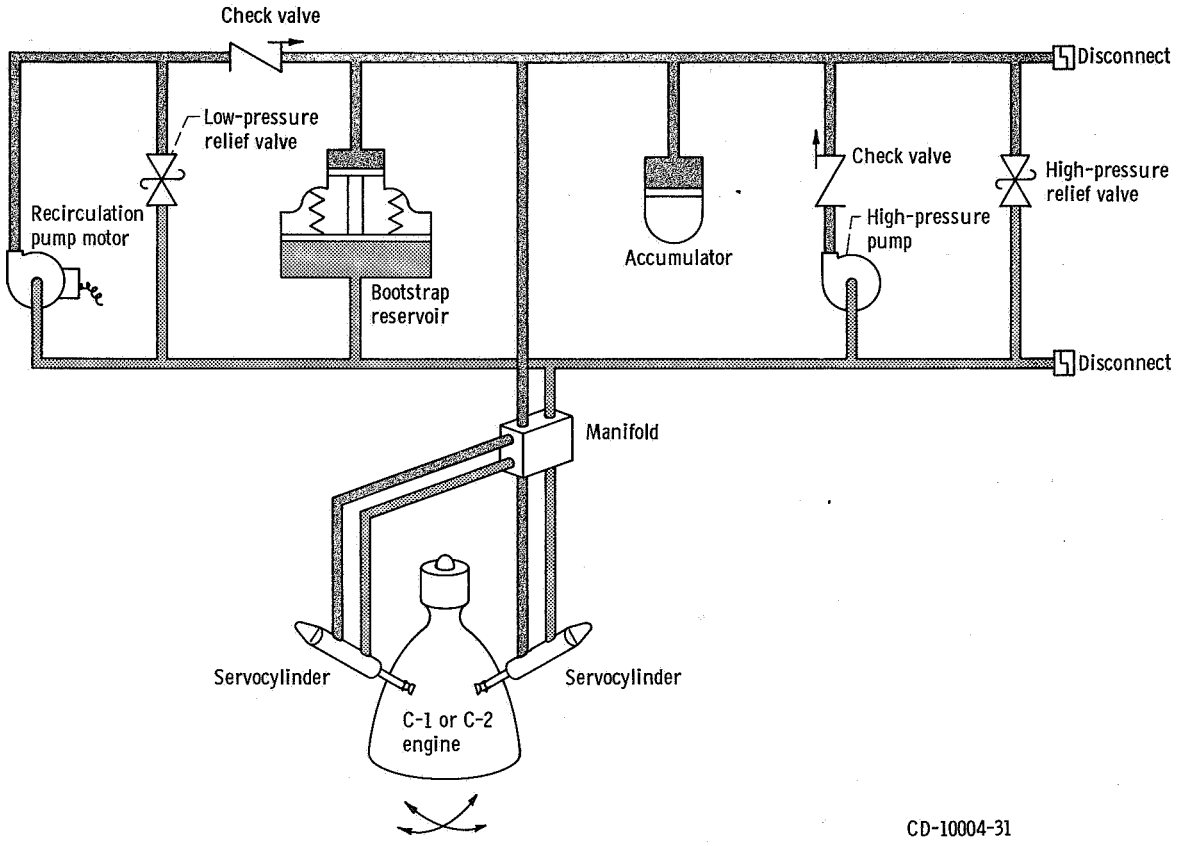

Figure VI-40. - Centaur hydraulic system; AC-13, AC-14, and AC-15.

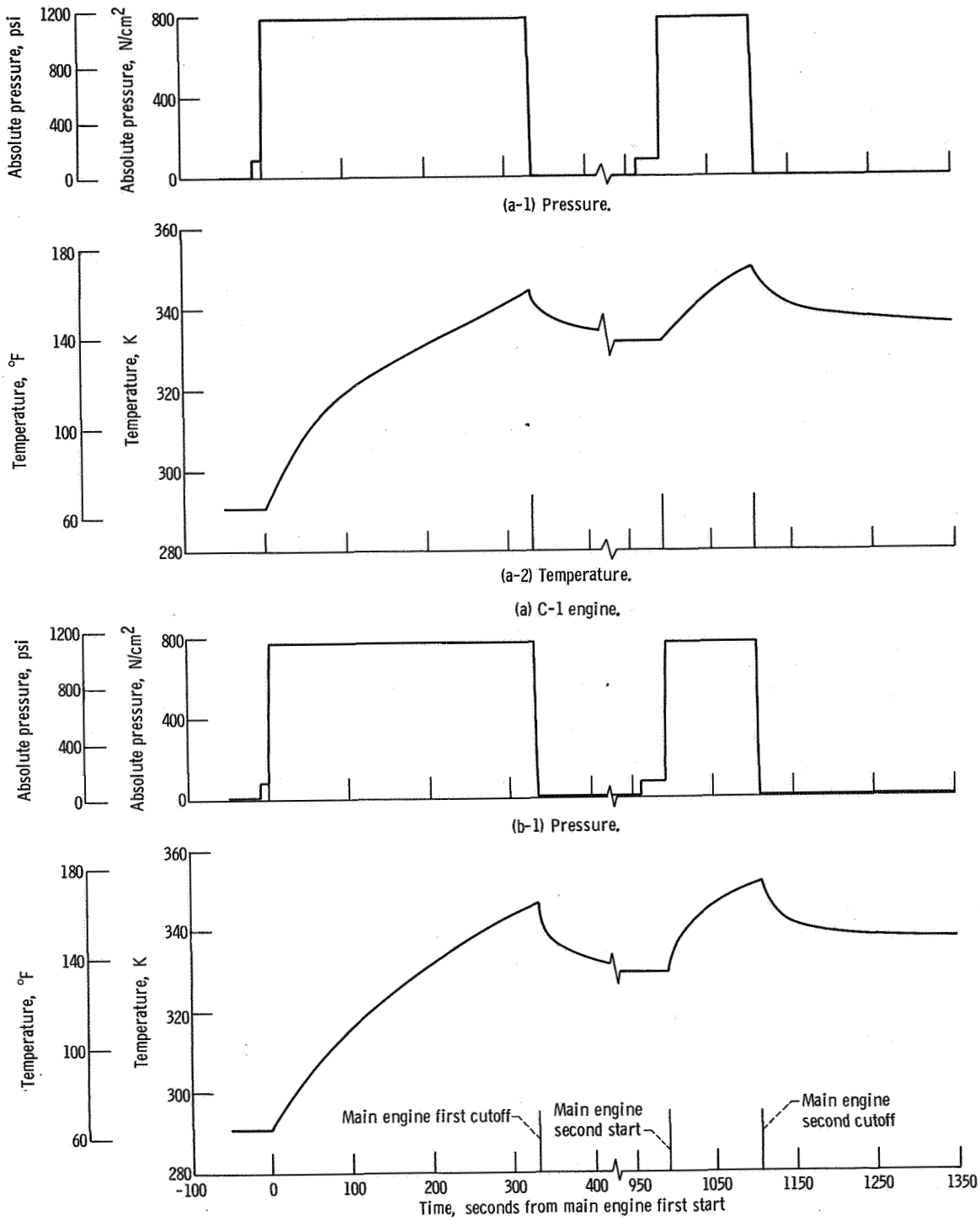

(a-1) Pressure.

(a-2) Temperature.

(a) C-1 engine.

(b-1) Pressure.

(b-2) Temperature.

(b) C-2 engine.

Figure VI-41. - Hydraulic system pressure and temperature, AC-13.

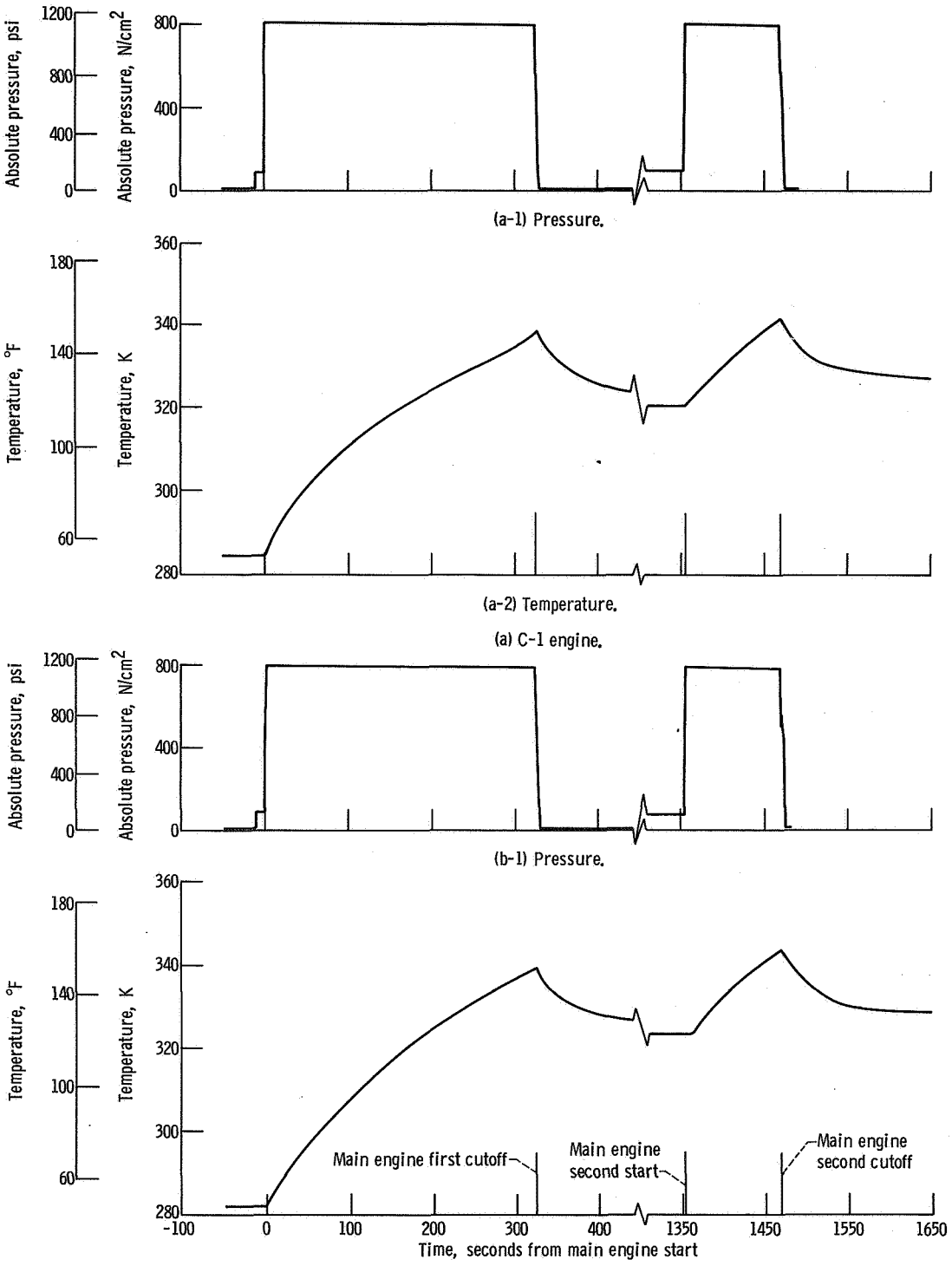

(a-1) Pressure.

(a-2) Temperature.

(a) C-1 engine.

(b-1) Pressure.

(b-2) Temperature.

(b) C-2 engine.

Figure VI-42. - Hydraulic system pressure and temperature, AC-14.

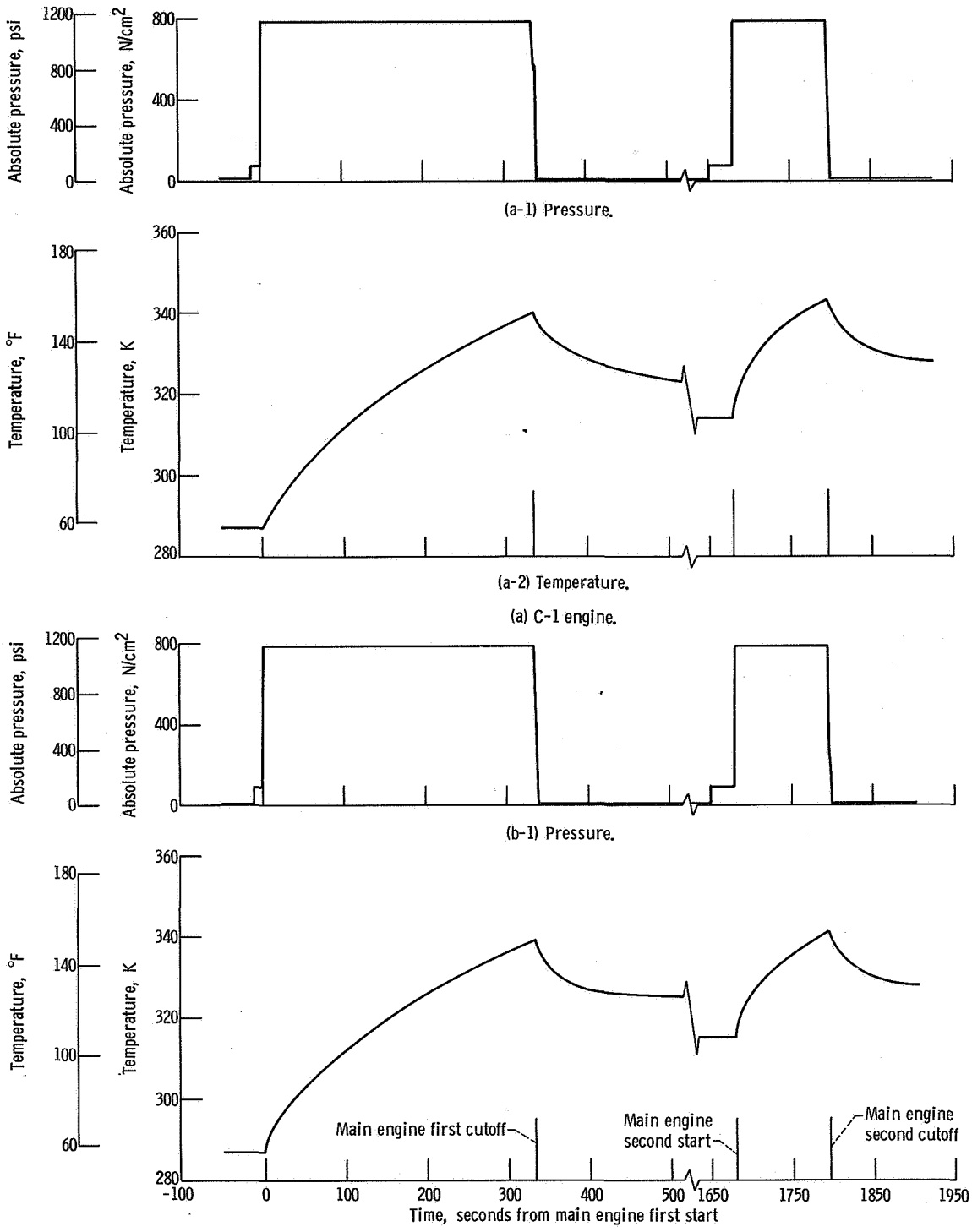

(a-1) Pressure.

(a-2) Temperature.

(a) C-1 engine.

(b-1) Pressure.

(b-2) Temperature.

(b) C-2 engine.

Figure VI-43. - Hydraulic system pressure and temperature, AC-15.

VEHICLE STRUCTURES

by Robert C. Edwards and Dana H. Benjamin

Atlas Structures

Atlas system description. - The Atlas vehicle primary structure is provided by the propellant tanks. These tanks are thin-walled, pressure-stabilized, monocoque sections of welded construction (see fig. VI-44). They require certain minimum pressures during various periods of flight in order to maintain structural stability. The strength of the tanks as pressure vessels determines the maximum allowable pressure in the propellant tanks.

Atlas tank flight pressures. - Because of varying loads and ambient pressures, the maximum allowable and minimum required tank pressures were not constant.

The Atlas vehicle was subjected to its highest design bending load between T + 60 and T + 110 seconds. The bending, axial inertia, and aerodynamic drag created compressive loads in the fuel and oxidizer tank skin. These loads were resisted by internal pressure to prevent buckling of the skin. The Atlas fuel and oxidizer tank ullage pressures during this time were above the minimum required to resist the combined bending and axial design loads, and did not approach the maximum allowable pressure at any time during the flight (see figs. VI-45 to VI-47).

The maximum allowable differential pressure between the oxidizer and fuel tanks was limited by the strength of the Atlas intermediate bulkhead. The fuel tank pressure must always be greater than the oxidizer tank pressure to stabilize the intermediate bulkhead (prevent bulkhead reversal). The bulkhead differential pressure was within the maximum allowable and minimum required pressure limits for all periods of flight (see figs. VI-45 to VI-47).

Quasi-steady-state load factors. - The increase of longitudinal inertia was as expected. A maximum value which was within the specified limits of 5.62 to 5.78 g's was reached at booster engine cutoff for all three flights (AC-13, 5.73 g's; AC-14, 5.76 g's; and AC-15, 5.78 g's).

Vehicle bending loads. - Flight bending loads were determined at station 461 on the Atlas interstage adapter for AC-13 and AC-15. Strain-gage data on the AC-14 vehicle exhibited drift, so no quantitative analysis was performed. However, a qualitative examination indicated AC-14 bending loads were similar to those of AC-13. The maximum flight bending moments were well within the maximum design bending moment as shown by figures VI-48 and VI-49.

Centaur Structures

Centaur system description. - The Centaur vehicle primary structure is provided by the propellant tanks. These tanks are thin-walled, pressure-stabilized, monocoque sections of welded construction (see fig. VI-50). They require certain minimum pressures during various periods of flight in order to maintain structural stability. The strength of the tanks, as pressure vessels, determines the maximum allowable pressure in the propellant tanks. The propellant tanks are vented, as required, during the flight to prevent excessive ullage pressures (see Centaur Pneumatics section).

Centaur tank flight pressures. - The maximum allowable and minimum required tank pressures were computed by using maximum design loads (as opposed to flight loads) with appropriate factors of safety. Because of varying loads and ambient pressures during flight, the maximum allowable and minimum required tank pressures were not constant. The tank locations and the criteria which determined the maximum allowable and minimum required tank pressures during different phases of flight are described in figure VI-51. The Centaur oxidizer and fuel tank ullage pressure profiles are compared with the design pressure profiles in figures VI-52, VI-53, and VI-54 for AC-13, AC-14, and AC-15, respectively.

The oxidizer tank pressure was of concern only near the time of booster engine cutoff (approx. T + 156 sec), when the high inertia load caused maximum tension loads on the aft bulkhead. At this time, the maximum allowable oxidizer tank absolute pressure was 22.7 newtons per square centimeter (33.0 psi). All three flight vehicles had oxidizer tank pressures less than this value (figs. VI-52(a), VI-53(a), VI-54(a)). The oxidizer tank pressure did not approach the minimum required for aft bulkhead stability during any period of the three flights.

The strength of the fuel tank was governed by the capability of the conical section of the forward bulkhead to resist hoop stress. Thus, the differential pressure across the forward bulkhead determined the maximum allowable fuel tank pressure. This allowable differential pressure was 18.5 newtons per square centimeter (26.8 psi). At no time during any of the three flights did the fuel tank ullage pressure exceed the maximum allowable pressure (see figs. VI-52 to VI-54).

Although well above the minimum required pressure at all times, the margin between fuel tank ullage pressure and the minimum required pressure was least during the following events:

(1) Prior to launch, the insulation panel pretensioning imposed local bending stresses on the fuel tank cylindrical skin. The minimum required fuel tank absolute pressure at this time was 13.1 newtons per square centimeter (19.0 psi). The actual fuel tank absolute pressures are shown in figures VI-52(a), VI-53(a), and VI-54(a).

(2) During the launch phase at T + 0 seconds, the payload imposed compression loads on the forward bulkhead as a result of inertia and lateral vibration. The minimum re-

quired fuel tank absolute pressure was 13.4 newtons per square centimeter (19.5 psi) at T + 0 seconds. The actual fuel tank absolute pressures are shown in figures VI-52(a), VI-53(a), and VI-54(a).

(3) From T + 60 to T + 110 seconds, the Centaur was subjected to maximum design bending moments. The combined loads due to inertia, aerodynamic drag, and bending imposed compression on the cylindrical skin at station 409.6. The minimum required fuel tank absolute pressure to resist this compression and the actual fuel tank ullage pressures are shown in figures VI-52(a), VI-53(a), and VI-54(a).

(4) At nose fairing jettison, the nose fairing exerted inboard radial loads at station 219. The minimum required fuel tank absolute pressure to resist these loads was 12.8 newtons per square centimeter (18.5 psi). The actual fuel tank ullage pressures are shown in figures VI-52(b), VI-53(b), and VI-54(b).

The maximum allowable differential pressure between the oxidizer and fuel tanks was limited by the strength of the Centaur intermediate bulkhead. The maximum design allowable differential pressure was 15.9 newtons per square centimeter (23.0 psi). The differential pressure was less than this maximum allowable for all periods of flight (see figs. VI-52 to VI-54).

The oxidizer tank pressure must always be greater than the fuel tank pressure to stabilize the intermediate bulkhead. The design minimum differential pressure was 1.4 newtons per square centimeter (2.0 psi). When the effect of the hydrogen fuel hydrostatic pressure was included, the differential pressure was still greater than this design minimum for all periods of flight (see figs. VI-52 to VI-54).

Vehicle Dynamic Loads

The Atlas-Centaur launch vehicle receives dynamic loading from several sources. The loads fall into three major categories: (1) external loads from aerodynamic and acoustic sources; (2) transients from engines starting and stopping and from the separation systems; (3) loads due to dynamic coupling between major systems.

Research and development flights of the Atlas-Centaur have shown that these loads were within the structural limits established by ground test and model analysis. For operational flights such as AC-13, AC-14, and AC-15, the number of dynamic flight measurements is limited by telemetry capacity. The instruments used and the parameters measured were as follows:

Instruments	Corresponding parameters
Low-frequency-range accelerometer	Launch vehicle longitudinal vibration
Centaur pitch rate gyro	Launch vehicle pitch plane vibration
Centaur yaw rate gyro	Launch vehicle yaw plane vibration
Angle-of-attack sensor	Vehicle aerodynamic loads
High-frequency-range accelerometers	Local spacecraft vibration

Launch vehicle longitudinal vibrations measured on the Centaur forward bulkhead are presented in figure VI-55, which depicts the presence of specific responses at the times noted. The frequency and amplitude of the vibration data measured on these three flights are shown together with comparable data from other flights.

During launcher release, longitudinal vibrations were excited. The amplitude and frequency of these vibrations were similar to those observed on vehicles prior to AC-13. Atlas intermediate bulkhead pressure fluctuations were the most significant effects produced by the launcher-induced longitudinal vibrations. The peak pressure fluctuations computed from these vibrations were 4.5×10^4 newtons per square meter (6.5 psi). Since the bulkhead static differential pressure measured at this time was 13.6×10^4 newtons per square meter (19.7 psi) (see fig. VI-46), the calculated minimum differential pressure across the bulkhead was 9.1×10^4 newtons per square meter (13.2 psi).

During Atlas flight between T + 50 and T + 140 seconds, intermittent longitudinal vibrations of 0.11 g, 11 hertz (AC-13); 0.12 g, 11 hertz (AC-14); 0.11 g, 12 hertz (AC-15) were observed on the forward bulkhead. These vibrations are believed to be caused by dynamic coupling between structure, engines, and propellant lines (commonly referred to as "POGO"). For AC-13, AC-14, and AC-15, the new SLV-3C Atlas booster configuration was flown. The SLV-3C incorporates, among other modifications, a modified propulsion system to provide an additional 6000 pounds of engine thrust and a 51-inch extension of the propellant tank. As a result, the parameters controlling the frequency and amplitude of these vibrations were changed slightly, but not significantly. For a detailed discussion of this low-frequency longitudinal vibration see reference 5.

During the booster engine thrust decay, short-duration longitudinal vibrations of 0.5 g, 14 hertz (AC-13); 0.6 g, 16 hertz (AC-14); 0.4 g, 13 hertz (AC-15) were observed. The analytical models did not indicate significant structural loading due to these transients.

During the boost phase of flight, the vehicle vibrates in the pitch and yaw planes as an integral body at all of its natural frequencies. Previous analyses and tests have defined these natural frequencies or modes and the shapes which the vehicle assumes when the modes are excited. The rate gyros on the Centaur provide data for determining the deflection of these modes. The maximum first-mode deflection was seen in the pitch

plane at T + 122 seconds for AC-13, T + 142 seconds for AC-14, and T + 145 seconds for AC-15 (figs. VI-56 to VI-58). The deflection was less than 15 percent of the allowable deflection. The maximum second-mode deflection was seen in the yaw plane at T + 42 seconds for AC-13, T + 34 seconds for AC-14, and T + 35 seconds for AC-15 (figs. VI-59 to VI-61). The yaw deflection was less than 23 percent of the allowable deflection.

Predicted angles of attack were based on upper wind data obtained from a weather balloon released before the time of launch. Vehicle bending moments were calculated using predicted angles of attack, booster engine gimbal angle data, vehicle weights, and vehicle stiffnesses. These moments were added to axial load equivalent moments and to moments resulting from random dispersions. The most significant dispersions considered were uncertainties in launch vehicle performance, vehicle center of gravity offset, and upper atmosphere wind. The total equivalent predicted bending moment (based on wind data) was divided by the design bending moment allowable to obtain the predicted structural capability ratio, as shown in figures VI-62 to VI-64. This ratio is expected to be greatest between T + 52 and T + 80 seconds as a result of high aerodynamic loads during this period. The maximum structural capability ratios predicted for this period were 0.70 for AC-13, 0.80 for AC-14, and 0.78 for AC-15.

Transducers located on the nose fairing cap provided differential pressure measurements in the pitch and yaw planes. Total pressure was computed from a trajectory reconstruction. Angles of attack were computed from these data and are compared with predicted angles of attack in figures VI-65 to VI-67. Since the actual angles of attack were within the expected dispersion values, it follows that the maximum predicted structural capability ratios of 0.70 for AC-13, 0.80 for AC-14, and 0.78 for AC-15 were not exceeded.

Local shock and vibration were measured by two continuous high-frequency accelerometers in the spacecraft area. The accelerometers were located on the forward end of the payload adapter (station 129).

A summary of the most significant shock and vibration levels measured by the two continuous accelerometers on AC-13, AC-14, and AC-15 together with comparable data from AC-10, AC-12, and AC-11 is shown in table VI-14. The most significant reason for the apparent discrepancy between the vibration data obtained from the new SLV-3C vehicle and that obtained from the old LV-3C vehicle is that the locations of the high-frequency-vibration accelerometers on the two vehicle configurations were different. On AC-10, AC-12, and AC-11, the one continuous accelerometer was installed on one of the retro-attach points of the spacecraft; however, on AC-13, AC-14, and AC-15, the two continuous accelerometers were installed on the forward end of the payload adapter (station 129). The data show that the payload adapter receives more vibration (especially during launch transient) than the spacecraft structure. The steady-state vibration levels were highest near lift-off, as expected. The maximum level of the shock loads

(12 g's) on all three flights occurred at Atlas-Centaur separation. These shock levels are of short duration (about 0.025 sec) and did not provide significant loads. An analysis of the data indicates that the levels were well within spacecraft qualification levels.

TABLE VI-14. - COMPARISON OF MAXIMUM SHOCK AND VIBRATION LEVELS AT MARK EVENTS[a]

Flight event	Flight								
	AC-10	AC-12	AC-11	AC-13	AC-14	AC-15	AC-13	AC-14	AC-15
	Accelerometer location								
	Retromotor attachment 1, station 125; quadrant I-IV; longitudinally sensitive; analysis band, 10 to 790 Hz			Payload adapter, station 129; quadrant III; longitudinally sensitive; analysis band, 10 to 790 Hz			Payload adapter, station 129; quadrant I-IV; radially sensitive[b]		
Launch:									
Acceleration, g's (rms)	0.68	0.65	0.53	1.5	1.4	1.2	2.5	2.9	2.1
Frequency, Hz	165	165	160 to 170	150, 300	163, 296, 397	225, 296, 389, 425	470	485	462, 478, 525
Booster engine cutoff:									
Acceleration, g's	0.8	1.2	0.7	1.2	0.96	1.7	0.83	0.38	0.6
Frequency, Hz	11	17	12	13	14	13	4.5	4.7	4.5
Booster jettison:									
Acceleration, g's	0.5	0.46	0.3	<1/2	<1/2	<1/2	<1/2	<1/2	<1/2
Frequency, Hz	16	16	23	---	---	14	---	---	6
Insulation panel jettison:									
Acceleration, g's	10	10.1	12	~14	~13	~14	~12	~12	~9
Frequency, Hz	700	600 to 700	600 to 700	500 to 600	500 to 600	500 to 600	500 to 600	500 to 600	500 to 600
Nose fairing jettison:	1.4	0.49	1.1	2.1	2.7	3.2	2.0	1.6	2.0
Acceleration, g's	1.4	0.49	1.1	2.1	2.7	3.2	2.0	1.6	2.0
Frequency, Hz	32	20	32	400 to 500	400 to 500	400 to 500	400 to 500	400 to 500	400 to 500
Atlas-Centaur separation:									
Acceleration, g's	12	13	12	~14	~13	~14	~12	~12	~9.5
Frequency, Hz	600	600 to 700	700	500 to 600	500 to 600	500 to 600	500 to 600	500 to 600	500 to 600
Main engine first start:									
Acceleration, g's	0.38	0.5	0.4	0.5	0.6	0.5	(c)	(c)	(c)
Frequency, Hz	20	20 to 21	19 to 20	22	20	22	(c)	(c)	(c)
Main engine first cutoff:									
Acceleration, g's	1.14	0.95	2.0	1.6	0.9	0.9	0.9	0.7	0.7
Frequency, Hz	33	22	27	23	23	23	400 to 500	400 to 500	400 to 500
Main engine second start:									
Acceleration, g's	(d)	0.66	(d)	0.7	0.6	0.6	(c)	0.5	(c)
Frequency, Hz	(d)	20 to 22	(d)	20 to 30	30	23	(c)	400 to 500	(c)
Main engine second cutoff:									
Acceleration, g's	(d)	0.97	(d)	0.9	0.9	0.9	1.1	1.5	3
Frequency, Hz	(d)	24	(d)	30	30	30	480	480	400 to 500

[a]Maximum shock and vibration levels at mark events are given in terms of maximum single amplitude (in g's) and the most predominant frequency (in Hz) except for rms levels which represent maximum levels observed at launch.

[b]A nonstandard Interrange Instrumentation Group filter of 600 Hz was used to analyze launch data on AC-13, AC-14, and AC-15. All other postlaunch data were analyzed with a 330-Hz filter.

[c]No detectable response.

[d]Single-burn missions.

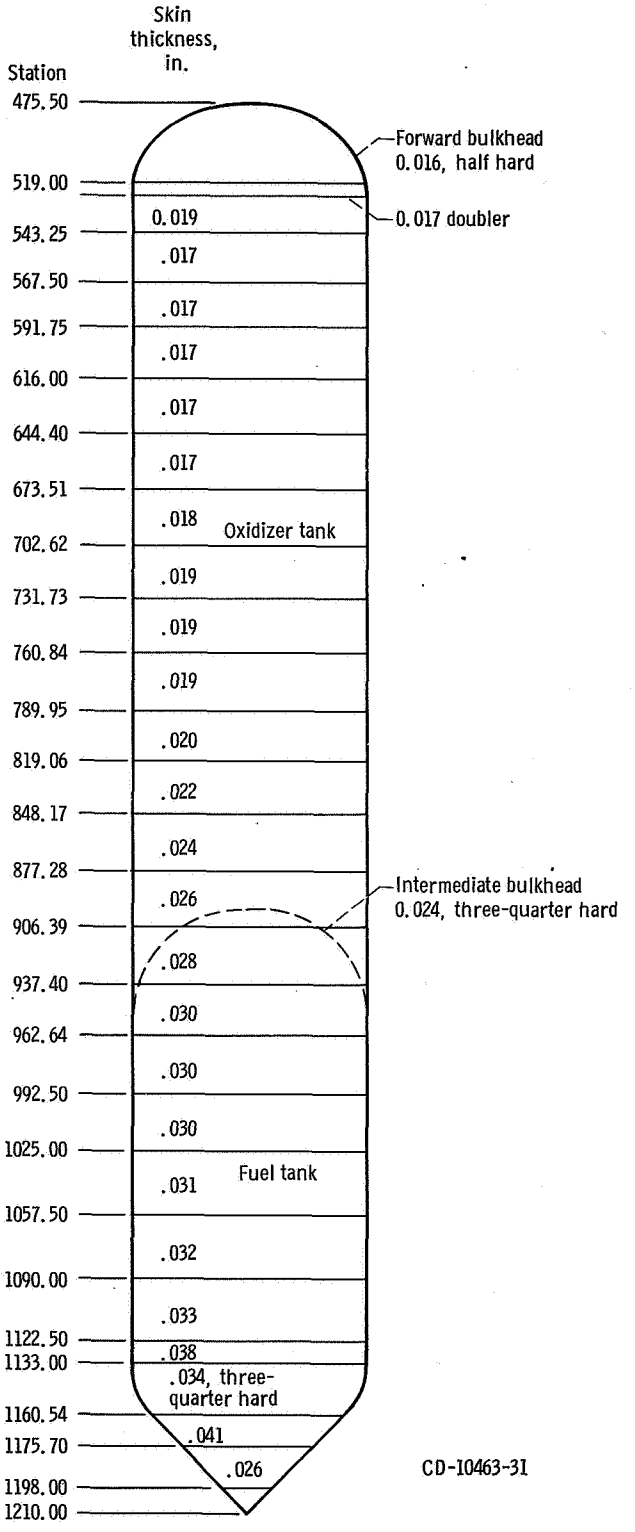

Figure VI-44. - Atlas propellant tanks; AC-13, AC-14, and AC-15. (Unless noted otherwise, all material is 301 extra-full-hard stainless steel.)

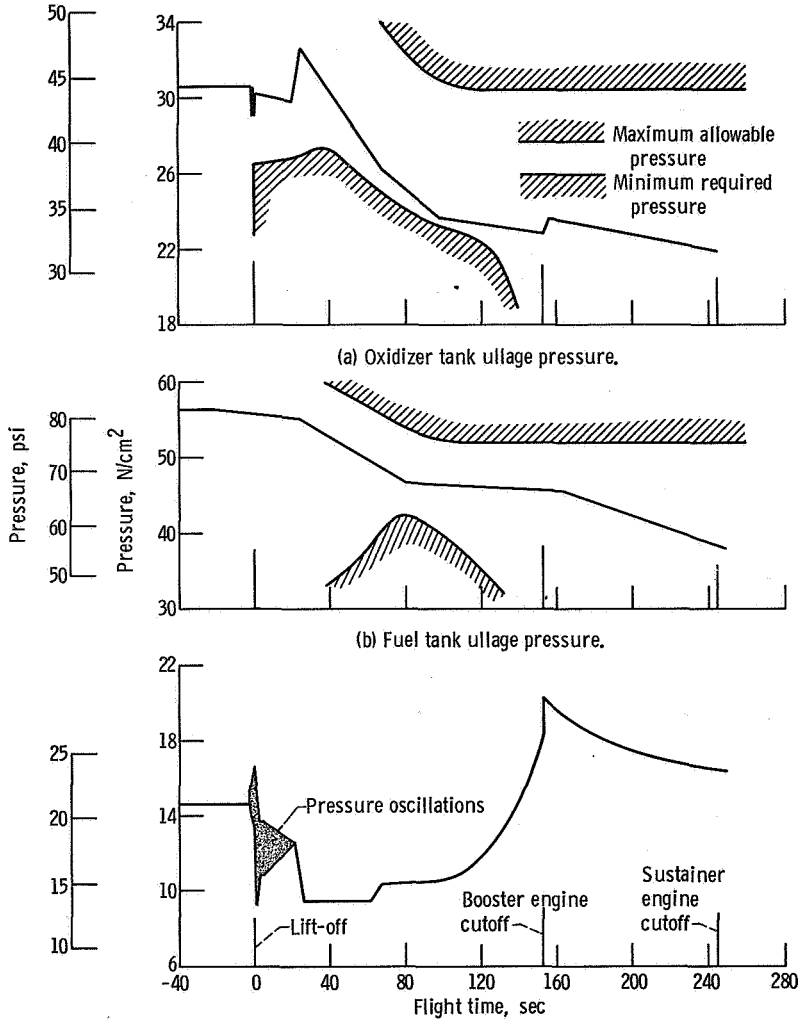

(c) Intermediate bulkhead differential pressure. Maximum allowable differential pressure, 42 newtons per square centimeter; minimum desirable differential pressure, 1.4 newtons per square centimeter.

Figure VI-45. - Atlas fuel and oxidizer tank pressures, AC-13.

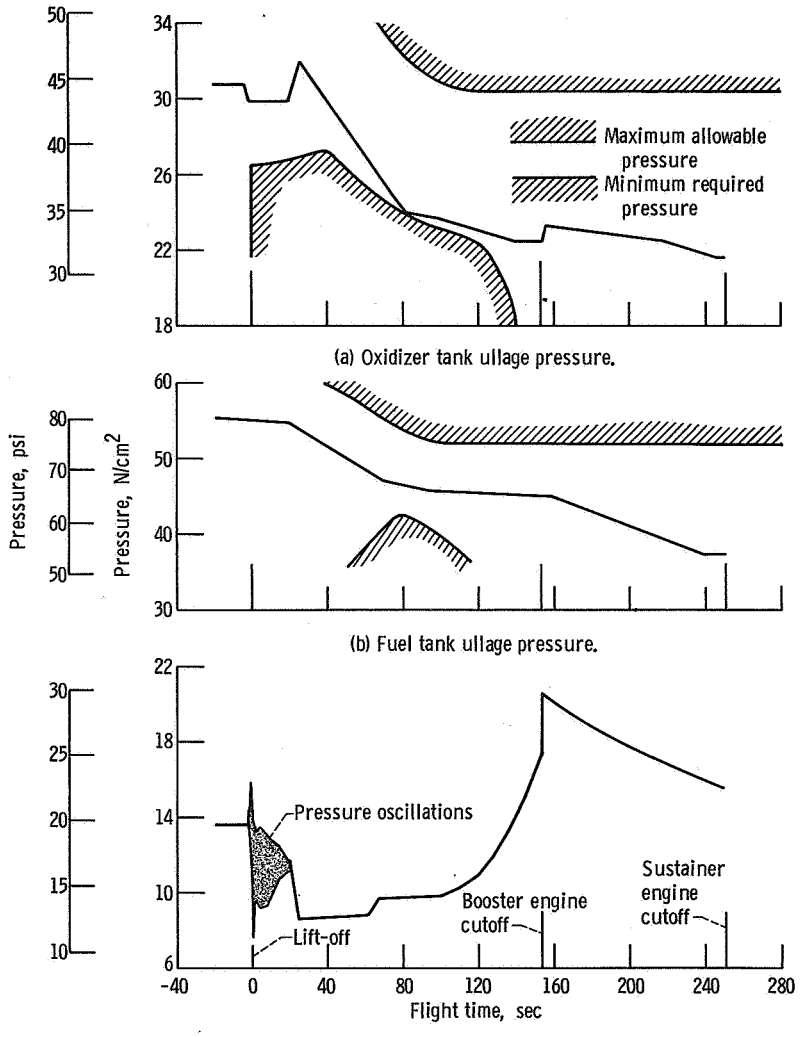

(c) Intermediate bulkhead differential pressure. Maximum allowable differential pressure, 42 newtons per square centimeter; minimum desirable differential pressure, 1.4 newtons per square centimeter.

Figure VI-46. - Atlas fuel and oxidizer tank pressures, AC-14.

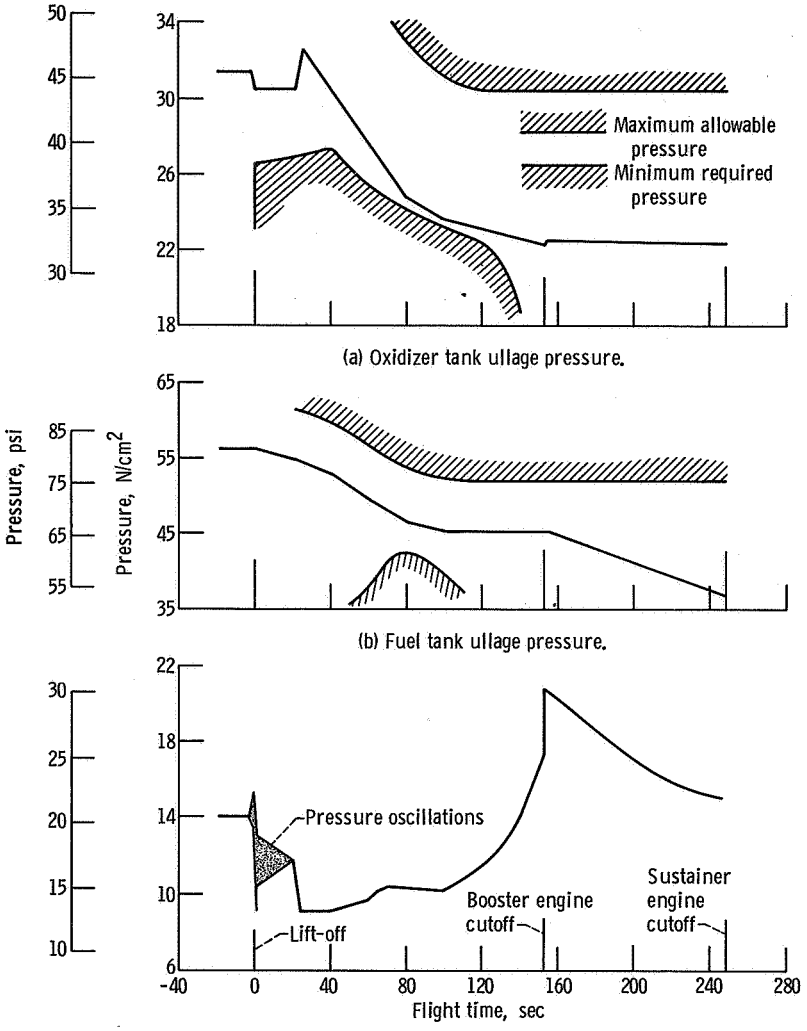

(c) Intermediate bulkhead differential pressure. Maximum allowable differential pressure, 42 newtons per square centimeter; minimum desirable differential pressure, 1.4 newtons per square centimeter.

Figure VI-47. - Atlas fuel and oxidizer tank pressures, AC-15.

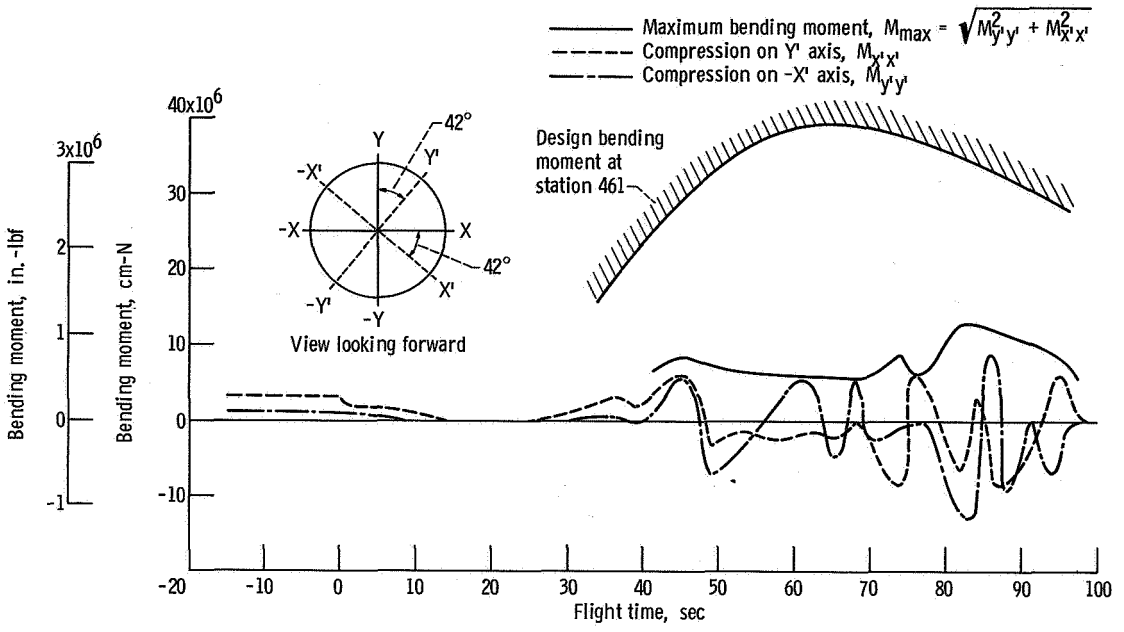

Figure VI-48. - Bending moment at station 461, AC-13.

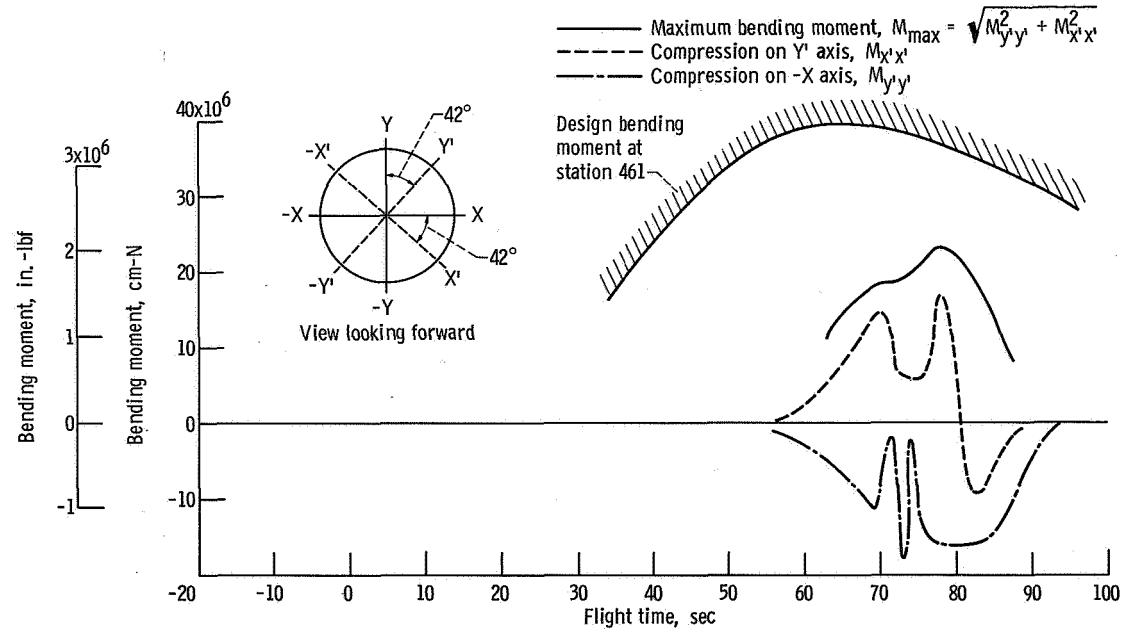

Figure VI-49. - Bending moment at station 461, AC-15

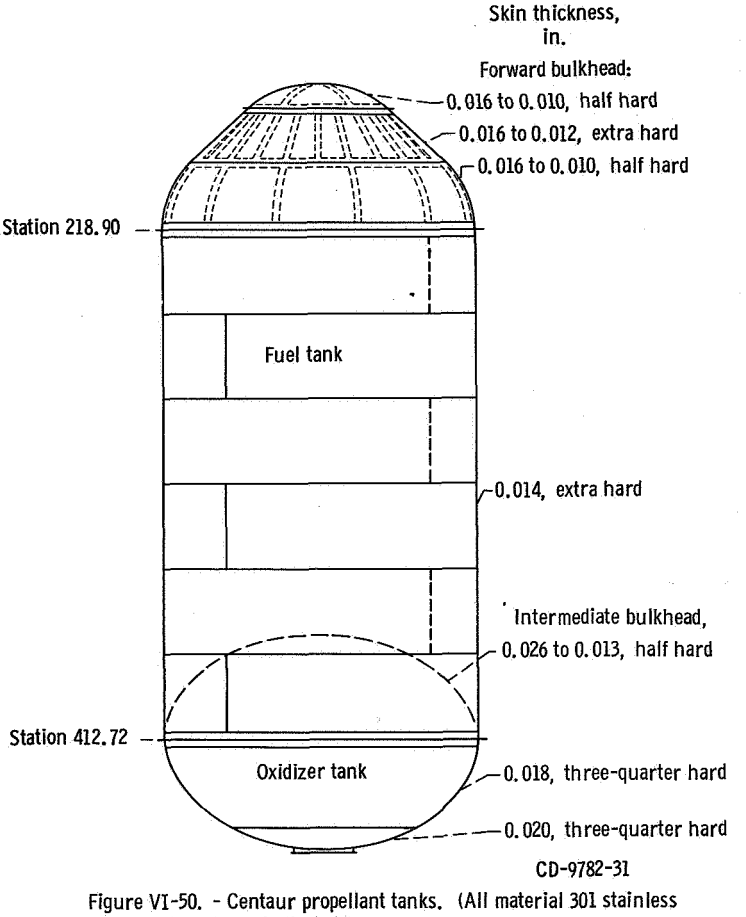

Figure VI-50. - Centaur propellant tanks. (All material 301 stainless steel, of hardness indicated.)

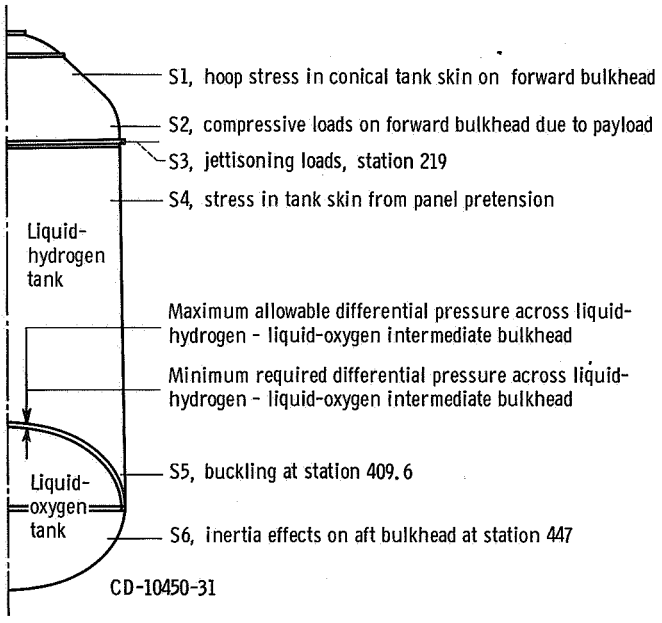

Figure VI-51. - Tank locations and criteria which determine allowable pressures.

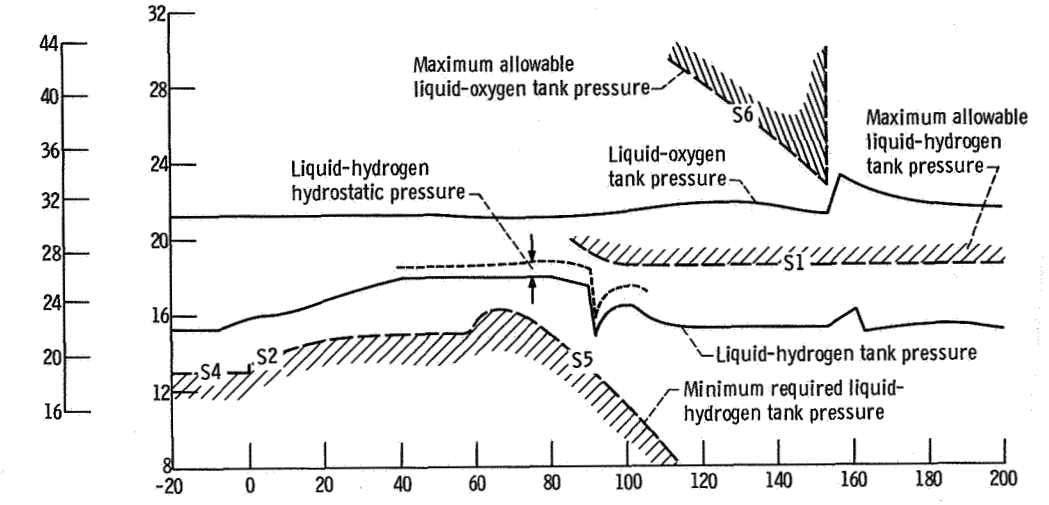

(a) Flight time, -20 to 200 seconds.

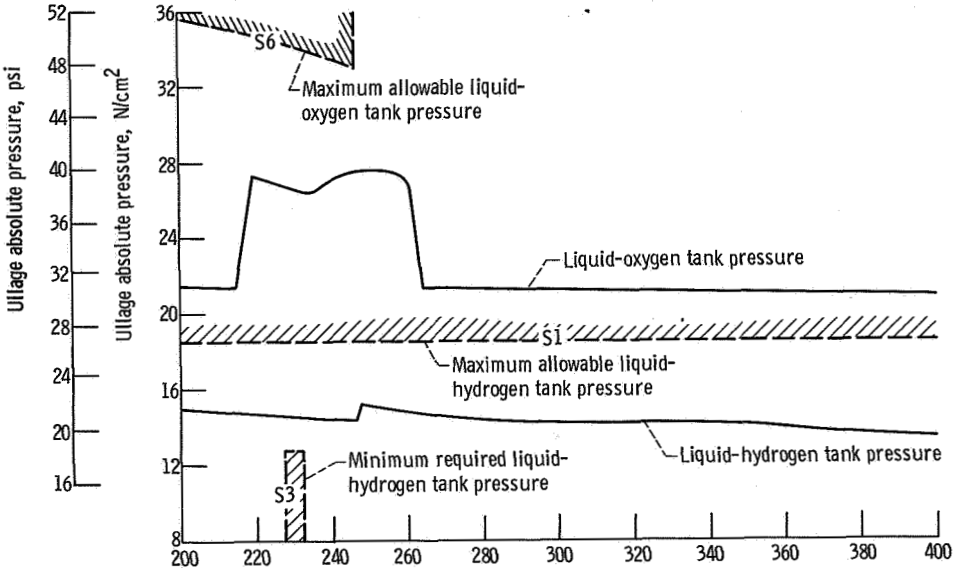

(b) Flight time, 200 to 400 seconds.

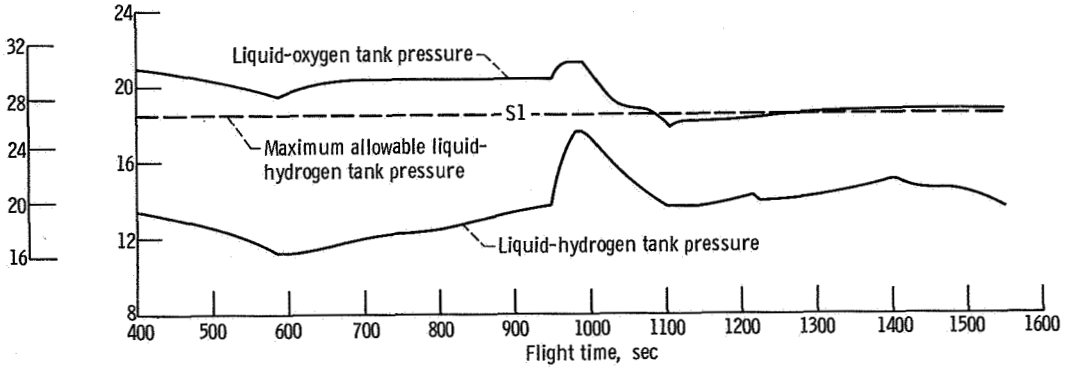

(c) Flight time, 400 to 1600 seconds.

Figure VI-52. - Centaur fuel and oxidizer tank pressure, AC-13. S1, S2, etc., indicate tank structure areas which determine the allowable tank pressure (see fig. VI-51).

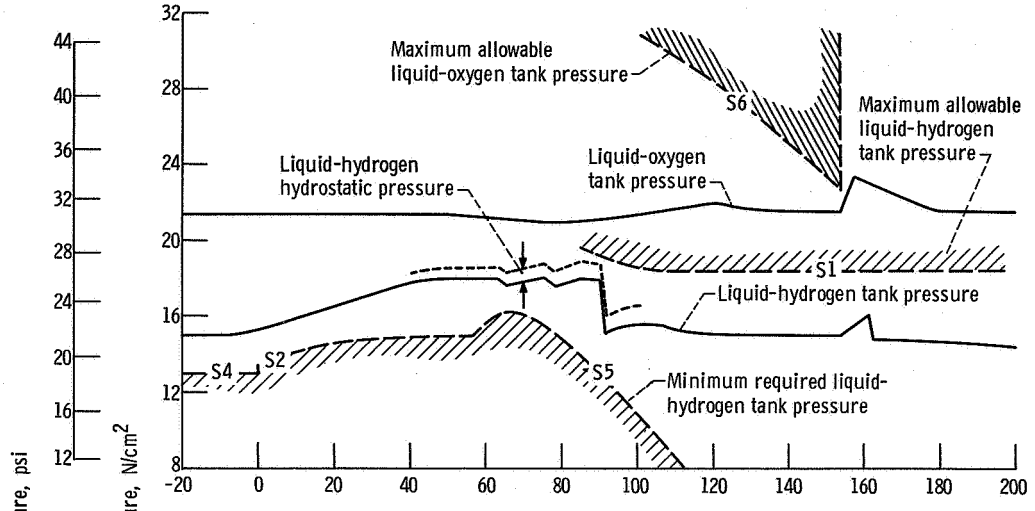

(a) Flight time, -20 to 200 seconds.

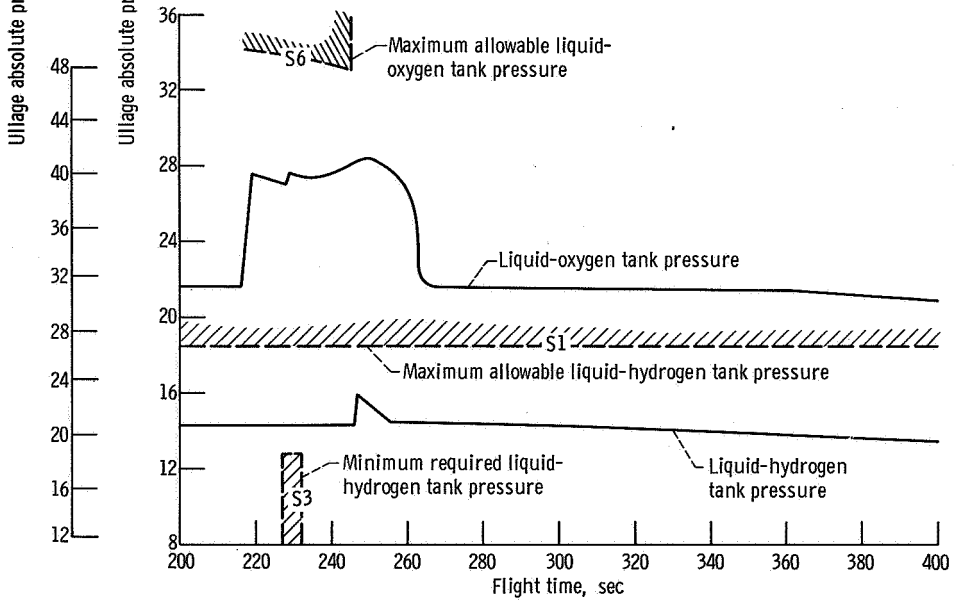

(b) Flight time, 200 to 400 seconds.

Figure VI-53. - Centaur fuel and oxidizer tank pressures, AC-14. S1, S2, etc., indicate tank structure areas which determine the allowable tank pressure (see fig. VI-51).

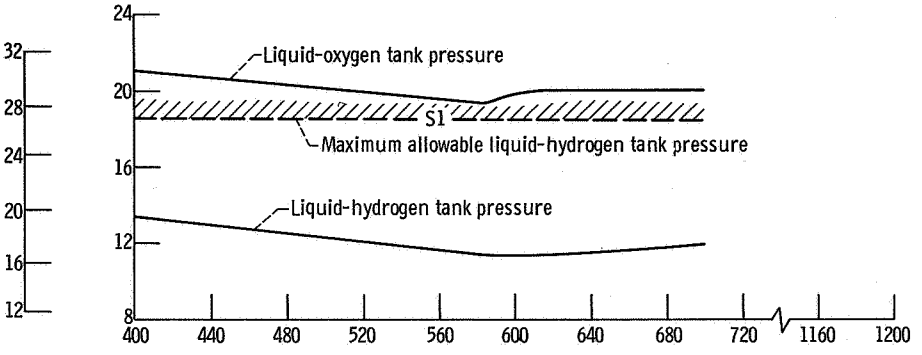

(c) Flight time, 400 to 1200 seconds. Data not available from 700 to 1200 seconds.

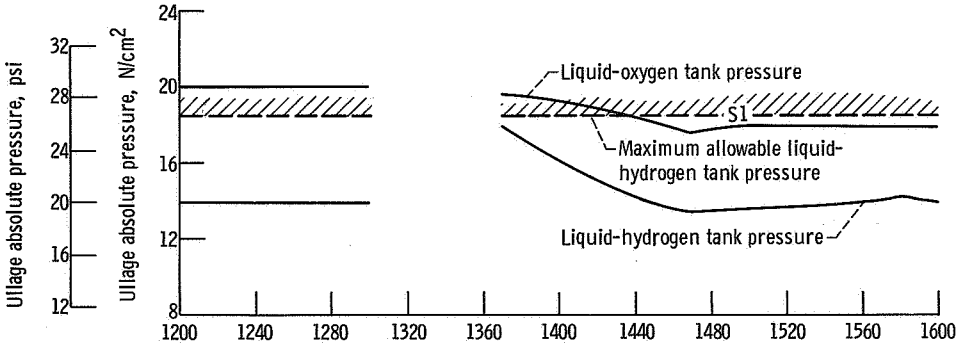

(d) Flight time, 1400 to 1600 seconds. Data not available from 1300 to 1370 seconds.

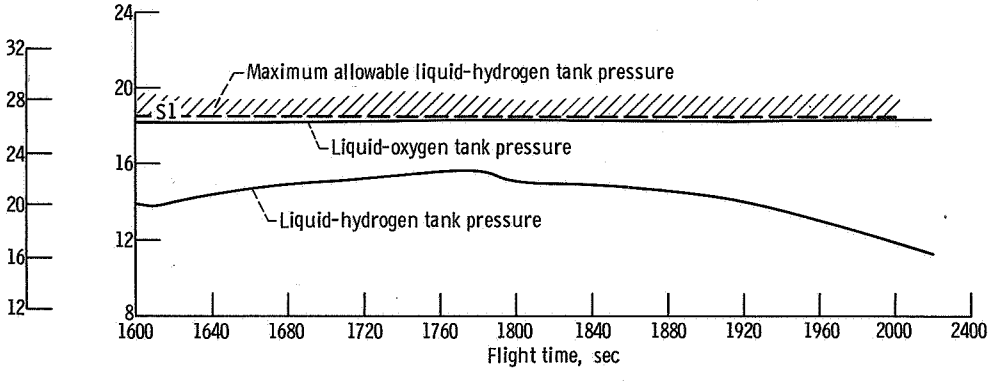

(e) Flight time, 1600 to 2400 seconds.

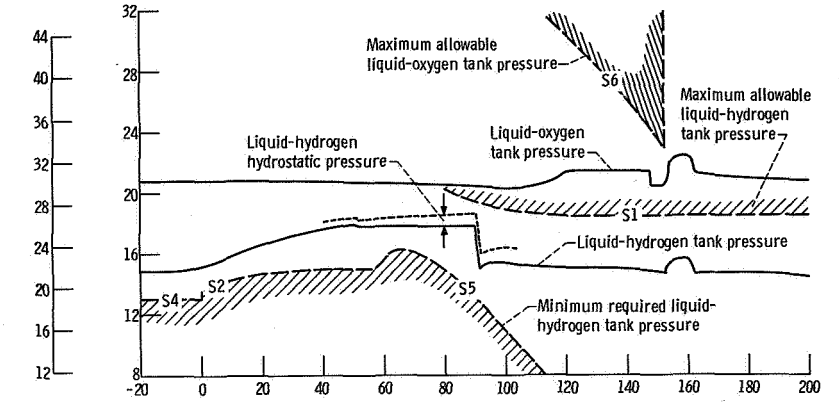

(a) Flight time, -20 to 200 seconds.

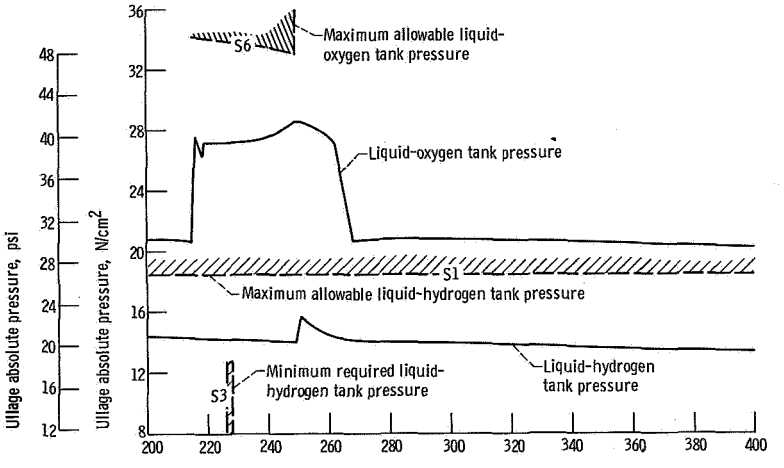

(b) Flight time, 200 to 400 seconds.

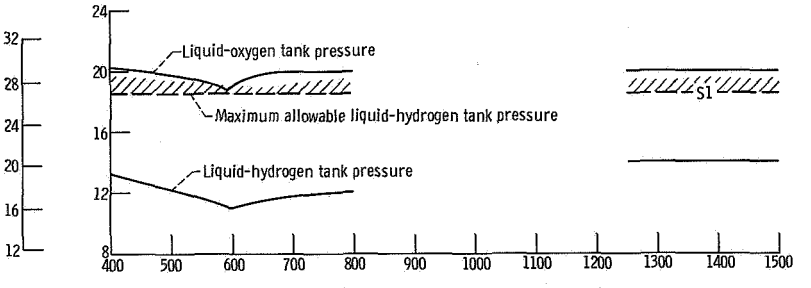

(c) Flight time, 400 to 1500 seconds. Data not available from 800 to 1250 seconds.

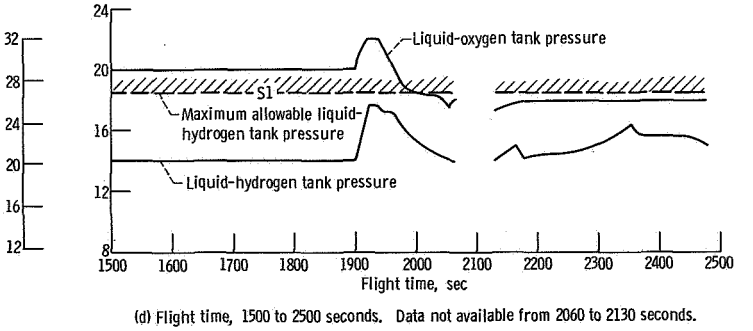

(d) Flight time, 1500 to 2500 seconds. Data not available from 2060 to 2130 seconds.

Figure VI-54. - Centaur fuel and oxidizer tank pressure, AC-15. S1, S2, etc., indicate tank structure areas which determine the allowable tank pressure (see fig. VI-51).

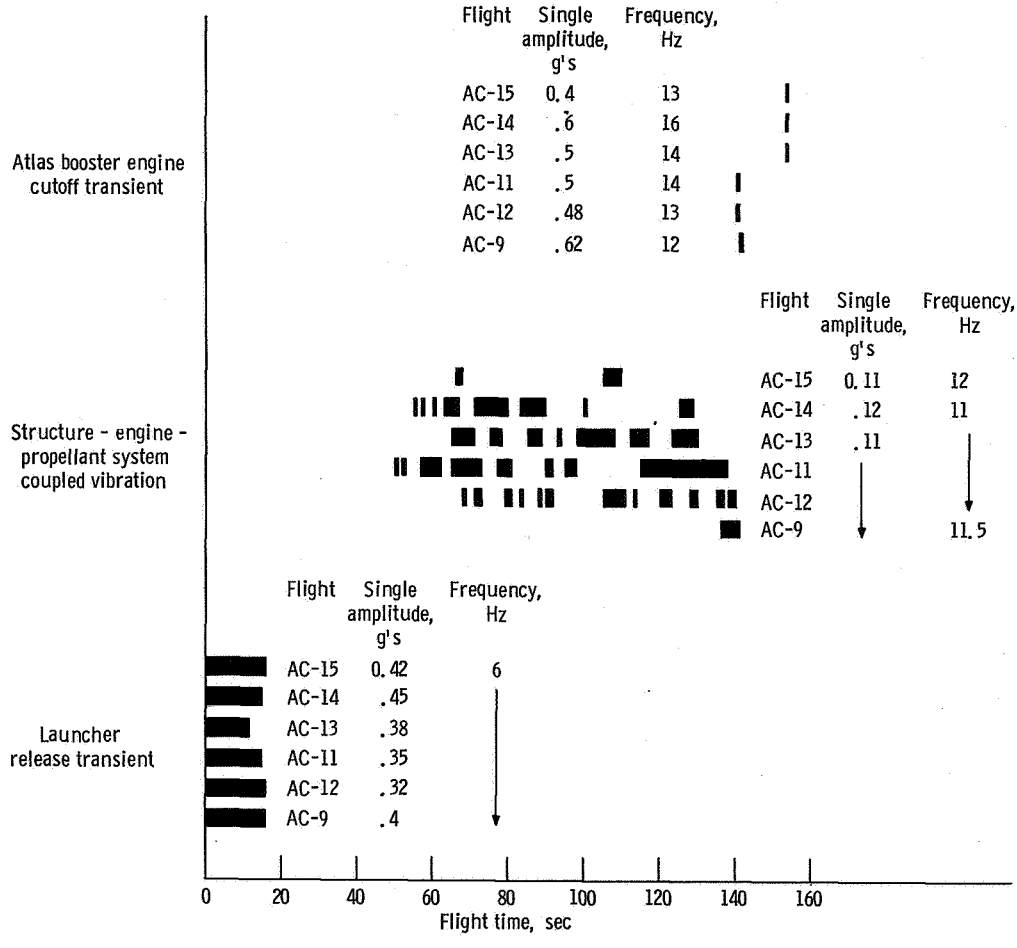

Figure VI-55. - Longitudinal vibrations for Atlas-Centaur flights.

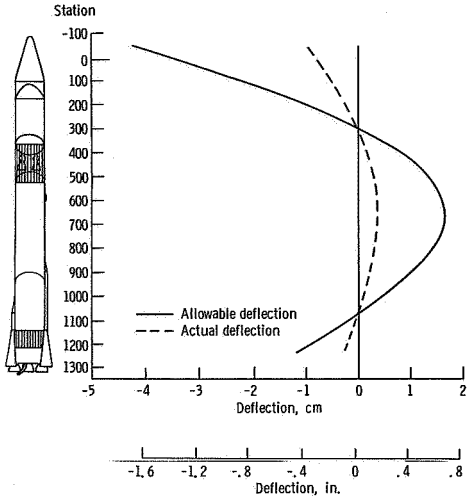

Figure VI-56. - Maximum pitch plane first-bending-mode amplitudes at T + 122 seconds, AC-13.

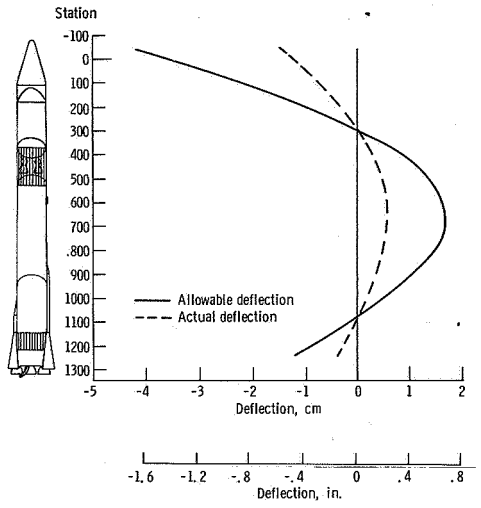

Figure VI-57. - Maximum pitch plane first-bending-mode amplitudes at T + 142 seconds, AC-14.

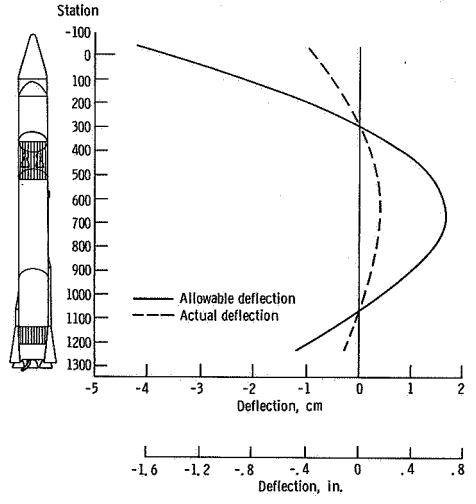

Figure VI-58. - Maximum pitch plane first-bending-mode amplitudes at T + 145 seconds, AC-15.

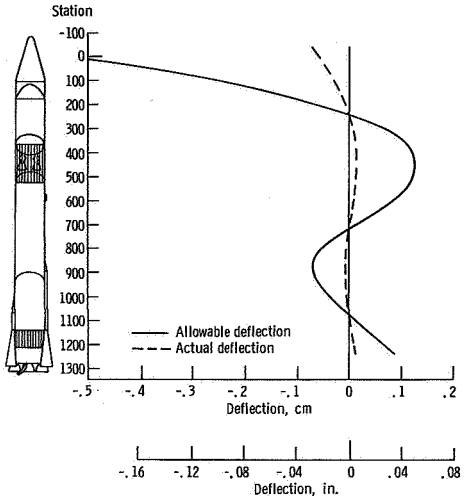

Figure VI-59. - Maximum yaw plane second-bending-mode amplitudes at T + 42 seconds, AC-13.

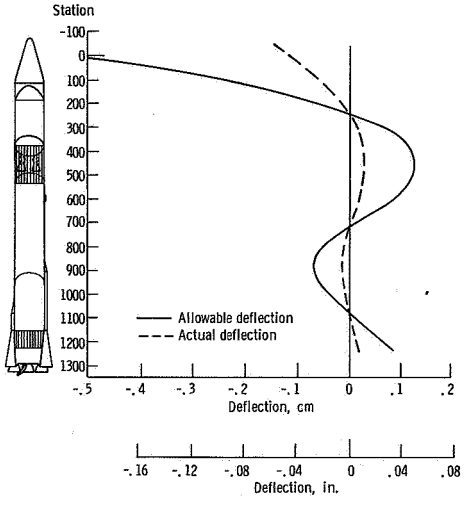

Figure VI-60. - Maximum yaw plane second-bending-mode amplitudes at T + 34 seconds, AC-14

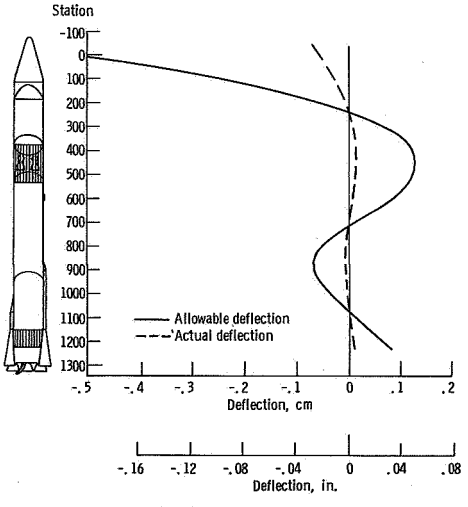

Figure VI-61. - Maximum yaw plane second-bending-mode amplitudes at T + 35 seconds, AC-15.

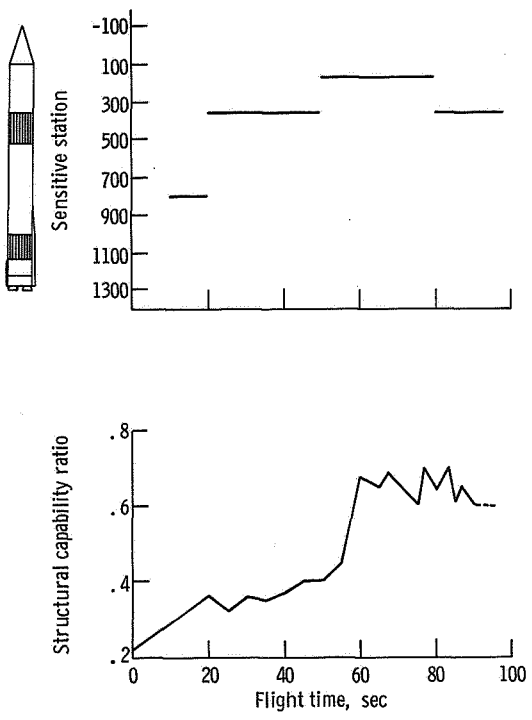

Figure VI-62. - Maximum predicted structural capability ratio (total equivalent predicted bending moment/bending moment allowable) and sensitive station, AC-13.

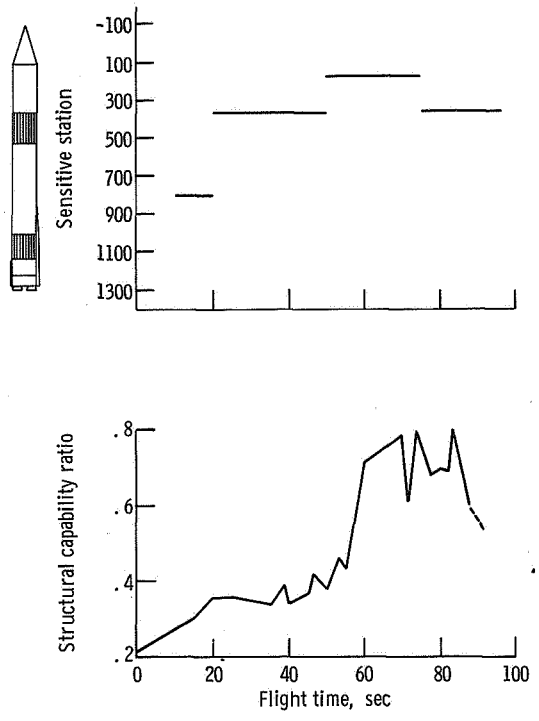

Figure VI-63. - Maximum predicted structural capability ratio (total equivalent predicted bending moment/bending moment allowable) and sensitive station, AC-14.

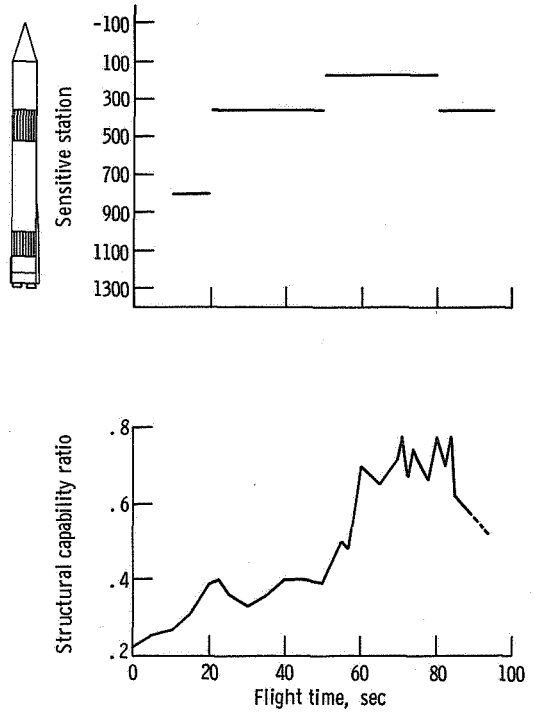

Figure VI-64. - Maximum predicted structural capability ratio (total equivalent predicted bending moment/bending moment allowable) and sensitive station, AC-15.

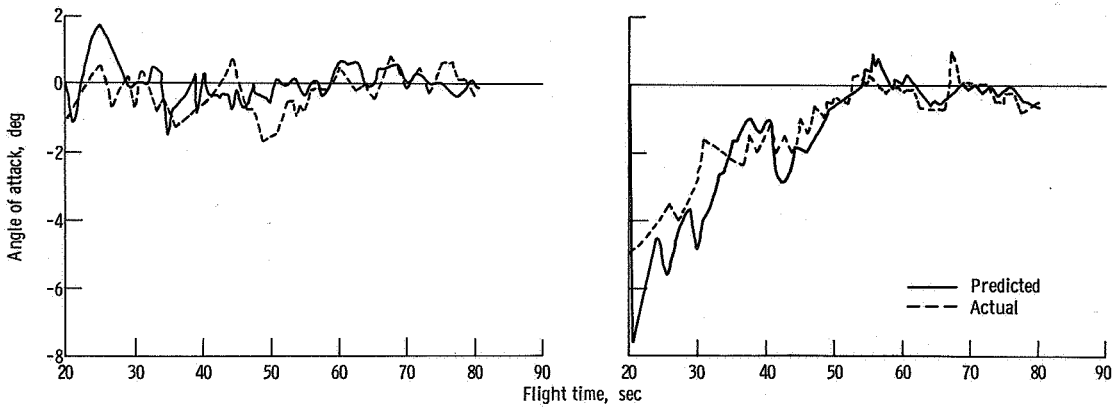

(a) Pitch. (b) Yaw.

Figure VI-65. - Predicted and actual angles of attack, AC-13.

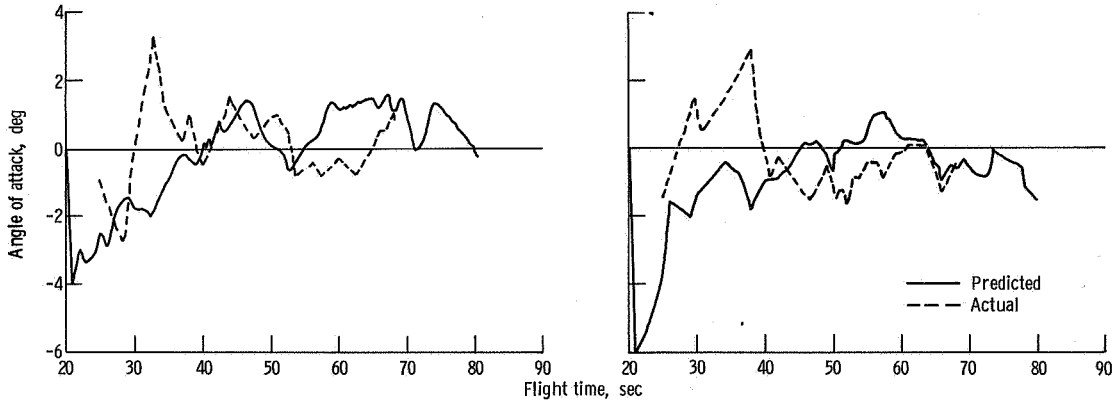

(a) Pitch. (b) Yaw.

Figure VI-66. - Predicted and actual angles of attack, AC-14.

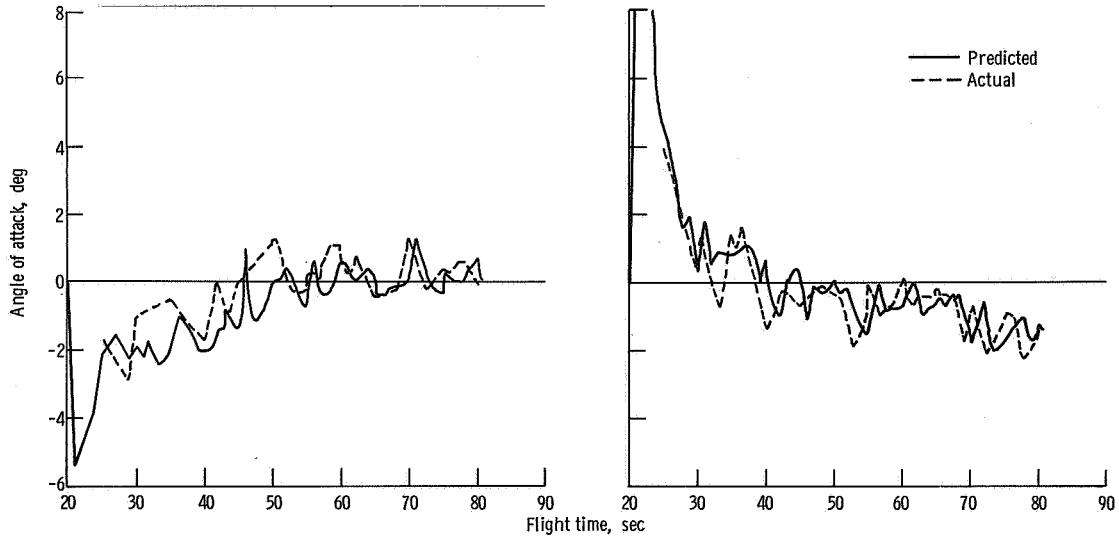

(a) Pitch. (b) Yaw.

Figure VI-67. - Predicted and actual angles of attack, AC-15.

SEPARATION SYSTEMS

by Thomas L. Seeholzer, Charles W. Eastwood, and Joseph E. Olszko

Separation Systems

System description. - Atlas-Centaur vehicles require systems for Atlas booster engine stage separation, Atlas-Centaur stage separation, and Centaur-Surveyor separation.

The Atlas booster engine stage separation system consists of 10 helium-gas-operated latch mechanisms. These latches (figs. VI-68(a) and (b)) are located circumferentially around the Atlas aft bulkhead thrust ring at station 1133. There is an explosive valve, which when activated connects a 2068 newton-per square-centimeter-gage (3000-psig) helium supply with the distribution manifold. The expanding gas flows through this manifold and causes actuation of the separation fittings. Actuation of these fittings results in the disengagement of the booster engine from the Atlas vehicle. Two tracks which extend from the thrust ring as shown in figure VI-69 are used to guide the booster engines as they separate from Atlas.

The Atlas-Centaur staging system consists of a flexible, linear, shaped charge mounted circumferentially near the forward end of the interstage adapter at station 412 (fig. VI-70). Separation force is provided by eight retrorockets mounted on the aft end of the Atlas (fig. VI-71).

The Surveyor spacecraft release system consists of three pyrotechnically operated pin puller latches mounted on the forward payload adapter (fig. VI-72). Separation force is provided by three mechanical spring assemblies, one mounted adjacent to each separation latch on the forward adapter. The spring stroke is 2.54 centimeters (1 in.).

Atlas booster engine staging system performance. - Atlas booster thrust section staging occurred at 3 seconds after booster engine cutoff for all three flights. This event was verified by cutoff data from the B-1 pitch actuator and initiation of data from the missile axial (fine) accelerometer. The following table summarizes the thrust section separation event times:

Flight	Booster engine cutoff, sec	Thrust section staging, sec
AC-13	T + 153.2	T + 156.3
AC-14	T + 153.2	T + 156.3
AC-15	T + 152.4	T + 155.5

Atlas-Centaur separation system performance. - The Atlas satisfactorily separated from Centaur on all three flights. Vehicle staging was initiated by the firing of the flexible, linear shaped charge. The eight retrorockets separated Centaur from Atlas 0.1 second later. Accelerometer data indicated that all eight retrorockets fired. During separation, 28 centimeters (11 in.) of clearance was available between Atlas and Centaur along the y-y axis (pitch motion). There was also 79 centimeters (31 in.) of clearance along the x-x axis (yaw motion). The following table lists the event times and Atlas pitch and yaw rotations and motions during staging for each flight:

Flight	Shaped-charge firing time, sec	Retrorocket firing time, seconds after shaped charge firing	Pitch rotation, deg	Pitch motion[a]		Yaw rotation[b], deg	Yaw motion	
				cm	in.		cm	in.
AC-13	T + 248.2	0.1	0.15	3.8	1.5	0.49	12.5	4.9
AC-14	T + 247.7	.1	.19	4.8	1.9	.34	8.6	3.4
AC-15	T + 250.6	.1	.29	7.4	2.9	.16	4.1	1.6

Spacecraft separation system performance. - The Surveyor spacecraft successfully separated from the Centaur vehicle on the AC-13, AC-14, and AC-15 flights. The separation produced forward motion of the spacecraft with no significant rotation. These facts were verified by Centaur rate gyro data and separation spring extensometer data. On AC-15, excessive disturbances in the separation spring extensometer data prevented its proper evaluation. However, successful separation from the AC-15 vehicle was verified by rate gyro data and by tracking data from the Pretoria tracking station. On the AC-13 and AC-14 flights, the extensometer data indicated that all three separation latches actuated within 0.002 second of each other. The three separation springs were calibrated at the Eastern Test Range prior to flight. These springs operated normally during separation and yielded approximately identical stroke against time data. Spring extensometer and calibration data for AC-13 and AC-14 are shown in figures VI-73 to VI-76. Spacecraft separation times for the three flights were T + 1165.6, T + 1528.9, and T + 2115.3 seconds for AC-13, AC-14, and AC-15, respectively.

Jettisonable Structures

System description. - Atlas-Centaur missions require jettisonable structures and their related separation systems. These consist of hydrogen tank insulation panels and a nose fairing.

The hydrogen tank insulation is made up of four panels. These panels are of fiber glass skin sandwich construction with a polyurethene-foam-filled core. They are bolted together along the longitudinal axis to form a cylindrical cover for the Centaur liquid-hydrogen tank. The panels are joined to the Centaur vehicle at their aft end by a metal ring, as shown in figure VI-77. At the forward end, a circumferential Tedlar and fiber glass cloth seal connects the panels to the base of the nose fairing at station 219, as shown in figure VI-78.

The insulation panel separation consists of flexible, linear shaped charged located at the forward, aft, and longitudinal seams (figs. VI-77 and VI-78). Each panel is hinged about two points located on the interstage adapter (fig. VI-79). Separation force is provided by (1) elasticity of the panels due to hoop tension, (2) center-of-gravity offset, and (3) residual in-flight purge pressure.

The nose fairing is a fiber glass honeycomb structure consisting of a cylindrical section approximately 1.83 meters (6 ft) long, bolted to a conical section approximately 4.87 meters (16 ft) long. It is assembled in two jettisonable halves with the split line along the x-x axis (fig. VI-80). Thermal protection, in the form of a subliming agent, is applied to the fairing to maintain necessary strength at high temperatures. The nose fairing separation system consists of a flexible, linear, shaped charge mounted circumferentially at the aft end of station 219, as shown in figure VI-78. There are also eight pyrotechnically actuated pin puller latches mounted as shown in figure VI-80. Separation force is provided by two nitrogen gas thrusters located at the forward end of the nose cone, one in each fairing half. Each fairing half is hinged at a single point on the Centaur hydrogen tank at station 219 on the y-y axis (see fig. VI-80).

Insulation panel separation system performance. - Jettison of the four panels was completely normal on the AC-13, AC-14, and AC-15 flights. Jettison was initiated by a command signal which was monitored on a commutated channel. Following issuance of the command, the linear shaped charge fired to sever the panel attachments. Shaped-charge firing times were determined from an axial accelerometer mounted on the spacecraft foot. The following table lists command and shaped-charge firing times for all three flights:

Event	Flight		
	AC-13	AC-14	AC-15
	Time, sec		
Separation command	T + 197.93	T + 197.99	T + 197.08
Shaped-charge firing	T + 197.95	T + 198.01	T + 197.10

Rotation of the panels to the 35° position was sensed by breakwire-type transducers. The panels were released from the Centaur vehicle after approximately 45° of rotation. Each panel was instrumented with a breakwire, extending from one of the hinge arms to the interstage adapter, adjusted to sever at 35° of panel rotation (fig. VI-81). Since the breakwire data were monitored on commutated channels, the data indicated a time dispersion for the event. Breakwire disconnect times for all three flights are shown in the following table:

Panel located in quadrants-	Hinge arm located in quadrant-	Panel 35°-rotation time, sec		
I-II	I	T + 198.36 to T + 198.38	T + 198.43 to T + 198.44	T + 197.50 to T + 197.51
II-III	III	T + 198.36 to T + 198.38	T + 198.46 to T + 198.48	T + 197.55 to T + 197.56
III-IV	III	T + 198.37 to T + 198.39	T + 198.42 to T + 198.43	T + 197.52 to T + 197.54
IV-I	I	T + 198.37 to T + 198.39	T + 198.42 to T + 198.43	T + 197.52 to T + 197.54

Average rotation velocities of the panels from the time of shaped-charge firing to the mean time of the 35° position of each panel are listed in the following table. The values also compare well with values from two previous flights, AC-11 and AC-12.

Panel located in quadrants-	Average rotation velocities from shaped-charge firing to mean time of 35° position, deg/sec				
	AC-11	AC-12	AC-13	AC-14	AC-15
I-II	79.6	84.6	83.8	82.6	87.5
II-III	89.6	72.9	83.8	76.5	77.5
III-IV	79.8	81.4	82.6	84.3	82.5
IV-I	85.8	75.6	79.4	78.0	76.5

Nose fairing separation system performance. - The jettisons of the AC-13, AC-14, and AC-15 nose fairings were fully successful events. Approximately 27 seconds prior to nose fairing jettison, a flexible, linear, shaped charge cut the aft joint attaching the nose fairing to the Centaur vehicle. This event was indicated by axial accelerometer data. The nose fairing jettison system was then activated by a programmed command. Eight pyrotechnically operated pin pullers unlatched the nose fairing split line. Approximately 0.5 second later, the two nitrogen thruster bottles were actuated, causing the fairings to rotate about their hinge points approximately 35^{o}. The fairing halves then jettisoned from the Centaur vehicle. Latch actuation and thruster firing times were determined from accelerometer data. Rotation of the fairing halves to the 3^{o} point was sensed by disconnect pins in the electrical connectors which separate at jettison. The following table summarizes significant nose fairing separation event times on all three flights:

Event	Time, sec		
	AC-13	AC-14	AC-15
Split line latch actuation	T + 227.2	T + 227.3	T + 226.4
Nitrogen thruster bottle actuation	T + 227.7	T + 227.8	T + 226.9
3^{o} fairing rotation[a]	T + 227.7 to T + 228.6	T + 227.8 to T + 228.5	T + 226.9 to T + 227.0

[a]Data from commutated channel.

During fairing jettison the payload compartment pressure remained at zero with no pressure surge occurring at thruster bottle discharge. Figure VI-82 shows the typical compartment pressure decay for the three flights.

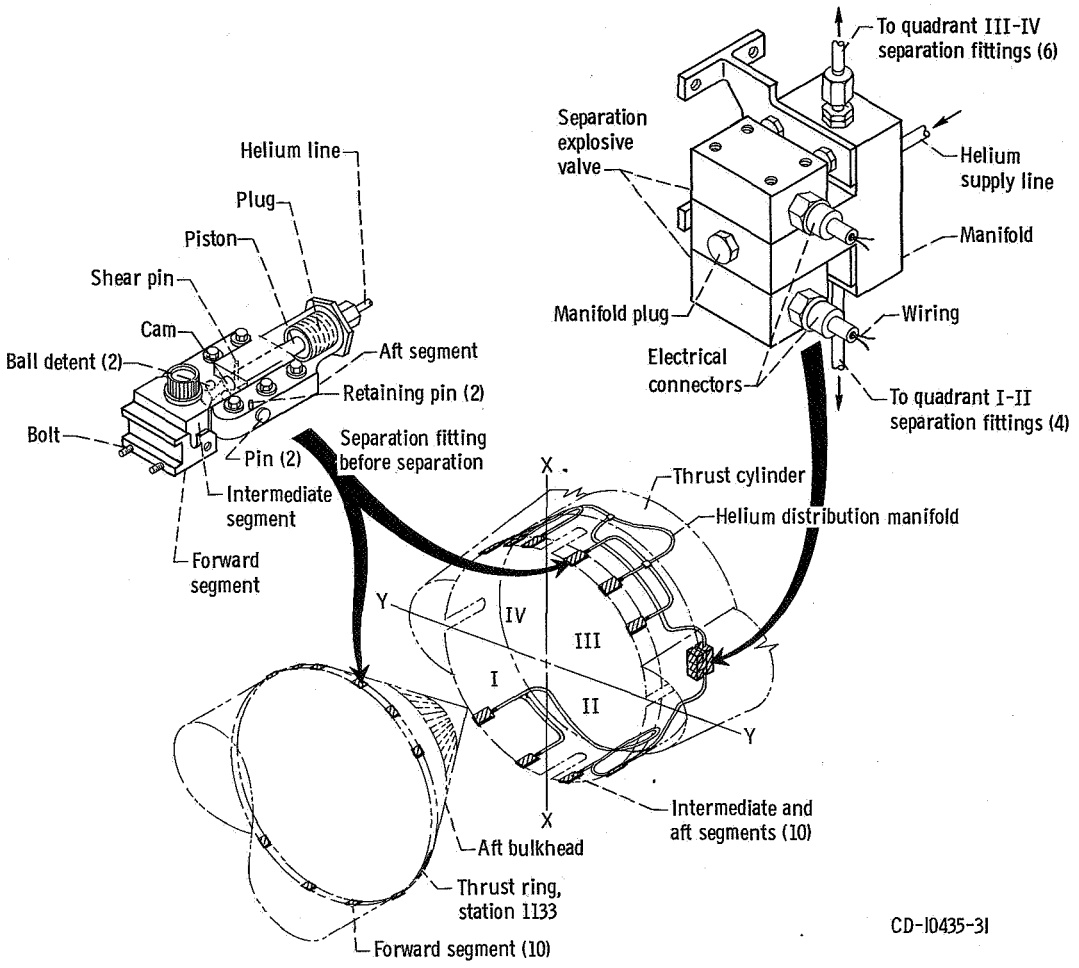

(a) Details of separation system.

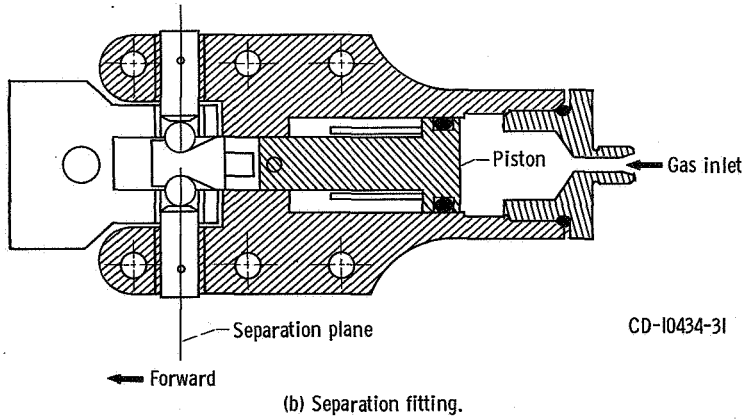

(b) Separation fitting.

Figure VI-68. - Atlas booster engine thrust section separation system; AC-13, AC-14, and AC-15.

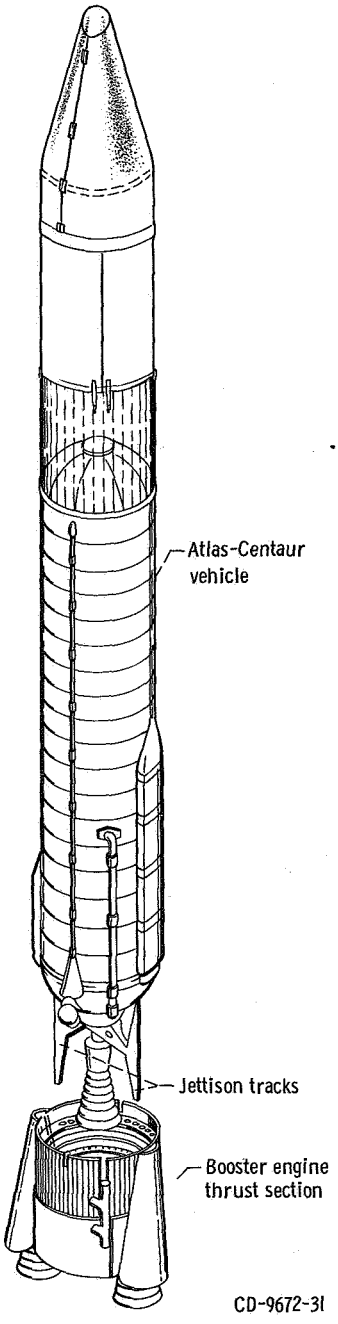

Figure VI-69. - Atlas booster engine thrust section staging system; AC-13, AC-14, and AC-15.

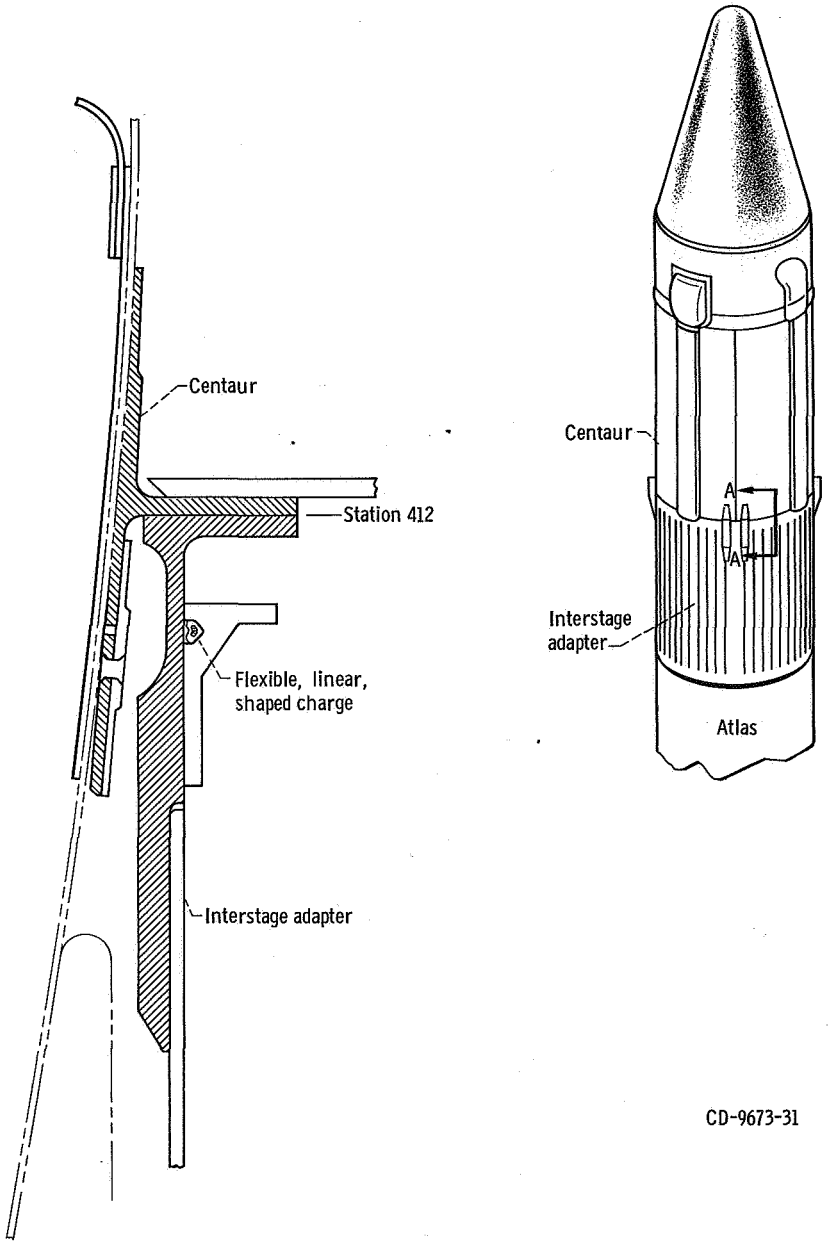

Figure VI-70. - Atlas-Centaur shaped-charge staging system; AC-13, AC-14, and AC-15.

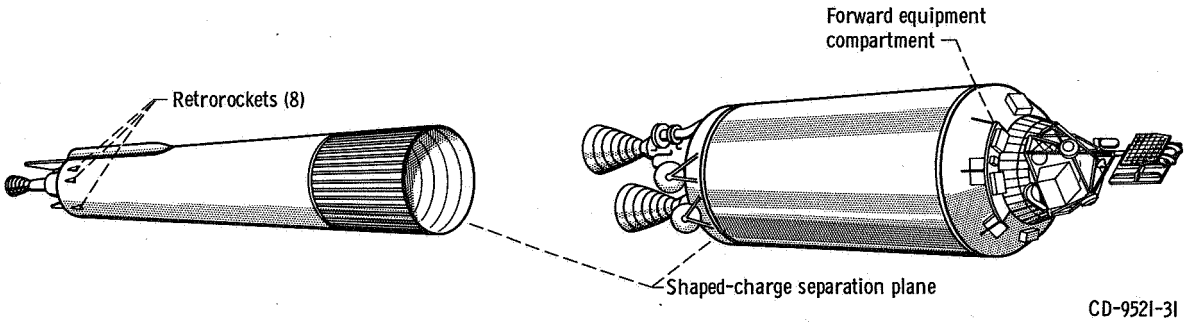

Figure VI-71. - Atlas-Centaur separation system; AC-13, AC-14, and AC-15.

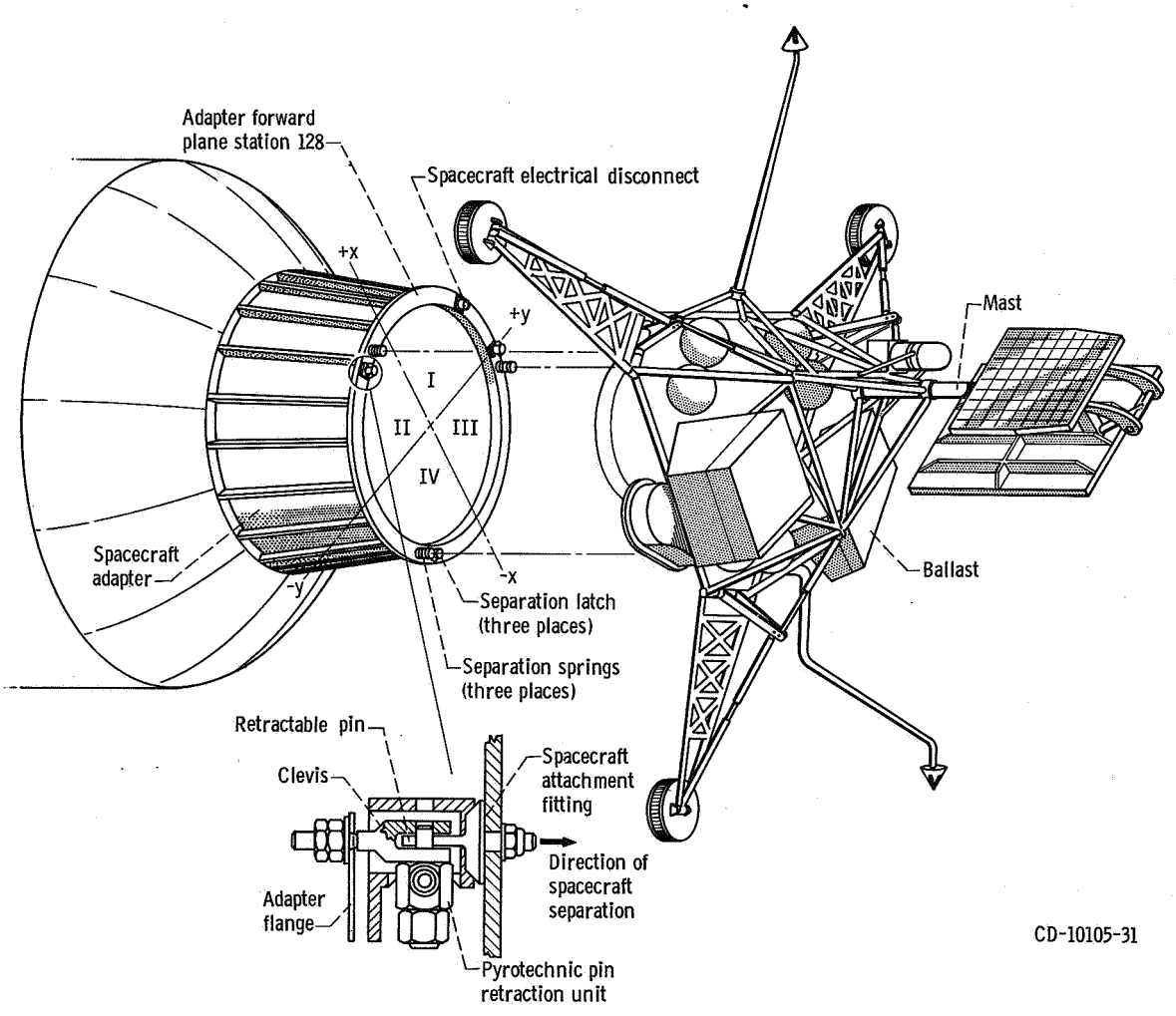

Figure VI-72. - Centaur-Surveyor separation system; AC-13, AC-14, and AC-15.

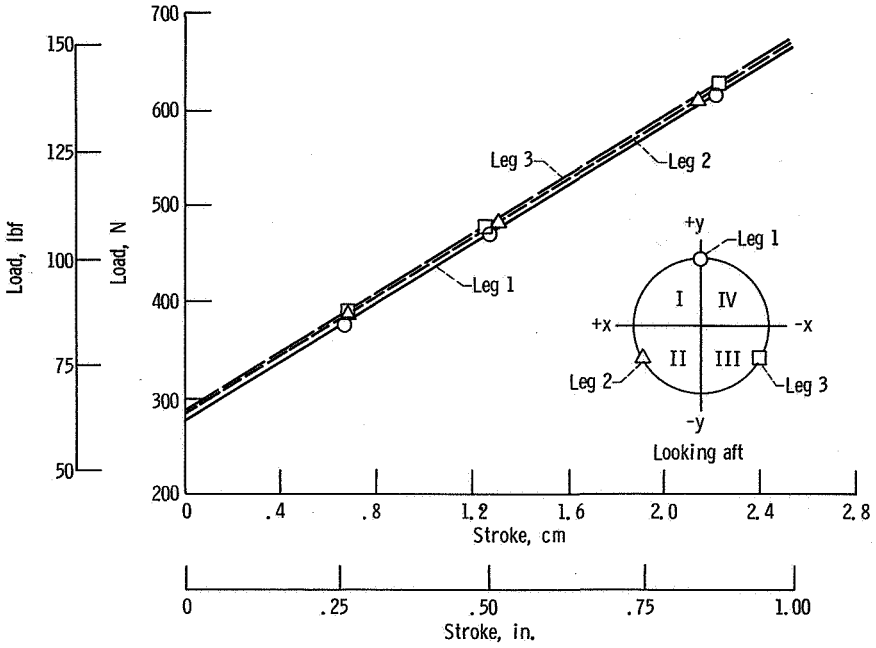

Figure VI-73. - Surveyor jettison spring calibration, AC-13.

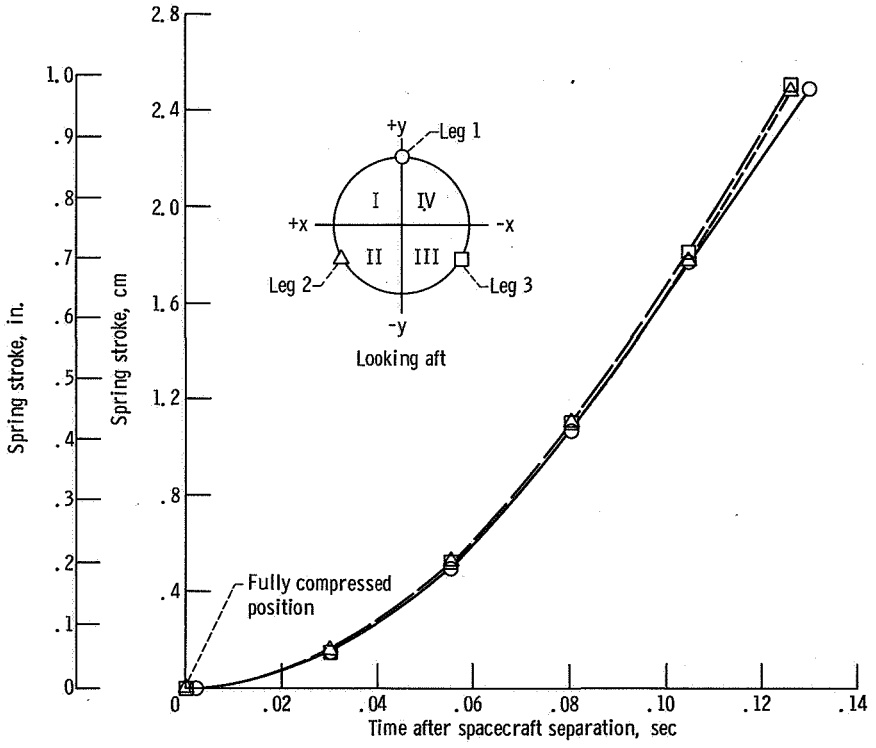

Figure VI-74. - Centaur-Surveyor separation spring release, AC-13.

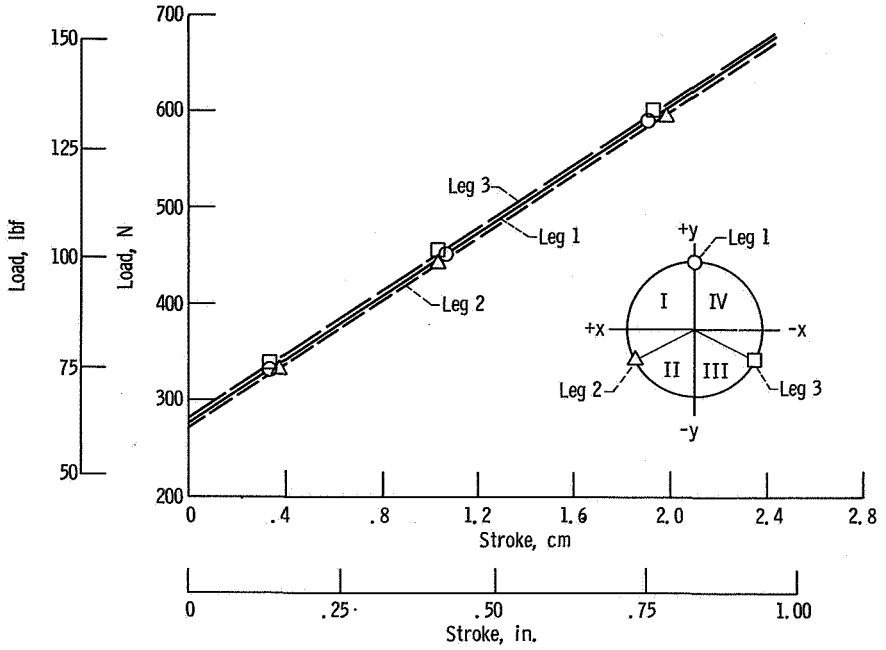

Figure VI-75. - Surveyor jettison spring calibration, AC-14.

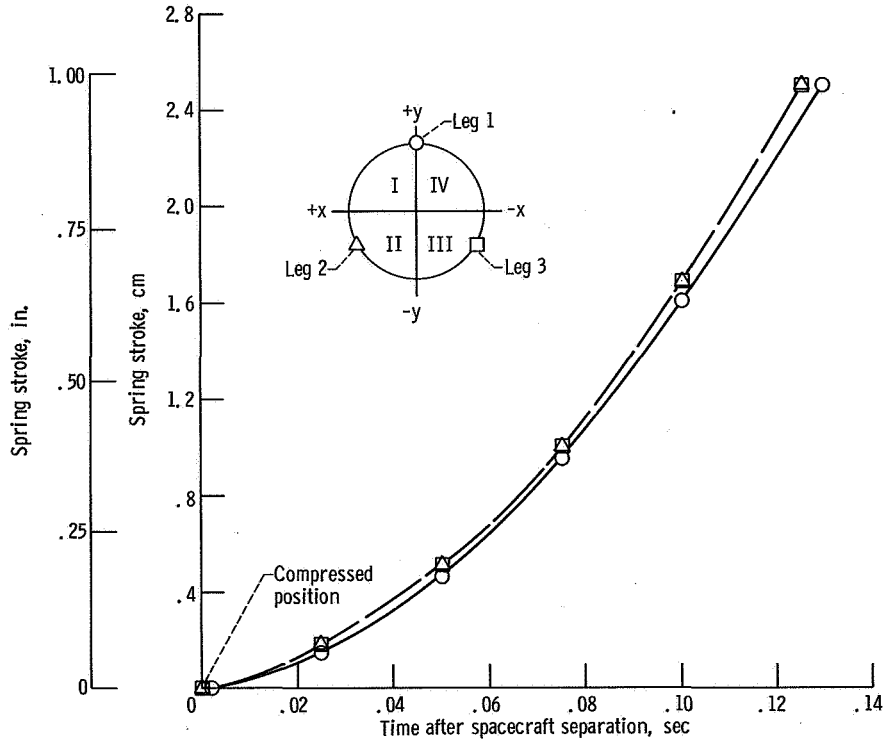

Figure VI-76. - Centaur-Surveyor separation spring release, AC-14.

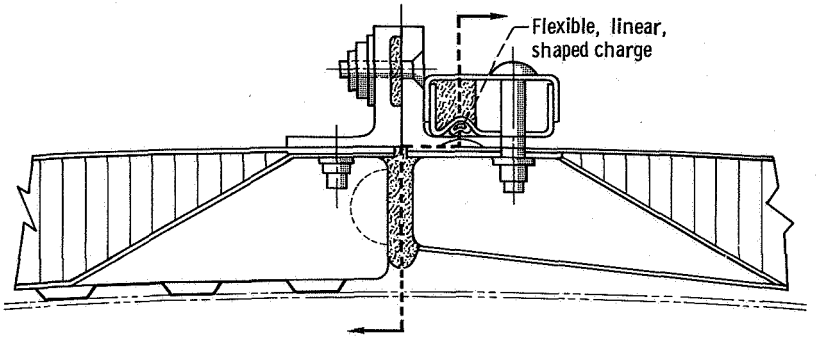

Section B-B. Longitudinal joint.

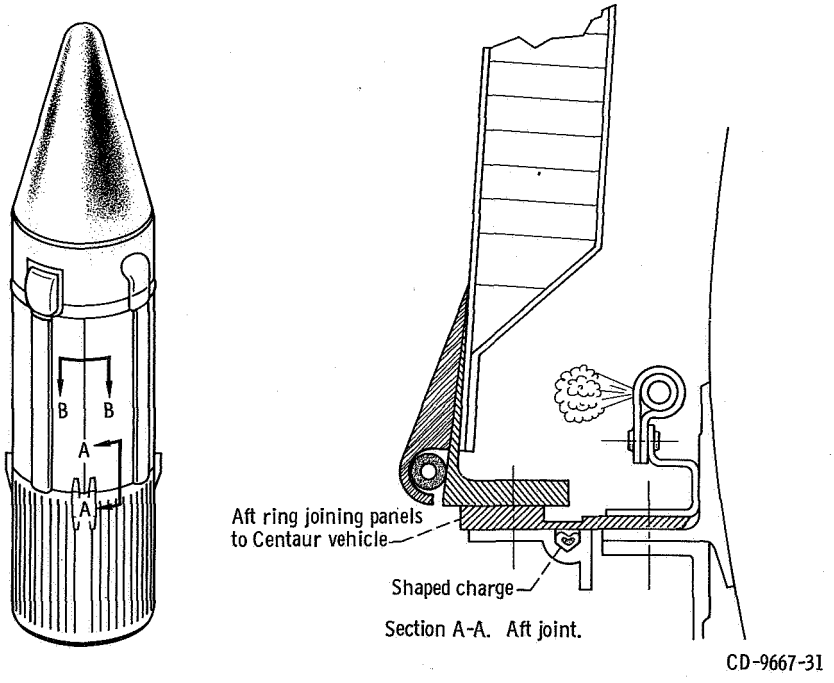

Figure VI-77. - Hydrogen tank insulation panels and separation system; AC-13, AC-14, and AC-15.

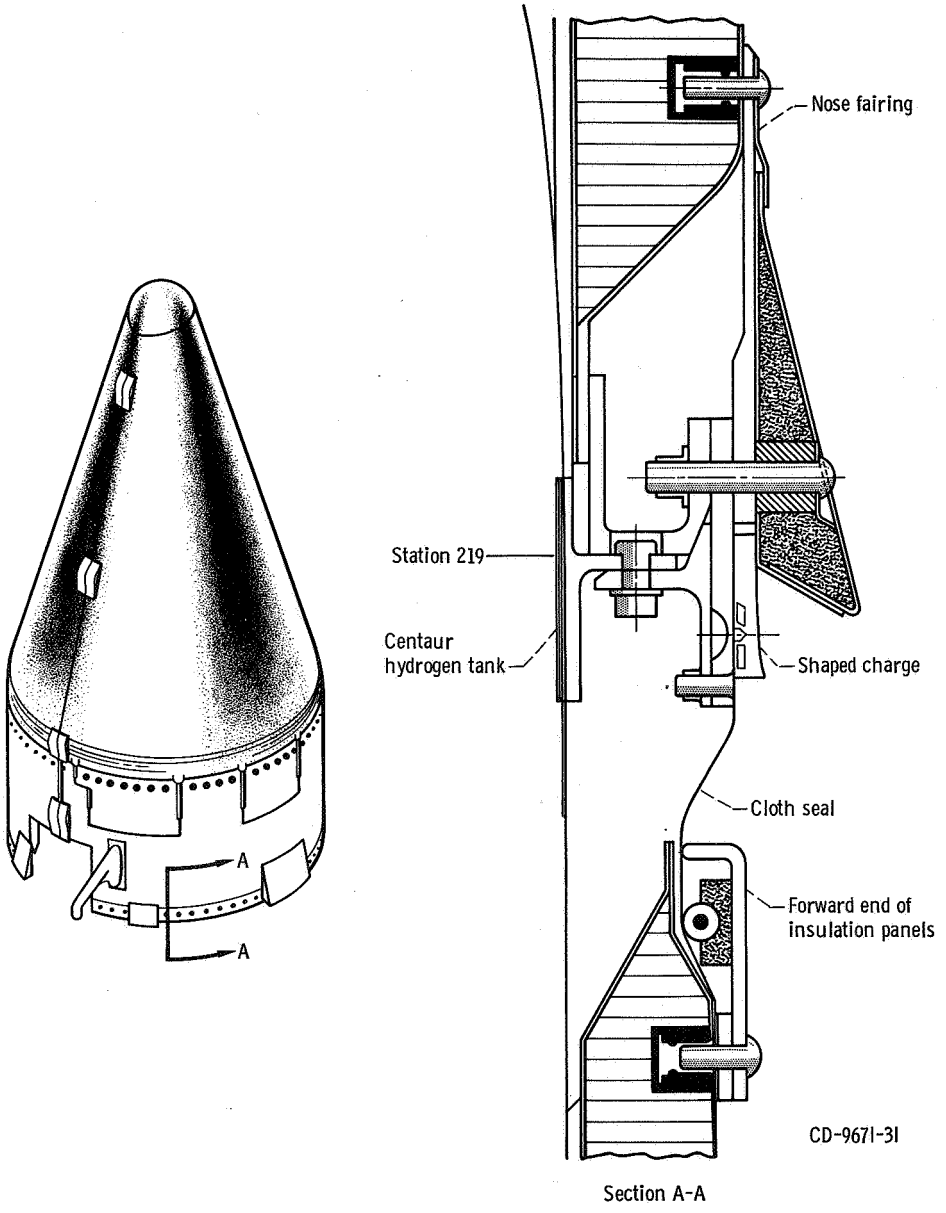

Figure VI-78. - Nose fairing aft separation system; AC-13, AC-14, and AC-15.

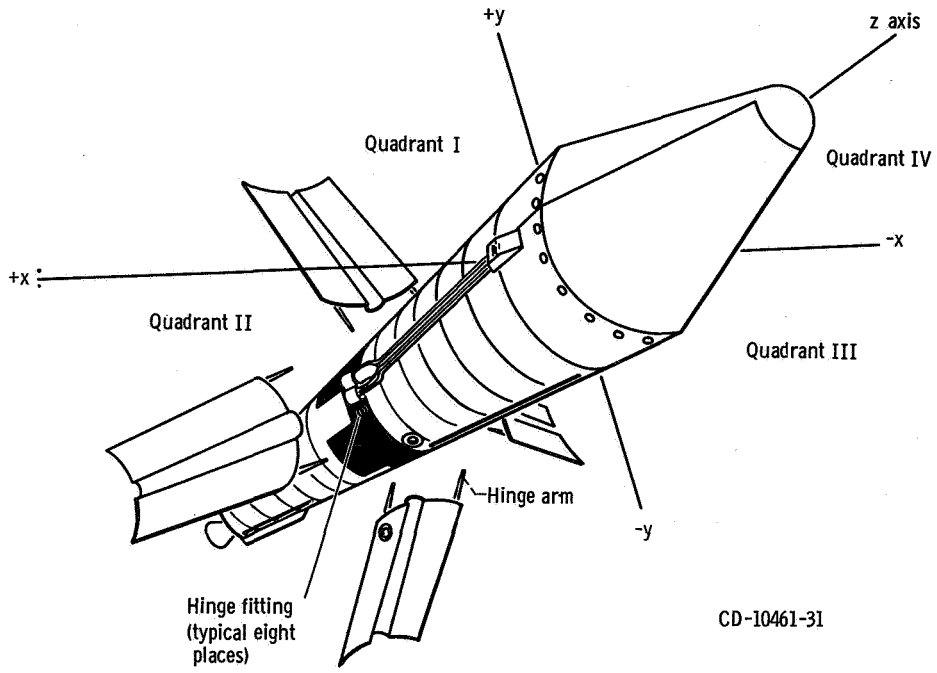

Figure VI-79. - Hydrogen tank insulation panel jettison system; AC-13, AC-14, and AC-15.

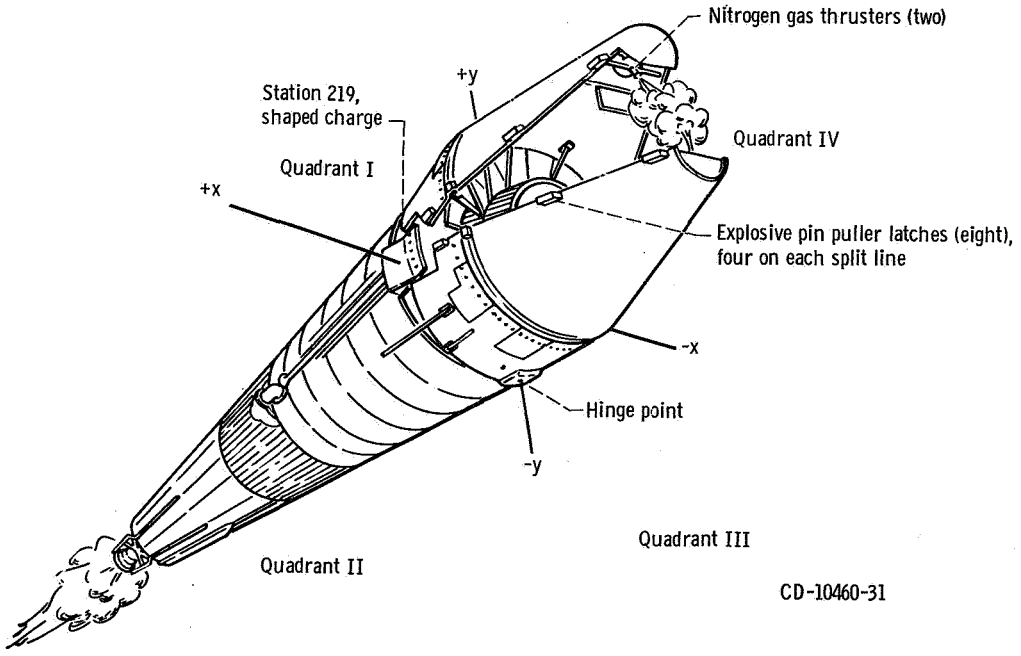

Figure VI-80. - Nose fairing jettison system, AC-13, AC-14, and AC-15.

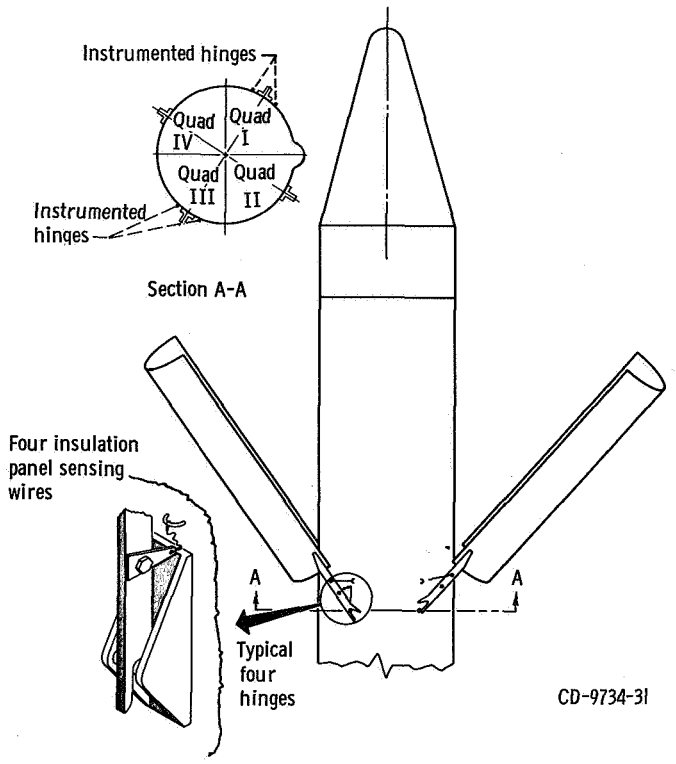

Figure VI-81. - Insulation panel breakwire locations; AC-13, AC-14, and AC-15.

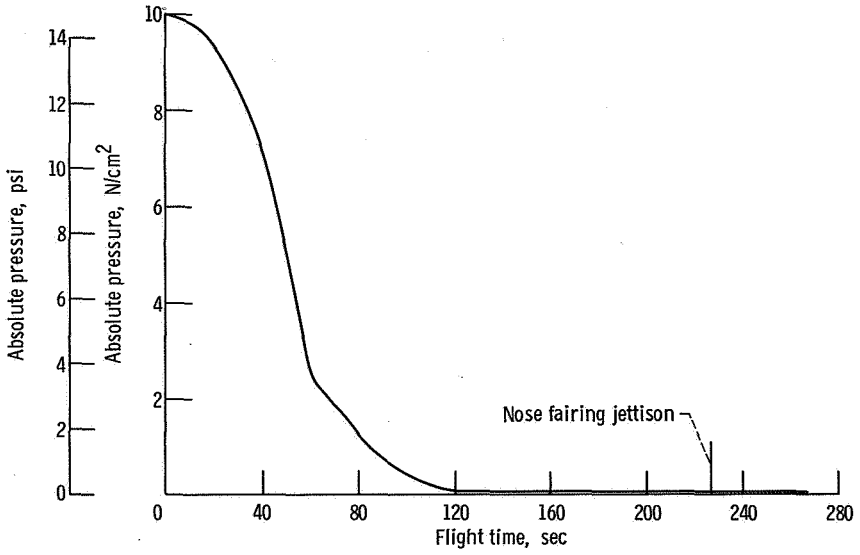

Figure VI-82. - Payload compartment pressure, typical for AC-13, AC-14, and AC-15.

ELECTRICAL SYSTEMS

by John M. Bulloch, Robert J. Freedman, John E. Moss,
John B. Nechvatal, and James Nestor

Power Sources and Distribution

System description - Atlas. - The Atlas power requirements are supplied by a main power battery, two range safety command (vehicle destruct) system batteries, two telemetry batteries (one only on AC-15), and a 400-hertz rotary inverter. Transfer of the Atlas electrical load from the external ground power supply to internal batteries is accomplished by the main power changeover switch at T - 2 minutes. The system block diagram is shown in figure VI-83.

System performance - Atlas. - All power sources performed satisfactorily throughout each flight. Battery voltage levels at lift-off were normal. Battery voltages were not monitored during flight; however, telemetered information on pyrotechnic systems, booster and sustainer cutoffs, range safety receiver operation, and all other vehicle systems indicated that all systems performed as planned. No deviations were observed in the electrical power systems performance.

The Atlas inverter performed normally. Phase voltages, monitored throughout each flight remained almost steady, with a decrease in voltage of less than 1/2 volt in the time from lift-off to Atlas-Centaur separation. The inverter frequencies remained quite steady, drifting slightly upward from the values at lift-off. The gradual drift in frequency is characteristic of the Atlas inverter and was observed on previous flights. The required frequency difference of 1.5 to 3.5 hertz between the Atlas and Centaur inverter frequencies was properly maintained. This difference prevents undesirable beat frequencies in the flight control system. Beat frequencies which are resonant with the slosh and natural structural resonant frequencies of the vehicle may cause the flight control system to issue false commands which may degrade vehicle stability. Voltage and frequency measurements at lift-off are given in table VI-15.

System description - Centaur. - The Centaur electric power system includes a main battery, two redundant range safety command (flight termination) system batteries, and two pyrotechnic system batteries. A three-phase, 400-hertz, solid-state inverter is powered from the main battery and provides alternating current to the guidance, flight control, and propellant utilization systems. A power changeover switch is used to transfer the Centaur electrical system to internal power at T - 4 minutes, and to turn off all systems except telemetry and tracking at the end of programmed flight.

System performance - Centaur. - The Centaur electric system voltages and currents were normal at lift-off. The system satisfactorily supplied power to all electrical loads

throughout the flight. Electrical data at lift-off were normal for all three flights. These data are shown in table VI-16. The main battery load profile was normal for all three flights and compared closely with values recorded on previous missions. Main battery current values observed at significant events are shown in table VI-17. The Centaur solid-state inverter supplied stable 400-hertz power for the guidance, flight control, and propellant utilization sytems. Telemetered voltage levels were normal and compared closely with values obtained during preflight testing. Voltage levels increased slightly during flight, a characteristic of the Centaur inverter. Table VI-15 summarizes the inverter performance in flight. Performance of the range safety command (vehicle destruct) subsystem batteries was satisfactory, as verified by telemetered data of the two receivers during launch and flight. Proper operation of the pyrotechnic subsystem was verified by the successful jettison of the insulation panels and nose fairing.

Tracking System

System description. - A C-band radar subsystem with associated ground stations provides position and velocity data to the range safety tracking system. These data are also used by the Deep Space Network for acquisition of the spacecraft, and for guidance and flight trajectory data analysis. The airborne equipment includes a lightweight transponder, a circulator (to channel receiving and sending signals), a power divider, and two antennas located on opposite sides of the tank. The locations of the Centaur antennas are shown in figure VI-84. The ground and ship stations use standard radar equipment and are located as shown in figures VI-85 to VI-87 for AC-13, AC-14, and AC-15, respectively. A block diagram of the AC-13, AC-14, and AC-15 C-band systems is shown in figure VI-88.

System performance. - For AC-13, C-band radar coverage was obtained up to T + 4619 seconds (fig. VI-89). Cape Kennedy, Grand Bahama Island, and Bermuda radar provided coverage during Atlas-Centaur powered flight. Bermuda, Canary Island, and Pretoria radar tracking stations provided data for near-real-time orbit calculation. The Grand Turk, Twin Falls, and Tananarive stations failed to provide data. The Carnarvon radar provided limited support.

For AC-14, C-band radar tracking was satisfactory, and coverage was obtained to T + 5296 seconds (fig. VI-90). Bermuda, Twin Falls, and Pretoria provided data for parking orbit, lunar transfer orbit, and postretromaneuver calculations. Cape Kennedy, Grand Bahama, Grand Turk, and Bermuda radar tracking stations provided coverage during Atlas-Centaur powered flight. The Tananarive radar station filed to track because of ground equipment problems.

For AC-15, C-band radar tracking was satisfactory, and coverage was obtained to T + 4686 seconds (fig. VI-91). Cape Kennedy, Grand Bahama, Grand Turk, and Bermuda

radar tracking stations provided coverage during Atlas-Centaur powered flight. Bermuda, Antigua, Ascension, Twin Falls, Pretoria, Tananarive, and Carnarvon provided data for parking orbit, lunar transfer orbit, and postretromaneuver calculations. Tananarive and Carnarvon had intermittent track as a result of marginal signal strength conditions at these stations.

Range Safety Command Subsystem

(Vehicle Destruct Subsystem)

Subsystem description. - The Atlas and Centaur stages each contained independent range safety command subsystems. These subsystems are designed to function simultaneously upon command from the ground stations. Each subsystem included redundant receivers, power control units, destructors, and batteries which operate independently of the main vehicle power system. Block diagrams of the Atlas and Centaur subsystems are shown in figures VI-92 and VI-93, respectively.

The Atlas and Centaur range safety command subsystems provide means of shutting down the engines only or shutting down the engines and destroying the vehicle if it leaves the safe flight corridor. To destroy the vehicle an explosive charge ruptures the propellant tanks and the liquid propellants of the Atlas and Centaur stages are dispersed. At the same time, the Surveyor retromotor is destroyed by a shaped charge.

Subsystem performance. - The Atlas and Centaur range safety command subsystems were prepared to execute destruct commands throughout the flight; however, engine cutoff or destruct commands were not needed nor were they inadvertently transmitted. The command from the Antigua ground station to disable the Centaur range safety command subsystem shortly after Centaur main engine first cutoff was properly received and executed. Figures VI-94 to VI-96 depict ground transmitter coverage to support the vehicle destruct systems for AC-13, AC-14, and AC-15, respectively.

Signal strength at the Atlas and Centaur range safety command receivers was satisfactory throughout the AC-13, AC-14, and AC-15 flights as indicated by telemetry measurements, with one exception. On AC-13, the signal strength at both Centaur range safety receivers indicated decreasing signal input at approximately T + 350 seconds. By T + 391 seconds, the signal strength at each receiver decreased to zero for approximately 2 seconds. The probable cause of the decrease in signal strength was the fact that Grand Turk had very poor look angles at this time.

Telemetered data indicated that both the Centaur receivers were deactivated shortly after main engine cutoff on AC-13, AC-14, and AC-15. This confirmed that the disable command was transmitted from the Bermuda station for AC-13 and AC-14 and the Antigua station for AC-15.

Instrumentation and Telemetry

System description - Atlas. - The Atlas telemetry system consists of two Pulse Amplitude Modulation/Frequency Modulation/Frequency Modulation (PAM/FM/FM) radiofrequency links for AC-13 and AC-14. A block diagram of this sytem is shown in figure VI-97. The standard first radiofrequency link monitors vehicle systems parameters and performance for AC-13, AC-14, and AC-15. It operates at a frequency of 229.9 megahertz. A second telemetry system was added for AC-13 and AC-14, operating at a frequency of 232.4 megahertz, to check the structural dynamics and the thermodynamics of the new SLV-3C vehicle. The two telemetry systems were located in the B-1 pod and connected to the B-1 and B-2 pod antennas.

Use of the PAM technique on all Atlas and Centaur commutated channels allows many measurements to be made on one subcarrier frequency. This increases the data handling capability of the telemetry system. The FM/FM technique takes discrete values from transducers and frequency modulates the subcarrier which, in turn, frequency modulates the carrier (radiofrequency link).

System performance - Atlas. - The telemetry coverage for the Atlas portion of the flights (figs. VI-98 to VI-100) lasted for approximately 525 seconds and was excellent. This time interval extends well beyond Atlas-Centaur separation and meets all telemetry coverage requirements. Station locations are shown in figures VI-85 to VI-87.

On AC-13 and AC-14 a total of 208 measurements each were telemetered for analysis (table VI-18), while on AC-15 only 131 measurements were telemetered (table VI-19). The difference was the extra link on AC-13 and AC-14.

On AC-13 all measurements were satisfactory, except two measurements which failed to provide completely useful data. The liquid-oxygen inlet duct lateral acceleration (AP18O) did not provide useful data after T + 30 seconds. Bias level shifts up to 50 percent information bandwidth were noted after this time. This is characteristic of amplifier saturation and could be caused by separation of the shield from one of the connectors on the coaxial cable which connects the transducer to its amplifier. The sustainer turbine exhaust duct pressure (AP98P) exhibited transients from T - 0 to T + 40 seconds and from T + 210 seconds to sustainer engine cutoff. (Cause of the transients is unknown; however, steady-state pressure levels were as expected and no data were lost.)

Of the 208 measurements made on AC-14 only four measurements showed unexpected outputs. These were the liquid-oxygen fill and drain value longitudinal accelerometer (AA306O) and the B-1 pod differential pressures (AA556P, AA557P, and AA558P). The AA306O measurement showed an erratic output from T + 156.55 seconds to T + 157.3 seconds, and thereafter the data were normal. This time is close to booster engine jettison, which could have caused this erratic output. Measurements AA556P, AA557P,

and AA558P indicate that the outside ports of the differential pressure transducers may have been plugged.

Of the 131 measurements made on AC-15, only one measurement failed. Sustainer hydraulic return pressure (AA601P) exhibited erratic data from T + 62 seconds to sustainer engine cutoff. The cause of failure is unknown.

System description - Centaur. - The Centaur telemetry system consists of one PAM/FM/FM radiofrequency link. A block diagram of this system is shown in figure VI-101. This system operates at 5 watts output at a frequency of 225.7 megahertz. A total of 163 measurements (table VI-20) were made on AC-13, while 161 measurements (table VI-21) were made on each of the AC-14 and AC-15 flights. All data on the vehicle system parameters and performance are transmitted through the omnidirectional antenna located on the forward umbilical island.

System performance - Centaur. - The telemetry coverage for the Centaur portion of flight (figs. VI-102 to VI-104) exceeded 5000 seconds. This time interval extended beyond power changeover and met all telemetry requirements. Station locations are shown in figures VI-85 to VI-87.

The coverage of AC-13 (fig. VI-102) was good. However, data received from the airplane Audit I were noisy from approximately 725 seconds to loss of data. The data from the range instrumentation ship Twin Falls were noisy from acquisition of signal to T + 905 seconds. Momentary losses of data of 1 to 15 seconds duration occurred after this time. Audit I and the Twin Falls covered primarily the coast phase of the AC-13 flight. Overlapping coverage was also provided by the airplane Audit II.

The coverage on AC-14 (fig. VI-103) was intermittent. The range instrumentation ship Coastal Crusader received noisy data for its entire view period. This resulted in the loss of important data during the main engine restart sequence. Although the restart sequence was lost, the Twin Falls did cover main engine second ignition. The gap in data which existed between T + 742 and T + 985 seconds occurred because no telemetry ship was stationed in the area.

The coverage on AC-15 (fig. VI-104) was fair. The only gap which existed was due to the absence of a telemetry ship and not a station malfunction. However, Pretoria's coverage was extremely noisy. This could have been caused by the ground antenna locking on to a minor lobe of the Centaur's antenna pattern.

Of the 160 measurements made on AC-13, three failed to yield data during portions of the flight. Liquid-oxygen boot pump turbine inlet pressure (CP26P) response was slow at main engine first start and main engine first cutoff. Cause of the failure is believed to be a frozen sensing line. Thermal insulation will be added to prevent reoccurrence of the problem on future flights. C-1 engine fuel pump temperature measurement (CP122T) failed to provide sufficient transient response. The probe is being

redesigned to improve response. S-4 chamber surface temperature measurement (CP693T) indicated lower than expected temperature during the S-4 half-on mode. The cause of this measurement failure is not known. However, such results would be expected if the sensor became partially detached from the surface.

Five the the 162 measurements on AC-14 failed during portions of flight. The nose cap angle-of-attach pitch pressure transducer (CA473P) opened at T + 68.3 seconds. C-1 liquid-oxygen pump temperature (CP124T) and C-1 engine fuel pump temperature (CP122T) measurements responded slowly, just as did CP122T on AC-13. The C-1 engine turbopump surface temperature measurement (CP728T) failed at T + 326 seconds. The response of liquid-oxygen boost pump turbine inlet pressure measurement (CP26P) was slow, as on AC-13.

Three of the 162 measurements on AC-15 lost data during portions of the flight. Two of these were the slow response of CP26P and CP122T, which also occurred on AC-13 and AC-14. Bias shifts occurred on the spacecraft leg number 1 radial vibration measurement (CA772O) at T + 1449 and T + 1586.5 seconds - less than 2 seconds of data was lost at each of these times.

TABLE VI-15. - INVERTER PERFORMANCE

Measurement	Units	AC-13		AC-14		AC-15	
		Lift-off	(a)	Lift-off	(a)	Lift-off	(a)
Atlas							
Phase A	V	115.3	-0.4	115.9	-0.4	114.9	-0.4
Phase B	V	115.8	-.4	116.0	±.2	115.8	-.8
Phase C	V	115.8	-.4	115.8	-.4	116.0	-.8
Frequency	Hz	402.7	+.3	402.7	-.3	402.6	+.4
Centaur							
Phase A	V	116.2	+0.2	115.6	+0.5	116.2	+0.4
Phase B	V	115.4	+.2	115.2	+.3	116.3	+.7
Phase C	V	115.5	+.1	115.6	+.2	115.2	+.4
Fre			-.2				
Frequency	Hz	400.0	0	400.0	0	400.0	0
Temperature	K	306	----	304	----	305	----
	°F	90.6	----	87.8	----	88.4	----

[a]Drift from lift-off value during programmed flight.

TABLE VI-16. - ELECTRICAL DATA AT LIFT-OFF

	Units	Flight		
		AC-13	AC-14	AC-15
Atlas				
Main battery	V	28.1	28.0	28.1
Telemetry battery:				
Number 1	V	28.5	28.5	28.4
Number 2	V	28.5	28.3	(a)
Range safety command battery:				
Number 1	V	29.8	29.0	29.2
Number 2	V	29.3	29.2	29.2
Centaur				
Main battery	A	44	45.5	44
Main battery	V	28.5	28.2	28.3
Range safety command battery:				
Number 1	V	32.6	32.6	32.5
Number 2	V	32.8	32.7	32.6
Pyrotechnic battery:				
Number 1	V	35.8	36.1	35.6
Number 2	V	36.0	35.9	35.2

[a]Not used on AC-15.

TABLE VI-17. - CENTAUR MAIN BATTERY LOAD PROFILE

Event	Main battery load, A		
	AC-13	AC-14	AC-15
Preload	13	13	13
Changeover, external power to battery	42.5	44	43
Lock liquid-hydrogen vent valve	45.5	47.5	46
Eject Centaur umbilicals	44	45.5	44
Lift-off (T - 0)	44	45.5	44
Unlock liquid-hydrogen vent valve	42	43	42.5
Lock liquid-hydrogen vent valve (booster engine cutoff)	44	45	43
Unlock liquid-hydrogen vent valve	42	43	42
Start boost pumps and lock liquid-oxygen vent valve	45.5	46.5	45.5
Lock liquid-hydrogen vent valve and pressurize tank (sustainer engine cutoff)	48	49.5	47.
Start hydraulic recirculating pumps and end pressurization of liquid-hydrogen tank	53	53.5	52
Prestart main engines	55	56	54
Energize igniters, start main engines (MES-1)	61	62	60
Igniters off, hydraulic recirculating pumps off	52	53	51
Main engine cutoff (MECO-1), boost pumps off, end prestart, verniers half on	48	49	48.5
Unlock liquid-hydrogen vent valves (MECO backup)	46	47	46.5
Vernier engines cutoff, start coast phase	44.5	45	45
Lock liquid-hydrogen vent valve, start tank burp pressurization	49	----	48.5
Start boost pumps, start hydraulic recirculating pumps	55	----	53.5
Stop liquid-oxygen tank burp pressurization	54	----	53.5
Energize liquid-oxygen and hydrogen prestart solenoids	56.5	----	55.5
Energize igniters, start main engines (MES-2), liquid-hydrogen tank burp pressurization	60	----	59.5
Stop hydraulic recirculating pumps	51	51.5	50.5
Stop boost pumps (MECO-2)	44.5	46.5	44
[a]Spacecraft electrical disconnect	----	----	----
[a]Spacecraft separation	----	----	----
Vernier engines to half on	47	47.5	47
Vernier engines off	45	45	44
Energize liquid-oxygen and hydrogen prestart solenoids, start hydraulic recirculating pumps, begin prestart	52.5	53	51
Unlock liquid-oxygen and hydrogen vent valves	48	50	48
Energize main power changeover switch	53	53.5	
[b]Power turnoff	0	0	0

[a]These measurements are not reliable because of the short duration of the pulse which may or may not appear on a commutated measurement.

[b]Telemetry and tracking remain on. However, main battery current cannot be monitored beyond power turnoff because of loss of 60-Hz excitation to the dc current probe.

TABLE VI-18. - ATLAS MEASUREMENT SUMMARY FOR AC-13 AND AC-14

System	Measurement type													
	Acceleration	Rotation rate	Displacement	Positions	Vibrations	Pressure	Frequency	Rate	Strain	Temperature	Voltages	Discretes	Acoustical	Totals
Airframe					17	9		4	4	22		4	1	61
Range safety											3	1		4
Electrical							1				4			5
Pneumatics						13				7				20
Hydraulics				2		8				4				14
Dynamics	1											2		3
Propulsion		3	6		2	26				14		6		57
Flight control			17					3			4	14		38
Telemetry										2				2
Propellants	1					2					1			4
Totals	2	3	23	2	19	58	1	7	4	49	12	27	1	208

TABLE VI-19. - ATLAS MEASUREMENT SUMMARY FOR AC-15

System	Measurement type											
	Acceleration	Rotation rate	Displacement	Vibration	Pressure	Frequency	Rate	Strain	Temperature	Voltage	Discretes	Totals
Airframe				4	3			4	14		4	29
Range safety										3	1	4
Electrical						1				4		5
Pneumatics					9				3			12
Hydraulics					6							6
Dynamics	1										2	3
Propulsion		3	3		18				6		6	36
Flight control			11				3			4	13	31
Telemetry									1			1
Propellants	1				2					1		4
Totals	2	3	14	4	38	1	3	4	24	12	26	131

TABLE VI-20. - CENTAUR MEASUREMENT SUMMARY FOR AC-13

Systems	Measurement type											
	Rotation rate	Current	Displacement	Vibrations	Pressure	Frequency	Rate	Temperature	Digital	Voltage	Discretes	Totals
Airframe								3			3	6
Range safety										2	3	5
Electrical		1				1				4		6
Pneumatics					5			3			2	10
Hydraulics					2			2				4
Guidance								1	1	16		18
Separation			1									1
Propulsion	4				12			20			20	56
Flight control							3			4	35	42
Propellants			2							2		4
Spacecraft			3	5	1			1	1			11
Totals	4	1	6	5	20	1	3	30	2	28	63	163

TABLE VI-21. - CENTAUR MEASUREMENT SUMMARY FOR AC-14 AND AC-15

System	Measurement type											
	Rotation rate	Current	Displacement	Vibration	Pressure	Frequency	Rate	Temperature	Digital	Voltage	Discretes	Totals
Airframe				2				3			3	8
Range safety										2	3	5
Electrical		1				1				4		6
Pneumatics					5			3			2	10
Hydraulics					2			2				4
Dynamics								1	1	16		18
Propulsion	4				12			22			20	58
Flight control							3			4	35	42
Propellant			2							2		4
Spacecraft			3		1			1	1			6
Totals	4	1	5	2	20	1	3	32	2	28	63	161

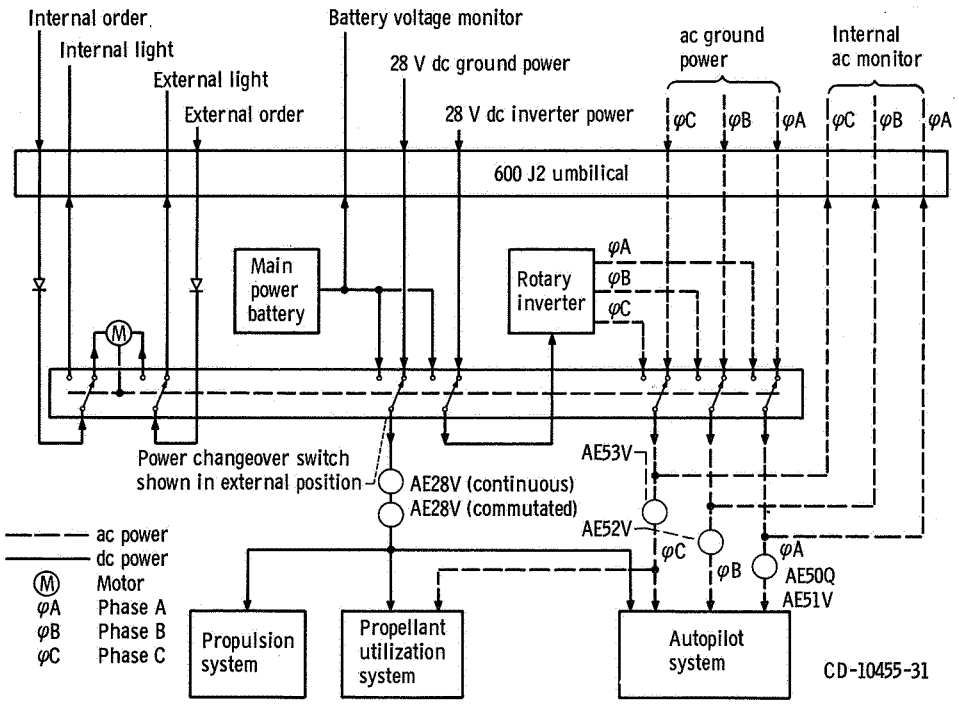

Figure VI-83. - Atlas electrical system block diagram; AC-13, AC-14, and AC-15.

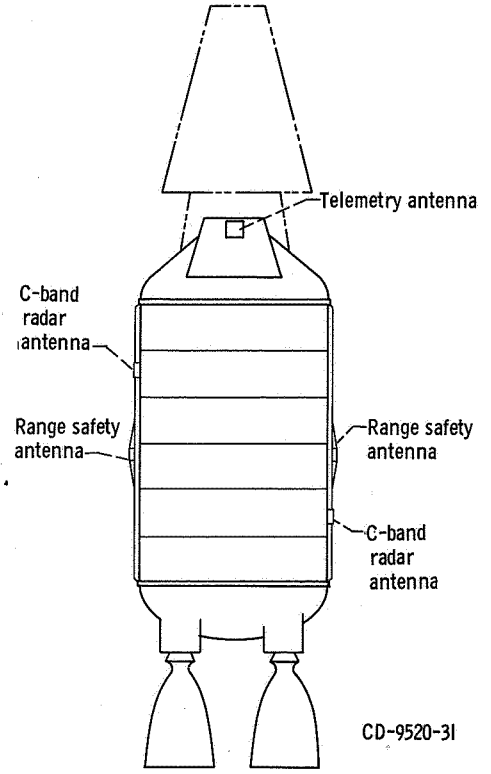

Figure VI-84. - Centaur antenna locations and radiofrequency subsystems; AC-13, AC-14, and AC-15.

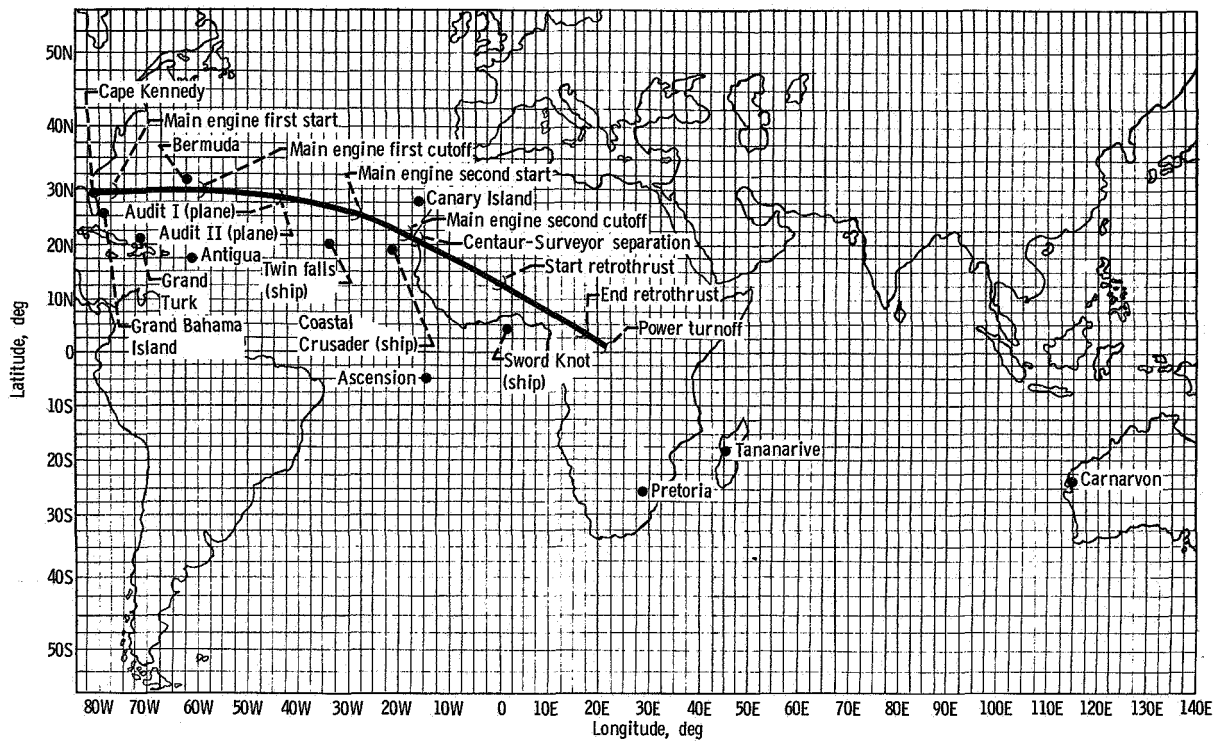

Figure VI-85. - Tracking station locations and vehicle trajectory Earth track, AC-13.

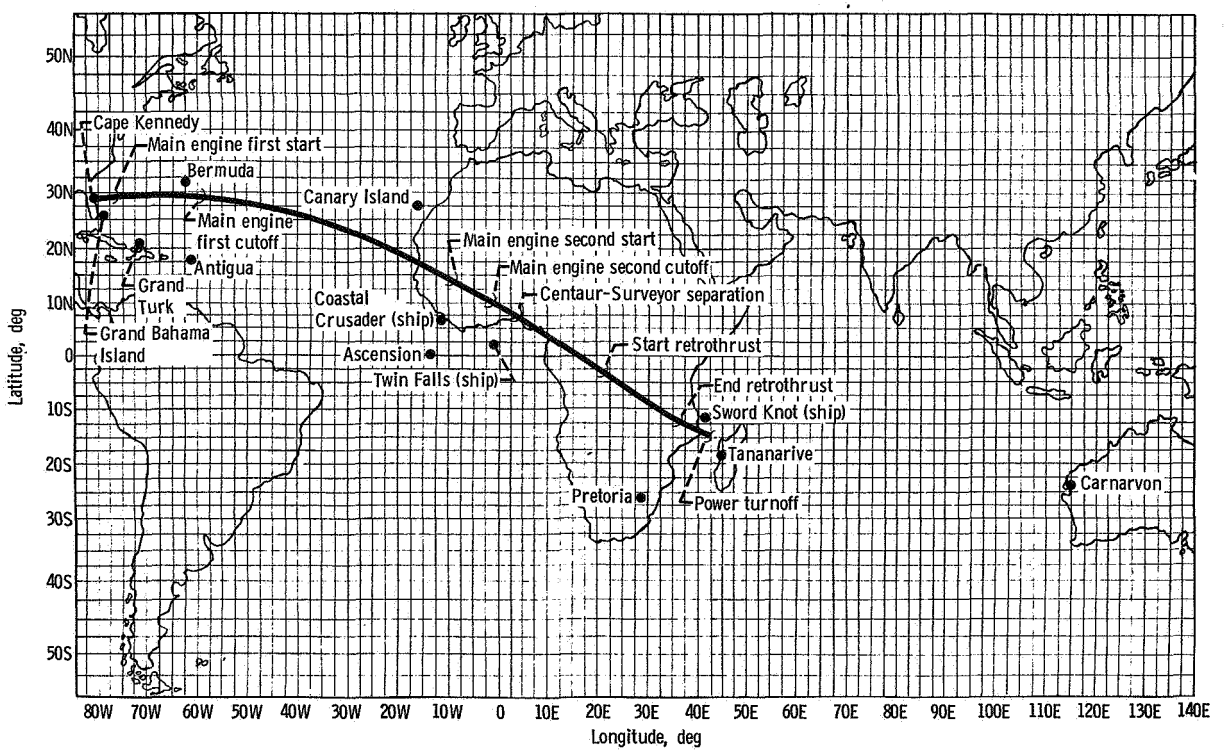

Figure VI-86. - Tracking station locations and vehicle trajectory Earth track, AC-14.

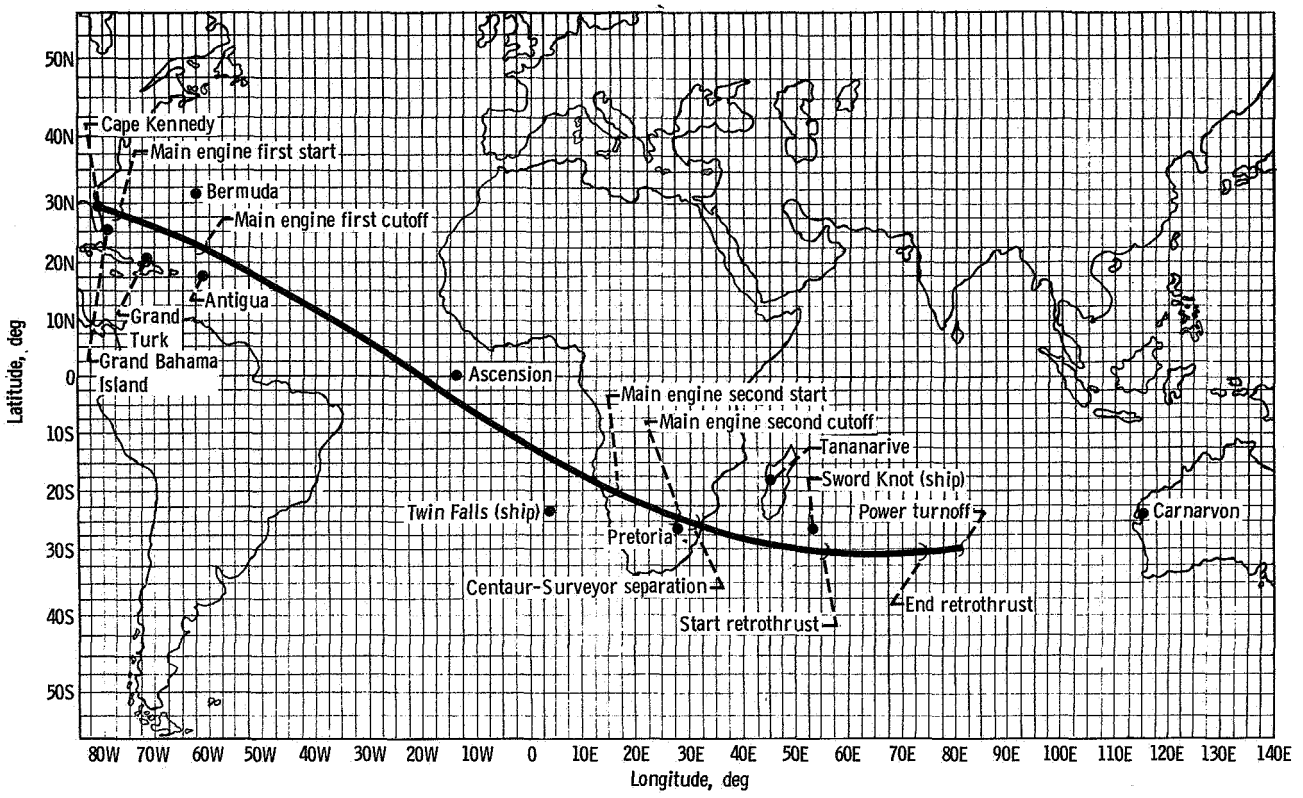

Figure VI-87. - Tracking station locations and vehicle trajectory Earth track, AC-15.

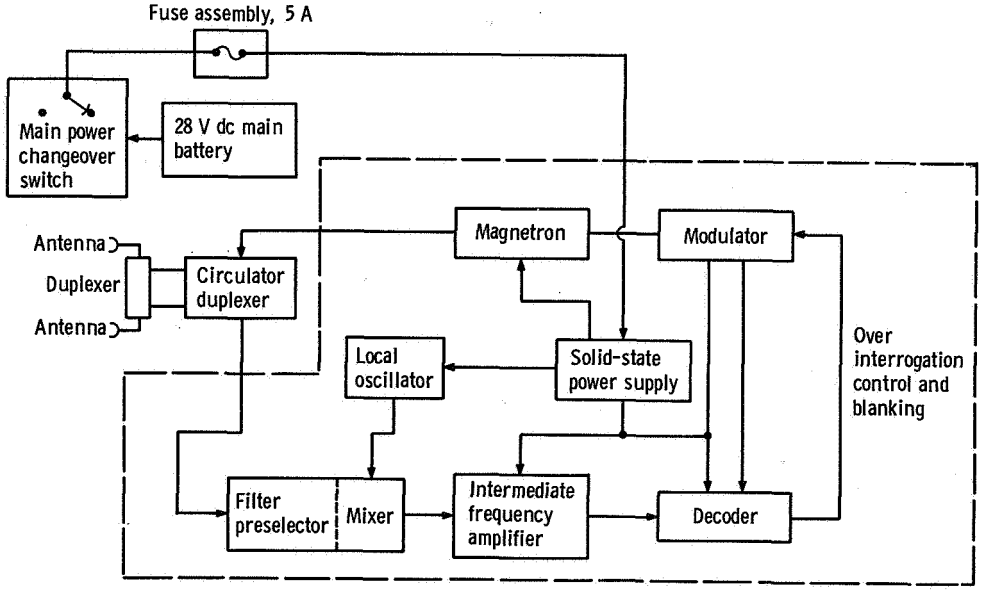

Figure VI-88. - Centaur C-band beacon subsystem; AC-13, AC-14, and AC-15.

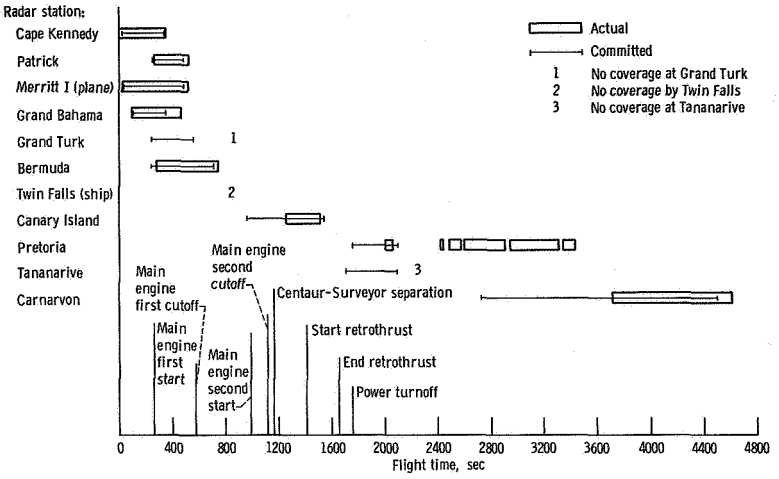

Figure VI-89. - C-Band radar coverage, AC-13. Coverage shown is for autobeacon track only.

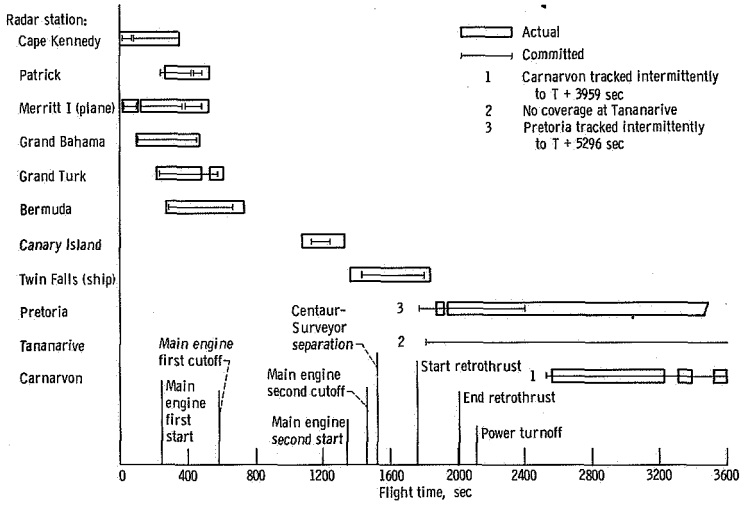

Figure VI-90. - C-Band radar coverage, AC-14. Coverage shown is for autobeacon track only.

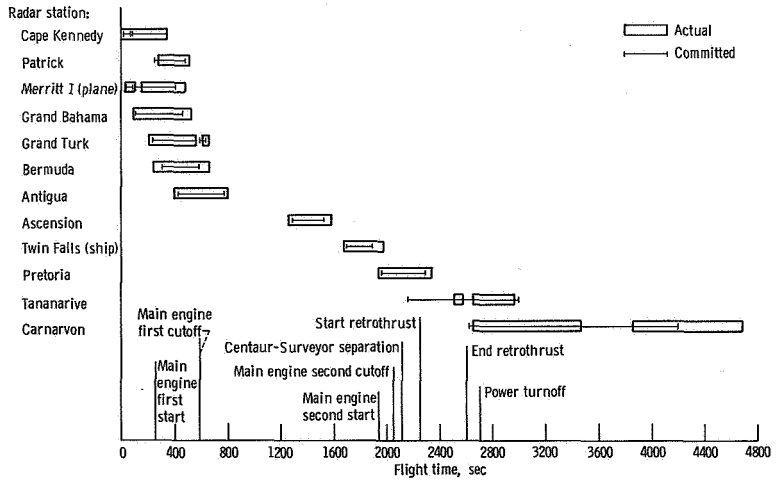

Figure VI-91. - C-Band radar coverage, AC-15. Coverage shown is for autobeacon track only.

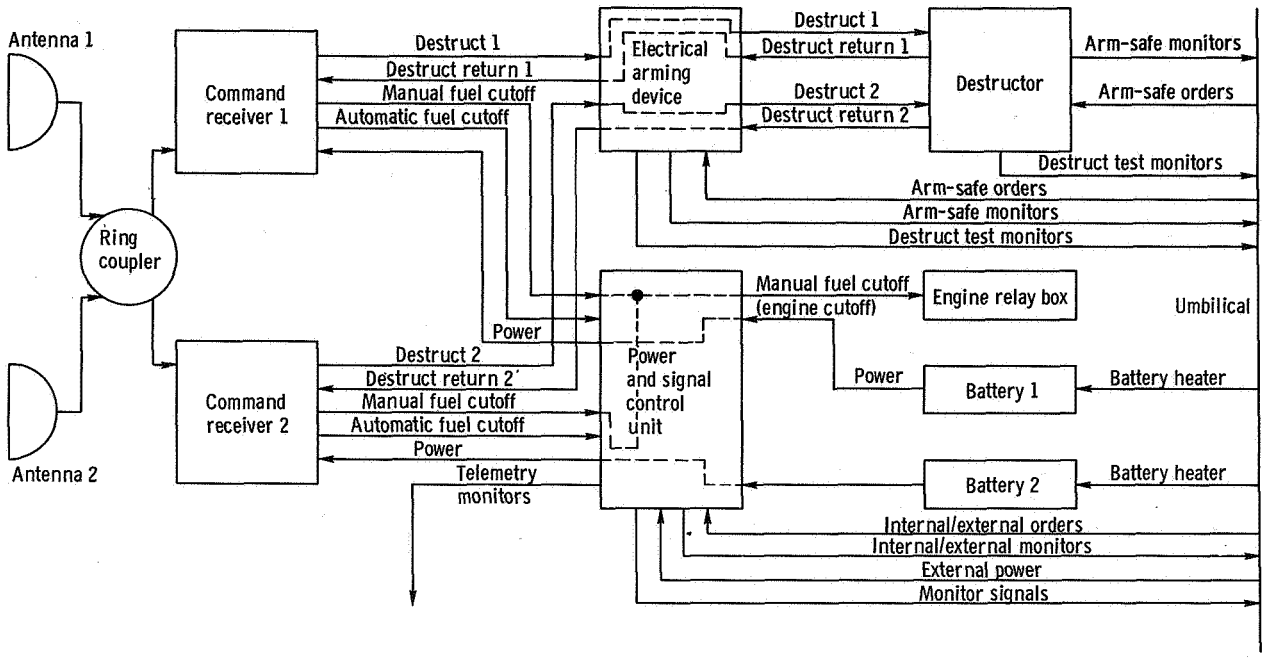

Figure VI-92. - Atlas vehicle destruct subsystem block diagram; AC-13, AC-14, and AC-15.

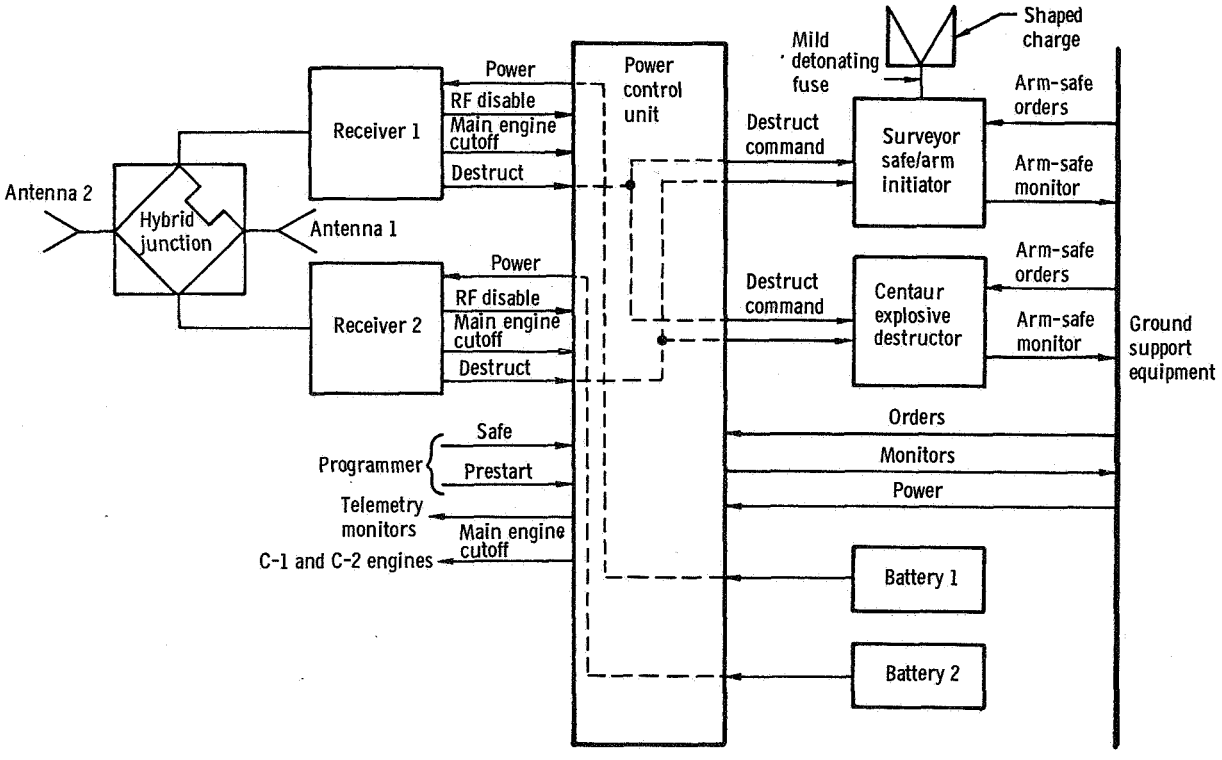

Figure VI-93. - Centaur vehicle destruct subsystem block diagram; AC-13, AC-14, and AC-15.

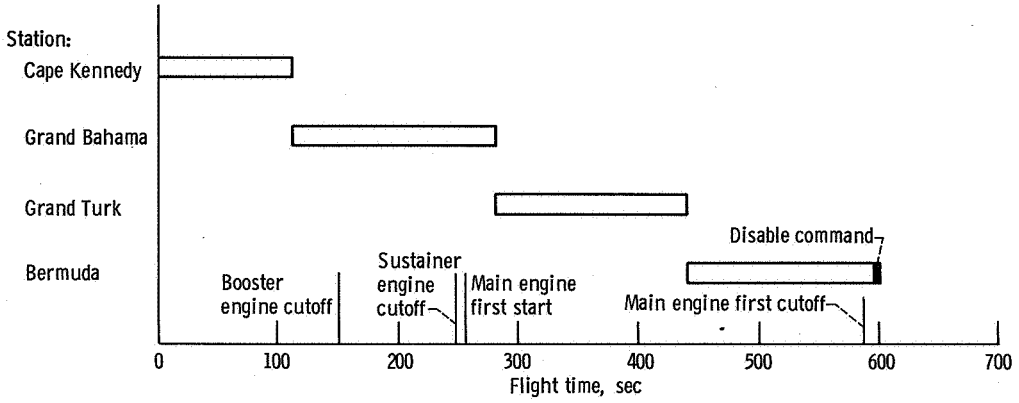

Figure VI-94. - Range safety command system transmitter coverage, AC-13.

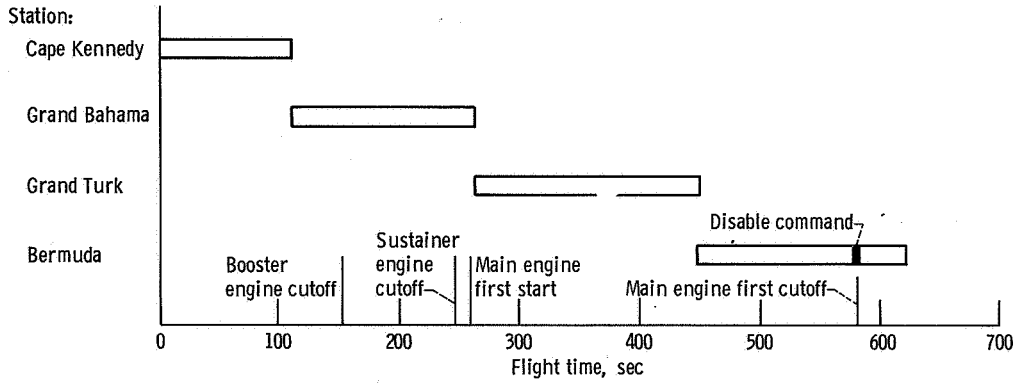

Figure VI-95. - Range safety command system transmitter coverage, AC-14.

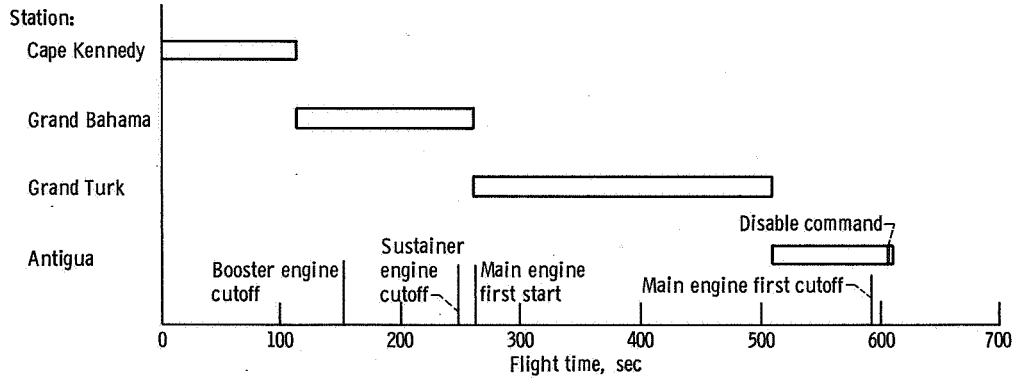

Figure VI-96. - Range safety command system transmitter coverage, AC-15.

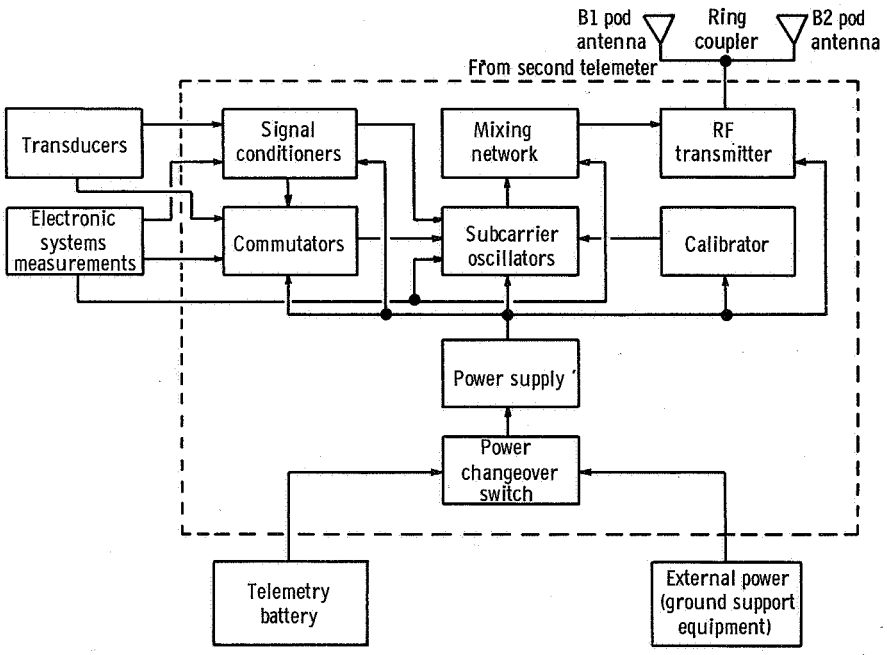

Figure VI-97. - Typical Atlas telemetry system; AC-13, AC-14, and AC-15. (Note: AC-15 has only one Atlas telemeter.)

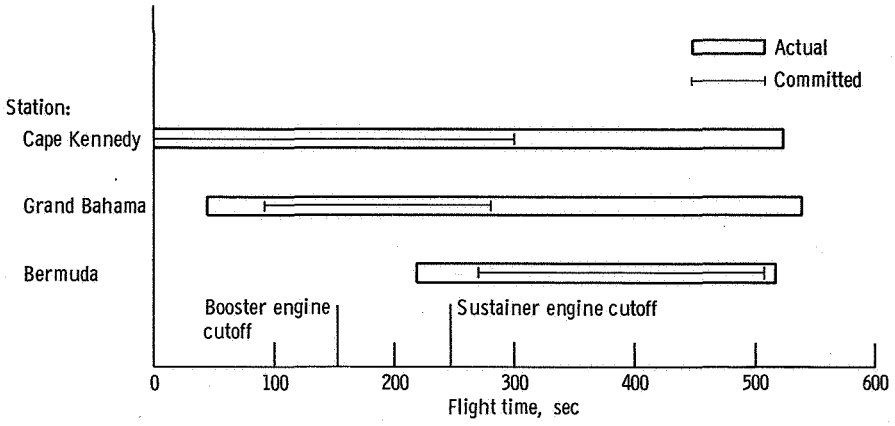

Figure VI-98. - Atlas telemetry coverage, AC-13.

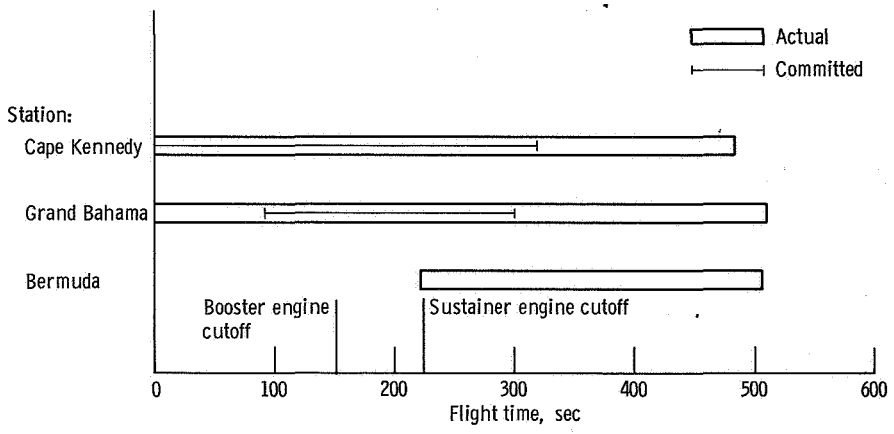

Figure VI-99. - Atlas telemetry coverage, AC-14.

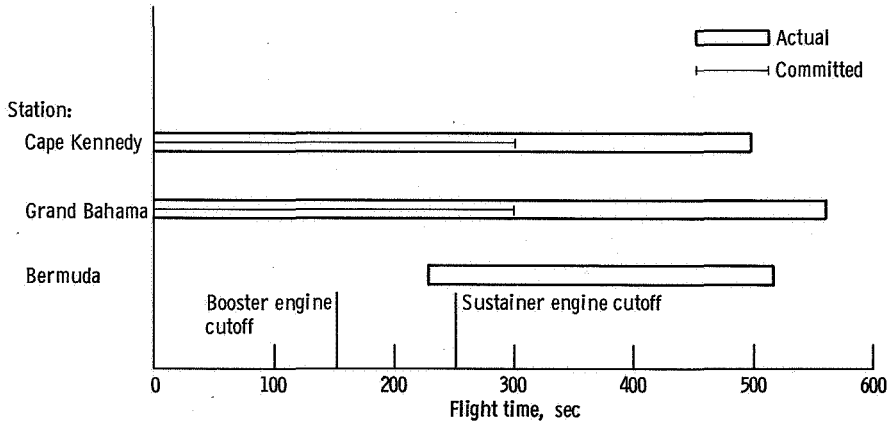

Figure VI-100. - Atlas telemetry coverage, AC-15.

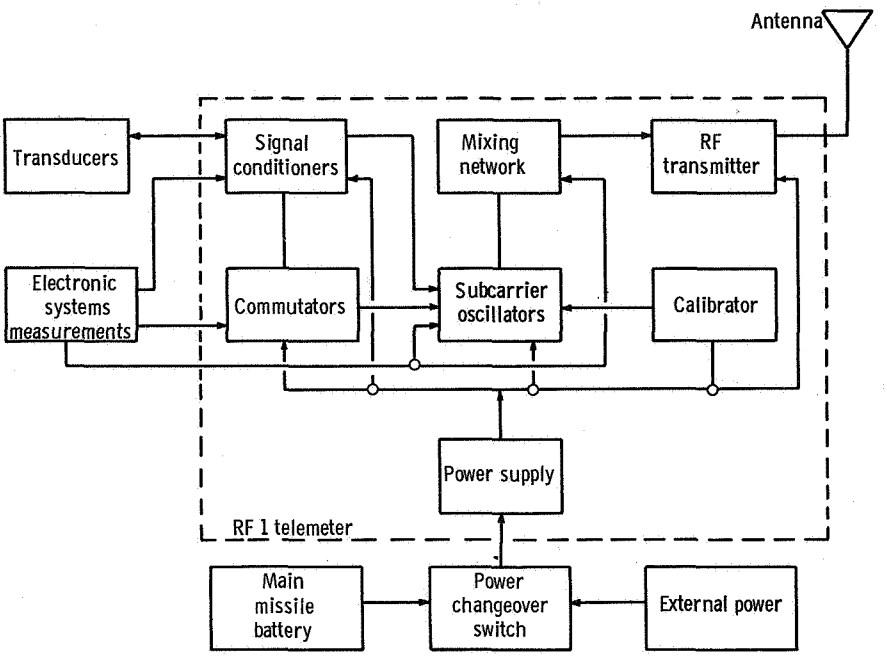

Figure VI-101. - Centaur telemetry subsystem block diagram; AC-13, AC-14, and AC-15.

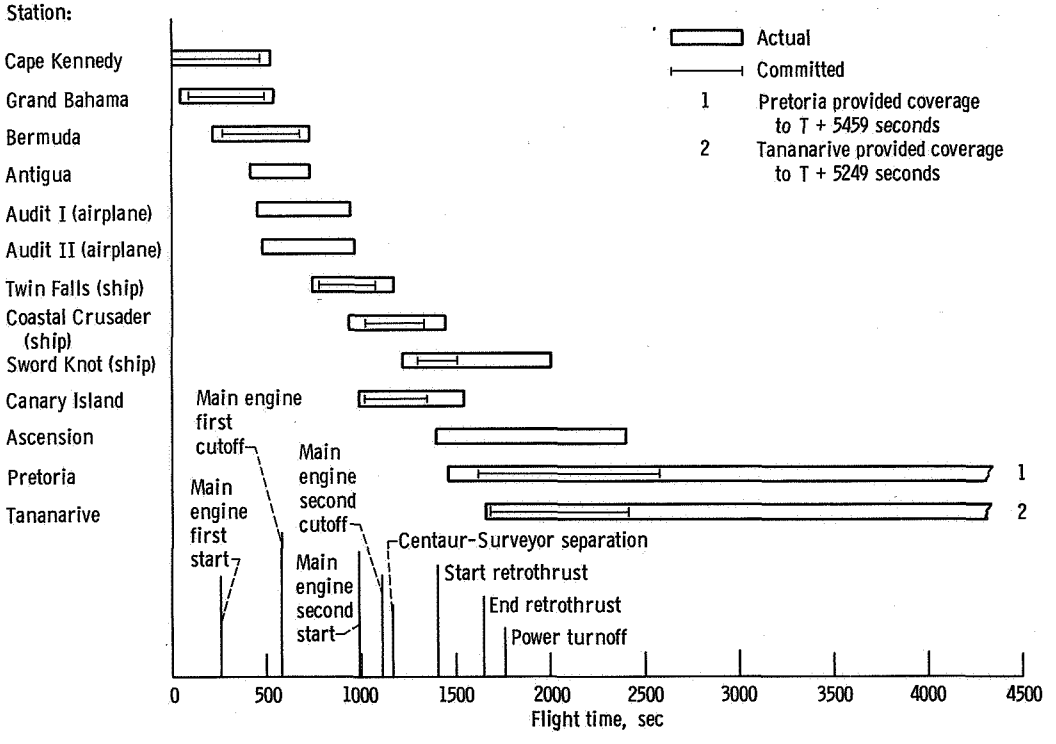

Figure VI-102. - Centaur telemetry coverage, AC-13.

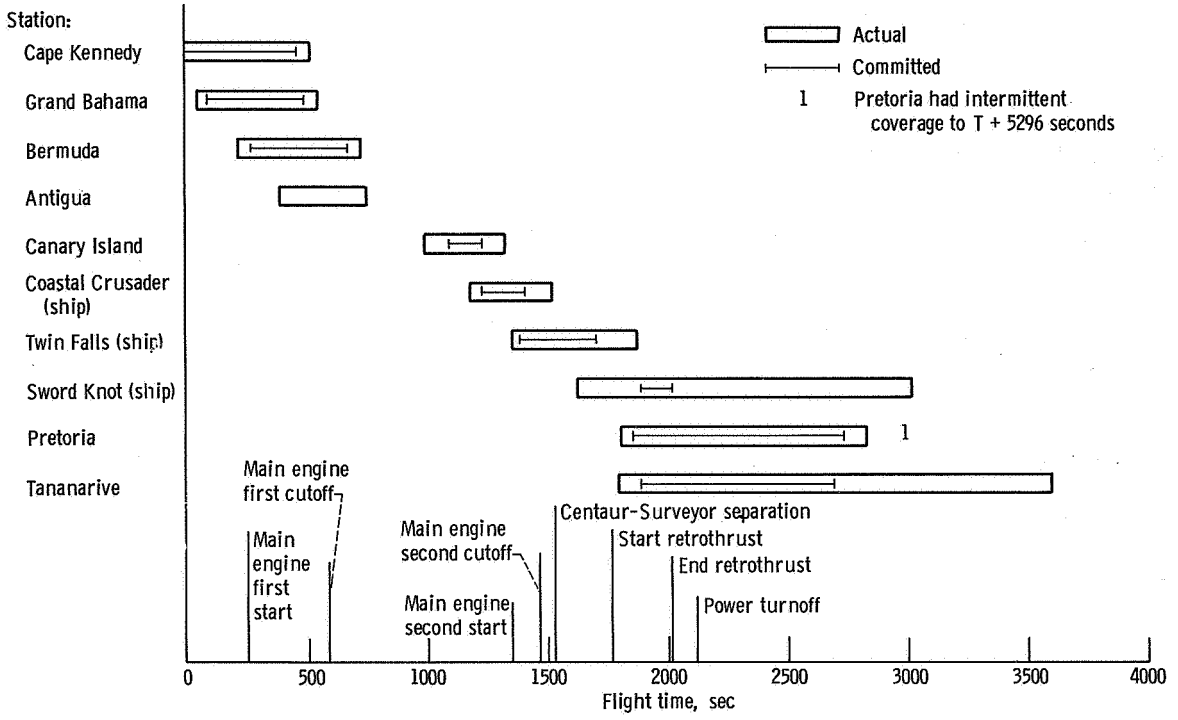

Figure VI-103. - Centaur telemetry coverage, AC-14.

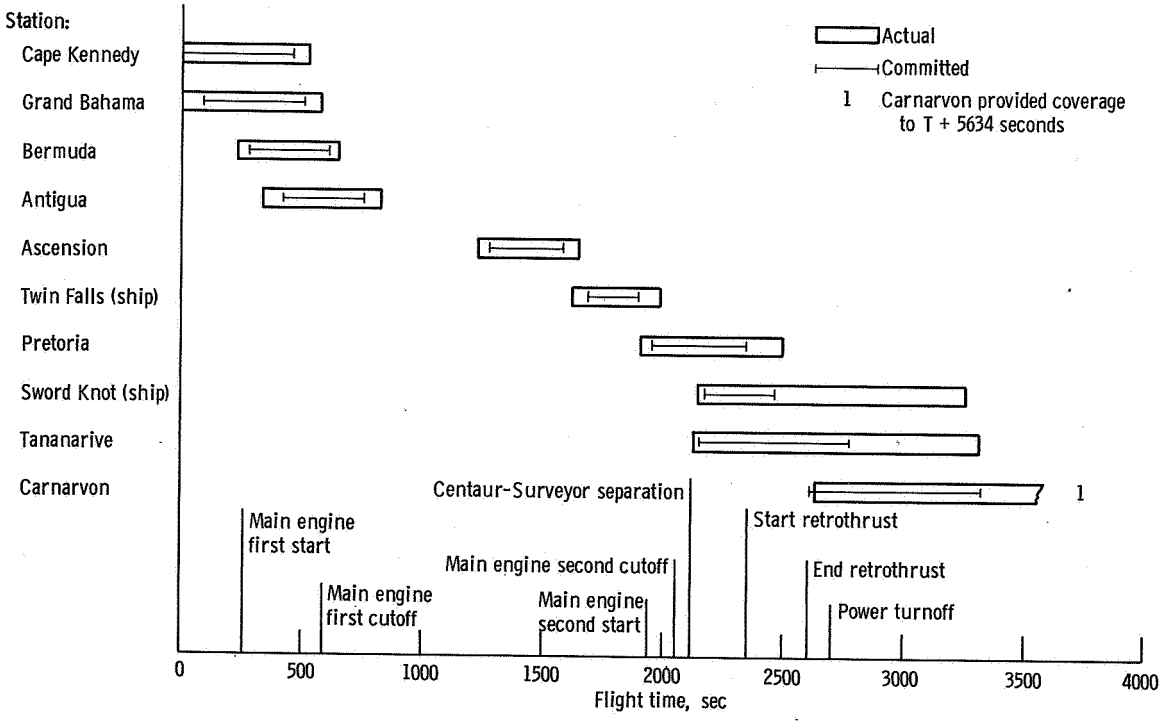

Figure VI-104. - Centaur telemetry coverage, AC-15.

GUIDANCE AND FLIGHT CONTROL SYSTEMS

by Michael Ancik, Larry Feagan, and Corrine Rawlin

The objectives of the guidance and flight control systems are to guide the launch vehicle to the orbit injection point and establish the vehicle velocity necessary to place the Surveyor spacecraft in a lunar transfer orbit. To accomplish these objectives the guidance and flight control systems provide vehicle stabilization, control and guide the vehicle along the flight path, and sequence flight events of the launch vehicle. These functions are performed at specified time periods from vehicle lift-off through completion of the Centaur retromaneuver after spacecraft separation. An inertial guidance system is installed on the Centaur stage. Separate flight control systems are installed on the Atlas and Centaur stages. The guidance system, operating with the flight control systems, provides the capability to stabilize the vehicle and compensate for trajectory dispersions resulting from thrust misalinement, winds, and vehicle performance variations.

Three modes of operation are used for stabilization, control, and guidance of the launch vehicle. These modes are rate stabilization only, rate stabilization and attitude control, and rate stabilization and guidance control. Block diagrams of the three modes are shown in figure VI-105. The flight times during which a particular mode is used are shown in figure VI-106. This figure also shows the modes of operation of the Centaur hydrogen peroxide attitude control system, which are discussed later in this section.

The flight control system controls the vehicle by gimbaling the engines to provide thrust vector control while the main engines are firing or by commanding various combinations of the hydrogen peroxide attitude control engines on or off during coast periods, when the main engines are not firing. In the rate-stabilization-only mode, output signals from rate gyros are used to control the vehicle. The output signal of each rate gyro is proportional to the angular rate of rotation of the vehicle about the input axis of the gyro. The vehicle angular rates are minimized, by the flight control system, to stabilize the vehicle. The rate-stabilization-only mode stabilizes the roll axis of the Centaur stage continuously after Atlas-Centaur separation except during Centaur-spacecraft separation. This mode is also used to stabilize the pitch and yaw axis of the Centaur stage for 12 seconds following Atlas-Centaur separation, 4 seconds following main engine second start, and the period between main engine second cutoff and Centaur-spacecraft separation. Rate stabilization is also combined with position (attitude) information in the other two modes of operation.

The rate-stabilization-and-attitude control mode is used for pitch, yaw, and roll control during the Atlas booster phase of flight and for roll control only during the Atlas sustainer phase of flight. This mode is termed attitude control since the displacement

gyros (one each for the pitch, yaw, and roll axes) provide a reference attitude to which the vehicle is to be alined. However, if the actual flight path differs from the desired flight path, there is no way of determining the difference and correcting the flight path. The reference attitude is programmed to change during booster phase. These changes in reference attitude cause the vehicle to roll to the programmed flight azimuth angle and to pitch downward. Vehicle stabilization is accomplished in the same manner as in the rate-stabilization-only mode. The rate stabilization signals are algebraically summed with the attitude reference signals. These resultant signals are used to control and stabilize the vehicle.

The rate-stabilization-and-guidance-control mode is used for the pitch and yaw axes during Atlas sustainer firing and Centaur main engine first and second firings, and during coast periods except for 12 seconds following Atlas-Centaur separation, 4 seconds following main engine second start, and the period between main engine second cutoff and Centaur-spacecraft separation. In this mode, the guidance system provides the attitude and direction reference. If the resultant flight path, as measured by the guidance system, is not the desired flight path, the guidance system issues steering signals to direct the vehicle to the desired flight path. Vehicle stabilization is accomplished in the same manner as in the rate-stabilization-only mode. The pitch and yaw rate stabilization signals are algebraically summed with the appropriate pitch and yaw steering signals from the guidance system. These resultant signals are used to control and stabilize the vehicle. Figure VI-107 is a simplified diagram of the interface between the guidance system and the flight control system.

Guidance System

System description. - The Centaur guidance system is an inertial system which becomes completely independent of ground control approximately 9 seconds before lift-off of the vehicle. The guidance system performs the following functions:

(1) Measures vehicle acceleration in fixed inertial coordinates
(2) Computes the values of actual vehicle velocity and position, and computes the vehicle flight path to attain the trajectory injection point
(3) Compares the actual position to the desired flight path and issues steering signals
(4) Issues discrete commands

A simplified block diagram of the guidance system is shown in figure VI-108.

Inertial measuring unit: Vehicle acceleration is measured by

(1) The inertial platform unit, which contains the platform assembly, gyros, and accelerometers

(2) The pulse rebalance, gyro torquer, and power supply unit, which contains the electronics associated with the accelerometers

(3) The platform electronics unit, which contains the electronics associated with the gyros

The inertial platform assembly uses four gimbals which provide a three-axis coordinate system. The use of four gimbals, instead of three, allows complete rotation of all three vehicle axes about the platform without gimbal lock. Gimbal lock is a condition in which two axes coincide, causing loss of one degree of freedom. A gimbal diagram is shown in figure VI-109. The azimuth gimbal is isolated from movements of the vehicle airframe by the other three gimbals. The inertial components (three gyros and three accelerometers) are mounted on the azimuth or inner gimbal. A gyro and an accelerometer are mounted as a pair with their sensing axes parallel. The gyro and accelerometer pairs are also alined on three mutually perpendicular (orthogonal) axes corresponding to the three axes of the platform.

The three gyros are identical and are of the single-degree-of-freedom, floated-gimbal, rate integrating type. Each gyro monitors one of the three axes of the platform. These gyros are elements of control loops, the sole purpose of which is to maintain each axis fixed in inertial space. The output signal of each gyro is connected to a servoamplifier whose output controls a direct-drive torque motor which moves a gimbal of the platform assembly. The orientation of the azimuth gimbal is fixed in inertial space, and the other roll gimbal is attached to the vehicle. The angles between the gimbals provide a means for transforming steering signals from inertial coordinates to vehicle coordinates. The transformation is accomplished by electromechanical resolvers, mounted between gimbals, to produce analog electrical signals proportional to the sine and cosine functions of the gimbal angles. These electrical signals are used for an analog solution of the mathematical equations for coordinate transformation by interconnecting the resolvers in a multiple resolver chain.

The three accelerometers are identical and are of the single-axis, viscous-damped, hinged-pendulum type. The accelerometer associated with each axis measures the change in vehicle velocity along that axis by responding to acceleration. Acceleration of the vehicle causes the pendulum to move off center. The associated electronics then produce precise current pulses to recenter the pendulum. These rebalance pulses are either positive or negative depending on an increase or decrease in vehicle velocity. These pulses, representing changes in velocity (incremental velocity), are then routed to the navigation computer unit for computation of vehicle velocity.

Proper flight operation requires alinement and calibration of the inertial measuring unit during launch countdown. The aximuth of the platform, to which the desired flight trajectory is referenced, is alined by ground-based optical equipment. The platform is alined perpendicular to the local vertical by using the two accelerometers in the hor-

izontal plane. Each gyro is calibrated to determine its characteristic constant torque drift rate and mass unbalance along the input axis. The scale factor and zero bias offset of each accelerometer are determined. These prelaunch-determined calibration constants and scale factors are stored in the navigation computer for use during flight.

Navigation computer unit: The navigation computer unit is a serial, binary, digital machine with a magnetic drum memory. The memory drum has a capacity of 2816 words (25 bits per word) of permanent storage, 256 words of temporary storage, and six special-purpose tracks. Permanent storage is prerecorded and cannot be altered by the computer. The temporary storage is the working storage of the computer. Incremental velocity pulses from the accelerometers are the information inputs to the navigation computer. The operation of the navigation computer is controlled by the prerecorded program. This program directs the computer to use the prelaunch equations, navigation equations, and guidance equations.

The prelaunch equations establish the initial conditions for the navigation and guidance equations. Initial conditions include (1) a reference trajectory; (2) launch site values of geographical position; and (3) initial values of navigation and guidance functions. Based on these initial conditions, the guidance system starts flight operation approximately 9 seconds before lift-off.

The navigation equations are used to compute vehicle velocity and actual position. Velocity is determined by algebraically summing the incremental velocity pulses from the accelerometers. An integration is then performed on the computed velocity to determine actual position. Corrections for the prelaunch-determined gyro and accelerometer constants are also made during the velocity and position computation to improve the navigation accuracy. For example, the velocity data derived from the accelerometer measurements are adjusted to compensate for the accelerometer scale factors and zero offset biases measured during the launch countdown. The direction of the velocity vector is also adjusted to compensate for the gyro constant torque drift rates measured during the launch countdown.

The guidance equations continually compare actual position and velocity with the position and velocity desired at the time of injection. Based on this position comparison, steering signals are generated to guide the vehicle along an optimized flight path to obtain the desired injection conditions. The guidance equations are used to generate eight discrete commands: (1) booster engine cutoff, (2) sustainer engine cutoff backup, (3) Centaur main engine first cutoff, (4) hydrogen peroxide settling engines cutoff, (5) B timer start (Centaur main engine second start sequence), (6) Centaur main engine second cutoff, (7) telemetry calibration on, and (8) telemetry calibration off. The booster engine cutoff command and the sustainer engine cutoff backup commands are issued when the measured vehicle acceleration equals predetermined values. The Centaur main engine first cutoff command is issued when the vehicle orbital energy equals the energy required for injec-

tion into the parking orbit. At this time the hydrogen peroxide engines are started. At 76 seconds after main engine first cutoff, the hydrogen peroxide settling engines cutoff command is issued. The B timer start command is issued when the angle between the position and target vectors, as computed by the guidance system, equals a prelaunch-determined angle. When the measured vehicle orbital energy equals the predetermined value required for injection into the proper lunar trajectory, the Centaur main engine second cutoff command is issued. The telemetry calibration commands are issued at fixed intervals after the B timer start command is issued.

During the booster phase of flight, the navigation computer supplies an incremental pitch signal and the total yaw signal for steering the Atlas stage. From a series of predetermined programs, one pitch program and one yaw program are selected based on prelaunch upper-air wind soundings. The selected programs are entered and stored in the computer during launch countdown. The programs consist of discrete pitch and yaw turning rates for specified time intervals from T + 15 seconds until booster engine cutoff. These programs permit changes to be made in the flight reference trajectory during countdown to reduce anticipated aerodynamic heating and structural loading conditions on the vehicle.

Signal conditioner unit: The signal conditioner unit is the link between the guidance system and the vehicle telemetry system. This unit modifies and scales guidance system parameters to match the input range of the telemetry system.

System performance. - The performance of all three guidance systems was excellent. The system performances were evaluated in terms of the resultant flight trajectories and the midcourse corrections that would have been required by the spacecrafts to impact the targets for which the trajectories were designed. In addition, the issuance of discrete commands, the operation of the guidance steering loops, gyro control loops, and accelerometer loops, and other measurements were evaluated in terms of general performance. Except where otherwise noted, all numbers indicative of performance are the maximums seen on any of the three flights.

Trajectory and midcourse requirements: The accuracy of the AC-13, AC-14, and AC-15 guidance systems was excellent. Parking orbit data and midcourse correction requirements (20 hr after injection) are listed in the following table:

Parking orbit data[a] and midcourse correction requirements	Units	Flights		
		AC-13	AC-14	AC-15
Injection altitude (parking orbit)	km	164.2	165.8	162.9
	n.mi.	88.6	89.5	87.9
Perigee parking altitude	km	153.4	157.7	162.1
	n.mi.	82.8	85.1	87.5
Apogee parking altitude	km	164.4	166.2	168.1
	n.mi.	88.7	89.7	90.7
Coast time	min	6.7	12.9	22.4
Midcourse correction - miss only[b]	m/sec	0.55	1.35	0.33
	ft/sec	1.80	4.43	1.08
Midcourse correction - miss plus time of flight[c]	m/sec	1.21	2.21	1.21
	ft/sec	-3.97	7.25	3.97

[a]These values are based on Centaur guidance data.

[b]Miss only denotes the velocity correction required to hit the preflight aiming point.

[c]Miss plus time of flight denotes the velocity correction required to hit the aiming point at the specified time.

The parking orbit injection altitude, for all three flights, was designed to be 166.7±9.3 kilometers (90±5 n. mi.), based on the spacecraft heating and payload considerations. The midcourse correction requirements were well within the established specification that a Surveyor spacecraft would not be required to perform a midcourse correction greater than 50 meters per second (164 ft/sec) for AC-13 and 30 meters per second (98.4 ft/sec) for AC-14 and AC-15. The slight inaccuracies at injection were introduced primarily by three main sources:

(1) Dispersions due to the computational limitations

(2) Dispersion between predicted and actual engine shutdown impulse

(3) Dispersions related to the guidance equipment limitations and to variations from the predicted values of the thrust produced by the hydrogen peroxide engines

The landing conditions which would have resulted had no midcourse maneuvers been made are listed in the following table:

	Units	Landing conditions					
		Designed			No midcourse correction		
		AC-13	AC-14	AC-15	AC-13	AC-14	AC-15
Selenographic latitude	------	0.83°N	0.42°N	4.95°S	2.33°N	3.24°S	5.72°S
Selenographic longitude	------	24.0°E	1.33°W	3.88°E	23.6°E	0.70°E	5.01°E
Unbraked impact velocity	m/sec	2642	2635	2660	2632	2635	2659
	ft/sec	8668	8643	8727	8735	8643	8723
Flight time to moon	days	2	2	2	2	2	2
	hr	15	16	18	15	16	18
	min	27	26	25	28	26	33
	sec	26.7	4.11	10.8	13.2	43.38	4.6
Projected miss distance	km	------	------	------	47.0	126	41.5
	n.mi.	------	------	------	25.4	68	22.4

Performance of the guidance systems was not evaluated in terms of the midcourse corrections actually executed. The actual midcourse corrections were different from those required to impact the targets for which the trajectories were designed. New targets were selected by the Surveyor Project to optimize the meeting of mission objectives. The selections were based on actual measurements of spacecraft position and velocity.

Discrete commands: All discrete commands were issued properly. Table VI-22 lists the discretes, the criteria for the issuance of the discretes, and the computed values at the time the discretes were issued. Actual and predicted times from lift-off are also show, for reference only.

Guidance steering loop: The pitch and yaw steering signals issued by the guidance system are proportional to the components of the steering vector (desired vehicle pointing vector) along the vehicle pitch and yaw axes. In this section of the report, the steering signals have been converted into the angular errors between the steering vector and the vehicle roll axis (vehicle pointing vector) in the pitch and yaw planes.

Guidance steering was activated 8.0 seconds after the booster engine cutoff command. At this time the steering signals were 6° (AC-15) or less. These vehicle attitude changes were required to correct for errors accumulated during the booster phase of the flights when the vehicles were under open-loop control. The steering signals were less than 1° throughout the remainder of the sustainer phase of the flights. Guidance steering was deactivated at sustainer engine cutoff in preparation for staging. When guidance steering was reactivated, about 4 seconds after Centaur main engine first start, the steering signals were 3° (AC-15) or less. During the remainder of the Centaur powered phase of the flights, the steering signals were less than 1.6°. During the coast phase of the flights, the steering signals did not exceed 5° in pitch and in yaw. Guidance steering was deactivated at Centaur main engine second start and was reactivated 4 seconds later. At this time the steering signals were 5° (AC-15) or less. During the remainder of the Centaur

powered phase of the flight, the steering signals were less than 1.5^{o}. Guidance steering was deactivated at Centaur main engine second cutoff. Vehicle stabilization was maintained by rate gyros and the hydrogen peroxide attitude control system during the periods of guidance deactivation except during spacecraft separation when the attitude control systems were also deactivated. Steering was reactivated for the retromaneuvers. At this time the steering signals commanded the vehicles to turn 180^{o} with respect to the vehicle velocity vector at injection. The signals caused the vehicles to pitch and yaw as required to accomplish the turnaround maneuvers. The AC-13, AC-14, and AC-15 vehicles turned 173^{o}, 170^{o}, and 172^{o}, respectively.

Gyro control loops and accelerometer loops: The inertial platforms were stable throughout the flights. The platform gimbal control loops operated satisfactorily. The maximum displacement errors on any flight were less than 20 arc-seconds (the dynamic accuracy tolerance was 60 arc-sec). Normal low-frequency oscillations (<2 Hz) were observed in all gyro control loops. These oscillations are attributed to vehicle dynamics. The accelerometer loops operated satisfactorily throughout the flights.

Other measurements: All of the guidance system signals and measurements which were monitored during the flights were normal and indicated satisfactory operation of the guidance systems.

Flight Control Systems

System description - Atlas. - The Atlas flight control system provides the primary functions required for vehicle stabilization, control, execution of guidance steering signals, and timed switching sequences.

The Atlas flight control system consists of the following major units:

(1) The displacement gyro unit consists of three single-degree-of-freedom, floated-gimbal, rate integrating gyros and associated electronic circuitry for gain selection and signal amplification. These gyros are mounted to the vehicle airframe in an orthogonal triad configuration, the input axis of a gyro alined to its respective vehicle axis of pitch, yaw, or roll.

Each gyro provides an electrical output signal proportional to the integral of the time rate of change of angular displacement from the gyro reference axis.

(2) The rate gyro unit contains three single-degree-of-freedom, floated-gimbal, rate gyros and associated electronic circuitry. These gyros are mounted in the same manner as the displacement gyro unit. Each gyro provides an electrical output signal proportional to the angular rate of rotation of the vehicle about the gyro input (reference) axis.

(3) The servoamplifier unit contains electronic circuitry to amplify, filter, integrate, and algebraically sum engine position feedback signals with position and rate signals.

The electrical outputs of this unit direct the hydraulic actuators, which in turn gimbal the engines to provide thrust vector control.

(4) The programmer unit contains an electronic timer, arm-safe switch, high-, low-, and medium-power electronic switches, the fixed pitch program, and circuitry to set the roll program from launch ground equipment. The programmer issues discrete commands to the following systems: other units of the Atlas flight control system, Atlas propulsion and pneumatic systems, vehicle separation systems, and Centaur flight control and propulsion systems.

System performance - Atlas. - The flight control system performances were satisfactory throughout the Atlas phase of the AC-13, AC-14, and AC-15 flights and compared well with previous flights. The corrections required to control the vehicles because of disturbances were well within the system capabilities. The vehicle dynamic responses resulting from each flight event were evaluated in terms of amplitude, frequency, and duration as observed on rate gyro data (table VI-23). In this table, the control capability is the ratio of engine gimbal angle used to the available total engine gimbal angle, in percent. The percent control capability used at the times of the flight events includes that necessary for correction of the vehicle transient disturbances and for steady-state requirements.

In the remainder of this section, all numbers indicative of performance are the maximum seen on any of the three flights. The programmer was started at 42-inch (1.1-m) rise, which occurred at approximately T + 1 second. At this time, the flight control system began to gimbal the engines for vehicle control. The significant vehicle transients were damped out within T + 4 seconds and required a maximum of 9 percent (AC-14) of the control capability. The roll program was initiated at approximately T + 2 seconds to roll the vehicles to the desired flight azimuths. The roll rate, which depended on the launch pad and flight aximuth orientations, continued for approximately 13 seconds. The pitch program was initiated at T + 15 seconds. The subsequent pitch rates varied for each flight according to its pitch program, which was selected in accordance with launch-day upper-air wind data. Rate gyro data indicated that the periods of maximum aerodynamic loading for the three flights were generally from T + 75 to T + 90 seconds. During these periods, a maximum of 30 percent (AC-15) of the control capability was required to overcome both steady-state and transient loading. The Atlas booster engines were cut off at approximately T + 153 seconds. The rates imparted to any of the vehicles by this transient required a maximum of 12 percent (AC-14) of the sustainer engine gimbal capability. The Atlas booster engines were jettisoned at about 3 seconds after booster engine cutoff. The rates imparted by this disturbance were nearly damped out by the time Centaur guidance was admitted.

During the Atlas booster phase of the flights, the Atlas flight control system provided the vehicle attitude reference. At approximately T + 161 seconds, the Centaur guidance

system provided the attitude reference. For AC-13, AC-14, and AC-15, a maximum of 38 percent (AC-15) of the total control capability was required to move the vehicles to the new references. The maximum vehicle rate transient during this change was a pitch rate of 3.88 degrees per second (peak to peak), with a duration of 15 seconds (AC-15). Insulation panels and nose fairings were jettisoned at average times of T + 197.7 and T + 227.5, respectively. The observed vehicle rate transients caused by these disturbances were damped within 8 seconds and required a maximum control capability of 13 percent (AC-13). Only small transients were observed at sustainer engine cutoff. Atlas-Centaur separation was smooth with transient rates of less than 1.1 degrees per second.

System description - Centaur. - The Centaur flight control system provides the primary means for vehicle stabilization and control, execution of guidance steering signals, and timed switching sequences for programmed flight events. A simplified block diagram of the Centaur flight control system is shown in figure VI-110.

The Centaur flight control system consists of the following major units:

(1) The rate gyro unit contains three single-degree-of-freedom, floated-gimbal, rate gyros with associated electronics for signal amplification. These gyros are mounted to the vehicle in an orthogonal triad configuration, the input axis of each gyro alined to its respective vehicle axis of pitch, yaw, or roll. Each gyro provides an electrical output signal proportional to the angular rate of rotation of the vehicle about the gyro input (reference) axis.

(2) The servoamplifier unit contains electronics to amplify, integrate, and algebraically sum engine position feedback signals with position and rate signals. The electrical outputs of this unit direct the hydraulic actuators, which in turn control the gimbaling of the engines. In addition, this unit contains the logic circuitry controlling the engines of the hydrogen peroxide attitude control system.

(3) The electromechanical timer unit contains a 400-hertz synchronous motor to provide the time reference. Two timer units, designated A and B, are needed because of the large number of discrete commands required for the parking orbit mission.

(4) The auxiliary electronics unit, which contains logic, relay switches, transistor power switches, power supplies, and an arm-safe switch. The arm-safe switch electrically isolates valves and pyrotechnic devices from control switches. The combination of the electromechanical timer units and the auxiliary electronics unit issues discretes to the following systems: other units of the flight control system and the propulsion, pneumatic, hydraulic, separation, propellant utilization, telemetry, spacecraft, and electrical systems.

Vehicle steering during Centaur powered flight is by thrust vector control, through gimbaling of the two main engines. There are two actuators for each engine to provide pitch, yaw, and roll control. Pitch control is accomplished by moving both engines to-

gether in the pitch plane. Yaw control is accomplished by moving both engines together in the yaw plane, and roll control is accomplished by moving the engines differentially in the yaw plane. Thus, the yaw actuator responds to an algebraically summed yaw-roll command. By controlling the direction of thrust of the main engines, the first control system maintains the flight of the vehicle on a trajectory directed by the guidance system. After main engine cutoff, control of the vehicle is maintained by the flight control system, using selected constant-thrust hydrogen peroxide engines. A more complete description of the engines and the propellant supply for the attitude control system is presented in the PROPULSION SYSTEMS section.

The logic circuitry which commands the 14 hydrogen peroxide engines, either on or off, is contained in the servoamplifier unit of the flight control system. Figure VI-111 shows the alphanumeric designations of the engines and their locations on the aft end of the vehicle. Algebraically summed position and rate signals are the inputs to the logic circuitry. The logic circuitry provides five modes of operation designated: all off, separate on, A and P separate on, V half on, and S half on. These modes of operation are used during different periods of the flight that are controlled by the timer unit. A summary of the modes of operation is presented in table VI-24. In this table, "threshold" designates the vehicle rate in degrees per second that has to be exceeded before the engines are commanded on.

System performance - Centaur. - The Centaur flight control system performances were satisfactory for AC-13, AC-14, and AC-15. Vehicle stabilization and control were maintained throughout the flights. All events sequenced by the timers were executed at the required time. The following evaluation is presented in paragraphs related to time-sequences portions of the flights. Except where otherwise noted, all numbers indicative of performance are the maximums seen in any of the three flights. For the typical time periods of guidance - flight control modes of operation and attitude control system modes of operation, refer to figure VI-106. Vehicle dynamics responses for selected flight events are tabulated in table VI-23.

Sustainer cutoff to main engine first cutoff: The Centaur A timers were started at sustainer engine cutoff by discrete commands from the Atlas programmers. Appropriate commands were issued to separate the Centaur stages from the Atlas stages and to initiate the main engine first firing sequences. There were no significant vehicle transients during separation for any of the flights. Disturbance torques were created prior to main engine start by boost pump exhaust and by chilldown flow through the main engines. Vehicle control was maintained by gimbaling the main engines. The maximum angular rate caused by main engine start transients was 3.23 degrees per second in pitch for AC-13. For AC-14 and AC-15, the vehicle transients during main engine start were small, indicating small differential impulses. When guidance steering was enabled, 4 seconds after main engine start, the maximum steering command for the three flights was 3^{o}

in pitch (AC-15). Vehicle transients resulting from guidance steering enabling and main engine start disturbances were damped out within 15 seconds in all three flights. Vehicle steady-state angular rates during the periods of closed-loop control were less than 0.5 degree per second. The angular rates imparted to the vehicles at main engine first cutoff were damped within 4 seconds. The maximum rate was measured in pitch and was 2.02 degrees per second.

Main engine first cutoff to main engine second prestart: At main engine first cutoff, the hydrogen peroxide attitude control systems were activated. During the coast period of the flights, the control requirements were well within the capabilities of the attitude control systems. Except for periods of noisy data, the rates were less than 0.5 degree per second.

Main engine second prestart to main engine second cutoff: The hydraulic recirculating pumps were activated 28 seconds prior to main engine second start, and the Centaur main engines were centered. The maximum angular rate observed at main engine second start was 2.72 degrees per second about the pitch axis (AC-13). Prestart and start operations resulted in a maximum vehicle attitude deviation of 2^{o} in pitch (AC-14) and 5^{o} in yaw (AC-15). These attitude errors were corrected when guidance steering was admitted approximately 4 seconds after main engine start. The control capability used to control these disturbances was a maximum of 28 percent (AC-15). Angular rates were low during the main engine second firing periods.

Main engine second cutoff to electrical power turnoff: At the time of Centaur main engine second cutoff, guidance-generated steering signals were temporarily discontinued. The hydrogen peroxide attitude control system quickly damped the low angular rates created by the main engine cutoff transients to within the 0.2-degree-per-second control threshold. The attitude control systems were deactivated for 5 seconds while the Surveyor spacecraft was separated from Centaur. The deactivation of the attitude control system during this time was to preclude a possibility of the Centaur interfering with the spacecraft during the separation phase. Angular rates prior to the retromaneuver did not exceed 0.60 degree per second. When the retromaneuver sequence was initiated, the Centaur was commanded to turn approximately 180^{o}. The attitude control systems were activated to turn the vehicle to the new steering vector. Approximately halfway (90^{o}) through the turnaround, the V engines were commanded to the V-half-on mode to provide 445 newtons (100 lbf) of thrust for 20 seconds. These maneuvers increased the lateral separations between Centaur and the spacecraft and minimized impingement of the residual propellants on the spacecraft during the subsequent periods of retrothrust. Guidance gimbal resolver data indicated that the AC-13 vehicle turned through an angle of 173^{o} in 110 seconds. The other vehicles turned through smaller angles. Following vehicle turnaround, the engine prestart valves were opened to allow the residual propellants to discharge through the main engines. Coincident with this propellant discharge, the

engine thrust chambers were gimbaled to aline the thrust vectors through the vehicle centers of gravity. Impulse from the propellant discharge provided adequate separation between Centaur and the Surveyor spacecraft. The minimum separation distance at the end of 5 hours was 1423 kilometers (AC-15). This was more than four times the separation distance required for a Surveyor mission.

TABLE VI-22. - DISCRETE COMMANDS; AC-13, AC-14, AND AC-15

Discrete command	Criteria for discrete to be issued	Discrete issued at this computed value			Actual time, T + sec			Predicted time, T + sec		
		AC-13	AC-14	AC-15	AC-13	AC-14	AC-15	AC-13	AC-14	AC-15
Booster engine cutoff	When square of vehicle thrust acceleration is greater than [a] $29.81(g's)^2$ $(5.46g's)^2$	$32.83(g's)^2$ $(5.73g's)^2$	$32.95(g's)^2$ $(5.74g's)^2$	$31.70(g's)^2$ $(5.6g's)^2$	153.2	153.2	152.4	153.5	153.6	153.4
Sustainer engine cutoff backup	When square of vehicle thrust acceleration is less than $0.53(g's)^2$	$0.12(g's)^2$	$0.34(g's)^2$	$0(g's)^2$	246.4	248.2	251.6	248.2	248.8	249.4
Centaur main engine first cutoff	When extrapolated orbital energy-to-be-gained is equal to zero	----------	----------	----------	587.0	581.2	593.2	579.9	577.3	580.5
Hydrogen peroxide settling engines cutoff	When time from main engine first cutoff discrete is greater than 74.45 sec	75.9	75.8	75.8	662.9	657	669	655.9	653.3	656.5
		Seconds after Centaur main engine first cutoff discrete								
B timer start (Centaur main engine second start sequence)	When sine of angle between position and target vectors is greater than 0.003052 (AC-13), 0.02406 (AC-14), and 0.02784 (AC-15)	0.00351	0.02523	0.02864	929.5	1293.2	1879.3	928.6	1292.2	1874.7
Centaur main engine second cutoff	When extrapolated orbital energy-to-be-gained is equal to zero	----------	----------	----------	1103.6	1468.6	2054.9	1099.8	1466.0	2048.1
Telemetry calibration on	When time from B timer start discrete is greater than 260.5 sec	261.3	260.5	260.6	1190.8	1553.7	2139.9	1189.9	1552.7	2135.3
		Seconds after B timer start discrete								
Telemetry calibration off	When time from B timer start discrete is greater than 264.5 sec	264.6	264.9	265.0	1194.1	1558.1	2144.3	1193.2	1557.1	2139.7
		Seconds after B timer start discrete								

[a] This value is lower than the vehicle thrust acceleration of 5.7±0.08g's required for issuing the discrete, to allow for time delays between the time when the computer determines the criteria are satisfied and the time when the discrete is actually issued.

TABLE VI-23. - VEHICLE DYNAMIC RESPONSE TO FLIGHT DISTURBANCES; AC-13, AC-14, AND AC-15

Event	Flight times[a], T + sec			Measurement	Rate gyro peak-to-peak amplitude, deg/sec			Transient frequency, Hz			Transient duration, sec			Required percent control capability		
	AC-13	AC-14	AC-15		AC-13	AC-14	AC-15	AC-13	AC-14	AC-15	AC-13	AC-14	AC-15	AC-13	AC-14	AC-15
Lift-off	0	0	0	Pitch	0.76	1.23	1.15	10	7.14	10	3.5	5.0	(b)	(c)	(c)	(c)
				Yaw	.84	.77	.75	10	6.67	7.7	3.5	8.0	(b)	(c)	(c)	(c)
				Roll	1.24	.77	.93	12.5	5.00	6.7	3.5	.4	(b)	(c)	(c)	(c)
42-Inch (1.1-m) rise	1	1	1	Pitch	1.7	2.52	2.75	10	6.67	10	2.5	4.0	1.5	3.3	9	4
				Yaw	.67	.06	.54	(b)	7.14	10	(b)	7.0	7.0	5	2	2
				Roll	1.0	1.81	2.11	17.3	7.14	1.43	(b)	6.0	.9	5	2	2
Maximum dynamic pressure	86	81	82-4	Pitch	1.36	1.30	1.15	0.25	0.24	0.50	4	26	15	26.5	20	30
	85	88	82-4	Yaw	1.09	1.12	1.32	.71	.50	.33	3	14	15	16.6	18	20
	84	76	82-4	Roll	1.25	1.54	1.06	1.0	.83	.72	5	Continues beyond max. g region	15	16.6	6	20
Booster engine cutoff	153.4	153.4	152.6	Pitch	2.98	2.52	1.88	5	4.55	1.25	3	3.0	2.0	8.3	10	8
				Yaw	1.67	2.10	2.03	10	5.0	5.0	1	3.0	3.0	10	12	2
				Roll	1.83	1.88	[d]0.99,1.52	1.33	.45	[d]10,0.55	3	2.5	1.5	10	10	2
Booster engine jettison	156.5	156.4	155.5	Pitch	1.7	1.36	2.02	1.25	0.72	1	4	4	5	(e)	(e)	(e)
	156.5	157.3	155.5	Pitch	-----	1.70	1.52	-----	10	5	-----	.9	5	(e)	(e)	(e)
	156.5	156.4	155.5	Yaw	2.92	2.52	2.98	10	.72	.91	5	4	5	(e)	(e)	(e)
	156.5	157.3	155.5	Yaw	-----	3.50	2.98	-----	25	6.7	-----	.9	5	(e)	(e)	(e)
	156.5	156.4	155.5	Roll	3.32	2.51	2.58	1.25	.67	.63	5	4	5	(e)	(e)	(e)
	156.5	157.3	155.5	Roll	3.82	1.47	2.04	50	25	25	Spike of negligable duration	.9	-----	(b)	18	(b)
Admit guidance	161.3	161.4	160.6	Pitch	3.57	1.09	3.88	0.16	0.22	0.18	7.5	17.5	15	37	12	38
				Yaw	1.0	3.21	3.79	.25	.14	.18	4	17.5	20	8.3	24	20
				Roll	.91	.70	.86	.91	1.25	.67	18	24.5	9	5	8	4
Insulation panel jettison	198	198	197.1	Pitch	2.73	3.94	2.58	50	25	40	0.7	2.0	0.8	13	8	6
				Yaw	1.17	1.68	[d]1.08,0.41	5	30	[d]40,5	7.0	1.8	5	8	6	10
				Roll	1.58	1.54	[d]0.79,2.54	12.5	4.43	[d]35,6.7	.7	2.4	[d]0.3,0.7	3	2	4

Nose fairing jettison	227.7	227.8	227.0	Pitch	4.42	4.09	$d_{4.74,2.16}$	25	25	$d_{30,0.67}$	2.0	3	$d_{2,6}$	15	4	10
				Yaw	1.0	2.10	1.76	33	25	40	1.2	3	2	8.3	6	12
				Roll	1.6	2.65	1.58	25	25	$d_{35,1.67}$	1.0	1	$d_{0.6,8}$	(b)	2	6
Sustainer engine cutoff	246.4	244.9	248.5	Pitch	Only	1.09	Only	(b)	20	(b)	(b)	2	(b)	(f)	(f)	(f)
				Yaw	Small	.63	Small	(b)	20	(b)	(b)	2	(b)	(f)	(f)	(f)
				Roll	Tran-	.84	Transient	(b)	.63	(b)	(b)	1.8	(b)	(f)	(f)	(f)
Atlas-Centaur separation	248.3	247.8	250.7	Pitch	Smooth	0.84	1.08	(b)	50	30	(b)	2.5	2.5	(f)	(f)	(f)
				Yaw	separ-	.56	.61	(b)	25	35	(b)	2.0	5	(f)	(f)	(f)
				Roll	ation	.42	.42	(b)	2.5	2.5	(b)	.2	.4	(f)	(f)	(f)
Main engine first start	257.8	258.7	262	Pitch	3.23	0.95	1.29	0.176	1.25	0.42	15	1.0	2.5	28	16	4
				Yaw	0.5 increase to 1.67	.49	.68	.173	.43	3.5	15	2.7	3	14	16	16
				Roll	2.16	2.23	1.95	1.1	.50	.55	4	4.0	3	14	16	16
Admit guidance	263	262.7	266	Pitch	0.85	1.36	2.01	0.176	0.20	0.33	11	10	10	12	20	16
				Yaw	1.67	1.61	.27	.173	.19	(b)	11	(b)	(b)	20	20	9
				Roll	(g)	(g)	.26	(g)	(g)	1	(g)	(g)	(b)	20	20	9
Main engine first cutoff	587	581.2	593.2	Pitch	3.74	4.64	$d_{4.74,3.16}$	33	33	$d_{35,6.7}$	4	2.5	2	12	16	16
				Yaw	3.01	3.92	3.12	50	33	35	3	2.2	2	20	24	28
				Roll	1.33	2.23	1.98	50	33	35	3	1.8	15	20	24	28
				Roll	-----	1.25	1.06	-----	.33	1.0	-----	1.8	15	-----	24	28
Main engine second start	990.9	1354.6	1940.5	Pitch	2.72	(h)	2.58	0.72	(h)	0.5	2.7	(h)	4	22	(h)	24
				Yaw	.84	(h)	1.15	.28	(h)	.5	2.7	(h)	4	22	(h)	24
				Roll	2.68	(h)	2.18	.56	(h)	.55	4.4	(h)	4	22	(h)	24
Admit guidance	993.7	1358.6	1944.5	Pitch	1.04	(h)	0.65	0.20	(h)	0.67	2.5	(h)	2.5	10	(h)	12
				Yaw	1.50	(h)	1.90	.22	(h)	.17	4	(h)	6.5	24	(h)	28
				Roll	(g)	(h)	.26	(g)	(h)	1.67	(g)	(h)	(g)	24	(h)	28
Main engine second cutoff	1103.9	1489.4	2055.0	Pitch	3.55	4.78	3.59	30	40	30	4	4.5	3	8	16	40
				Yaw	3.17	3.50	2.16	30	40	40	6	2.0	3	8	24	24
				Roll	1.41	2.23	2.38	40	$d_{40,0.45}$	14.3	11	1.3	1.2	8	24	24

[a] Initiation of disturbances as observed on rate gyro data.

[b] Data too small to be measured.

[c] Autopilot control not yet activated.

[d] Two disturbances were seen at the same time.

[e] Only verniers controlling in roll at this time.

[f] Control deactivated during this period.

[g] All that exists is damped rate from main engine start distrubance.

[h] No measurable data.

TABLE VI-24. - DESCRIPTION OF ATTITUDE CONTROL SYSTEM MODES OF OPERATIONS; AC-13, AC-14, AND AC-15

[V engines, 50 lb (222.4 N) thrust; S engines, 3.0 lb (13.3 N) thrust; A engines, 3.5 lb (15.6 N) thrust; P engines, 6.0 lb (26.7 N) thrust.]

Mode	Flight period	Description
All off	1. Powered phases 2. 5 sec during spacecraft separation sequence	This mode prevents the operation of all attitude control engines regardless of error signals.
Separate on	1. Main engine second cutoff until start of spacecraft separation sequence 2. End of lateral thrust during turnaround until end of retrothrust	When in the separate on mode, a maximum of two A and two V engines and one P engine fire. These engines fire only when appropriate error signals surpass their respective threshold. A engines: when 0.2 deg/sec threshold is exceeded, suitable A engines fire to control in yaw and roll. A_1A_4 and A_2A_3 combinations are inhibited. P engines: when 0.2 deg/sec threshold is exceeded, suitable P engine fires to control in pitch. P_1P_2 combination is inhibited. S engines: off V engines: when 0.3 deg/sec threshold is exceeded, suitable engines fire (as a backup for higher rates). V_1V_3 and V_2V_4 combinations are inhibited.
A and P separate on	End of spacecraft separation sequence until start of lateral thrust	This mode is the same as separate on mode, except V engines are inhibited.
V half on	1. Main engine first cutoff until main engine first cutoff plus 76 sec 2. Main engine second start minus 40 sec until main engine second start 3. During lateral thrust phase 4. Last 100 sec prior to Centaur power turnoff	A engines: when 0.2 deg/sec threshold is exceeded, suitable A engines fire to control in roll only. P engines: off S engines: off V engines: when there are no error signals, V_2V_4 combination fires continuously. This continuous firing serves various purposes: to settle propellants in flight periods 1 and 2, to provide lateral and added longitudinal separation between Centaur and spacecraft in flight period 3, and to deplete hydrogen peroxide supply in order to determine the amount of usable propellant remaining at end of mission in flight period 4. When 0.2 deg/sec threshold is exceeded, a minimum of two and a maximum of three V engines fire to control in pitch and yaw.
S half on	1. Main engine first cutoff plus 76 sec until main engine second start minus 40 sec	A engines: when 0.2 deg/sec threshold is exceeded, suitable A engines fire to control in roll only. P engines: off S engines: when there are no error signals, S_2S_4 combination fires continuously for propellant retention purposes. When 0.2 deg/sec threshold is exceeded, a minimum of two and a maximum of three S engines fire to control in pitch and yaw. V engines: when 0.3 deg/sec threshold is exceeded, a minimum of one and a maximum of two V engines fire to control in pitch and yaw. When a V engine fires, a corresponding S engine is commanded off.

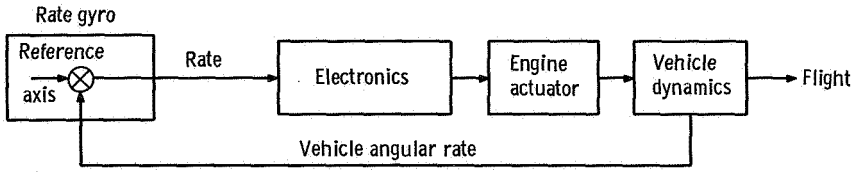

(a) Rate-stabilization-only mode.

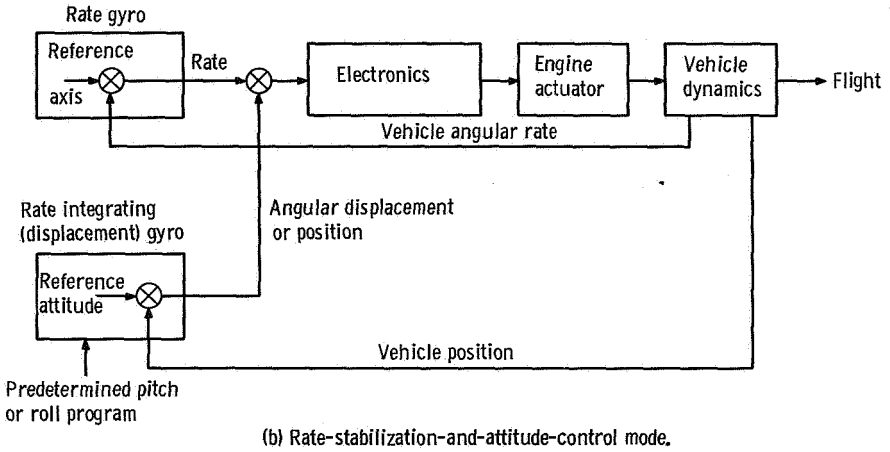

(b) Rate-stabilization-and-attitude-control mode.

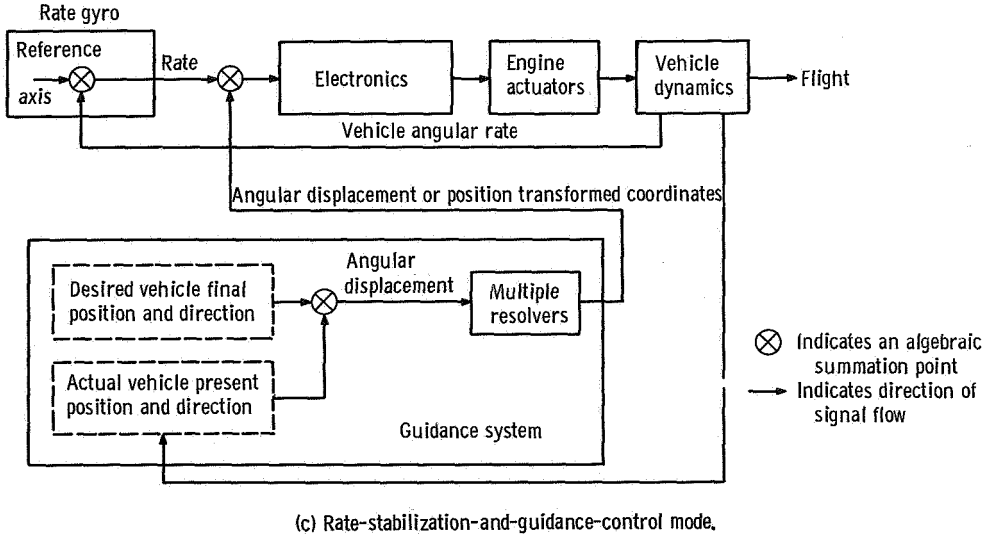

(c) Rate-stabilization-and-guidance-control mode.

Figure VI-105. - Block diagrams of guidance - flight control system operation; AC-13, AC-14, and AC-15.

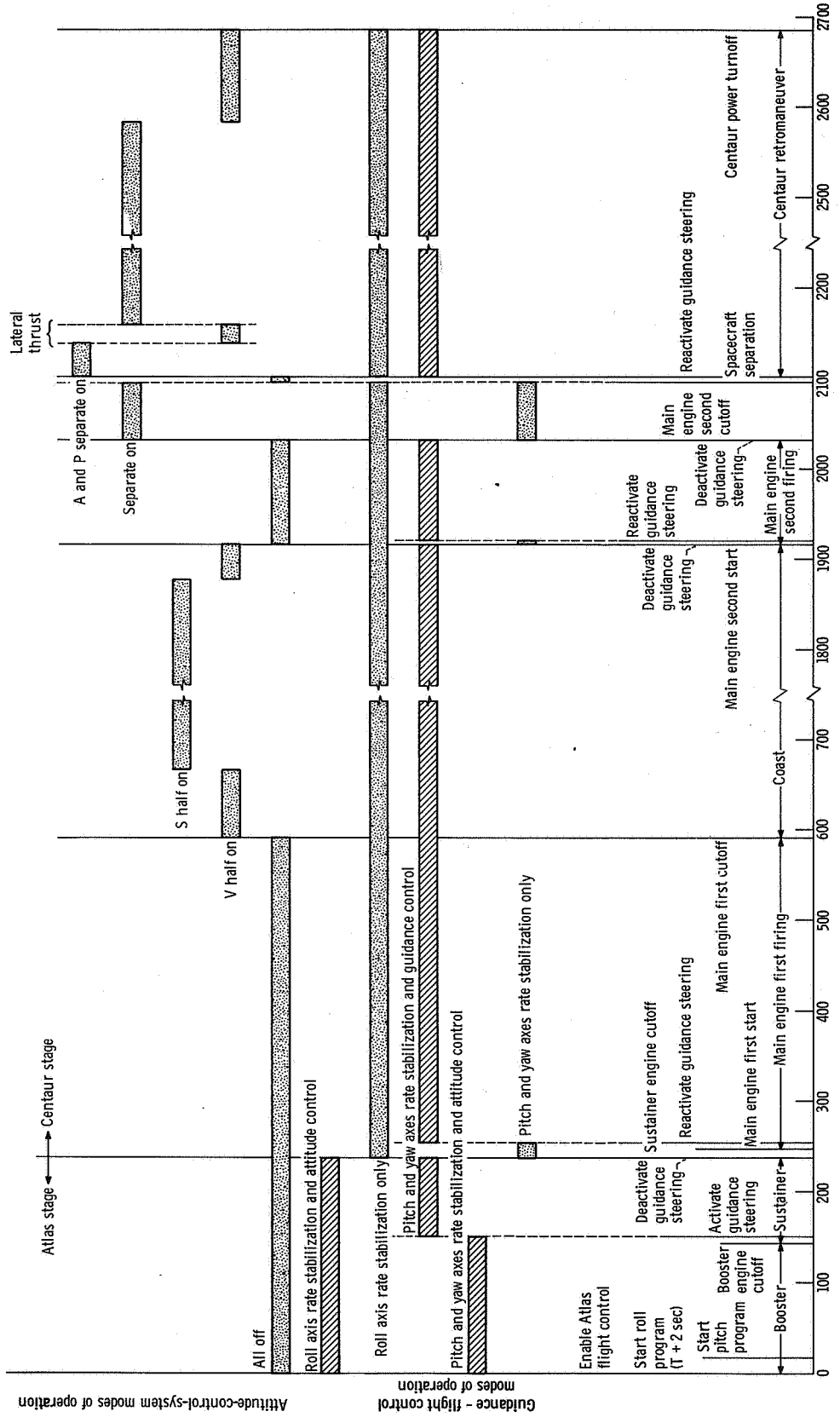

Figure VI-106. - Typical time periods of guidance - flight-control and attitude-control-system modes of operation, AC-13, AC-14, and AC-15. (There is no rate control during a 3.5-second period following sustainer engine cutoff because the engines are not developing thrust.)

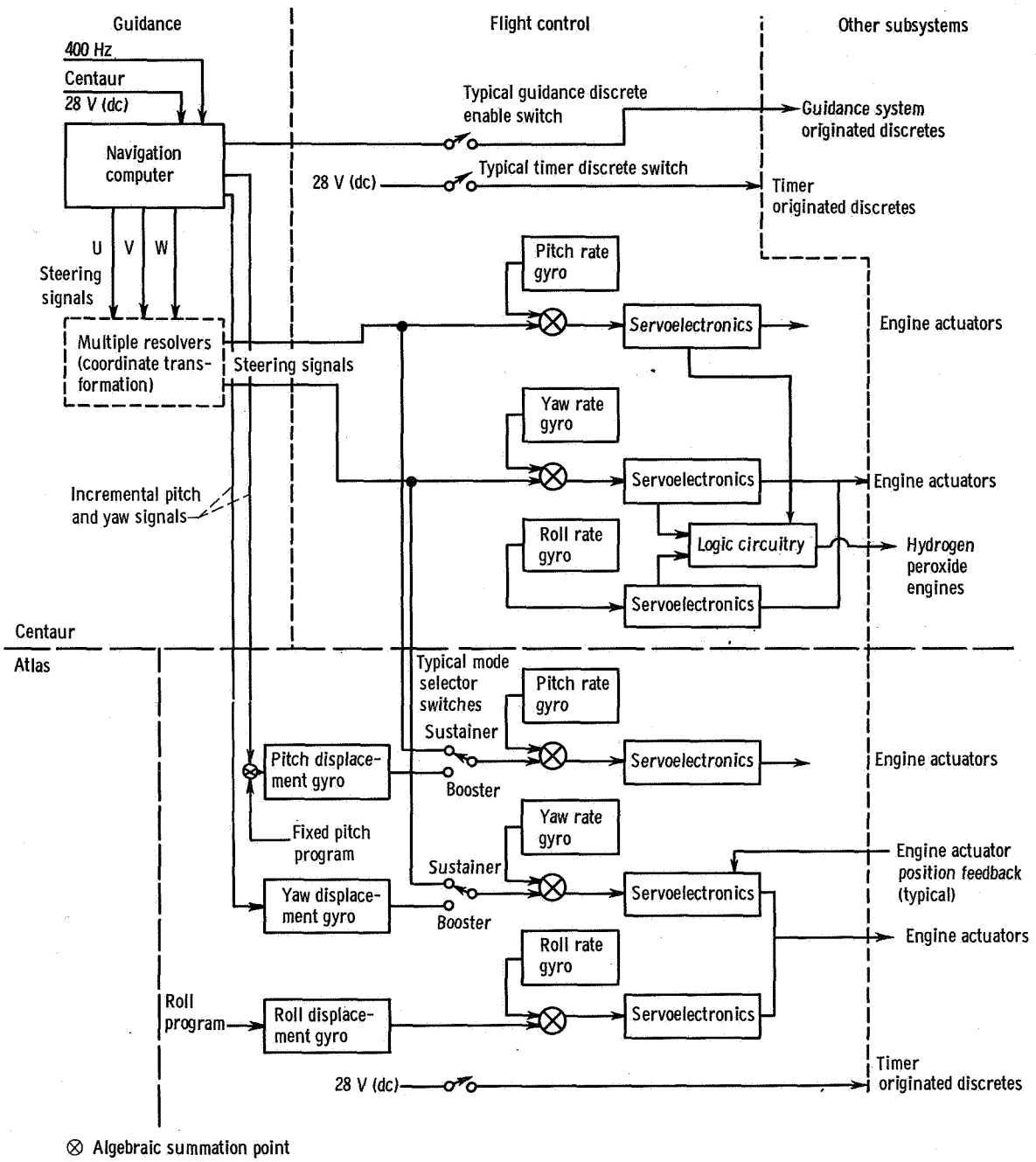

Figure VI-107. - Simplified guidance and flight control systems interface; AC-13, AC-14, and AC-15.

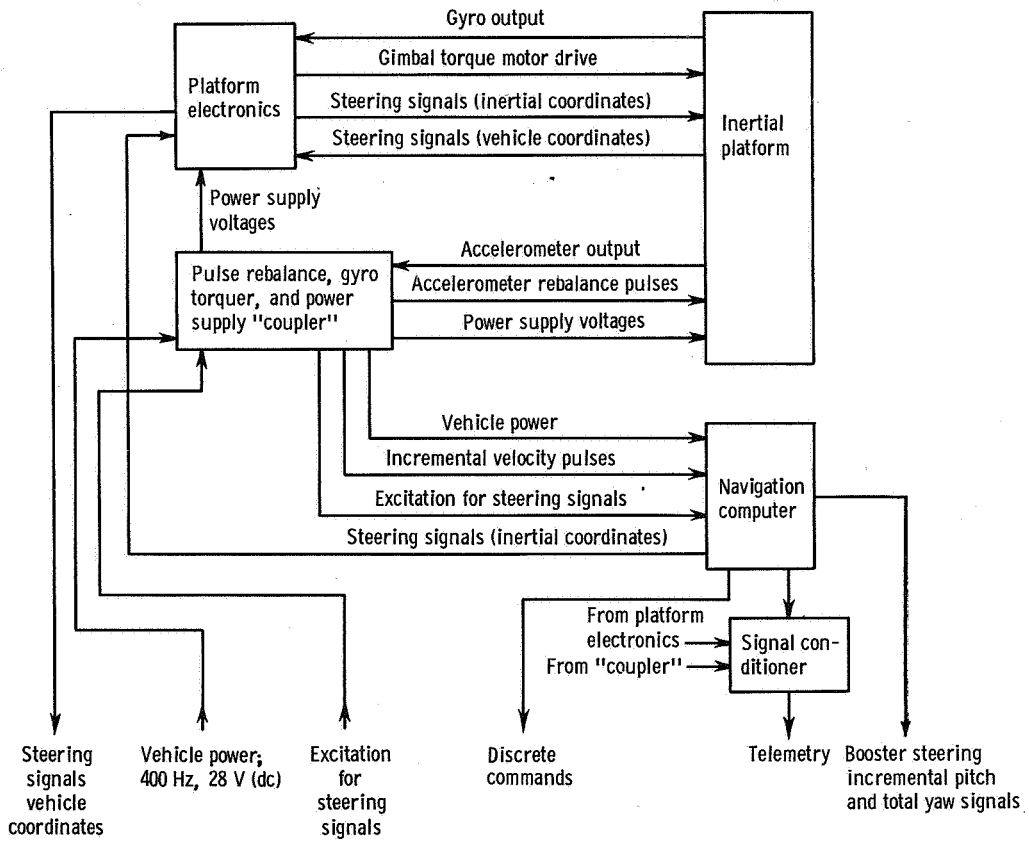

Figure VI-108. - Simplified block diagram of Centaur guidance system; AC-13, AC-14, and AC-15.

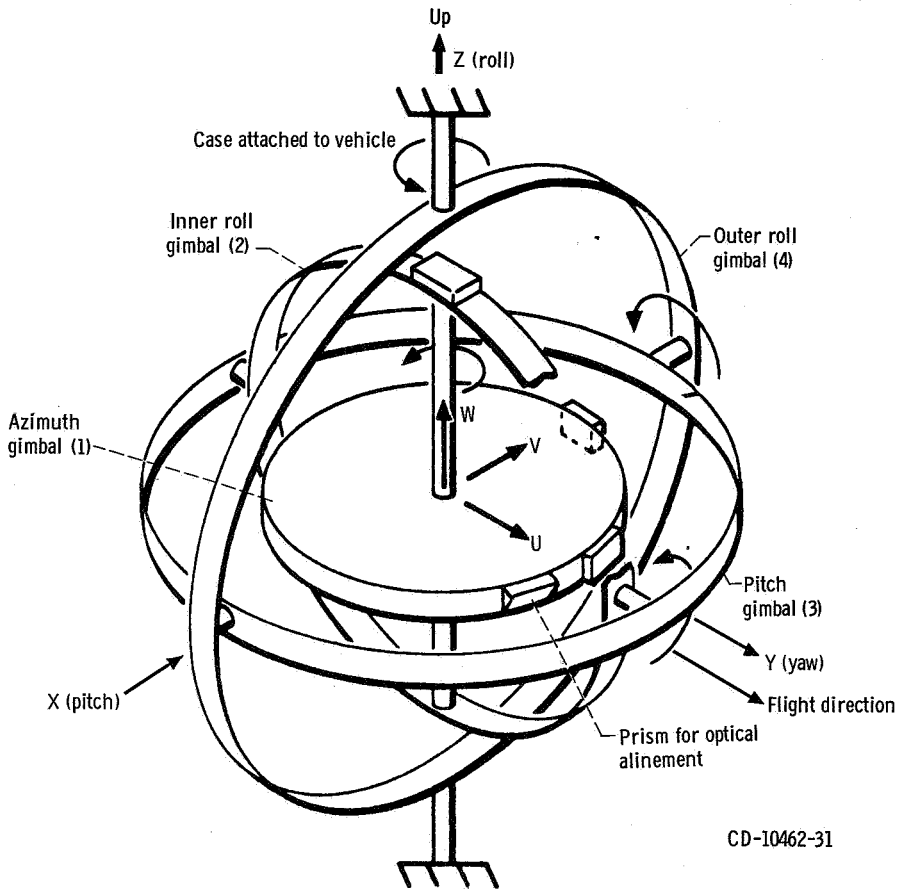

Figure VI-109. - Gimbal diagram. Launch orientation: inertial platform coordinates, U, V, and W; vehicle coordinates, X, Y, and Z; AC-13, AC-14, and AC-15.

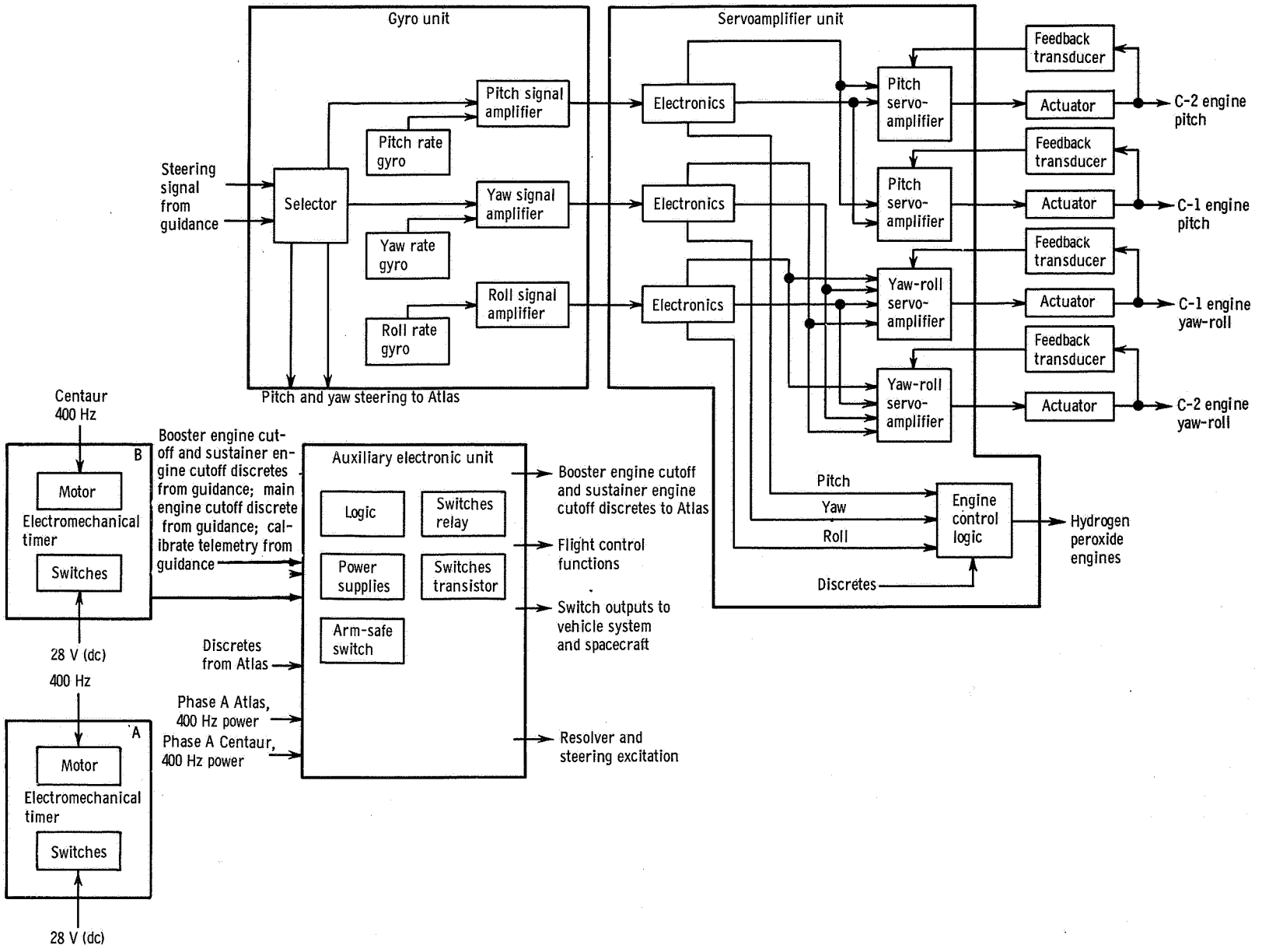

Figure VI-110. - Centaur flight control system; AC-13, AC-14, and AC-15.

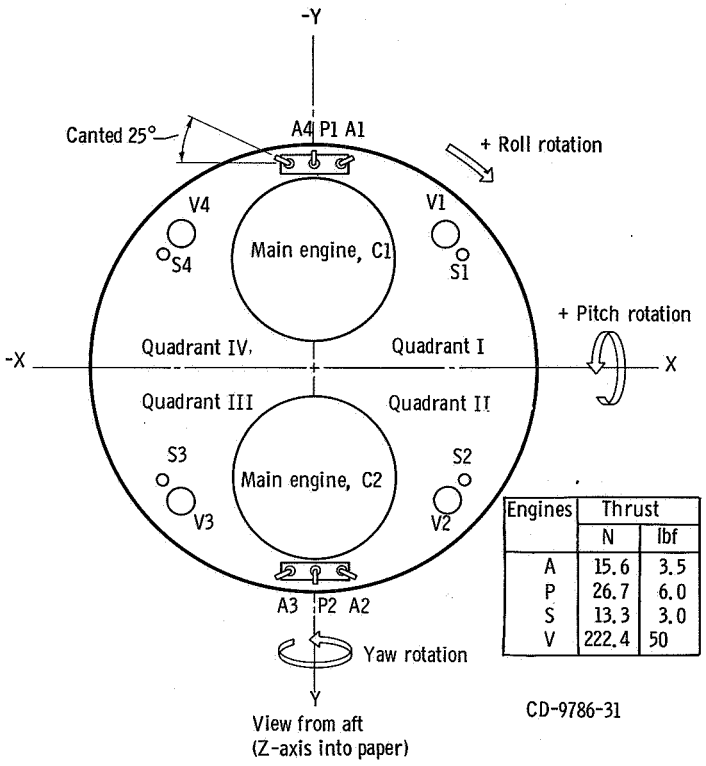

Engines	Thrust	
	N	lbf
A	15.6	3.5
P	26.7	6.0
S	13.3	3.0
V	222.4	50

Figure VI-111. - Attitude engines alphanumeric designations and locations; AC-13, AC-14, and AC-15. Signs of axes are convention for flight control system.

VII. CONCLUDING REMARKS

The AC-13, AC-14, and AC-15 launch vehicles were the last of a series of seven operational Atlas-Centaur vehicles for the Surveyor lunar landing program. The final launch (AC-15) with Surveyor VII took place on January 7, 1968. All seven launches were completely successful. Two spacecraft, Surveyor II (AC-7) and Surveyor IV (AC-11), failed to complete their missions. These failures were unrelated to the launch vehicle.

The new uprated SLV-3C Atlas booster used on AC-13, AC-14, and AC-15 flights did not cause any significant vibration changes in the spacecraft environment. For these three missions, the largest midcourse velocity correction (miss plus time of flight) that would have been required approximately 20 hours after injection for the spacecraft to impact the designed target was required by AC-14 and was 2.21 meters per second. (A midcourse velocity correction of 2.21 m/sec at approx. 20 hr after injection corresponds to 126 km on the lunar surface.)

The Centaur propulsion system performed satisfactorily on all flights. The AC-13 flight had the least propellant reserve of any of the three vehicles; if required, this reserve would have been sufficient to provide at least an additional 8.3 seconds of main engine firing.

On the AC-14 vehicle, a momentary cavitation of the oxidizer boost pump occurred at Centaur main engine second start. This cavitation probably resulted from insufficient pressurization of the oxidizer tank. A change was made on the AC-15 vehicle to increase the tank pressurization level just prior to main engine second start. No evidence of boost pump cavitation was observed on AC-15.

Lewis Research Center,
National Aeronautics and Space Administration,
Cleveland, Ohio, June 4, 1969,
491-05-00-03-22.

APPENDIX A

SUPPLEMENTAL FLIGHT, TRAJECTORY, AND PERFORMANCE DATA

by John J. Nieberding

Trajectory data for Atlas-Centaur (AC-13 and AC-14) launch vehicle flights are presented in tables A-1 to A-7 and figures A-1 to A-10. These data are not discussed and are presented for reference only.

Spacecraft Midcourse Velocity Correction

The midcourse velocity correction is a ground-commanded maneuver performed in flight by the spacecraft to ensure arrival at the desired target, at the desired time, and with the desired landing conditions. The following table summarizes the midcourse velocity corrections and landing parameters for Surveyors V, VI, and VII:

Surveyor	Time of correction, hr	Midcourse correction (miss only)		Midcourse correction (miss and time of flight)		Total midcourse correction		Final planned target coordinates, deg	Actual lunar touchdown coordinates, deg	Time of touchdown on lunar surface (GMT)
		m/sec	ft/sec	m/sec	ft/sec	m/sec	ft/sec			
V	T + 18	0.52	1.71	0.56	1.84	14.01	45.96	0.93 N 24.4 E	1.41 N 23.18 E	00:46:44.3 9/11/67
VI	T + 18.5	1.18	3.87	1.25	4.10	10.06	33.00	.42 N 1.13 W	.47 N 1.38 W	01:01:05.5 11/10/67
VII	T + 17	11.05	36.25	11.05	36.25	11.08	36.35	40.87 S 11.37 W	40.92 S 11.45 W	01:05:37.6 1/10/68

The second column gives the approximate time after lift-off at which the midcourse maneuver was performed. The third column gives the velocity correction required to hit the final target. Hence, it is called the miss-only correction. In order to ensure the proper arrival time as well as arrival at the final target, additional correction, known as the miss-plus-time-of-flight correction, is required. This velocity correction is given in column 4. In addition to arriving at the desired target at the desired time, it is usually necessary to optimize the spacecraft unbraked impact speed prior to firing the Surveyor braking motor and to optimize spacecraft propellant weight at retromotor burn-

out. These optimizations require additional midcourse velocity correction. The total correction performed to arrive at the final target (column 6) at the correct time with optimized spacecraft conditions is given in column 5. The actual touchdown locations and touchdown times are included in columns 7 and 8, respectively.

The miss-only and miss-plus-time-of-flight corrections quoted above are not to be confused with the miss-only and miss-plus-time-of-flight corrections used to evaluate the accuracy with which the Centaur injected the spacecraft into the trajectory designed prior to launch. Prior to launch, a particular target and associated arrival time are selected. The spacecraft trajectory is then designed to meet these target conditions. Centaur injection accuracy is then measured by the amount of the miss-only and miss-plus-time-of-flight corrections required by the spacecraft to achieve these prelaunch conditions. In reality, after launch, a new, more favorable target was usually selected. This new target is the target quoted in column 6. The midcourse corrections relating to this new target are those quoted in the table. The correction required to achieve the prelaunch target conditions and, hence, those used to evaluate Centaur injection accuracy are quoted in the GUIDANCE AND FLIGHT CONTROL SYSTEMS section.

Countdown History

AC-13

The AC-13 countdown on September 8, 1967 was smooth and trouble-free until the programmed hold at T - 5 minutes. The hold was extended an additional 18 minutes to allow investigation of a low pressure indication on the system which stabilizes the vehicle in the launcher. Analysis indicated that the system was satisfactory. The count was resumed and proceeded to lift-off without difficulty.

AC-14

Lift-off of AC-14 occurred on November 7, 1967, 1.075 seconds after the planned lift-off time of 0239 eastern standard time. The opening of the launch window was revised from 0222 to 0239 eastern standard time after the start of the countdown to improve downrange data coverage. This was accomplished by extending the T - 5 hold by 17 minutes.

AC-15

The AC-15 countdown on January 7, 1968 was trouble-free. The planned 60-minute hold at T - 90 minutes was extended 35 minutes to ensure optimum tracking coverage.

TABLE A-1. - CENTAUR PARKING ORBIT PARAMETERS, AC-13 AND AC-14

Parameter[a]	Units	Flight value for -	
		AC-13	AC-14
Time from 2-inch motion	sec	669.9	671.7
Epoch (GMT)	hr	0808:10.9 (Sept. 8, 1967)	0750:12.8 (Nov. 7, 1967)
Apogee altitude	km	164.3	168.5
	n. mi.	89.0	91.0
Perigee altitude	km	157.4	159.3
	n. mi.	85.0	86.0
Injection energy, C_3	km^2/sec^2	-60.89	-60.96
	ft^2/sec^2	-65.541×10^7	-65.62×10^7
Semimajor axis	km	6545	6539
	n. mi.	3534	3531
Eccentricity	------	0.00197	0.00065
Orbital inclination	deg	29.833	28.982
Period	min	87.89	87.71
Inertial velocity at Centaur main engine first cutoff	m/sec	7753.33	7863.03
	ft/sec	25 437.43	25 797.33
Earth relative velocity at Centaur main engine first cutoff	m/sec	7354.80	7171.24
	ft/sec	24 129.91	23 526.98
Geocentric latitude at Centaur main engine first cutoff	deg, North	29.813	28.676
Longitude at Centaur main engine first cutoff	deg, West	59.671	59.514

[a]Based on tracking data.

TABLE A-2. - SURVEYOR ORBIT PARAMETERS, AC-13 AND AC-14

Parameter	Units	Flight value for -	
		AC-13	AC-14
Time from 2-inch motion	sec	1104.0	1470.0
Epoch (GMT)	hr	0815:24.95 (Sept. 8, 1967)	0803:31.1 (Nov. 7, 1967)
Apogee altitude	km	549 654	684 614
	n. mi.	296 789	369 662
Perigee altitude	km	166.7	168.5
	n. mi.	90.0	91.0
Injection energy, C_3	km^2/sec^2	-1.417	-1.1428
	ft^2/sec^2	-1.525×10^7	-1.23×10^7
Semimajor axis	km	281 289	348 769
	n. mi.	151 884	188 320
Eccentricity		0.97673	0.98123
Orbital inclination	deg	29.840	29.003
Injection (spacecraft separate) true anomaly	deg	10.54	10.85
Injection (spacecraft separate) flight path angle	deg	5.41	5.59
Period	days	17.17	23.72
Longitude of ascending node	deg	316.13	4.285
Argument of perigee	deg	124.20	154.91

TABLE A-3. - CENTAUR POSTRETROMANEUVER ORBITAL PARAMETERS, AC-13 AND AC-14

Parameter	Units	Flight value for -	
		AC-13	AC-14
Time from 2-inch motion	sec	3736.9	2644.8
Epoch (GMT)	hr	0859:17.9 (Sept. 8, 1967)	0823:05.9 (Nov. 7, 1967)
Apogee altitude	km	346 337	401 708
	n. mi.	187 007	216 905
Perigee altitude	km	168.5	168.5
	n. mi.	91.0	91.0
Injection energy, C_3	km^2/sec^2	-2.21	-1.92
	ft^2/sec^2	-2.3788×10^7	-2.06667×10^7
Semimajor axis	km	179 631	207 317
	n. mi.	96 993	111 942
Eccentricity		0.96355	0.96842
Orbital inclination	deg	29.873	28.979
Period	days	8.77	10.87

TABLE A-4. - CENTAUR POSTFLIGHT VEHICLE WEIGHT SUMMARY, AC-13 AND AC-14

Item	Weight			
	AC-13		AC-14	
	lbm	kg	lbm	kg
Basic hardware:				
Body	963	437	941	427
Propulsion group	1 224	555	1 223	555
Guidance group	329	149	333	151
Control group	151	68	152	69
Pressurization group	187	85	187	85
Electrical group	287	130	283	128
Separation group	80	36	79	36
Flight instrumentation	251	114	255	116
Miscellaneous equipment	141	64	143	65
Total	3 613	1 638	3 596	1 632
Jettisonable hardware:				
Nose fairing	2 075	941	2 067	938
Insulation panels	1 211	549	1 223	555
Ablated ice	62	28	50	23
Total	3 348	1 518	3 340	1 516
Centaur residuals:				
Liquid hydrogen	201	91	235	107
Liquid oxygen	722	327	843	382
Gaseous hydrogen	75	34	65	29
Gaseous oxygen	173	78	170	77
Hydrogen peroxide	77	35	65	29
Helium	4	2	5	2
Ice	12	5	12	5
Total	1 264	572	1 395	631

Item	Weight			
	AC-13		AC-14	
	lbm	kg	lbm	kg
Centaur expendables:				
Main impulse hydrogen	4 805	2 180	4 780	2 168
Main impulse oxygen	24 294	11 020	24 201	10 077
Gas boiloff on ground, hydrogen	14	6	16	7
Gas boiloff on ground, oxygen	17	8	0	0
In-flight chill hydrogen	71	32	71	32
In-flight chill oxygen	102	46	102	46
Booster phase vent, hydrogen	53	24	53	24
Booster phase vent, oxygen	66	30	66	30
Sustainer phase vent, hydrogen	30	14	30	14
Sustainer phase vent, oxygen	60	27	60	27
Engine shutdown loss, hydrogen				
First shutdown loss	6	3	6	3
Second shytdown loss	6	3	6	3
Engine shutdown loss, oxygen				
First shutdown loss	18	8	18	8
Second shutdown loss	18	8	18	8
Parking orbit vent, hydrogen	6	3	8	4
Parking orbit vent, oxygen	0	0	0	0
Parking orbit leakage, hydrogen	0	0	1	1
Parking orbit leakage, oxygen	1	1	2	1
Hydrogen peroxide	159	72	171	78
Helium	10	5	6	3
Total	29 753	13 497	29 615	13 434
Total tanked weight	37 978	17 225	37 946	17 213
Minus ground vent	31	14	16	7
Total Centaur weight at lift-off	37 947	17 211	37 930	17 206

TABLE A-5. - ATLAS POSTFLIGHT VEHICLE WEIGHT SUMMARY,

AC-13 AND AC-14

Item	Weight			
	AC-13		AC-14	
	lbm	kg	lbm	kg
Booster jettison weight:				
Booster dry weight	6 380	2 894	6 324	2 869
Oxygen residual	554	251	554	251
Fuel (RP-1) residual	487	221	487	221
Unburned lubrication oil	22	10	21	9
Total	7 443	3 376	7 386	3 350
Sustainer jettison weight:				
Sustainer dry weight	6 060	2 749	6 112	2 772
Oxygen residual	315	143	609	276
Fuel (RP-1) residual	355	161	236	107
Interstage adapter	1 046	474	1 032	468
Unburned lubrication oil	16	7	15	7
Total	7 792	3 534	8 004	3 630
Flight expendables:				
Main impulse fuel (RP-1)	83 029	37 661	83 381	37 821
Main impulse oxygen	185 301	84 051	185 279	84 041
Helium-panel purge	5	2	5	2
Oxygen vent loss	15	7	15	7
Lubrication oil	200	91	201	91
Total	268 550	121 812	268 881	121 962
Ground expendables:				
Fuel (RP-1)	529	240	496	225
Oxygen	1 665	755	1 593	723
Lubrication oil	3	1	4	2
Exterior ice	54	24	24	24
Liquid nitrogen in helium shrouds	250	113	250	113
Pre-ignition gaseous oxygen loss	450	204	450	204
Total	2 951	1 337	2 847	1 291
Total Atlas tanked weight	286 736	130 061	287 118	130 235
Minus ground run	2 951	1 337	2 847	1 291
Total Atlas weight at lift-off	283 785	128 722	284 271	128 944
Spacecraft	2 217	1 006	2 219	1 007
Total Atlas-Centaur-spacecraft lift-off weight	323 949	146 941	324 420	147 157

TABLE A-6. - FLIGHT EVENTS RECORD, AC-13

Event	Programmer time, sec	Preflight time, sec	Actual time, sec	Event	Programmer time, sec	Preflight time, sec	Actual time, sec
Lift-off (2-in. motion	T + 0.0	T + 0.0	T + 0.0	Start Centaur boost pumps	MES-2 - 28	T + 958.9	T + 961.5
Start roll	T + 2.0	T + 2.0	T + 2.0	Centaur main engine second start (MES-2)	MES-2	T + 986.9	T + 989.5
End roll	T + 15.0	T + 15.0	T + 15.0				
Start pitchover	T + 15.0	T + 15.0	T + 15.0	Stop propellant settling engines	MES-2	T + 986.9	T + 989.5
Booster engine cutoff (BECO)	BECO	T + 153.5	T + 153.2				
Jettison booster engines	BECO + 3.1	T + 156.6	T + 156.3	Centaur main engine second cutoff	MECO-2	T + 1099.8	T + 1103.6
Jettison insulation panels	BECO + 45	T + 198.5	T + 198.0				
Start Centaur boost pumps	BECO + 62	T + 215.5	T + 215.0	Preseparation arming signal; extend landing gear signal	MES-2 + 134	T + 1120.9	T + 1123.6
Jettison nose fairing	BECO + 75	T + 228.5	T + 228.2				
Sustainer engine cutoff (SECO); vernier engine cutoff; start Centaur programmer	SECO	T + 248.2	T + 246.3	Unlock omnidirectional antennas on signal	MES-2 + 144.5	T + 1131.4	T + 1133.8
				High power transmitter on signal	MES-2 + 165	T + 1151.9	T + 1154.0
Atlas-Centaur separation	SECO + 1.9	T + 250.1	T + 248.2				
Centaur main engine first start (MES-1)	SECO + 11.5	T + 259.7	T + 257.8	Spacecraft separate	MES-2 + 176.0	T + 1162.9	T + 1165.5
				Start turnaround	MES-2 + 181.0	T + 1167.9	T + 1170.5
Centaur main engine first cutoff (MECO-1)	MECO-1	T + 579.9	T + 587.0	Start propellant settling engines	MES-2 + 221.0	T + 1207.9	T + 1210.5
Start propellant settling engines	MECO-1	T + 579.9	T + 587.0	Stop propellant settling engines	MES-2 + 241.0	T + 1227.9	T + 1230.5
Stop propellant settling engines; start propellant retention engines	MECO-1 + 76	T + 655.9	T + 662.9	Start discharge of Centaur residual propellants	MES-2 + 416.0	T + 1402.9	T + 1405.5
				End discharge of Centaur residual propellants; start propellant settling engines[a]	MES-2 + 666	T + 1652.9	T + 1655.5
Stop propellant retention engines; start propellant settling engines	MES-2 - 40	T + 946.9	T + 949.5				
				Energize power changeover	MES-2 + 766	T + 1752.9	T + 1755.5

[a]Postmission hydrogen peroxide depletion experiment.

TABLE A-7. - FLIGHT EVENTS RECORD, AC-14

Event	Programmer time, sec	Preflight time, sec	Actual time, sec
Lift-off (2-in. motion)	T + 0.0	T + 0.0	T + 0.0
Start roll	T + 2.0	T + 2.0	T + 2.0
End roll	T + 15.0	T + 15.0	T + 15.0
Start pitchover	T + 15.0	T + 15.0	T + 15.0
Booster engine cutoff (BECO)	BECO	T + 153.6	T + 153.2
Jettison booster engines	BECO + 3.1	T + 156.7	T + 156.3
Jettison insulation panels	BECO + 45	T + 198.6	T + 198.0
Start Centaur boost pumps	BECO + 62	T + 215.6	T + 215.4
Jettison nose fairing	BECO + 75	T + 228.6	T + 228.1
Sustainer engine cutoff (SECO); vernier engine cutoff; start Centaur programmer	SECO	T + 248.8	T + 245.8
Atlas-Centaur separation	SECO + 1.9	T + 250.7	T + 247.7
Centaur main engine first start (MES-1)	SECO + 11.5	T + 260.3	T + 257.3
Centaur main engine first cutoff (MECO-1)	MECO-1	T + 577.3	T + 581.2
Start propellant settling engines	MECO 1	T + 577.3	T + 581.2
Stop propellant settling engines; start propellant retention engines	MECO 1 + 76	T + 653.3	T + 657.0
Stop propellant retention engines; start propellant settling engines	MES-2 - 40	T + 1312.9	T + 1312.9
Start Centaur boost pumps	MES-2 - 28	T + 1324.9	T + 1324.9
Centaur main engine second start (MES-2)	MES-2	T + 1352.9	T + 1352.9
Stop propellant settling engines	MES-2	T + 1352.9	T + 1352.9
Centaur main engine second cutoff	MECO-2	T + 1466.0	T + 1468.6
Preseparation arming signal; extend landing gear signal	MES-2 + 134	T + 1486.9	T + 1486.9
Unlock omnidirectional antennas on signal	MES-2 + 144.5	T + 1497.4	T + 1497.4
High power transmitter on signal	MES-2 + 165	T + 1517.9	T + 1517.9
Spacecraft separate	MES-2 + 176.9	T + 1528.9	T + 1528.9
Start turnaround	MES 2 + 181.0	T + 1533.9	T + 1533.9
Start propellant settling engines	MES 2 + 221.0	T + 1573.9	T + 1573.9
Stop propellant settling engines	MES-2 + 241.0	T + 1593.9	T + 1593.9
Start discharge of Centaur residual propellants	MES-2 + 416	T + 1768.9	T + 1768.9
End discharge of Centaur residual propellants; start propellant settling engines[a]	MES-2 + 666	T + 2018.9	T + 2018.9
Energize power changeover	MES-2 - 766	T + 2118.9	T + 2118.9

[a]Postmission hydrogen peroxide depletion experiment.

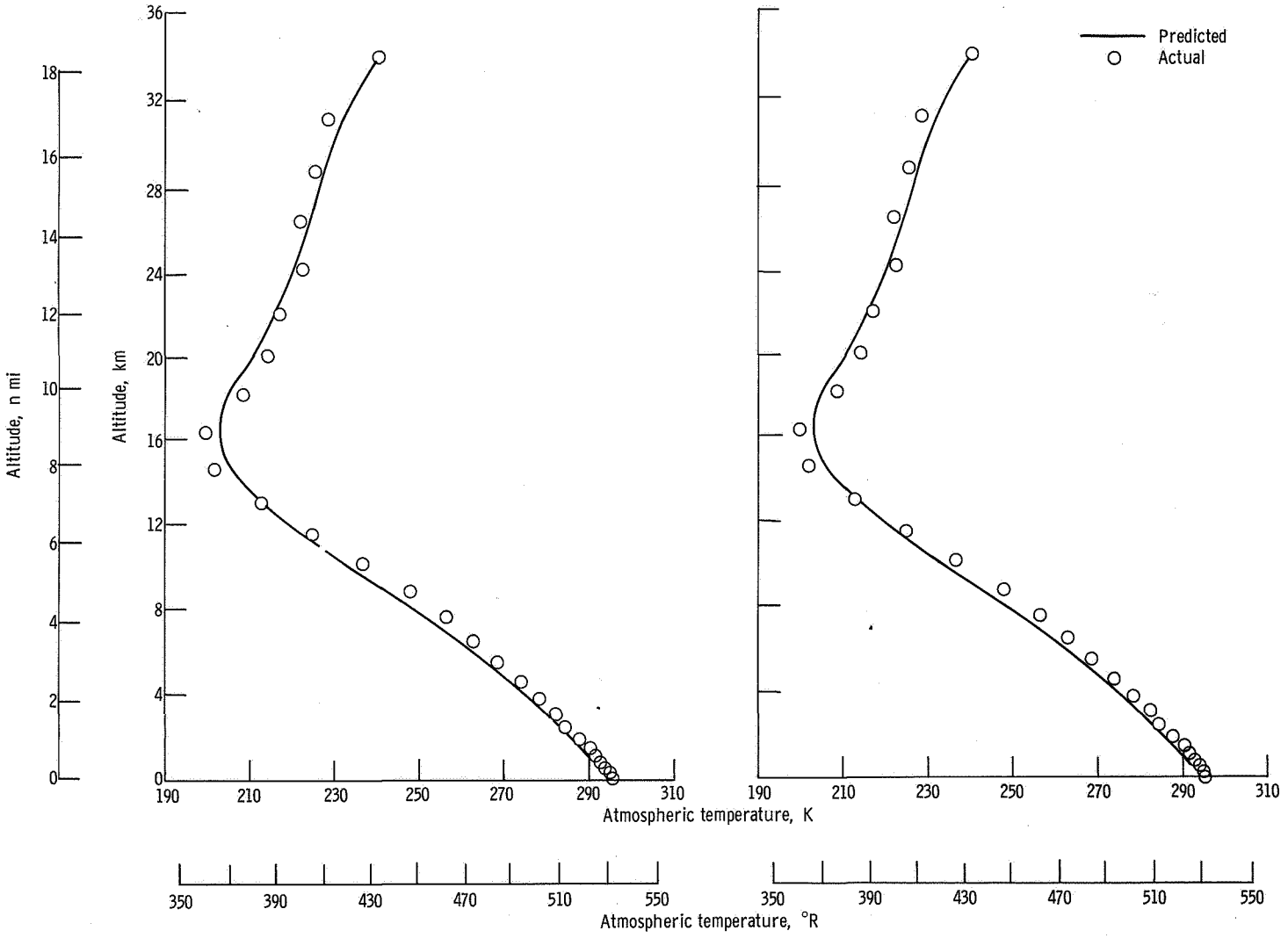

Figure A-1. - Altitude as function of temperature.

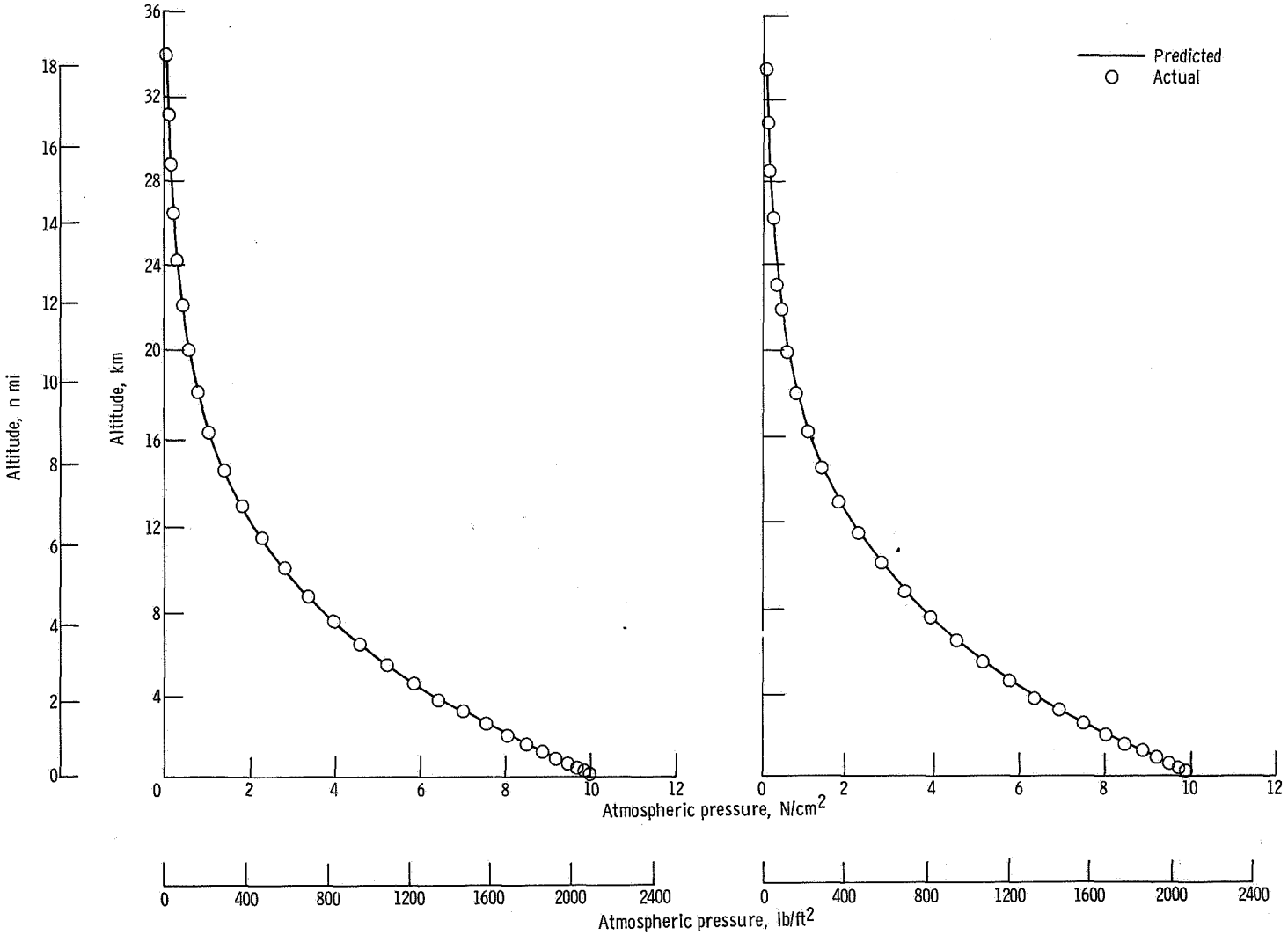

Figure A-2. - Altitude as function of pressure.

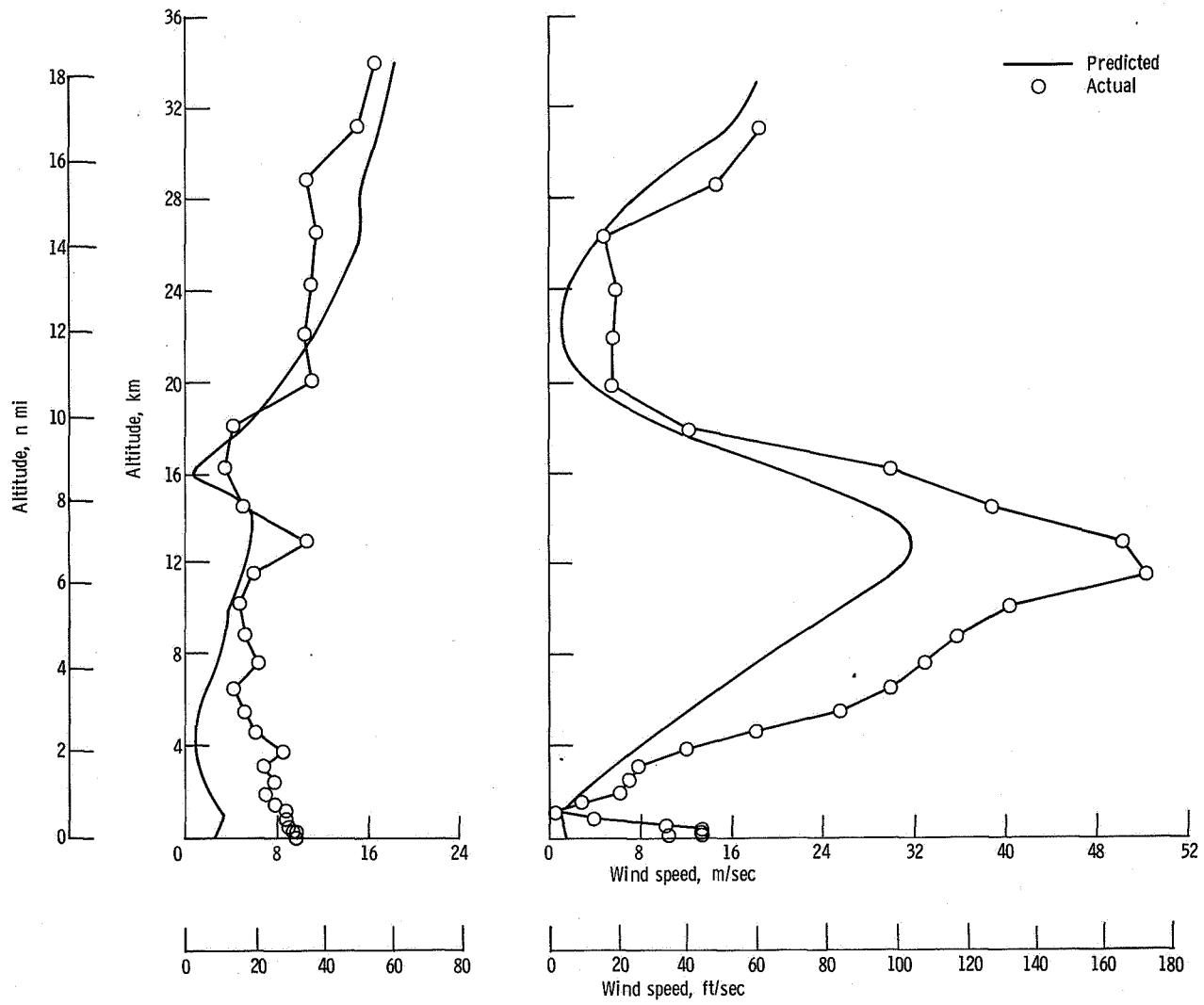

(a) AC-13.

(b) AC-14.

Figure A-3. - Altitude as function of wind speed.

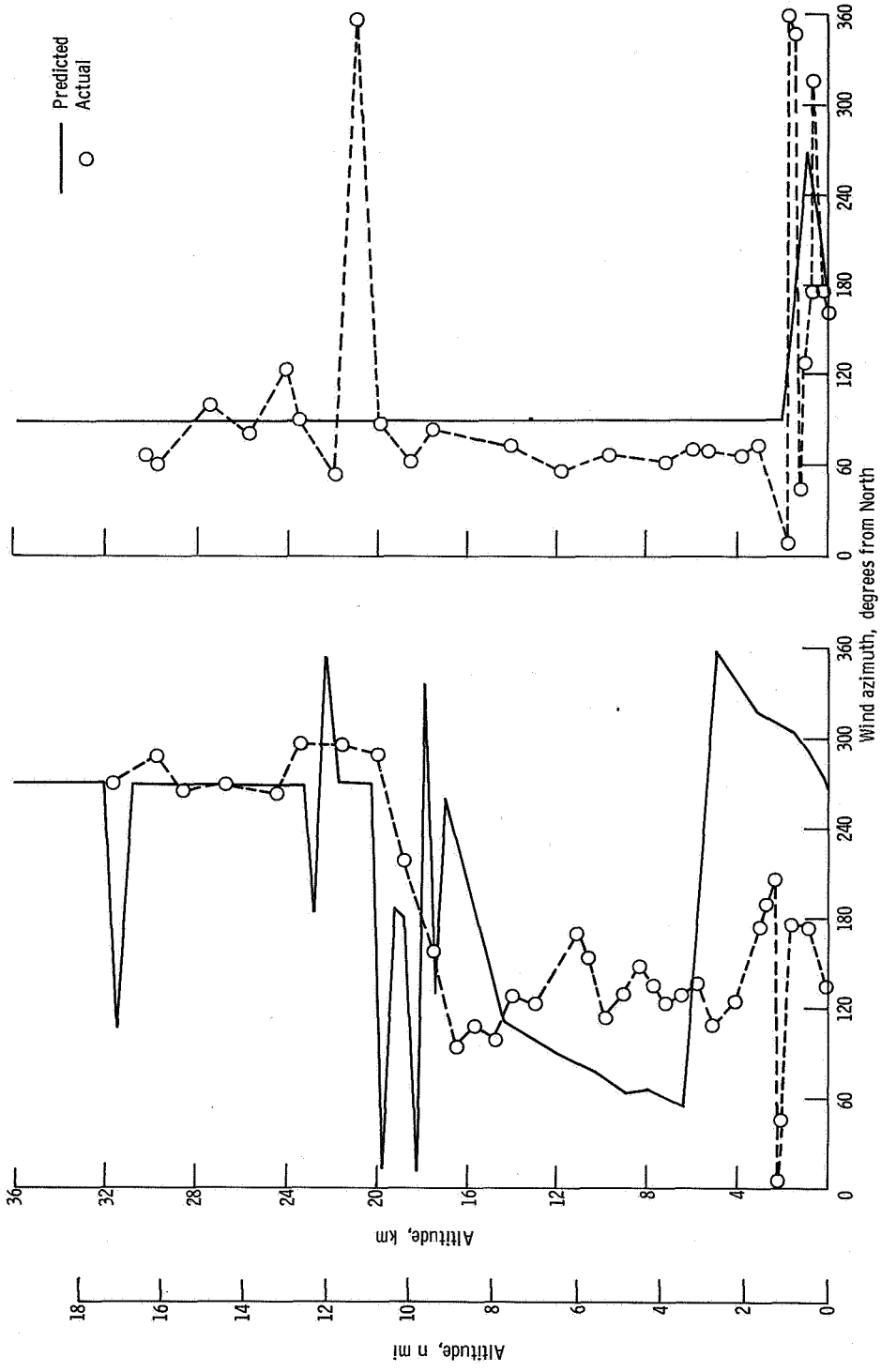

(a) AC-13.

(b) AC-14.

Figure A-4. - Altitude as function of wind azimuth.

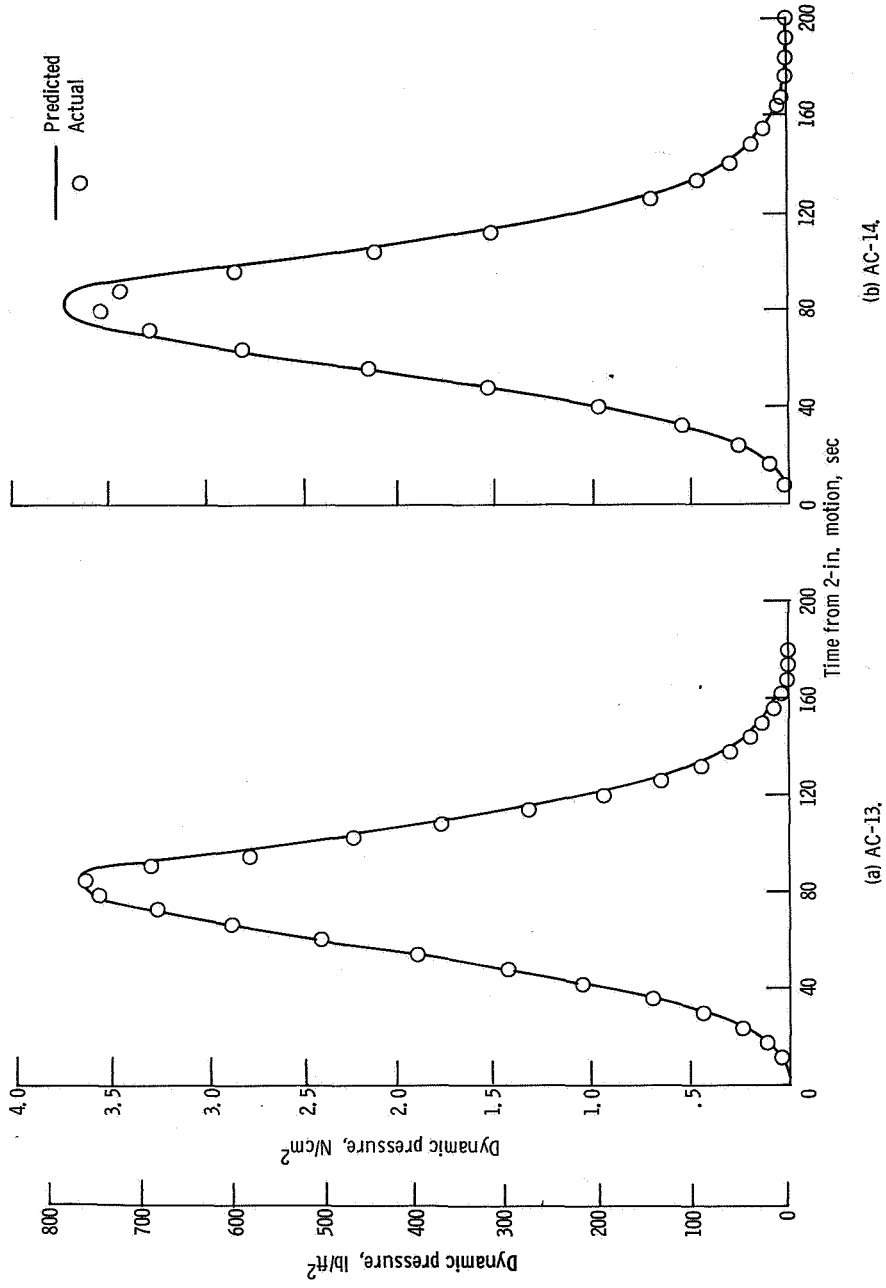

Figure A-5. - Dynamic pressure as function of time.

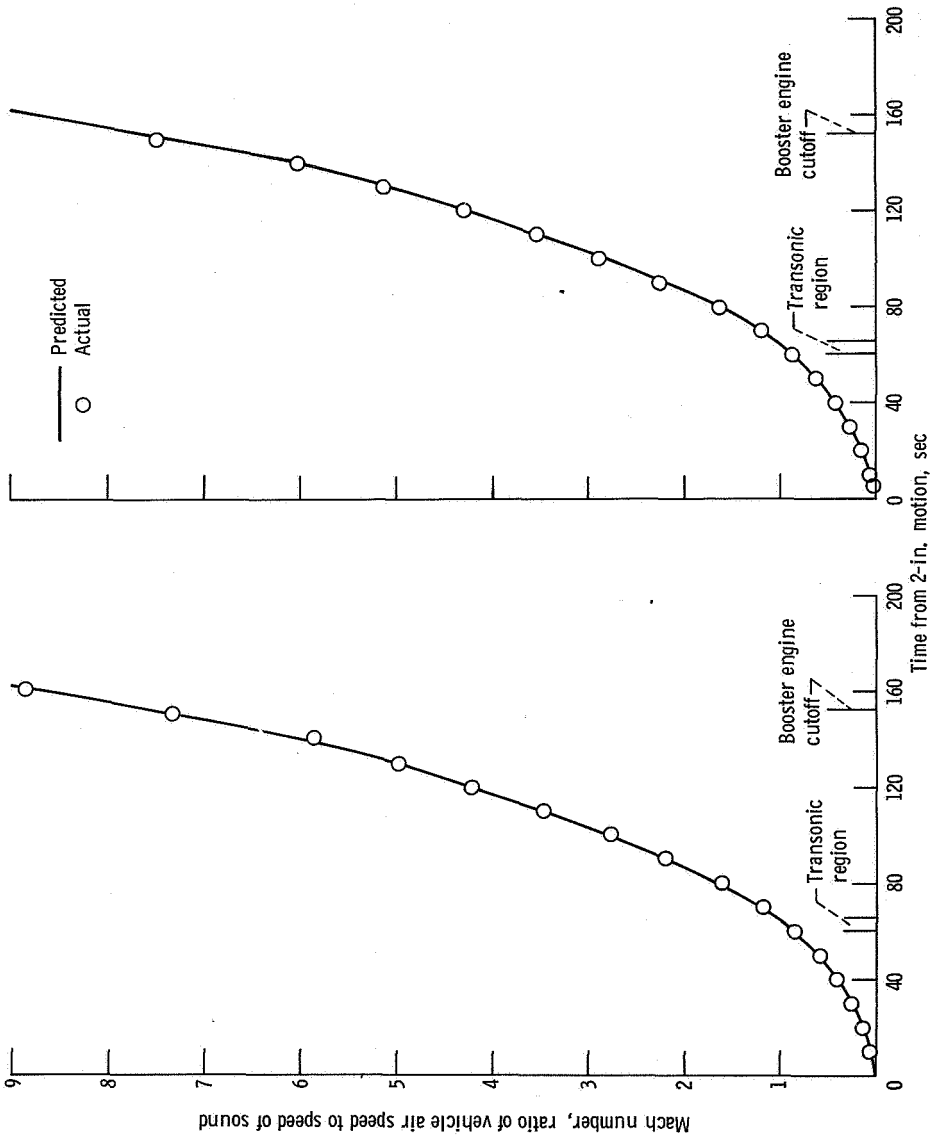

Figure A-6. - Mach number as function of time.

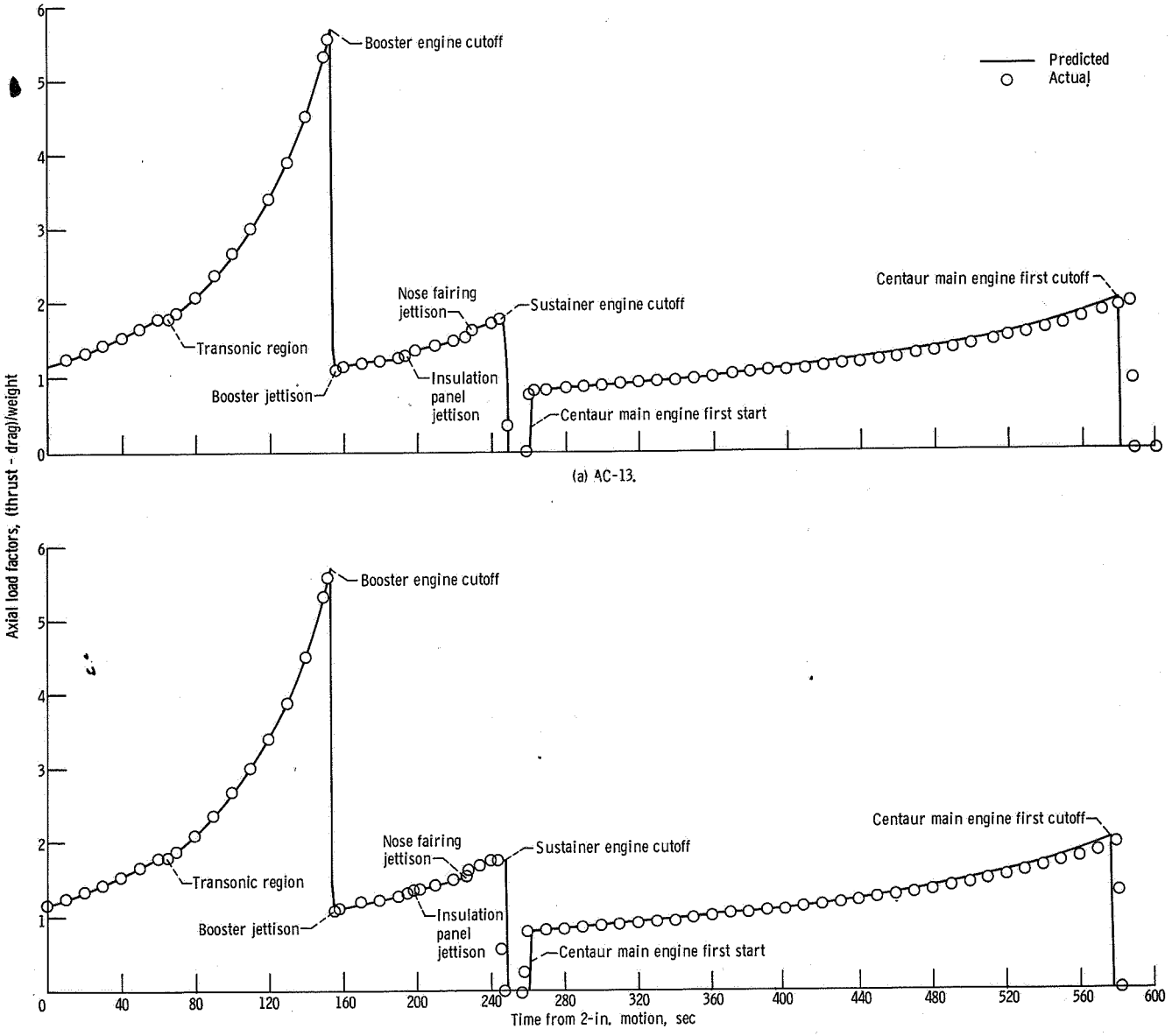

(a) AC-13.

(b) AC-14.

Figure A-7. - Axial load factor as function of time.

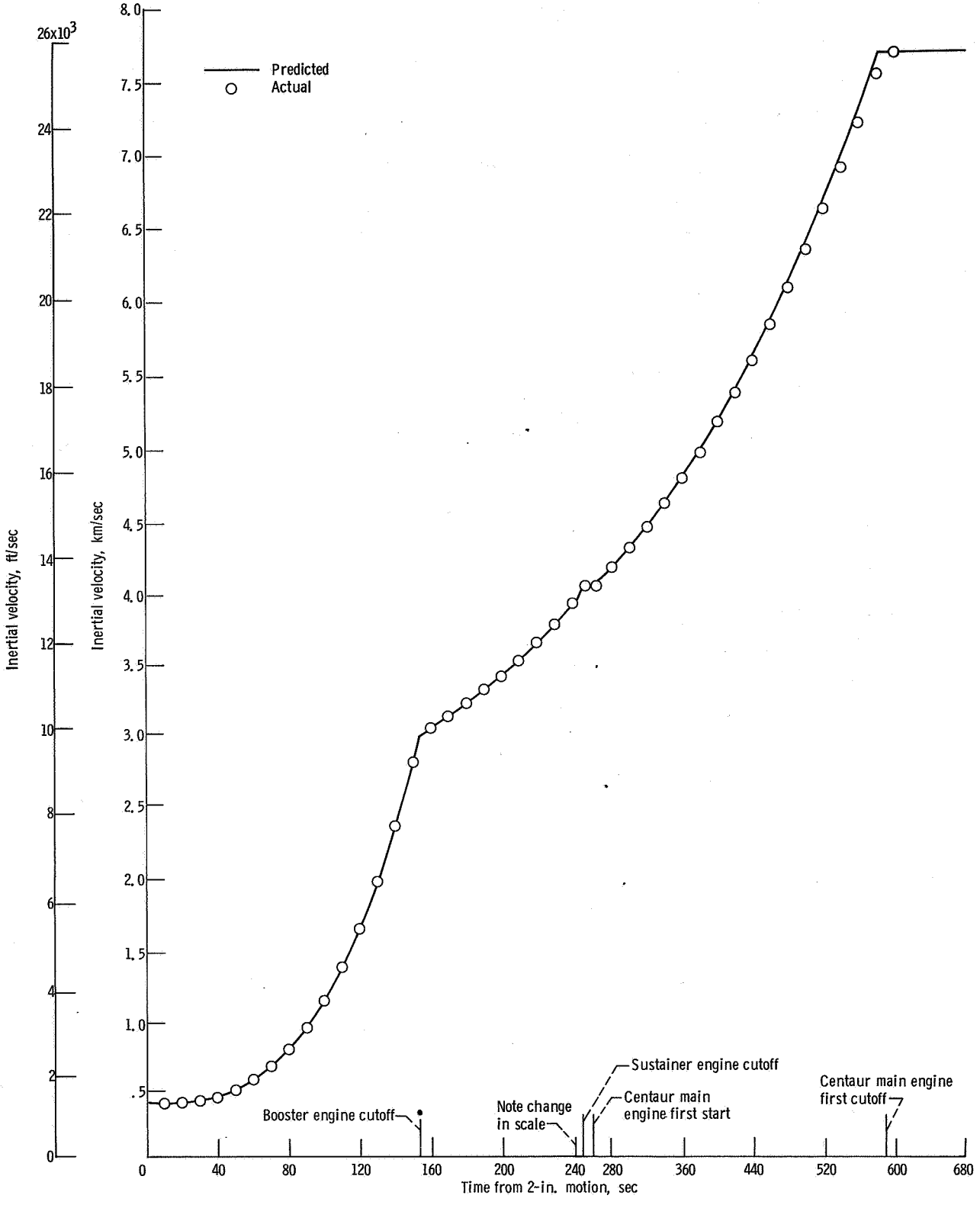

(a) AC-13.

Figure A-8. - Inertial velocity as function of time.

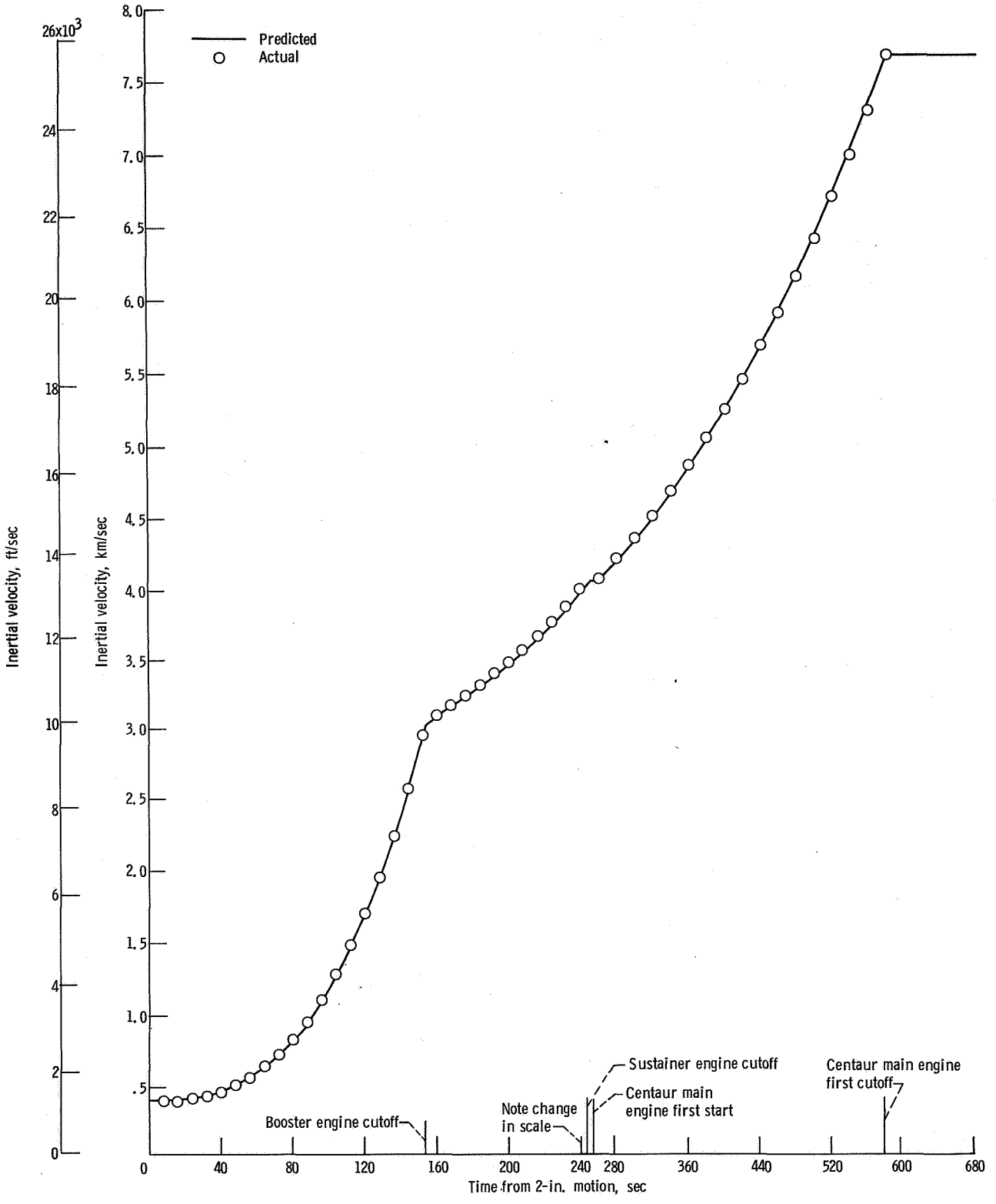

(b) AC-14.

Figure A-8. - Concluded.

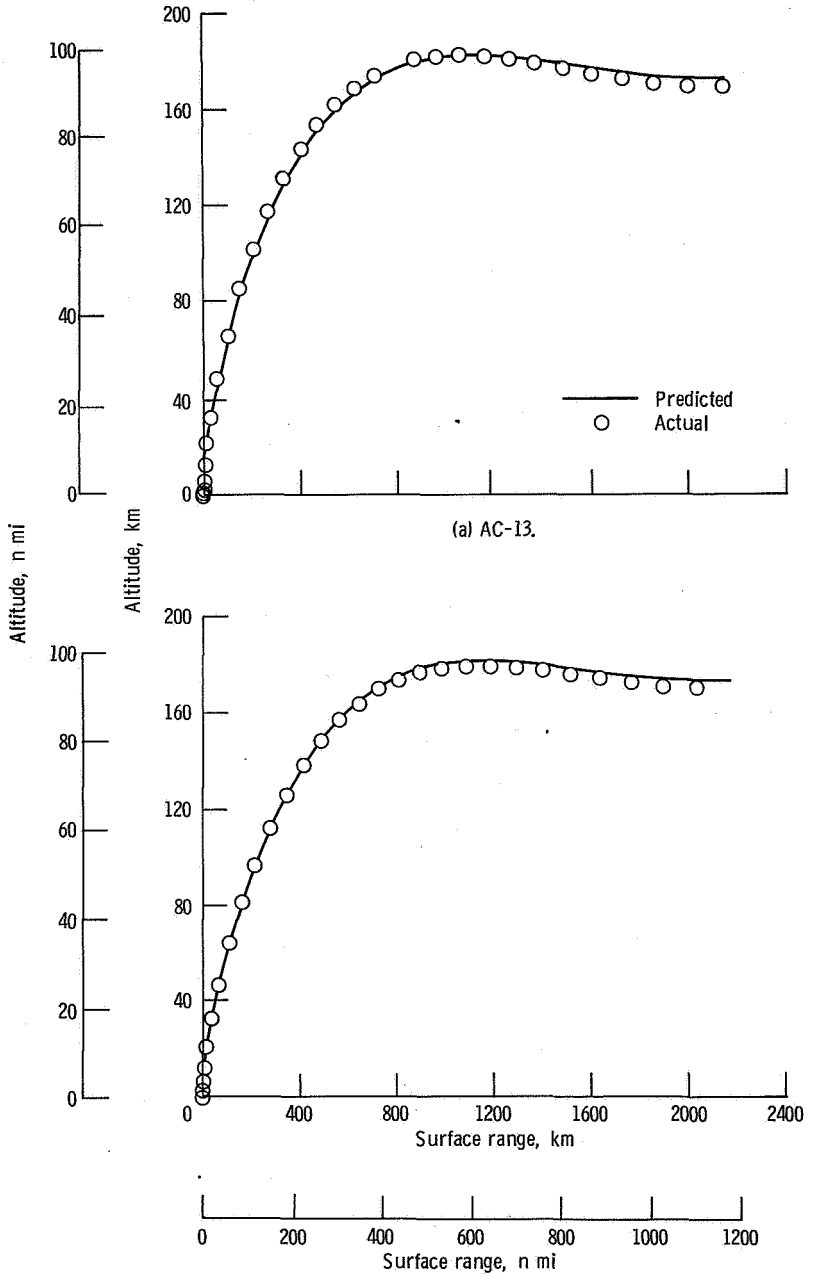

Figure A-9. - Altitude as function of surface range.

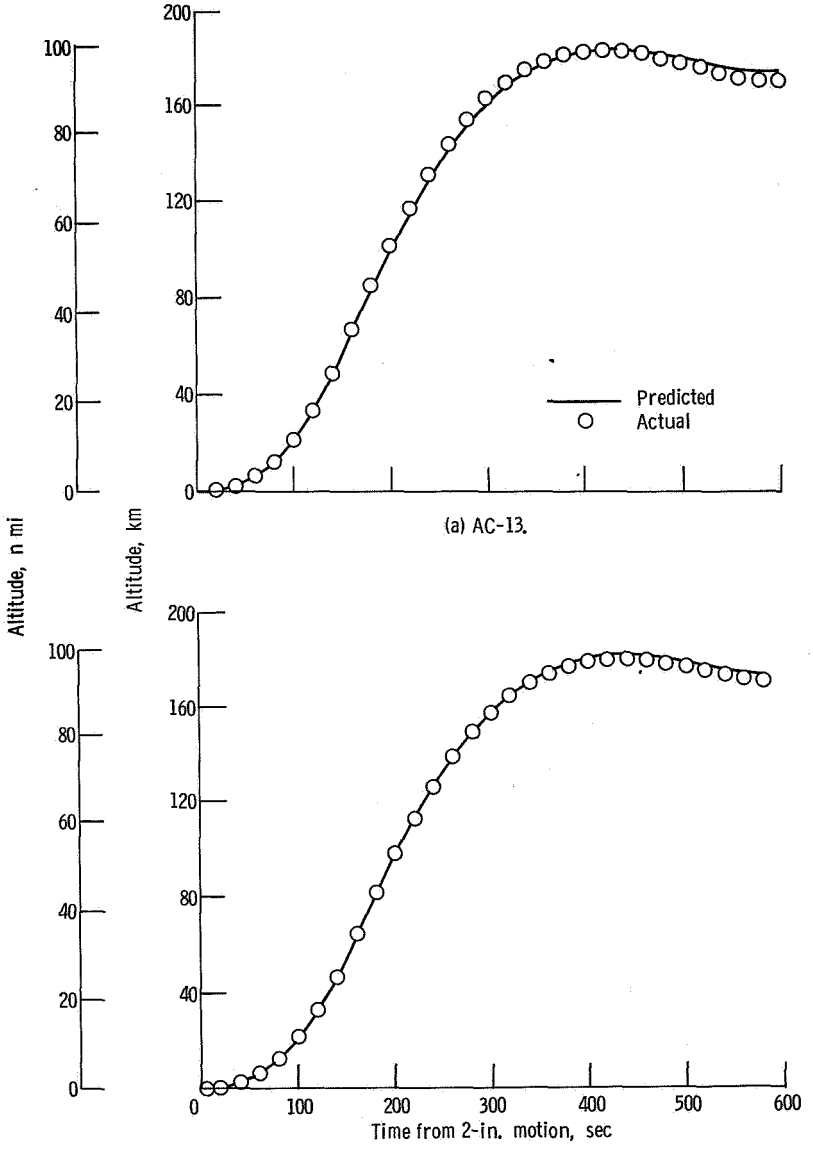

(a) AC-13.

(b) AC-14.

Figure A-10. - Altitude as function of time.

APPENDIX B

CENTAUR ENGINE PERFORMANCE CALCULATIONS

by Ronald W. Ruedele

Flight values of engine thrust, engine specific impulse, and oxidizer to fuel mixture ratio were calculated by using the Pratt & Whitney characteristic velocity (C*) iteration and the Pratt & Whitney regression methods. The Pratt & Whitney techniques are used to calculate individual engine performance at discrete times. These two calculation techniques are discussed in the following sections.

PRATT & WHITNEY C* TECHNIQUE

This technique is an iteration process for determining engine performance parameters. Flight data are used with calibration coefficients obtained from the engine acceptance tests. Calculations are made to determine C*, individual propellant weight flow rates, and subsequently, specific impulse and engine thrust. The procedure is as follows:

(1) Calculate the hydrogen flow rate by using acceptance test calibration data and venturi measurements of pressure and temperature as obtained from telemetry.

(2) Assume a given mixture ratio and calculate corresponding oxidizer flow rate and total propellant flow rate.

(3) Obtain C* ideal from performance curve as a function of mixture ratio.

(4) Correct to C* actual by using characteristic exit velocity efficiency factor obtained from acceptance test results.

(5) Calculate total propellant flow rate, using C* actual:

$$\dot{\omega}_t = \frac{P_o A_t g}{C^*}$$

where $\dot{\omega}_t$ is the total engine propellant flow rate, P_o is the measured chamber pressure from telemetry, A_t is the thrust chamber throat area, g is the gravitational constant (32.17 ft/sec/sec), and C* is the characteristic (actual) exhaust velocity.

(6) Determine the mixture ratio by using the calculated total propellant flow rate and the measured hydrogen flow rate.

(7) Compare the calculated mixture ratio with that assumed in step (2).

(8) If two values of mixture ratio do not agree, assume a new value of the mixture ratio and repeat the process until agreement is obtained.

(9) When the correct mixture ratio is determined, obtain the ideal specific impulse from the performance curve as a function of actual mixture ratio.

(10) Correct to actual specific impulse by using specific impulse efficiency factor determined from acceptance test results.

(11) Calculate engine thrust as a product of propellant flow rate and specific impulse.

PRATT & WHITNEY AIRCRAFT REGRESSION TECHNIQUE

This program determines engine thrust, specific impulse, and propellant mixture ratio from flight values of engine inlet pressures, engine inlet temperatures, and propellant utilization valve angle. The program is strongly dependent on engine ground testing. The method in which ground testing is correlated with the flight is as follows:

A large group of RL10A3-1 engines was ground tested. An average level of engine performance was obtained as a function of engine pump pressures, inlet temperatures, and the propellant utilization valve angle. During any specific engine acceptance test, the differences in performance from this average level are noted.

Flight performance is then determined in two steps: (1) the average engine level of performance is obtained for flight values of engine inlet conditions and propellant utilization valve angle and (2) corrections are made for the difference between the average engine level and the specific engine as noted during the engine acceptance test.

REFERENCES

1. Staff of the Lewis Research Center: Postflight Evaluation of Atlas-Centaur AC-8 (Launched April 7, 1966). NASA TM X-1343, 1967.
2. Lewis Research Center: Performance Evaluation of Atlas-Centaur Restart Capability in Earth Orbit. NASA TM X-1647, 1968.
3. Staff of the Lewis Research Center: Postflight Evaluation of the Atlas-Centaur AC-6 (Launched August 11, 1965). NASA TM X-1280, 1966.
4. Lacovic, Raymond F.; and Berns, James A.: Capillary Rise in the Annular Region of Concentric Cylinders During Coast Periods of Atlas-Centaur Flights. NASA TM X-1558, 1968.
5. Foushee, B. R.: Liquid Hydrogen and Liquid Oxygen Density Data for Use in Centaur Propellant Loading Analysis. Rep. AE62-0471, General Dynamics Corp., May 1, 1962.
6. Pennington, K., Jr.: Liquid Oxygen Tanking Density for the Atlas-Centaur Vehicles. Rep. BTD 65-103, General Dynamics Corp., June 3, 1965.

NASA-Langley, 1970 —— 31 E-5057

"The aeronautical and space activities of the United States shall be conducted so as to contribute . . . to the expansion of human knowledge of phenomena in the atmosphere and space. The Administration shall provide for the widest practicable and appropriate dissemination of information concerning its activities and the results thereof."

—NATIONAL AERONAUTICS AND SPACE ACT OF 1958

NASA SCIENTIFIC AND TECHNICAL PUBLICATIONS

TECHNICAL REPORTS: Scientific and technical information considered important, complete, and a lasting contribution to existing knowledge.

TECHNICAL NOTES: Information less broad in scope but nevertheless of importance as a contribution to existing knowledge.

TECHNICAL MEMORANDUMS: Information receiving limited distribution because of preliminary data, security classification, or other reasons.

CONTRACTOR REPORTS: Scientific and technical information generated under a NASA contract or grant and considered an important contribution to existing knowledge.

TECHNICAL TRANSLATIONS: Information published in a foreign language considered to merit NASA distribution in English.

SPECIAL PUBLICATIONS: Information derived from or of value to NASA activities. Publications include conference proceedings, monographs, data compilations, handbooks, sourcebooks, and special bibliographies.

TECHNOLOGY UTILIZATION PUBLICATIONS: Information on technology used by NASA that may be of particular interest in commercial and other non-aerospace applications. Publications include Tech Briefs, Technology Utilization Reports and Notes, and Technology Surveys.

Details on the availability of these publications may be obtained from:

SCIENTIFIC AND TECHNICAL INFORMATION DIVISION

NATIONAL AERONAUTICS AND SPACE ADMINISTRATION

Washington, D.C. 20546